Alma Mater Studiorum – Università di Bologna

DOTTORATO DI RICERCA IN

Biologia Cellulare e Molecolare

Ciclo XXVIII

Settore Concorsuale di afferenza: 05/A2 – Fisiologia Vegetale

Settore Scientifico disciplinare: BIO/04 – Fisiologia Vegetale

DISENTANGLING THE ROLE OF TRANSITORY STARCH STORAGES IN PLANT DEVELOPMENT AND IN OSMOTIC STRESS RESPONSE

Presentata da: Claudia Pirone

Coordinatore Dottorato
Chiar.mo Prof.
Giovanni Capranico

Relatore
Chiar.ma Prof.ssa
Francesca Sparla

Esame finale anno 2016

SINTESI

L'amido, dopo la cellulosa, è il secondo biopolimero in termini di biomassa (Geigenberger, 2011) ed è formato da lunghe catene di unità di glucosio legate da legami α-1,4 (Berg et al., 2002). Oltre a rappresentare la maggiore riserva di carboidrati nelle piante superiori è anche di fondamentale importanza per l'alimentazione umana (fornendo circa il 60% dell'apporto calorico giornaliero) e animale (Geigenberg, 2011), nonché per l'industria e per la produzione di energia rinnovabile (Davis et al., 2003; Smith, 2008). Nelle piante superiori, grazie alla fotosintesi ossigenica una parte del carbonio organicato viene utilizzato per la produzione di amido (Zeeman et al., 2010). L'amido può essere per semplicità distinto in amido di riserva (anche detto secondario) o transitorio (anche detto primario), a seconda che sia immagazzinato dalla pianta per lunghi o brevi periodi. Infatti, l'amido secondario si trova nei plastidi degli organi di riserva della pianta, come semi, tuberi o radici e viene degradato per fornire zuccheri e, quindi energia, necessari in casi specifici, come durante la germinazione o la secrezione del nettare (Fincher, 1989; Razem and Davis, 1999). L'amido primario invece viene sintetizzato nei cloroplasti delle foglie durante il giorno e viene degradato durante la successiva notte per fornire gli zuccheri che sono necessari a supportare i processi metabolici della cellula stessa o che vengono trasportati negli organi in cui è richiesta energia, permettendo la crescita della pianta anche nei periodi in cui la mancanza di luce non consente ulteriore fissazione di CO_2 (Zeeman et al., 2007). L'amido transitorio viene anche accumulato temporanemanete nei semi oleosi e nei frutti di alcune specie vegetali (Schaffer and Petreikov, 1997; Baud et al., 2002; Andriotis et al., 2010) o nelle radici (per esempio negli statoliti della columella), per svolgere alcune funzioni specifiche. L'amido è quindi di fondamentale importanza per la crescita della pianta.

L'amido forma granuli semi-cristallini, con schemi caratteristici di diffrazione ai raggi-X, di differenti dimensioni, compatti e osmoticamente inerti (Jane et al., 1994). Questi granuli sono composti da amilosio e da amilopectina, generalmente in un rapporto di 1:3 circa (Buléon et al., 1998). Mentre l'amilosio è una lunga molecola prevalentemente lineare, l'amilopectina contiene ramificazioni, date da unità di glucosio legate da legami α-1,6, ed è responsabile della natura semi-cristallina dei granuli d'amido (McPherson and Jane,

1999; Gérard et al., 2002). Data la sua importanza, l'amido è presente in molte specie vegetali e in quasi tutti gli organi. In base alla sua origine botanica può avere diverse composizioni e strutture, caratteristiche che a loro volta si riflettono sulle sue proprietà chimico-fisiche (Alcázar-Alay and Meireles, 2015), per esempio temperatura di gelatinizzazione, viscosità, etc. Amidi con minore contenuto di amilosio, per esempio, hanno una maggiore resistenza al congelamento e allo scongelamento (caratteristica interessante per la preparazione dei cibi) (Jobling, 2004), mentre amidi con maggior contenuto di amilosio sono importanti a fini nutrizionali, dato che quest'ultimo è più resistente alla digestione umana nell'intestino tenue e può quindi raggiungere l'intestino crasso dove svolge la stessa funzione delle fibre alimentari (Nugent, 2005; Topping, 2007). La complessa struttura dell'amido è il risultato dell'azione di diversi enzimi, sia biosintetici che degradativi, che ne modificano le proprietà e che quindi sono rilevanti anche per applicazioni nutrizionali e industriali (Ball and Morrel, 2003; James et al., 2003; Jeon et al., 2010; Zeeman et al., 2010).

L'orzo (*Hordeum vulgare* L.) è il quarto più importante cereale in termini di area coltivata e tonnellate raccolte e la produzione globale è utilizzata principalmente come mangime animale e per l'industria del malto (http://faostat.fao.org). I semi di orzo contengono nell'endosperma il 50-60% di amido di riserva rispetto al peso secco del seme. Questo amido è immagazzinato in due tipi di granuli di differenti forme e dimensioni (Mazanec et al., 2011; Howard et al., 2011): i granuli di tipo A, che hanno maggiori dimensioni (in cui si trova la maggior parte dell'amido) e i granuli di tipo B, più piccoli, ma più numerosi. I granuli di tipo A sono più facilmente attaccati dagli enzimi idrolitici, mentre i granuli di tipo B sembrano essere più protetti, causando problemi tecnici durante la produzione della birra (MacGregor, 1991). In una prima parte del progetto di dottorato è stato analizzato il fenotipo (con particolare riguardo alla quantità e alla struttura dei granuli d'amido) di nove mutanti di orzo, ottenuti tramite strategia TILLING, che portavano mutazioni missenso o non-senso in cinque geni collegati al metabolismo dell'amido, noti per essere espressi nell'endosperma dell'orzo durante il riempimento del seme: *BMY1* (β-amilasi 1), *GBSSI* (amido sintasi associata al granulo I), *LDA1* (Limit Dextrinasi 1), *SSI* (amido sintasi I), *SSIIa* (amido sintasi IIa). Mentre BMY1 è prevalentemente coinvolta nella degradazione, come anche LDA1, gli enzimi codificati dagli altri tre geni sono principalmente coinvolti nella sintesi del granulo d'amido. È stato osservato che sette

linee mutanti presentavano amido con caratteristiche interessanti per applicazioni alimentari e industriali, come per esempio un alterato rapporto amilosio/amilopectina, un'alta percentuale di granuli di tipo A oppure granuli di tipo A più grandi rispetto a quelli di piante wild-type. I risultati hanno inoltre confermato il ruolo dell'enzima GBSSI nella biosintesi dell'amilosio e il ruolo della proteina SSIIa nella sintesi dell'amilopectina. Sorprendentemente, la proteina LDA1 sembra essere coinvolta nell'iniziazione della sintesi dei granuli, mentre l'enzima SSIIa è implicato nel controllo della dimensione dei granuli.

La pianta modello *Arabidopsis thaliana* è stata di fondamentale importanza per lo studio del metabolismo dell'amido fogliare, sia perché converte più del 50% del carbonio fissato durante il giorno in amido transitorio, sia perché il suo genoma è interamente sequenziato, sia perché sono disponibili una serie di servizi pubblici, tra cui banche dati di semi mutanti che permettono di ottenere specifici *knock out* (KO). È stato proprio attraverso lo studio di piante KO con alterato metabolismo dell'amido che il *pathway* di degradazione dell'amido transitorio è stato compreso (per una *review*, Zeeman et al., 2010).

Mentre amido transitorio e amido di riserva condividono la medesima via biosintetica, la loro degradazione avviene tramite differenti *pathway*. Alla degradazione dell'amido di riserva prendono parte α-amilasi, β-amilasi, enzimi deramificanti (nello specifico LDA) e α-glucosidasi. Al contrario, per la normale degradazione dell'amido fogliare non è richiesta nessuna attività α-amilasica (Yu et al., 2005), ma è indispensabile un iniziale passaggio di fosforilazione del granulo, necessario a rendere la sua superficie accessibile ad una serie di enzimi degradativi (Blennow et al., 2000; Edner et al., 2007; Santelia et al., 2015). Il genoma di Arabidopsis codifica per tre enzimi in grado di fosforilare l'amido. A seconda del substrato che utilizzano, questi enzimi vengono suddivisi in glucano, acqua dichinasi (GWD1 e GWD2) e fosfoglucano, acqua dichinasi (PDW). I primi sono in grado di fosforilare in posizione C-6 i residui di glucosio dell'amilopetina (Ritte et al., 2002), i secondi sono invece in grado di fosforilare in posizione C-3 i residui di glucosio di catene di amilopectina già pre-fosforilate (Baungaard et al., 2005; Kötting et al., 2005). Il livello di fosforilazione delle catene di glucano influisce sulla capacità di degradazione dell'amido, così come può variarne le proprietà chimico-fisiche. Ad eccezione della GWD2, le proteine GWD1 e PWD sono localizzate nello stroma del cloroplasto (Ritte et al., 200; Baunsgaard

et al., 2005), dove l'amido si accumula durante il giorno. GWD2 è invece un enzima citoplasmatico, prevalentemente espresso nel tessuto vascolare e nel periodo di senescenza della pianta (Glaring et al., 2007) e sembra non essere coinvolto nella normale degradazione dell'amido primario. Molti esperimenti sottolineano l'importanza di GWD1 e PWD nell'assicurare la corretta degradazione dell'amido fogliare: piante di Arabidopsis mancanti di GWD1 sono incapaci di degradare l'amido anche dopo un periodo prolungato di buio e sono perciò caratterizzate da un forte accumulo di amido nelle foglie, detto fenotipo *starch excess* (*sex*) (Lorberth et al., 1998). Piante KO mancanti della proteina PWD hanno un fenotipo *sex* più lieve, mentre in accordo con la sua localizzazione extra-plastidiale, piante mancanti di GWD2 non presentano fenotipo *sex* (Glaring et al., 2007).
Sono stati effettuati molti studi su piante con alterata espressione di geni coinvolti nel metabolismo dell'amido (Lloyd et al., 2005), tuttavia è stata posta maggiore attenzione sui mutanti che presentavano i fenotipi più severi ed i dati si riferiscono spesso a singole fasi di sviluppo della pianta o ad organi specifici. Quindi, è stato deciso di analizzare durante l'intero ciclo vitale e in differenti organi il fenotipo di piante di Arabidopsis mancanti dei geni *GWD1*, *GWD2* e *PWD*. È stato osservato che, a parte il noto fenotipo *sex* delle piante *gwd1* e *pwd*, solo le piante *gwd1* apparivano chiaramente differenti dalle piante *wild type*, richiedendo circa il 50% del tempo in più per raggiungere la fase riproduttiva, probabilmente primariamente a causa della deplezione di zuccheri durante la notte. Di conseguenza, il numero delle foglie della rosetta nelle piante *gwd1* era circa 1,3 volte superiore a quello del wild-type. La crescita delle piante in condizioni di luce continua a bassa intensità luminosa (che permette la continua produzione ed un continuato apporto di zuccheri alla pianta), causava la reversione del fenotipo, anche se non completa, suggerendo che i mutanti *gwd1* non soffrivano unicamente per la carenza di zuccheri. Considerando che l'incremento in termini di biomassa delle piante *gwd1* è associato a una piccola perdita di produttività (in termini di numero di semi prodotti e delle loro dimensioni), questa mutazione potrebbe essere di interesse industriale, fornendo piante con maggiore biomassa, maggior contenuto di amido nelle foglie (incrementando il valore della materia prima), buona produttività e semi con maggior contenuto di amido e minor contenuto lipidico. Sono stati inoltre evidenziati ulteriori tratti fenotipici sia nelle piante *pwd* che nelle piante *gwd2*, come per esempio ridotta crescita radicale, minor contenuto di lipidi nei semi, insorgenza del fenotipo *sex* nelle

foglie in piante esposte a luce continua, minore produttività della pianta (minor numero di foglie nella rosetta e di fiori, di silique e di semi sullo scapo principale) rispetto al wild-type. L'enzima PWD è normalmente presente nei cloroplasti dove contribuisce alla degradazione dell'amido, sebbene agisca a valle dell'enzima GWD1 e quindi, quando assente, dia un fenotipo *sex* meno severo. Perciò, i dati ottenuti per i mutanti *pwd* possono essere ascritti a un mancato apporto di carboidrati necessari a sopperire alle richieste energetiche. Inoltre, sorprendentemente, questi risultati suggeriscono che anche GWD2 possa avere un ruolo nel mantenimento di un bilanciato apporto di zuccheri alle diverse parti della pianta. Vista la sua localizzazione nell'apparato vascolare e l'incrementata espressione durante le fasi avanzate dello sviluppo (Glaring et al., 2007), GWD2 potrebbe avere un ruolo nella mobilitazione degli zuccheri (sotto forma di eteroglicani solubili) nel floema o nella degradazione e nella ri-mobilitazione dell'amido rilasciato dai tessuti senescenti.

Dopo un'iniziale fase di fosforilazione e defosforilazione, il granulo d'amido viene degradato dalle β-amilasi e dagli enzimi deramificanti. Mentre gli enzimi deramificanti sono in grado di scindere i legami α-1,6 tra le molecole di glucosio, le β-amilasi sono eso-amilasi che rilasciano maltosio, idrolizzando i legami α-1,4 tra molecole di glucosio, a partire dalle estremità non riducenti delle catene lineari poliglucosidiche di amilosio e amilopectina. Il genoma di Arabidopsis codifica per 9 β-amilasi (BAM1-9), 4 delle quali (BAM1-4) a localizzazione cloroplastica. Mentre BAM3 sembra essere la principale responsabile della normale degradazione notturna dell'amido transitorio, BAM1 sembra avere un ruolo nella degradazione dell'amido nelle cellule del mesofillo in piante sottoposte a stress osmotico (Valerio et al., 2011; Monroe et al., 2014). Lo stress idrico ha un impatto forte e negativo sulla crescita della pianta e sulla sua produttività (Cattivelli et al., 2008; Rockström and Falkenmark, 2010; Osakabe et al., 2014). Un tratto comune a molte piante colpite da siccità o stress salino è l'accumulo di osmoprotettori, come per esempio prolina, betaina o zuccheri alcolici (Szabados and Savouré, 2009; Liang et al., 2013). La prolina non solo è un soluto compatibile, ma ha anche una funzione di detossificazione nei confronti delle specie reattive dell'ossigeno (ROS), proteggendo la cellula dallo stress ossidativo (Matysik et al., 2002; Bartels and Sunkar, 2005). Nelle piante la sintesi della prolina avviene sia nel citosol che nei cloroplasti e gli scheletri carboniosi necessari provengono dal metabolismo primario attraverso il *pool* del glutammato. Non

essendo noto se la degradazione dell'amido fosse coinvolta in questo processo e con lo scopo di indagare più approfonditamente il ruolo delle β-amilasi nella risposta allo stress osmotico in Arabidopsis, sono stati analizzati mutanti mancanti di BAM1 o di BAM3 sottoposti a uno stress osmotico moderato (150 mM mannitolo) e prolungato (fino a una settimana). È stato dimostrato che le foglie di piante *bam1* sottoposte a stress osmotico accumulavano più amido e meno zuccheri solubili durante il giorno delle piante *bam3* e wild-type. Inoltre, è stato osservato che le piante *bam1* presentavano un inficiato accumulo di prolina e soffrivano di una maggiore perossidazione lipidica rispetto alle piante *bam3* e wild-type. Questi dati suggeriscono quindi che gli scheletri carboniosi derivanti dalla degradazione diurna dell'amido transitorio ad opera di BAM1 supportano la biosintesi di prolina necessaria a fronteggiare lo stress osmotico. Questo potrebbe essere un tratto interessante per il miglioramento della tolleranza allo stress nelle piante coltivate.

Il genoma di Arabidopsis codifica inoltre per tre α-amilasi, endo-amilasi capaci di idrolizzare l'amido, una delle quali, AMY3, citosolica (Seung et al., 2013). Nonostante AMY3 sia un'amilasi attiva, piante mancanti di questa proteina (come quelle mancanti di BAM1) degradano l'amido normalmente in condizioni normali di crescita (Yu et al., 2005; Kaplan and Guy et al., 2005; Kötting et al., 2009). Tuttavia, quando altri enzimi degradativi sono assenti, la mancanza di AMY3 (come quella di BAM1), accentua il fenotipo *sex*. Inoltre, è stato dimostrato che AMY3 e BAM1 sono responsabili della degradazione diurna dell'amido nelle cellule di guardia, processo che sostiene l'apertura stomatica (Valerio et al., 2011; Horrer et al., 2016) e che le due proteine agiscono sinergicamente nella degradazione dell'amido *in vitro* (Seung et al., 2013). Un'altra similitudine fra le due proteine è che sembrano essere le uniche amilasi redox regolate. Vengono infatti attivate dalla luce mediante la riduzione di un ponte disolfuro intra-molecolare. L'espressione di AMY3, parallelamente a quella di BAM1, sembra anche essere promossa in Arabidopsis durante stress osmotico nelle cellule del mesofillo (Dr. Santelia, comunicazione personale). Tutto ciò suggerisce la possibilità di una via degradativa alternativa dell'amido transitorio in condizioni di luce, in piante sottoposte a stress osmotico, che coinvolge enzimi che non sono normalmente richiesti. Nelle ultime decadi, la glutationilazione è emersa come modificazione redox post-traduzionale alternativa, che consiste nella formazione di un ponte disolfuro fra una cisteina reattiva di una proteina e una molecola

di glutatione e che avviene prevalentemente in condizioni di stress, momento in cui la produzione di specie reattive dell'ossigeno (ROS) è esacerbata (Zaffagnini et al., 2012b). Questa modificazione sembra avere diversi ruoli, tra cui la protezione di tioli proteici dall'ossidazione irreversibile, la modulazione dell'attività enzimatica e la segnalazione cellulare. Dato il coinvolgimento di AMY3 e BAM1 nella degradazione diurna dell'amido in condizioni di stress, le due proteine ricombinanti sono state espresse e purificate e ne è stata analizzata la suscettibilità all'ossidazione e alla glutationilazione, saggiando l'attività enzimatica in presenza di acqua ossigenata (H_2O_2), in presenza o in assenza di glutatione ridotto (GSH). È stato osservato che entrambi gli enzimi venivano inibiti dal trattamento con H_2O_2, ma in presenza di GSH i tassi di inibizione erano minori per BAM1 o assenti per AMY3, suggerendo che entrambi le proteine fossero soggette a glutationilazione. Questa ipotesi è stata confermata tramite western blot e analisi di spettrometria di massa. Per identificare i residui coinvolti nella glutationilazione, tutte le varianti Cisteina/Serina sia di BAM1 che di AMY3 sono state analizzate mediante western blot utilizzando glutatione biotinilato e anticorpi anti-biotina, senza però ottenere risultati univoci. Tuttavia è stato osservato che la formazione del ponte disolfuro in BAM1 preveniva la glutationilazione e che i residui coinvolti sembravano essere due, facendo supporre che le cisteine interessate fossero le medesime. È quindi stato ipotizzato un ruolo della glutationazione nella prevenzione dell'inattivazione enzimatica causata da ossidazione e da formazione del ponte disolfuro. Per AMY3 non è stata evidenziata una interazione fra glutationilazione e ossidazione mediata da formazione del ponte disolfuro. Tuttavia è stato evidenziato che una delle due cisteine coinvolte nella regolazione redox era anche essenziale per la catalisi enzimatica e sembrava avere un pK_a di 7.2, facendone un potenziale bersaglio anche per la glutationilazione. Ulteriori esperimenti sono necessari per verificare queste ipotesi. In generale, questi dati suggeriscono un ruolo della glutationilazione nella protezione di BAM1 e AMY3 da una veloce e irreversibile ossidazione in condizioni di stress ossidativo.

In conclusione, in passato l'amido era considerato un biopolimero abbastanza statico, data la sua natura cristallina ed il suo ruolo di sostanza di riserva energetica non osmoticamente attiva. Sulla capacità delle piante di immagazzinare amido si basano anche l'industria alimentare ed energetica. Tuttavia nel corso degli anni è stato dimostrato che l'amido ha anche una natura transitoria ed altamente dinamica. È stato infatti evidenziato

che l’amido non funge solo da riserva di energia a lungo termine ma è anche una fonte di carbonio che viene rapidamente utilizzata dalla pianta non solo per la crescita ma anche per supportare specifiche funzioni, come l’apertura stomatica e la produzione di osmoliti, in funzione degli stimoli esterni e delle condizioni ambientali. Per fare questo è necessaria una concertata e fine regolazione degli enzimi responsabili sia del suo accumulo che della sua degradazione. La comprensione di questi meccanismi, della modalità di ripartizione del carbonio derivante dalla degradazione dell’amido nella pianta e tra le differenti vie metaboliche e più in generale del ruolo dell’amido in risposta alle condizioni esterne ed agli stress, è particolarmente importante e può avere in futuro rilevanza applicativa.

Preface: organization and brief description of the topics.

This PhD thesis is composed of four chapters:

- Chapter 1: “New starch phenotypes produced by TILLING in barley”;
- Chapter 2: “Starch phosphorylating enzymes are required for a proper development of Arabidopsis plants”;
- Chapter 3: “β-amylase 1 (BAM1) degrades transitory starch to sustain proline biosynthesis during drought stress”;
- Chapter 4: “BAM1 and AMY3, two redox sensitive enzymes involved in Arabidopsis starch degradation, are target of glutathionylation”;

having starch metabolism as leitmotif and corresponding to different stand-alone experimental works. More in detail, the first chapter deals with storage starch metabolism, whereas the other three discuss about transitory starch degradation; the third and fourth chapter also investigate the relationship between starch degradation and plant stress responses and stress redox physiology, respectively. The four chapters are preceded by a “General introduction” that aims to give an idea of the knowledge about plant carbon partitioning and about storage and transitory starch metabolism. References of this introductory chapter can be found at the very end of the thesis.

Table of contents

GENERAL INTRODUCTION

Starch is the second bio-polymer on earth in term of biomass after cellulose (Geigenberger, 2011). Such as cellulose, starch is a polysaccharide composed by glucose units. The difference between cellulose and starch is that, in starch, glucose units are joined together by α-glycosidic bonds, whereas in cellulose by β-glycosidic bonds (Berg et al., 2002). This seemingly trivial diversity results in large differences in function, structure, physicochemical properties and enzyme susceptibility. Indeed, starch is the most abundant energy storage in plants and the most important carbohydrate in animal and human diet (Geigenberger, 2011). On the contrary, most animals including humans cannot digest cellulose.

In higher plants, starch is produced and stored in plastids, either in photosynthetic and non-photosynthetic cells. It exists in form of insoluble and semi-crystalline inert granules and this allow storing a large amount of energy in a relatively small volume without affecting the osmotic balance of the cell (Valerio et al., 2011). Primary starch is synthesized in chloroplasts as a consequence of photosynthesis (Zeeman et al., 2007). Starch is then degraded by night to provide carbon to sustain leaf respiration and to produce sugars that are exported via vascular tissues to sustain plant growth even in absence of light (Zeeman et al., 2007). Because of its great fluctuations in content between day and night, primary starch is also named transient starch. Starch is also temporarily accumulated in oilseeds and fruits (Schaffer and Petreikov, 1997; Baud et al., 2002; Andriotis et al., 2010) of some plant species or in roots (i.e. columella statoliths), to exploit some specific function, and for the same reason also this type of starch can be considered as transient (Baud et al., 2002; Andriotis et al., 2010). On the contrary, storage or secondary starch is retained in amyloplasts of perennating organs for longer periods and it is subsequently remobilized to give sugars to meet specific energy demands, as in case of germination or nectar secretion (Fincher, 1989; Razem and Davis, 1999). While transitory and storage starch share the same biosynthetic pathway, their degradation occurs in a different manner (Zeeman et al., 2010).

The harvested part of our staple crops are starch storage organs (i.e. seeds, roots and tubers). Storage starch provides about the 60% of the human dietary energy supply (Food

and Agriculture Organization of the United Nations, values for 2014; www.fao.org). About 2500 million tons of starch crops are produced per year, and even if the edible plants species are about 50.000, only 15 provide the 90% of the world's food energy intake, the 60% of which is due to three plant species (rice, maize and wheat) (Burrel, 2003; Food and Agriculture Organization of the United Nations, values for 2014; www.fao.org). Moreover, since the ancient times, prior by the Egyptians and then by the Romans, starch was used as adhesive and for medical preparations. Also nowadays starch is demanded for non-food industry (Davis et al., 2003) and in the last decades, it is employed for the production of biofuels such as bioethanol, given that it can easily be converted into fermentable sugars (Smith, 2008).The world population is projected to increase (from almost 8 billion in 2020 to about 9 billion in 2050) and the per capita calories consumption is rising, while the problem of hunger in some part of the world is still far to be defeated (Food and Agriculture Organization of the United Nations, values for 2014; http://faostat.fao.org). Recent studies suggest a growth in food demand of about 70 to 100% by 2050 (Food and Agriculture Organization of the United Nations, values for 2014; www.fao.org). This imposes profound challenges in meeting the future food requirements. The need to increase staple crops yield can't be faced by bringing into cultivation some new land, because of the necessity of defend biodiversity and natural ecosystems, but also because, as a matter of facts, available agricultural land is decreasing due to urbanization, desertification, salinization, soil erosion and unsustainable land management (Food and Agriculture Organization of the United Nations, values for 2014; www.fao.org). In addition, climate changes and the increasing competition for the use of the fields for biofuels production rather than for alimentary purposes are likely to exacerbate this scenario.

There are still many "mysteries" concerning starch metabolism, structure and properties, despite the progresses in our understanding of its deposition processes, composition and characteristics. In fact, starch from different botanical sources have different polymer compositions and structures and therefore, different chemical-physical properties (gelatinization temperature, viscosity of cooked pastes and gels, etc.) (Alcázar-Alay and Meireles, 2015). For all these reasons, understanding the pathways by which starch is synthetized and degraded in model plants as *Arabidopsis thaliana* will facilitate the improvement of crops for both food and non-food uses. For example, this knowledge can

be exploited to increase starch accumulation in harvested organs, to prevent or increase starch degradation (depending upon the needing), as well as facilitate its structural modification to diversify its functionality and qualities as food and as industrial material. Obviously, the study of the model plants alone cannot provide sufficient information for this purposes and it must be accompanied in parallel by progresses in the study of these pathways in staple crops.

Photosynthesis and starch

Photosynthetic organisms are able to reduce CO_2 into biomass using energy derived from light. In plants, algae and cyanobacteria, photosynthesis releases oxygen (oxygenic photosynthesis) to convert carbon dioxide into sugars (carbon fixation). On the contrary, some types of bacteria carry out anoxygenic photosynthesis, consuming carbon dioxide without releasing oxygen, and water is therefore not used as an electron donor (Bryant and Frigaard, 2006).

Then, oxygenic photosynthesis is the only biological process able to collect solar energy to give organic carbon compounds starting from inorganic molecules as CO_2 and water. As photosynthetic organisms, plants are at the bottom of the food chain, providing eatable biomass and thus energy to almost all the other living organisms. In addition, they are also a reservoir of energy, in the form of fuel, for the planet in either recent (biofuels) or ancient times (fossil fuels). In higher plants, photosynthesis take place in chloroplasts. The outfitted tissue for photosynthesis in plants is leaf mesophyll, which contains many chloroplasts. Photosynthesis can be divided in two parts colloquially called the “light phase” and the “dark phase”. The light reactions of photosynthesis, so called because they need the direct contribution of the light, occur on specialized internal membranes of the chloroplast, called thylakoid. Proteins and chlorophylls of the photosystems absorb the light energy and use it to rip electrons from water to produce oxygen gas and to reduce nicotinamide adenine dinucleotide phosphate ($NADP^+$) to NADPH, meanwhile generating a trans-membrane proton gradient necessary for adenosine triphosphate (ATP) synthesis. NADPH and ATP are subsequently used for the reactions of the Calvin-Benson cycle, occurring in the chloroplast stroma. These reactions represents the dark phase of photosynthesis, in which carbon dioxide is used for the production of triose-phosphates (TPs). Triose-phosphates are finally converted in sucrose. Sucrose can be employed to

support cell metabolism in the cytosol, exported through the phloem to sink organs, or spent for the synthesis of starch and hence retained in the chloroplast as dense insoluble granules. In some plant species, other carbohydrates are accumulated, for example fructans in barley (Vijn and Smeekens, 1999; Cairns et al., 2000), or exported, such as galactosyl-sucrose oligosaccharides in Cucurbita and Arabidopsis, sorbitol in apple trees and mannitol in celery (Edwin et al., 2009; Noiraud et al., 2001). Stems, roots and young leaves uses exported sugars to grow. In storage organs sugars are subsequently used to produce storage polysaccharides. Typically in tubers and grains secondary starch is accumulated and degradaded to boost other specific growth phases or to meet locally high demand for carbon (Fincher, 1989; Razem and Davis, 1999).

In some species (e.g. soybean, sugar beet and Arabidopsis) starch is the major storage form and the ratio among sucrose and starch production in leaves is almost constant during the day (Upmeyer and Koller, 1973; Fondy et al., 1989; Zeeman and ap Rees, 1999). On the contrary, in other species (e.g. french bean and spinach), sucrose as well as starch accumulates in leaves during the day and starch biosynthesis is promoted when sucrose production overcomes the storage capacity of the leaf or the needing of the sink tissues (growth sites) (Fondy et al., 1989; Stitt et al., 1983). Therefore, the division of assimilates between starch and sucrose can be variable between species. The balance between these two pathways is regulated by the amount of specific key metabolites as orto-phosphate, triose-phosphates and fructose-2,6-diphosphate.

Due to the fact that starch is the main storage product in leaves of many plant species, mutations affecting starch metabolism (biosynthesis or degradation) significantly affect plant growth. For example, Arabidopsis mutant lines that are not able to produce and degrade starch have impaired growth rates in many conditions (Caspar et al., 1985; Caspar et al., 1991; Lin et al., 1991; Zeeman et al., 1998). However, these mutations have been instrumental to define the metabolic pathway of starch and are giving first indication of the mechanism that controls it.

Starch composition, structure and architecture

Starch granules are present in a wide array of species and almost in all plant organs including leaves, seeds, fruits, stems and roots. They may differ in size (from 1 to 100 µm in diameter); shape (round, lenticular, polygonal); size distribution (uni- or bi- modal);

association as individual (simple) or clusters (compound) and composition (moisture, association with lipids or proteins and mineral content, in particular phosphorus) (Jane et al., 1994). In general leaf starch granules are very small compared with storage starch granules and have a discoid or irregular shape rather than spherical or oval, probably to increase the surface available to synthetic and degrading enzymes responsible for the daily primary starch turnover (Badenhuizen, 1969). Independently from its shape, starch is always composed by amylose and amylopectin (Buléon et al., 1998). The relative amount of the two polymers varies according to the plant species, typically from 18-33% for amylose and 72-82% for amylopectin (Buléon et al., 1998). However, waxy starches containing less than 15% amylose as well as high amylose starches containing more than 40% amylose, are known (Buléon et al., 1998). The building block of both amylose and amylopectin is the six-carbon sugar D-glucose.

Amylose is a linear polymer mainly composed by α-1,4-linked glucose units (Fig. 1), though some α-1,6 branching points (typically less than 1%) are present in the molecule. The average number of chains in a single, branched molecule varies from 5 (rice and maize) to 21 chains (wheat) (Shibanuma et al., 1994), with chain lengths between 4 and >100 glucose units. The size of the polymer is more frequently given as the degree of polymerization (DPn, number of molecules composing the polymer) than as molecular weight values (DPw). Amylose possesses a broad molecular weight and DPn distribution, differing both between and within plant species and is thought to be smaller compared to amylopectin (10^5-10^6Da; DPn 500-5000). For example, amylose from barley (Takeda et al., 1999) was reported to have DPn 1570 (DPw 5580) and maize (Takeda et al., 1988) possessed DPn 930–990 (DPw 2270–2500). The DPn in different wheat varieties ranged from 830 to 1570 (Shibanuma et al, 1994).

Amylopectin is an highly branched molecule (about 5% of α-1,6 bonds) (Fig. 1) with a bigger molecular weight (10^7-10^9 Daltons). The DPn values of amylopectin range from 0.7 to 26.5 x 10^3 (Perez and Bertoft, 2010).

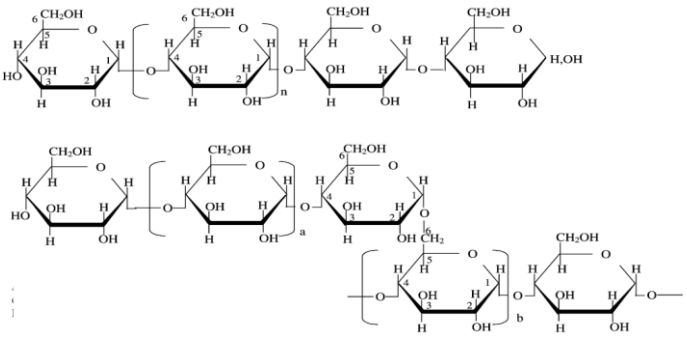

Figure 1. Starch glucosidic bonds. Structure of amylose (upper panel) and amylopectin (lower panel). Amylose is a long polymer of glucose residues linked together by α-1,4 bonds. In amylopectin α-1,4 glucose chains are linked together by α -1,6 linkages. Adapted from Tester et al., 2004.

Current models for amylopectin fine structure suggest two populations of chains, A- and B-chains, so designated for their relative position in the macromolecule, which are present in almost equal proportions. A-chains are unbranched and attached to B-chains by a single linkage, whereas B-chains are branched and connected to two or more other chains. Each amylopectin molecule will also possess a single C-chain, which contains the sole reducing group. The different population of chains can be grouped depending on their size. The smaller chain size (DPn ~15) are prevalently composed of A-chains and small B-chains. Larger chains population (DPn ~45) is thought to comprise long B-chains. The chains are assembled in a cluster structure (French, 1973; Robin et al. 1974; Nikuni, 1978; Hizukuri 1986).

The packaging of amylose and amylopectin within the granule is not random. In bigger granules, concentric “growth rings” can be seen (Fig. 2). These rings, which are between 100 and 400 nm thick, originate from the alternation between semi-crystalline and amorphous shells (Gallant et Guilbot, 1971; Yamaguchi et al., 1979; French, 1984; Gallant et al., 1997).

The semi-crystalline regions are so called due to an alternation between crystalline and amorphous layers, with a periodicity of about 9 nm (Fig. 2) (Blanshard et al., 1984; Oostergetel et al., 1989; Pérez and Bertoft, 2010). This seems to be a universal feature in the structure of starch, independent of botanical source. Furthermore, it suggests a common mechanism for starch deposition (McDonald et al., 1991). Amylopectin, which is organized radially between such structures, is responsible for the formation of the semi-crystalline regions. In fact α-glucans, although illustrated as straight chain structures, are

actually often helical. The helices formed by the branching chains of amylopectin can form double helices that can strictly interact with each other, forming crystalline layers that are generally 6 nm thick, while the branching zones of amylopectin, in which the interaction between helices is more lax, give rise to the amorphous layer (usually about 3 nm thick).
Conversely, amylose helices are prevalently found in bundles between amylopectin clusters, randomly interspersed among clusters and in the amorphous shells (Blanshard, 1987; Jane et al., 1992; Kasemsuwan and Jane, 1994).
In the less strictly ordered zones, the hydrophobic regions of the helices can interact with other compounds as free fatty acids, lysophospholipids, iodine (this being an important diagnostic function for starch characterization). These set of crystalline structures (composed by several amylopectin molecules) integrated in amorphous material (given by less branched structures like amylose and lipids) are called blocklets. Blocklets can be seen as supramolecular structures that are not prone to be enzymatically digested (Oates, 1997).
Whereas amylopectin is a key factor for overall structure of starch granules, amylose does not (McPherson and Jane, 1999; Gérard et al., 2002), even if it seems to have a role in connecting semi-crystalline shells, contributing to its strength and flexibility.
The diffraction patterns obtained from starch powders treated by mild acid hydrolysis to remove amorphous materials can be used to identify different allomorphs (Buléon et al., 1998) and to group starches according with their physical properties. In general, most cereal starches give the so-called A-type pattern, some tubers (such as potato and lesser yam), rhizomes (e.g. canna), and cereal starches rich in amylose yield the B-pattern; legume starches generally have a mixed pattern of A-type and B-type pattern, defined as C-type (Gidley, 1987; Pérez and Bertoft, 2010). An additional form, called V-type, occurs in swollen granules and is typical of the complexes formed by amylose and lipids (Buléon et al., 1998; Perez and Bertoft, 2010).

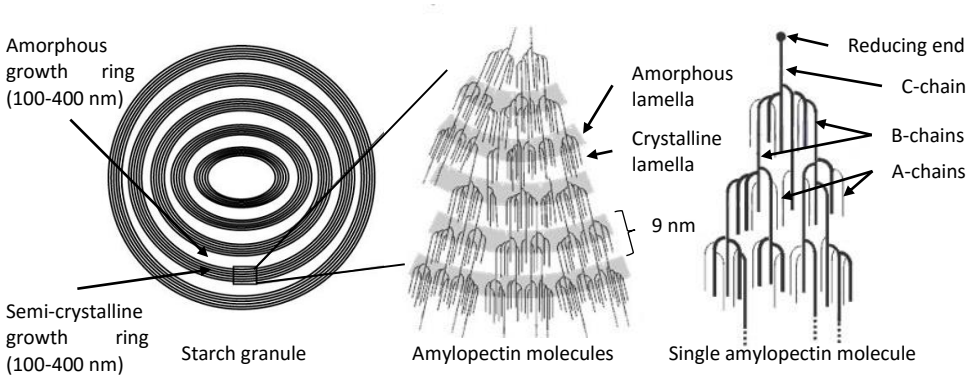

Figure 2. Starch lamellar structure, adapted by O'Neill and Field (2015). In starch granules, concentric growth rings, formed by semi-crystalline (drawn as black rings in the granule) and amorphous regions (white rings), can be seen. The semi-crystalline shells (magnificated in the middle panel) are in turn formed by an alternation of crystalline (white portion of amylopectin molecules) and amorphous lamellae (grey portion), with a periodicity of 9 nm. On the right, a schematic representation of a single amylopectin molecule. Different types of chains are highlighted.

Sucrose and starch are the products of carbon organication

In mesophyll cells, sucrose and starch are synthesized in two different compartments. The biosynthetic pathway of sucrose takes place into the cytosol while the production of starch takes place into the chloroplast (Huber and Bickett, 1984; Stitt et al., 1984; Stitt and Quick, 1989; Ekkehard Neuhaus and Stitt, 1990). Despite their different subcellular localization, the two pathways compete for carbon skeletons deriving from the photosynthetic processes (Sage, 1990; Sage, 1994; Eichelmann and Laisk, 1994; Stitt 1996). Because of the phosphate/triose-phosphates translocator (TPT), newly synthesised triose-phosphates (TPs) can be exported to the cytosol from the chloroplast in exchange for inorganic phosphate (Pi). Due to its mechanism of translocation, this antiporter control the ratio between TPs and Pi, reflecting the metabolic state of the two compartments (for a review see Flügge, 1999). Ultimately, TPs/Pi ratios control whether photosynthates are required in starch or sucrose production. Typically high levels of Pi in the cytosol, lead to the export of TPs to sustain sucrose biosynthesis, while low levels of Pi drive starch production in the stroma (reviewed by Pettersson and Ryde-Pettersson, 1990). Moreover, Pi and TPs control the activity of several enzymes belonging to both sucrose and starch

biosynthesis; for example the activity of ADP-glucose pyrophosphorylase (AGPase) is promoted by 3-phosphoglyceric acid (3PGA) and inhibited by Pi (Morell et al., 1988; Kleczkowski et al., 1993; Gómez-Casati and Iglesias, 2002; Crevillén et al., 2003; Lee et al., 2007; Tuncel et al., 2014) (see also the following section).

Once exported or retained into the stroma, TPs are the substrates of aldolases. Fructose-1,6-bisphosphate deriving from TPs aldolic condensation, is de-phosphorylated in fructose-6-phosphate (Fru6P) by fructose-1,6-phosphatase. Hexose phosphate isomerase (Phospho Glucose Isomerase, PGI) catalyses the conversion of Fru6P in glucose 6-phosphate (Glc6P), that is in turn the substrate for a phosphoglucomutase (PGM) responsible of the production of glucose 1-phospate (Glc1P) (Zeeman et al., 2010; Geigenberger, 2011). Fru6P, Glc6P and Glc1P collectively form the hexose-phosphate pool whose concentration is kept close to equilibrium (Smith, 2009).

Both sucrose and starch synthesis pathway begins with a primary event of activation of Glu1P. In starch synthesis, Glc1P is converted to ADP-glucose (ADPGlc) via AGPase, in a reaction that requires ATP and generates pyrophosphate (PP_i) (Geigenberger, 2011). In the case of sucrose, Glc1P is used by the UDP-glucose pyrophosphorylase to catalyse the formation of UDP-glucose (UDPGlc) and PPi, consuming UTP (Kleczkowski, 1994). In plastids the PP_i is suddenly removed by inorganic pyrophosphatase, displacing the equilibrium of the AGPase reaction and pushing toward the formation of ADPGlc (Weiner et al., 1987; George et al., 2010). In the cytosol an inorganic pyrophosphatase is missing, but PPi can be used by other enzymes for trans-phosphorylation reactions (Weiner et al., 1987; George et al., 2010).

Mechanisms of AGPase regulation

As mentioned above, AGPase is responsible for the conversion of Glc1P and ATP into PPi and ADPGlc, the activated glucosyl donor required for starch synthesis. Once formed, ADPGlc is transferred to a short chain of malto-oligosaccharides (Recondo and Leloir, 1961). Arabidopsis mutants with impaired activities in the chloroplast isoforms of PGI, PGM1 or AGPase, display greatly reduced levels of leaf starch (Caspar et al., 1985; Lin et al.,1988a; Lin et al., 1988b; Yu et al., 2000).

In higher plants, AGPase is a heterotetrameric enzyme composed by two small and two large subunits (Fig.3) (Lin et al., 1988a; Lin et al., 1988b; Crevillén et al., 2003; Ventriglia

et al., 2008). The small subunit is the catalytically active portion of the protein while the large subunit plays the regulatory function (Crevillén et al., 2003). Arabidopsis genome encodes two different small subunits (APS1 and APS2, with the latter considered non-functional) (Crevillén et al., 2003) and four large subunits (APL1-4) (Lin et al., 1988a; Ventriglia et al., 2008). APS1 and APL1 are the prevailing subunits in leaf enzyme, but other large subunits are expressed after treatment with exogenous sugars and are probably involved in starch synthesis in non-photosynthetic tissues (Fritzius et al., 2001; Crevillén et al., 2005; Ventriglia et al., 2008). As consequence, it has been proposed that the association of APS1 with different APL subunits can change the kinetic and the regulatory properties of the enzyme to better respond to environmental changes (Fig. 3) (Crevillén et al., 2003; Crevillén et al., 2005; Ventriglia et al., 2008).

Typically the reaction catalysed by AGPase is promoted by 3-phosphoglycerate (3PGA) and inhibited by Pi (Fig. 3) (Iglesias et al., 1993). When photosynthesis is active and the production of TPs exceed the demand for sucrose synthesis, a negative feedback prevents the TPs export from the chloroplast. Consequently, the stromal concentration of 3PGA increases whereas the Pi concentration decreases. The high ratio 3PGA/P_i promotes the activation of AGPase and the synthesis of starch (Stitt and Quick, 1989; Streb and Zeeman, 2012). AGPase activity is also redox regulated (Fu et al., 1998; Hädrich et al., 2012; Li et al., 2012). The presence or absence of light itself can limit carbon assimilation, but light can also act as a signal for the plant to switch its metabolism. Part of the electrons transported across the photosystems lead to the reduction of ferredoxin (Fdx), which in turn reduces the ferredoxin-thioredoxin reductase (FTR) able to reduce the small regulatory proteins named thioredoxins (Trxs) (Schürmann and Buchanan, 2008). Promoting a disulfide/dithiol exchange, several Trxs-target enzymes are regulated, including the AGPase (Schürmann and Buchanan, 2008). In AGPase, because of oxidation, the cysteine residues 81 at the N-terminal domain of the two small subunits form an inter-molecular disulfide bond (Fu et al., 1998). This bond decreases the protein activity, making the enzyme less sensitive to the activation mediated by 3PGA and increasing the K_M for ATP. On the contrary, reduction monomerises the small subunits and the enzyme becomes more active (Ballicora et al., 2000; Tiessen et al., 2002; Hendriks et al., 2003). In this way starch biosynthesis is actually coordinated with photosynthesis.

However, the extent of redox-activation of AGPase is also influenced by metabolites, independently from light. For example, it has been reported that 3PGA is required for fully activate the enzyme by Trxs (Ballicora et al., 2000; Hendriks et al., 2003; Geigenberger et al., 2005). Furthermore, AGPase can also be reduced by the NADP-thioredoxin reductase C (NTRC) (Michalska et al., 2009), a bimodular protein containing both an NADPH-dependent thioredoxin reductase (NTR) domain and a Trx domain on a single polypeptide chain (Serrato et al., 2004; Pascual et al., 2011). In the light NTRC can consume the NADPH produced by the ferredoxin-NADP reductase (FNR), complementing the classical Fdx/Trx system (Michalska et al., 2009). NTRC seems also to play an important role in regulating AGPase activity in response to sugars, in particular glucose, in darkened leaves and in non-photosyntetic tissues (i.e. roots), exploiting NADPH reducing power provided by the initial reactions of oxidative pentose phosphate pathway (Serrato et al., 2013). This mechanism could link the metabolic processes taking place in sink organs with light, processed via photosynthesis in source organs, through sugars transported via the phloem. Additionally sucrose, unlike glucose, can act independently from NADPH and NTRC on AGPase (Kolbe et al., 2005). Its mechanism seems to be linked to trehalose-6-phosphate (Tre6P), a signal metabolite that promotes redox activation of AGPase, most likely by modifying its interaction with Trxs (Kolbe et al., 2005; Lunn et al., 2006). In Arabidopsis, it has been demonstrated that Tre6P production is enhanced at the onset of the light period as a consequence of carbohydrate depletion occurring after an extended night, and it is preceded by a rapid sucrose accumulation (Gibon et al., 2004; Lunn et al., 2006). Given that, Tre6P is suggested to promote a greater partitioning of photo-assimilates into starch compared to the previous light period to meet the energy request for another extended night (Lunn et al., 2006). Hexokinase (for glucose) and SnRK1 kinase (for sucrose) have also been proposed to take part in this cytosolic sugar signalling process that lead to redox activation of starch biosynthesis (Tiessen et al., 2003). Although details need to be worked out, the interactions among these metabolites are likely required for the fine redox control of AGPase as the plant encounters changing environmental conditions.

Overall, the convergence of regulation on AGPase confirm the idea that it represent an important checkpoint to determine how much starch should be produced to supply the plant in the subsequent night, and how much carbohydrates are necessary for growth during the day (Smith and Stitt, 2007).

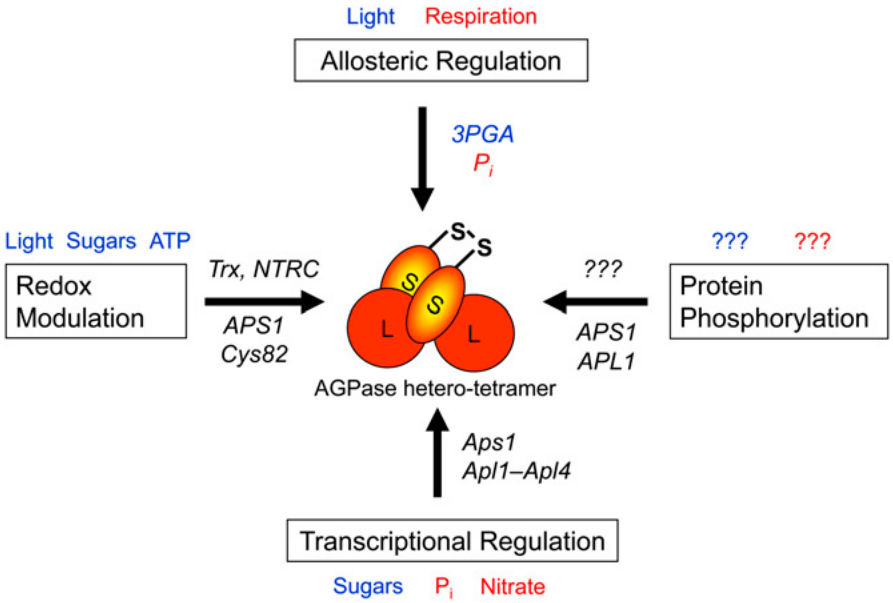

Figure 3. Regulation of plastidial AGPase by multiple mechanisms, from Geigenberger (2011). Plastidial AGPase is a heterotetramer that contains two large (APL; 51 kDa) and two slightly smaller (APS; 50 kDa) subunits, which both have regulatory functions. Allosteric regulation mediated by 3PGA and Pi (top) operates in a time frame of seconds to adjust the rate of starch synthesis. Posttranslational redox modulation (left) involves reversible disulfide bond formation between Cys82 of the two small APS1 subunits, leading to changes in AGPase activity in response to light and sugar signals in a time frame of minutes to hours. The signaling components leading to redox modulation of AGPase involve Trx and NTRC, which are linked to photoreduced Fdx and interact with different sugar signals. In Arabidopsis leaves, APS1 and APL1 have been identified as potential targets for reversible protein phosphorylation (right). Transcriptional regulation in response to changes in carbon and nutrient supply (bottom) allows more gradual changes in AGPase activity, which may require up to days to develop. Red font indicates inhibition, blue font indicates activation, and question marks indicate unknown.

Starch biosynthetic enzymes

In addition to AGPase, several other enzymes are involved in the biosynthesis of starch granules (Fig. 4). First, ADPGlc acts as the glucosyl donor for starch synthases, which catalyse the formation of a new α-glucosidic linkage by adding glucose to the non-reducing end of an existing chain (Recondo and Leloir, 1961). Starch synthases can be divided into five subclasses based on amino-acid sequence comparisons (Ral et al., 2004;

Patron and Keeling, 2005; Leterrier et al., 2008): one granule-bound starch synthase (GBSS) and four types of soluble starch synthases (SS1–4). Arabidopsis genome contains one gene for each subclass. GBSS is exclusively found associated with the starch granule and it is responsible for amylose production (Tsai, 1974). Several plant species lacking GBSS produce starch containing only amylopectin (known as waxy starch) (Denyer et al., 2001; Szydlowski et al., 2011). Cereals and eudicots have two isoforms of GBSS, GBSSI and GBSSII. While GBSSI expression is likely to be confined in storage tissues, GBSSII is mainly localized in the chloroplast (Cheng et al., 2012). GBSSs have a high affinity for starch granule and act in a processive manner, extending the same primer glucan to produce relatively long amylose molecules, but with the possibility to operate also on side chains of amylopectin (Zeeman et al., 2010). For these properties GBSS remains sheathed within the granule as amylopectin crystallises. Then, the newly synthesized amylose is not accessible for further modification and remains mostly linear (Streb and Zeeman, 2012). Even if starch granule consists up to about 30% of its weight of amylose, this is not required for granule crystallinity. However, amylose synthesis may be important for starch density, improving the efficiency of carbon storage, thus justifying the conservation of GBSS in higher plants (Zeeman et al., 2010). The four starch synthases (SS1-4) are prevalently situated in the stroma and are involved in the elongation of amylopectin chains (Streb and Zeeman, 2012). From the analyses of Arabidopsis mutants and other plant species, it has emerged that they act preferentially on different length chains. SS1 preferentially elongates chains of 9-10 glucose units (Delvallé et al., 2005; Fujita et al., 2006), SS2 chains of 13-22 glucose units (Craig et al., 1998; Morell et al., 2003), whereas SS3 act on chains longer than 25 glucose units (Zhang et al., 2005). In this way, SS1 produces the substrate for SS2 and SS2 for SS3. Studies performed on single and multiple SS mutants shown that plants can still synthetize starch, although with different distribution in chains length compared to wild-type, indicating that SSs have overlapping functions and that they can, in combination with other enzymes (i.e. branching enzymes), generate all the different-length chains (for an overview see Santelia and Zeeman, 2011). The *ss3ss4* double mutant seems to be the only exception because of its inability to initiate granules (Szydlowski et al., 2009). A recent study on Arabidopsis *ss4* mutant revealed that SS4 is essential to coordinate the granule formation during chloroplasts division in leaf

expansion and to determine the abundance and the flattened, discoid shape of leaf starch granules (Crumpton-Taylor et al., 2012).

Amylopectin is a highly branched molecule. Indeed, as soon as the linear chains reach a sufficient length (12 glucose units), two classes of starch branching enzymes (SBE 1 and 2, or B and A; Burton et al., 1995) introduce branching points. SBEs are glucanotransferases that can cut an existing α-1,4-linked chain and transfer this segment (with a minimum length of 6 glucose units) to another linear chain, creating a new α-1,6 linkage (Takaha et al., 1993). Studies on cereals and potato genes suggest that SB1 and SB2 differ in the length of the transferred chains, with SBE1 preferring longer chains than SBE2 (Takaha et al., 1993; Guan et al., 1997; Morell et al., 1997; Rydberg et al., 2001; Nakamura et al., 2010). In Arabidopsis, the situation is out of the ordinary because there are only members of SBE2 subclass (BE2 and BE3) and the lack of only one of the two SBE2 enzymes does not affect starch structure, suggesting functional redundancy. There is also a third gene related to the SBE1 subclass (BE1), but it is not likely to encode for a functional BE (Dumez et al., 2006; Wang et al., 2010). Mutant analyses in potato, maize, and rice suggest that the loss of subclass I of SBEs, leads only to minor alterations in starch structure compared to the wild-type plants. Conversely, the absence of SBE2 subfamily, brings to altered starch content, structure and properties (i.e. longer chains and less branches), indicating that SBE2 can compensate for the loss of SBE1, but not vice-versa (Safford et al., 1998; Blauth et al., 2001; Blauth et al., 2002; Satoh et al., 2003; Stinard et al., 1993; Mizuno et al., 1993). Potato plants in which both SBE1 and 2 are repressed show severe reduced levels of starch, prevalently composed by amylose (Schwall et al., 2000).

Initially it was thought that SSs and BEs were sufficient for amylopectin synthesis and starch granule formation (Zeeman et al, 2007b). Subsequently emerged that two types of starch debranching enzymes (DBEs), designated as isoamylases (ISA) and limit-dextrinases (LDA, also named pullulanase or R-enzyme), were involved in this process, overcoming the idea of their mere participation in starch degradation (Streb and Zeeman, 2012). Mutants depleted of particular classes of DBEs show a partial or complete replacement of starch with phytoglycogen (James et al., 1995; Burton et al., 2002; Delatte et al., 2005; Wattebled et al., 2005; Mouille et al., 1996), a very highly branched and water-soluble polysaccharide, with a high proportion of glucose short chains and a different distance between branching points in comparison to amylopectin (Ball et al., 1996). As suggested

by its name, phytoglycogen is rather similar to glycogen, a soluble polyglucan accumulated as storage compound in animals, fungi and bacteria (Ball et al., 1996). Different models have been proposed to explain the accumulation of phytoglycogen in the absence of DBEs. Currently the prevailing model suggests that during starch biosynthesis, DBEs selectively trim misplaced branches introduced by BEs, allowing the self-organization of amylopectin into the crystalline layers of starch granule (Ball et al., 1996; Myers et al., 2000; Streb et al., 2008).

ISAs can in turn be divided in three subgroups (ISA1-3) (Hussain et al., 2003). Whereas mutations in ISA1 in cereals and in ISA1 or ISA2 in potato and Arabidopsis result in the production of phytoglycogen, mutations in genes encoding for LDA and ISA3 do not, suggesting a role of the latter enzymes in starch degradation rather than in synthesis (Streb and Zeeman, 2012). In Arabidopsis, potato and rice ISA1 and ISA2 form a heteromultimer (Bustos et al., 2004; Delatte et al., 2005; Utsumi and Nakamura, 2006; Utsumi et al., 2011), while in cereal endosperm the biosynthetic activity of DBEs is given by homomultimeric protein containing only ISA1 subunits (Kubo et al., 2010). Interestingly, ISA2 is catalytically inactive and it has been suggested to have a regulatory function, probably conferring substrate specificity to the catalytically active ISA1 subunit (Kubo et al., 2010; Utsumi et al., 2011). Despite their important role in amylopectin synthesis, the relative contribution of DBEs is still puzzling, presumably because of their redundancy. There are variations in the severity of the phytoglycogen-accumulation in ISA1-deficient plants, within the same plant and between different plant species (Delatte et al., 2005, Mouille et al., 1996; Dauvillée et al., 2001; Burton et al., 2002; Posewitz et al., 2004). In fact, in plants lacking ISA1, starch is still synthesized, albeit with an altered structure, outside of the leaf mesophyll, for example in epidermal cells. Moreover, the entire complement of starch-synthesizing enzymes in the cell can influence the *isa1* phenotype, since double mutant plants lacking ISA1 and other SSs or BEs, make less phytoglycogen compared with starch granules. The Arabidopsis quadruple mutant *isa1isa2isa3lda* does not have starch granules at all, pointing toward the idea that DBEs activity is essential for starch granule synthesis (Wattebled et al., 2008; Streb et al., 2008). However, a more careful analysis overturns this view due to the fact that the loss of starch is the result of the action of starch degrading enzyme (such as α- and β-amylases, see sections “Degradation of storage starch” and “Degradation of transitory starch”) on

branched glucans (Streb et al., 2008). Indeed, DBEs-free mutants accumulate phytoglycogen, small-branched malto-oligo saccharides and maltose, the latest of which are produced by β- and α-amylase (Streb et al., 2008). This is also consistent with the evidence that starch granule production is partially restored in DBEs-free mutants that additionally lack AMY3 (an α-amylase able to hydrolyse α-1,4-glucosidic linkages) (Streb et al., 2008; Streb et al., 2012).

All these results highlight the fact that such a complex granule structure is the outcome of the synergistic action of both biosynthetic and degradative enzymes, and that all these processes are interconnected. Therefore, the removal of branch points by ISA1 during starch synthesis enhances amylopectin crystallization. This crystallization itself can make starch inaccessible to other interfering enzymes and can prevent starch degradation, that otherwise would result in the futile cycling of sugars into and out of starch. According to this hypothesis, α-amylases usually does not influence starch biosynthesis.

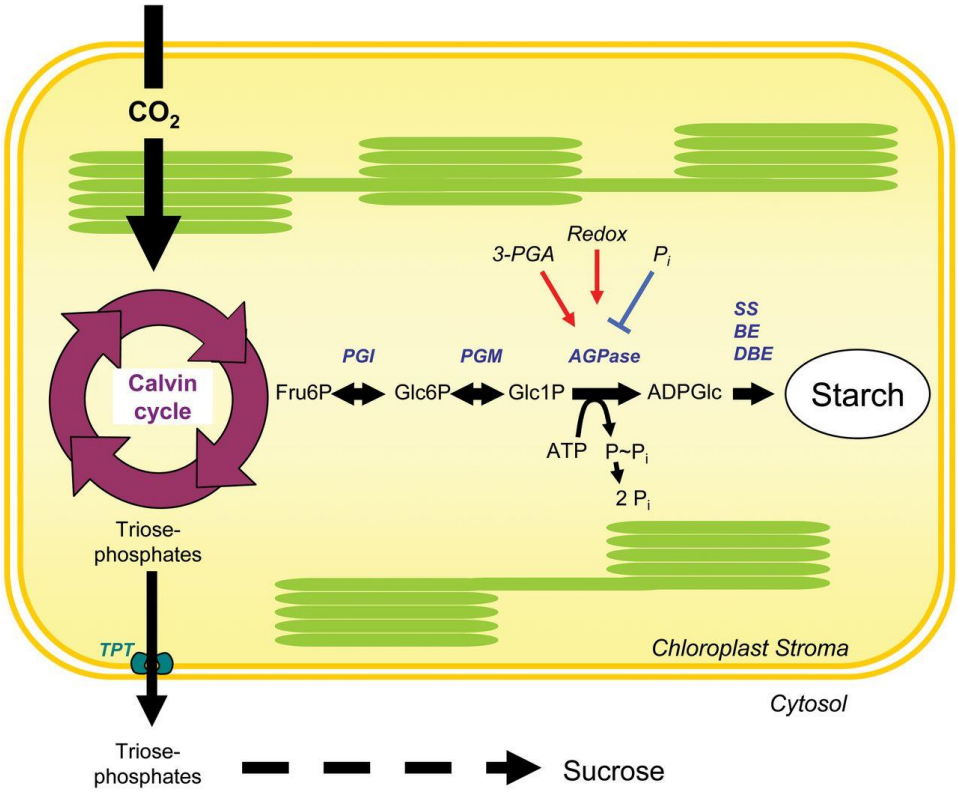

Figure 4. Pathway of starch synthesis in chloroplasts (Zeeman et al., 2007). Carbon is assimilated via the Calvin cycle. Part of the carbon give triose-phosphates that are exported to the cytosol for sucrose synthesis, whereas another part is retained in the chloroplast for starch synthesis. The limiting step of starch biosynthesis, AGPase activity, is controlled by allosteric and redox regulation and the reaction is pushed

toward the formation of ADPGlc by PPi degradation. Then, ADPGlc is the substrate for starch synthases (SSs). The complex structure of starch is given by the simultaneous action of SSs, BEs and DBEs. Fru6P, fructose-6-phosphate; Glc1P, glucose-1-phosphate; Glc6P, glucose-6-phosphate; TPT, triose-phosphate/phosphate translocator.

Degradation of storage starch

In cereals storage starch degradation has been well characterized. Cereal grains consist of a seed coat (also named testa) surrounding both endosperm and embryo (Fig. 5). In mature seeds, the endosperm (the largest organ in the seed and the major site of storage) is a dead tissue without cellular integrity and composed by cell walls, starch granules and proteins surrounded by a single layer of living cells, the aleurone layer (Fig. 5) (Emes et al, 2003). The embryo is formed by an embryonic root, a hypocotyl, a single cotyledon and the scutellum. Scutellum, that is composed by embryo living cells and is adjacent to the endosperm, can capture the final product of starch degradation, generally glucose, originating from the endosperm (Emes et al., 2003; Zeeman et al., 2010).

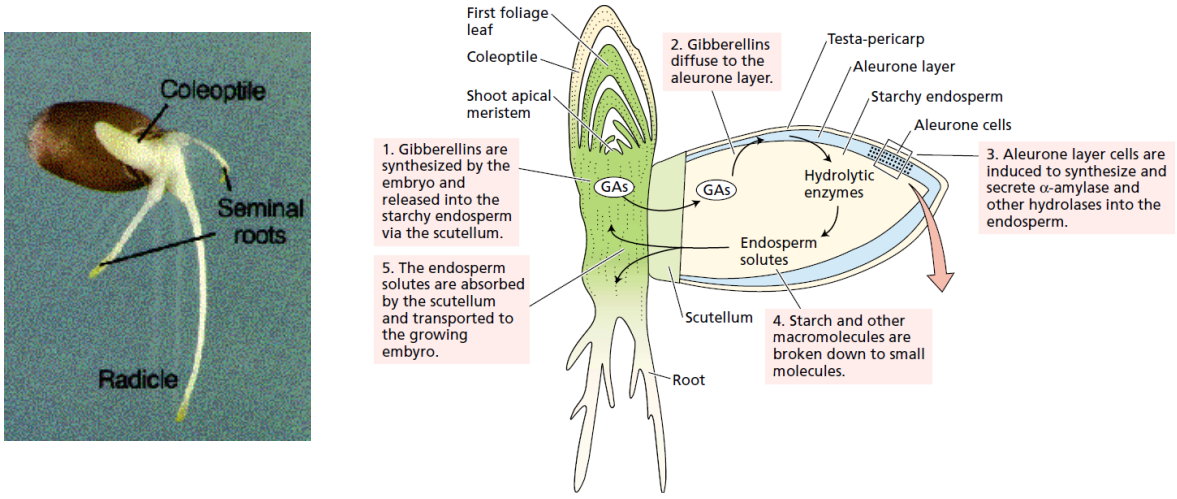

Figure 5. Seed germination. Left panel, developing seed morphology (http://corn.agronomy.wisc.edu/Crops/Wheat). Right panel, barley seed structure during germination and key biochemical steps of endosperm degradation (adapted from Taiz and Zeiger, Plant physiology, Fifth edition).

Several studies confirmed the involvement of four enzymes in endosperm starch degradation: α-amylases, β-amylases, DBEs (specifically LDA) and α-glucosidases (Tab. 1) (Kristensen et al., 1999; Mikami et al., 1999; Frandsen et al., 2000; Bozonnet et al., 2007). Alfa- and β-amylases are respectively endo- and exo-amylolitic enzymes. Both can

specifically hydrolyze α-1,4 glucose likages. Alfa-amylases can act randomly on soluble starch or amylose to produce a mixture of soluble linear and branched oligosaccharides (dextrins), whereas β-amylases can only cleave the non-reducing end of linear polyglucan chains, giving maltose as final product (Zeeman et al., 2010). Unlike α-amylases, β-amylases cannot overcome α-1,6 glucose linkages. Alfa-glucosidases (or maltases) can degrade maltose and malto-oligosaccharides, producing glucose (Sun and Henson, 1990). As mentioned above (see section "Starch biosynthetic enzyme"), DBEs are debranching enzymes able to cleave α-1,6 linkages (Delatte et al., 2006).

Enzyme	Activity	Substrate	Products	Cleaved bond
α-amylase	Endo-amylase	Branched and linear glucans	Linear and branched oligosaccharides	α-1,4
β-amylase	Exo-amylase	Linear glucans	Maltose	α-1,4
Limit dextrinase	Debranching-enzyme	Small branched oligosaccharides	Linear dextrins	α-1,6
α-glucosidases	Exo-hydrolase	Maltose or linear and branched oligosaccharides	Glucose	α-1,4 and α-1,6

Table 1. Storage starch degrading enzymes. The first attack on starch granules is accomplished by α-amylases. Alfa-amylases start to randomly cleave internal α-1,4 bonds of amylose and amylopectin, giving linear and branched oligosaccharides (or dextrins), that are further degraded by β-amyases, only able to cleave α-1,4 glucosidic bonds from the non-reducing end of glucan-chains, but not to overcome α-1,6 linkages. Beta-amylases release maltose and leave intact small branched glucans (limit dextrins). The α-1,6 bonds in branched limit dextrins are cleaved by limit-dextrinases (LDA), that release linear small oligosaccharides. Finally α-glucosidases, exo-hydrolysing enzymes able to cleave α-1,4 glucosidic bond from the non-reducing end of oligosaccharide chains, can act on both branched and linear small oligosaccharides as on maltose and maltotriose, producing glucose.

Even if these enzymes are well biochemically characterized, little is known about their relative contribution in storage starch breakdown. In cereal endosperm it is widely accepted that α-amylases are the major player in storage starch degradation (Fincher et al., 1989; Ritchie et al., 2000). In response to hormonal stimuli, α-amylases are synthesized in aleurone and scutellum and are released in the endosperm, where they can initiate the attack of starch granule surface, probably at specific sites known as pores (Fincher et al., 1989; Ritchie et al., 2000; Zeeman et al., 2010). Subsequently, α-glucosidases come into

play. It has been proven that α-glucosidases act synergistically with α-amylases to remove glucose directly from starch granule surface (Sun and Henson, 1991; Stanley et al., 2011). In some cereal species (i.e. barley) β-amylases are accumulated in an inactive form in the endosperm and only during germination they are activated by proteolytic digestion triggered by aleurone cells (Sopanen and Laurière, 1989; Smith et al., 2005; Zeeman et al., 2010).

Differently from cereal endosperm, for other storage organs the situation is much less clear. For example, during potato sprouting, starch degradation occurs in the tuber without an increase in starch degrading amylolitic or phosphotolytic enzymes (Davies and Ross, 1984; Davies and Ross, 1987; Davies, 1990), while during cold-sweetening the activity of a specific isoform of β-amylase increase, although its contribution in starch degradation is unknown (Deiting et al., 1998; Nielsen et al., 1997). A further suggestion of several initiation mechanisms comes from the different morphology of the starch granules surface (Fig. 6). Indeed, starch degradation in cereals begins from the pitting on the starch surface, while none or few pores are present on potato starch (Fig. 6).

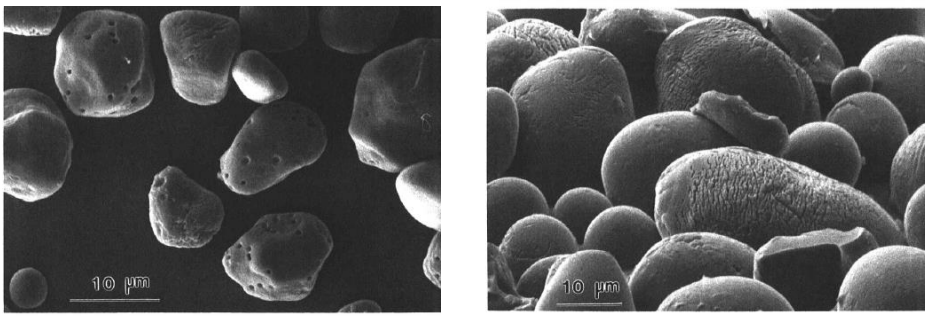

Figure 6. Enzyme treated starch granules. Common corn starch granules (left panel) and potato starch granules (right panel), treated with amyloglucosidase (from Fannon et al., 1992). The enzyme attacks corn starch granules in surface patterns resembling those of normal pores distribution, thus indicating that pores might be areas of lesser molecular association and major susceptibility. The same enzyme do not produce recognizable patterns when degrading root or tuber starches (i.e. potato) and no pores are present on the granule surface.

In storage organs other than cereal endosperm, starch is extensively phosphorylated, implying a possible role of the enzymes for transient glucan phosphorylation (see "Degradation of transitory starch), (phospho)glucan, water dikinases (GWDs and PWD) and glucan phosphatases, in controlling degradation. In potato, mung bean seeds and

Curcurma zeadoaria, starch phosphate levels are higher than that found in Arabidopsis leaf starch and GWD homologues occur in a wide range of species, indicating that the enzyme may be ubiquitous in higher plants (Blennow et al., 2000a; Blennow et al., 2002; Ritte et al., 2002). For potato tubers, there are indirect evidences that GWD is required for normal rates of starch degradation. In fact, transgenic potatoes with greatly reduced levels of GWD had very low levels of phosphate in tuber starch and were less prone to starch loss and sugar accumulation when stored at low temperatures (cold-induced sweetening, see below) implying that mobilization of starch was impaired in these conditions (Lorberth et al., 1998). In contrast, even if the genes encoding for starch phosphorylation are conserved in cereals, the starch of most cereal endosperms contains almost undetectably low levels of phosphate. It is doubtful whether GWD plays a role in degradation in these organs (Blennow et al., 2000a; Blennow et al., 2002).

Degradation of transitory starch

During the day, sucrose and starch are produced simultaneously as result of photosynthetic carbon assimilation. The ratio between sucrose and starch synthesis depends on plant species and environmental conditions (Upmeyer and Koller, 1973; Stitt et al., 1983; Fondy et al., 1989; Zeeman and ap Rees, 1999). Most of the current knowledge on leaf starch degradation derives from the model plant *Arabidopsis thaliana*, which typically allocates about the 50% of the newly fixed carbon into starch (Zeeman and ap Rees, 1999). Furthermore, Arabidopsis is a skilful model organism for the study of leaf starch metabolism due to the availability of a fully sequenced genome and to public facilities, such as databanks of mutated seeds that enable to get specific knockout (KO) mutants. It was through an exhaustive analysis of several KO mutants impaired in starch degrading enzymes that about 10 years ago primary starch degradation pathway was discovered (Caspar et al., 1991; Lorberth et al., 1998; Yu et al., 2001; Critchley et al., 2001; Scheidig et al., 2002; Niittyla et al., 2004; Chia et al., 2004; Lu and Sharkey, 2004; Kötting et al., 2005; Baunsgaard et al., 2005; Kaplan and Guy, 2005; Delatte et al., 2006; Zeeman et al., 2007; Kötting et al., 2009). Mutants impaired in key enzymes are characterized by a *starch excess* (*sex*) phenotype (Fig. 7), featured by a high amount of primary starch even after a prolonged period of dark (Zeeman et al., 1998). In particular, the analysis of a peculiar class of Arabidopsis mutants, named *sex1*, led to the identification of the

(phospho)glucan, water dikinase gene family, composed by three genes coding for the three proteins glucan, water dikinase 1 and 2 (GWD1 and 2) and phosphoglucan, water dikinase (PWD) (Fig. 7) (Ritte et al., 2002; Baunsgaard et al., 2005; Kötting et al., 2005; Glaring et al., 2007).

At the beginning, studies performed on potato plants showed that the lack of a starch bound protein of unknown function, originally named R1, caused starch accumulation in leaves and reduced levels of sweetening in cold-stored tubers, indicating low rates of starch degradation (Lorberth et al., 1998). In the same mutant, the amylopectin component of both leaf and tuber starch showed a decrease in the covalently bound phosphate groups (Lorberth et al., 1998). Around the same period, Yu group's discovered an Arabidopsis mutant with high starch content in seeds, flowers and root tips, and completely unable to degrade leaf starch (Caspar et al.,1991; Trethewey and ap Rees, 1994; Yu et al., 2001). As for potato R1, also in Arabidopsis mutant the amylopectin component was free of phosphate groups (Yu et al., 2001) and further studies led to the identification of GWD1 as the enzyme responsible of the phosphorylation in C-6 position of glucose units belonging to amylopectin chains (Ritte et al., 2002; Mikkelsen et al., 2004). Unlike GWD, PWD phosphorylates pre-phosphorylated glucan chains in C-3 (Baunsgaard et al., 2005; Kötting et al, 2005; Ritte et al., 2006). As a consequence, the activity of PWD is strictly dependent by the previous action of GWD and lack of PWD brings to a less severe *sex* phenotype (Zeeman et al., 2007). Amylopectin phosphorylation mediated by GWD and PWD is required in transitory starch breakdown in both photosynthetic and non-photosynthetic tissues (Fig. 8) (Lorberth et al., 1998; Yu et al., 2001), mainly because phosphate groups positively affect the hydrophilicity of amylopectin, speeding up its subsequent hydrolysis (Blennow et al., 2000a; Blennow et al., 2000b; Blennow et al., 2002).

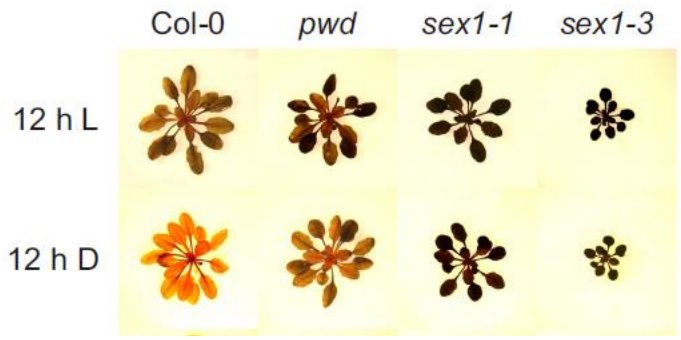

Figure 7. Comparison of wild-type, *pwd* mutant and *sex1* mutants (from Kötting et al., 2005). Plants were grown in a 12 h light (approximately 100 µmol quanta $m^{-2}s^{-1}$)/12 h dark cycle. Plants were harvested at the end of the light period (12 h L) and at the end of the dark period (12 h D), and chlorophyll was extracted in 80% ethanol. Starch was visualized by iodine staining. The sex1-3mutant is a GWD knock-out, sex1-1 contains a mutated form of GWD and approximately 20-30% of starch phosphate compared with wild-type (Yu et al., 2001). *sex1* plants show high starch content even after the period of dark, whereas *pwd* plants show a milder phenotype. Moreover, *sex1-3* showed reduced growth.

Since in cereal endosperm α-amylases can attack the surface of insoluble starch grains, releasing soluble and ramified glucans that facilitate the action of other degrading enzymes (Beck and Ziegler, 1989; Sun and Henson, 1990), the role of the three chloroplast target α-amylases (AMY1, AMY2, AMY3) coded by Arabidopsis genome, was investigated (Stanley et al., 2002; Yu et al., 2005). Differently from cereal endosperm, plants lacking of AMY1, AMY2 or AMY3 as well as the triple mutant *amy1amy2amy3*, showed a normal starch degradation rate at night, suggesting that α-amylases were not relevant for transitory starch breakdown in Arabidopsis (Yu et al., 2005). Similarly, α-glucan phosphorylases do not appear to take part in this metabolism (Zeeman et al., 2004). Further studies on Arabidopsis and potato transitory starch revealed a progressive degradation of the granule by exo-amylolysis and debranching enzymes. The loss of β-amylase 3 (BAM3) in Arabidopsis or of its homologous PCT BMY1 in potato (Beck and Ziegler, 1989; Lao et al., 1999; Scheidig et al., 2002; Kaplan and Guy, 2005; Fulton et al., 2008), as well as the loss of ISA3 (both in Arabidopsis and potato) led to a reduced rate of starch breakdown and to the onset of a *sex* phenotype, suggesting their involvement (Wattebled et al., 2005). In support to this hypothesis, it was observed that *in vitro* starch granules degradation mediated by β-amylases was enhanced in the presence of GWDs, and that in turn β-amylolysis caused an increased incorporation of phosphate by GWDs

(Edner et al., 2007). The interplay among BAM3, ISA3 and GWD was also confirmed by the observation that both BAM3 and ISA3 recombinant proteins have small activity on intact starch granules, and a much greater activity on soluble starch, according to the idea that they might require a previous phosphorylation of the substrate catalysed by GWD (Edner et al., 2007; Kötting et al., 2009). Finally, with the aid of ISA3-GFP construct it was demonstrated that ISA3 preferentially localizes at the starch granule surface, in agreement with its role (Delatte et al., 2006). Currently the proposed model (Fig. 8) suggests that BAM3 acts on the outer chains of the branched glucan, and since it is not possible for the enzyme to overcome the branched points, it produces on the grain a surface of short chains, on which it is not anymore able to act. The short chains could be removed by ISA3, uncovering other longer chains that become substrates for BAM3 (Delatte et al., 2006; Streb and Zeeman, 2012). Since mutations affecting BAM3 and ISA3 genes do not completely abolish starch breakdown, the involvement or the partial compensation of other enzymes has been hypothesized (Delatte et al., 2006). In fact, whereas in Arabidopsis plants lacking LDA there was no detectable phenotypic trait, plants in which ISA3 and LDA were simultaneously loss, starch breakdown was further compromised in respect to the *isa3* single mutant, indicating that when ISA3 is missing LDA carries out a compensatory function (Delatte et al., 2006). Due to the inability of β-amylases to work in proximity of phosphate groups (Takeda and Hizukuri, 1981), the proposed model seemed uncertain until the discovery in Arabidopsis plants of two phosphoglucan phosphatases. Starch Excess 4 (SEX4) and Like Sex Four 2 (LSF2) (Fig. 8) are two chloroplast enzymes able to dephosphorylate amylopectin (Gentry et al., 2007; Kötting et al, 2009; Santelia et al., 2011) in C-3 and C-6 position and in C3 position only, respectively (Hejazi et al., 2010; Santelia et al., 2011). As for ISA3 and LDA, the double mutant *sex4lsf2* displayed a more severe *sex* phenotype compared to single mutants (Santelia et al., 2011; Streb and Zeeman, 2012), and evidence of phosphorylation/dephosphorylation cycles derives from *in vitro* experiments where the addition of SEX4 enhanced the release of soluble glucans from the granules in the presence of GWD1 and hydrolytic enzymes (Kötting et al, 2009). Moreover, SEX4 acts preferentially on insoluble granules rather than on phospho-oligosaccharides, confirming that phosphorylation and dephosphorylation can occur concurrently on the granule surface (Kötting et al, 2009; Streb and Zeeman, 2012).

The end products of such a model are maltose, maltotriose and small oligosaccharides, made by debranching enzymes (Fig. 8). Disproportionating enzymes (DPEs) metabolize maltotriose (Lloyd et al., 2005) transferring an oligosaccharide unit to the C-4 position of an acceptor sugar, releasing glucose and a longer glucan chain (Jones and Whelan, 1969; Llooyd et al., 2005). Two isoforms of DPEs (Fig. 8) are present in Arabidopsis, namely DPE1 and DPE2. DPE2 is localized in the cytosol and it is not involved primary starch breakdown (Chia et al., 2004; Lu and Sharkey, 2004). Instead, DPE1 is chloroplast-targeted and is important for normal starch degradation, given that its absence causes accumulation of starch and malto-oligosaccharides (Critchley et al., 2001). Albeit at different extent, the final products of primary starch degradation are maltose and glucose (Streb and Zeeman, 2012), both exported to the cytoplasm through specific membrane transporters according to their concentration gradients (Fig. 8) (Weber et al., 2000; Niittylä et al., 2004). Maltose transporter is called MEX1 (Niittylä et al., 2004) and mutations in its locus give rise to the characteristic *sex* phenotype, corroborating the idea that maltose is the main product of transitory starch degradation at night (Niittylä et al., 2004), while two glucose transporters (GLT and GT) are responsible for glucose export and none relevant phenotypic traits were observed when mutated (Cho et al., 2011; Flügge et al., 2011).

Once in the cytosol, maltose is metabolised to glucose by DPE2 (Chia et al., 2004; Lu and Sharkey, 2004; Lu et al., 2006). Then, glucose is converted to hexose phosphates through the action of hexokinase (HKN) (Fig. 8). The fate of the second glucosidic portion of maltose, resulting from hydrolysis by DPE2, is not well understood. However, some studies suggest that it might be transferred to a cytosolic carbohydrate, such as a specific soluble arabinogalactan, found in leaves of many plant species (Fettke et al., 2005; Fettke et al., 2006; Lu et al., 2006).

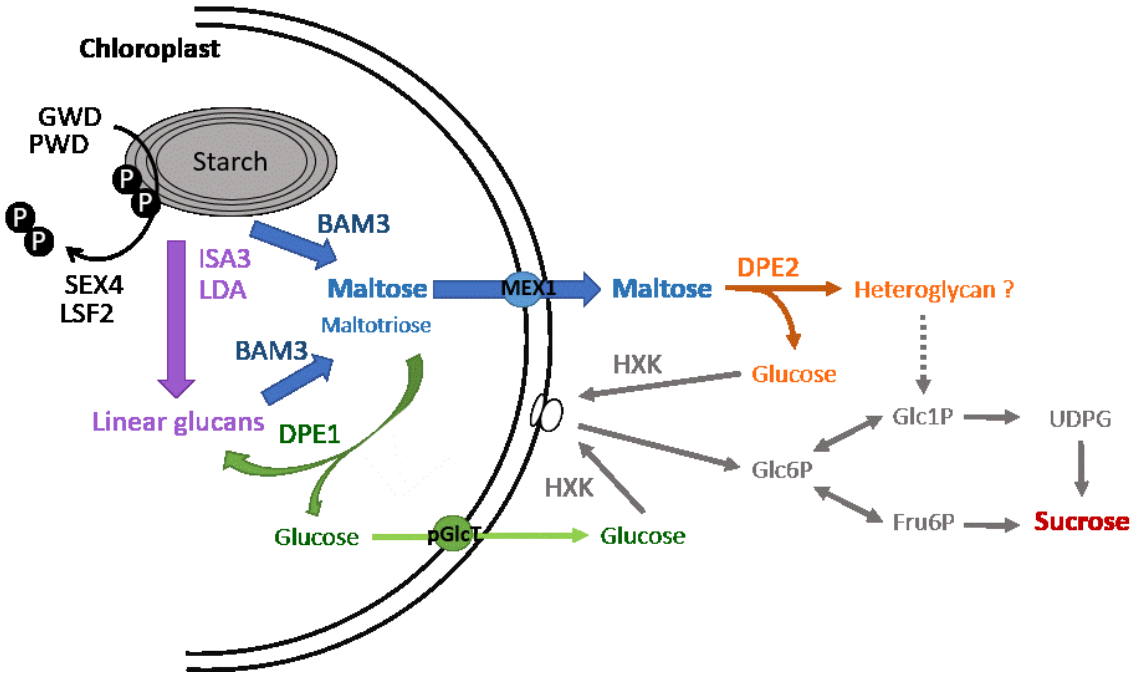

Figure 8. Pathway of hydrolytic leaf starch degradation, adapted from Weise et al., 2006. The products of the hydrolytic pathway are maltose and glucose, which are exported to the cytosol to make sucrose. Hatched arrows indicate steps that are currently uncertain. pGlcT, glucose transporter (GLT or GT).

Hints on starch metabolism regulation

As we have seen from the previous paragraphs, starch metabolism in higher plants requires the concerted and controlled action of a plethora of enzymes (Fig. 9). The large number of enzymes and reactions form a complex network that must be adjusted to meet the metabolic needs of the plant (Fig. 9, for an overview of regulation of starch metabolism in Arabidopsis chloroplasts).

Firstly, different protein isoforms are involved in the process and may have slightly different role depending on plant tissue, developmental stage, and conditions sensed by the plant, within the same plant species but also between different plant species. In Arabidopsis leaves carbon is partitioned into starch during the day at a linear rate. Starch degradation, that mainly provides carbon for respiration, follows a near-linear rate and starch is almost but not completely exhausted at dawn (Geiger and Servaites, 1994; Graf et al., 2010; Stitt and Zeeman, 2012). This allows to invest newly fixed carbon into growth, minimizing the risk of starvation at the end of the night (Rasse and Tocquin, 2006; Graf et al., 2010; Stitt and Zeeman, 2012).

Carbon partitioning is affected by developmental and source/sink relationship, by environmental factors such as light intensities, CO_2 concentrations and photoperiod. When carbon is poorly available (e.g. short days, low light), a larger proportion of the photosynthates is accumulated as starch in the light and the rate of starch degradation is decreased during the subsequent night (Chatterton and Silvius, 1979, 1980; Smith and Stitt, 2007; Stitt et al., 2007). It was recently shown that starch degradation is adjusted almost immediately to respond to the rapid changes in the light regime (Lu et al., 2005; Graf et al., 2010) and temperature (Pyl et al., 2012) and that the circadian clock regulates starch breakdown (Graf et al., 2010), although the underlying mechanism is still unknown (Graf and Smith, 2011; Scialdone et al., 2013). It was reported that the transcriptional levels of many enzymes involved in starch degradation show a diurnal pattern of expression in leaves and that the expression of some of them was under the light-dependent circadian control (Lu et al., 2005). However, when protein levels have been analysed, they did not change at the same extent, suggesting that additional post-translational regulatory mechanisms may occur (Yu et al., 2001; Ritte et al., 2003; Kötting et al., 2005; Skeffington et al., 2014). Indeed, the activity of several starch metabolising enzymes has been demonstrated to be affected by reducing or oxidising conditions, indicating that it can be regulated by the redox potential of the stroma (Glaring et al., 2012).

AGPase, the first enzyme of the biosynthetic pathway, has been object of several studies and its redox regulation has been treated in the previous paragraph (see Section "Mechanisms of AGPase regulation"). In addition to AGPase, other enzymes involved in starch metabolism have been reported to be affected by redox regulation (Fig. 9). Among them, GWD and SEX4 proteins, both required in the first steps of transitory starch degradation, are activated by reducing conditions (see below for more details) (Sokolov et al., 2006; Silver et al., 2013), as well as BAM1 and AMY3, two enzymes mainly involved in starch degradation under stress condition and in guard cells, known to be active when reduced and inactive when oxidized (Sparla et al., 2006; Seung et al., 2013). The redox regulation of GWD and SEX4 is somehow counter-intuitive, because during the day when photosynthetic process is active, the chloroplast stroma represents a reducing environment (Schürmann and Buchanan, 2008). As a consequence, GWD and SEX4 would be more active during starch synthesis rather than during starch degradation. However,

starch phosphorylation commonly occurs during starch degradation and SEX4 is more active in the dark (Kötting et al., 2009). For BAM1 and AMY3 it has been suggested that they may have different roles in different tissues or under specific growth conditions. Indeed, BAM1 was suggested to be involved in stress tolerance, namely in diurnal starch degradation in mesophyll cells under osmotic stress conditions (Valerio et al., 2011; Zanella et al., 2016), as well as in guard cells under drought stress (Prasch et al., 2015). Moreover, BAM1 and AMY3 seem also to have a role in physiological diurnal starch degradation in guard cells (Valerio et al., 2011; Horrer et al., 2016).

Further regulatory mechanisms, including protein phosphorylation and supramolecular complexes formation (Fig. 9), are suggested to be involved in starch metabolism (Kötting et al., 2010). Phosphorylation is a common post-translational modification able to control protein function. Many Arabidopsis proteins have been identified by large-scale phosphoproteomic approaches, as phosphorylated *in vivo* (Fig. 9). Some of them are involved in starch metabolism, i.e. PGI, PGM1, AGPase, SS3, GWD1 and GWD2, DPE2, AMY3, BAM1 and BAM3, LDA, pGlcT and MEX1 (see Kötting et al., 2010), however the specific effect of the phosphorylation is poorly known.

Multi-enzyme complexes, containing different SSs and BEs isoforms, have been identified in wheat and maize endosperm, during grain filling (Tetlow et al., 2004; Hennen-Bierwagen et al., 2008; Tetlow et al., 2008; Hennen-Bierwagen et al., 2009). Since some of the enzymes forming the complexes have been demonstrated to be phosphorylated (Tetlow et al., 2004; Tetlow et al., 2008; Hennen-Bierwagen et al., 2009), complex formation has been proposed to be dependent on protein phosphorylation. Dephosphorylation of complex components by the addition of alkaline phosphatase resulted in subunit disassociation. Although, protein kinases and phosphatases determining the phosphorylation status of enzymes that form the complexes remain to be identified. It is also unknown if the formation of such complexes is functionally significant. It is plausible that different combinations of physically associated enzymes could produce specific structures within the starch granule that would not be produced by the free, soluble enzymes (Kötting et al., 2010).

In Arabidopsis, such protein complexes have never been identified. However, it was suggested (Sehnke et al., 2001) that 14-3-3 proteins, which can bind phosphorylated proteins mediating protein-protein interaction (Fu et al. 2000; Huber, 2007), could have a

role in starch metabolism regulation. Indeed, 14-3-3 proteins seem to associate with starch granules and the repression of plastid localized 14-3-3 isoforms changed starch properties and content in Arabidopsis leaves (Streb and Zeeman, 2012). In agreement with this hypothesis, in barley, among 14-3-3 proteins targets, several endosperm enzymes involved in starch metabolism have been identified, such as GBSSI, SSI, SSII, BEIIa, α- and β-amylases (Alexander and Morris, 2006)

In addition, other interesting chloroplast proteins may be involved in supramolecular complexes formation in Arabidopsis. Among them, a protein containing a carbohydrate binding module (CBM) and a coiled coil domain, by which it can interact with other starch related proteins, has been found. This protein lacks of any obvious enzymatic domain and could act as a scaffold to recruit other proteins on the starch granule (Lohmeier-Vogel et al., 2008).

LSF1 (Like SEX Four 1), likewise LSF2, is a homolog of SEX4. *lsf1* mutants have a *sex* phenotype, albeit milder than that of *sex4* (Comparot-Moss et al., 2010), suggesting that LSF1 is required for normal starch breakdown. However, the *lsf1* mutant leaf extracts misses any reduction in phosphoglucan phosphatase activity and *lsf1* mutant, unlike *sex4*, does not accumulate phospho-oligosaccharides. Indeed, LSF1 protein seems to lack any phosphoglucan phosphatase activity (Comparot-Moss et al., 2010). Consequently, LFS1 has been proposed to have a regulatory role (Streb and Zeeman, 2012). Interestingly, this protein has a CBM, allowing it to bind starch granules, but it also possess a putative PDZ-type protein-protein interaction domain. Recently it was discovered that LSF1 forms a stable complex together with the chloroplastic β-amylase BAM1, which may serve to target the β-amylase on the granule surface during starch degradation (Streb and Zeeman, 2012).

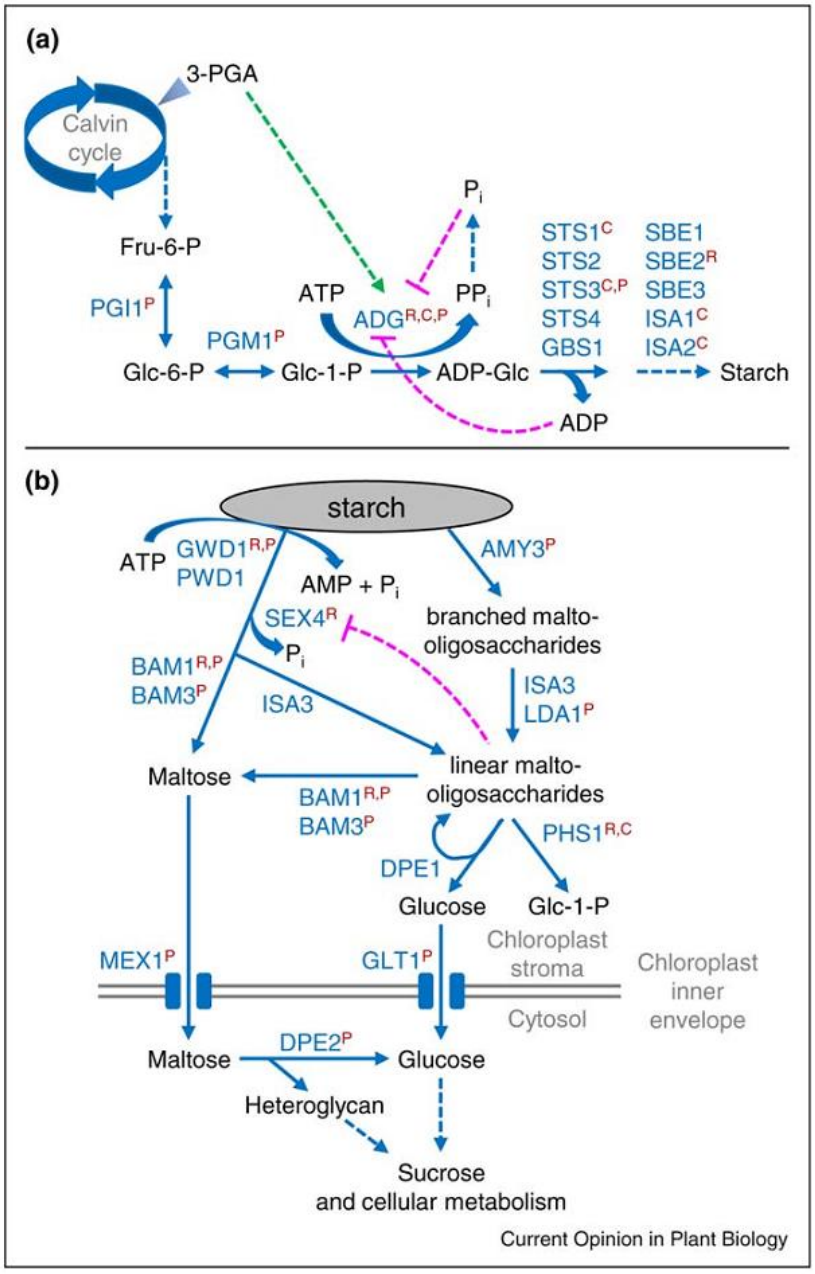

Figure 9. Model (Kotting et al., 2010) for the regulation of starch synthesis and degradation in Arabidopsis chloroplasts. In the box (a): synthesis. In the box (b): degradation. Potential regulatory mechanisms are highlighted with superscript red letters: R (redox), C (complex formation), P (protein phosphorylation). Regulation by metabolites: green dotted arrows (stimulation), magenta dotted lines (inhibition). Protein names are shown in blue, metabolites in black and cellular compartments and constituents in grey. ADG, AGPase; GLT, glucose transporter; MEX, maltose transporter; PGI, phosphoglucoisomerase; PGM, phosphoglucomutase; STS, starch synthase.

The transport of sugars through the plant

Between dicot and monocot leaves there are differences in the sucrose phloem loading pathway. Because Arabidopsis is a dicot Angiosperm, I will focus my attention only on dicots phloem loading.

Sucrose, resulting from photosynthetic carbon assimilation or from starch breakdown, is the primary transported sugar in most plants. From the mesophyll (M) cells, sucrose moves cell to cell, until arriving into bundle sheath (BS) cells, neighbouring the veins, and then into the vein for long distance transport out of leaf. In dicots, sucrose moves from smallest veins to larger veins, until reaching the midvein. Then, sucrose exits the leaf and moves into the stem vasculature. In each vein, there are two long distance transport tissues, xylem and phloem. Xylem transports water and minerals from the roots to the shoots and usually is situated in the inner part of the vein. Phloem usually carries sugars and other organic compounds from source (usually photosynthetic tissues) to sink organs (usually non-photosythetic tissues). Phloem is composed of three cell types:

- sieve elements (SEs) that conduct assimilates;
- companion cells (CCs) that genetically and metabolically support the SEs;
- the phloem parenchyma (PP) cells;

SEs are connected end-to-end longitudinally to form a sieve tube (ST), through which sucrose is transported (Evert, 1982). Phloem system can be also divided in three functional regions (van Bel, 1996):

- the collection phloem, located in the small veins of source leaves and responsible for sucrose entry into the vein (phloem loading);
- release phloem, located in the sink tissues and responsible for the exit of sucrose (phloem unloading) from the phloem into the surrounding tissues for utilization or storage;
- transport phloem, that connects collection and release phloem and represents the largest portion of the integrated phloem network in a plant (van Bel., 2003).

An hydrostatic pressure gradient between source and sink organs drive the flux of solutes through the STs (Lalonde et al., 2003; Patrick, 2013). This pressure is osmotically generated by sucrose. In source organs, sucrose enters into the collection phloem and increases the solute concentration. In response, water from the xylem flows into the STs

by osmosis, raising the pressure. In sink tissues, sucrose-unloading decreases the solute concentration in the STs and water diffuses out of them, lowering the pressure.

According to leaf anatomy, there are three possible pathways for phloem loading (van Bel, 1993; Rennie and Turgeon, 2009; Slewinski and Braun, 2010a):

- symplasmic loading (Fig. 10);
- apoplasmic loading (Fig. 10);
- polymer trapping loading;

The symplasmic phloem loading is also passive, because there is no need of energy input for sucrose to enter ST. In fact, the entire process, from M cells to ST, is driven only by diffusion down a concentration gradient. All the intervening cells are connected through plasmodesmata (PD), pores in the cell wall connecting the cytoplasm of adjacent cells, and their cytoplasm is joined into a single symplasm (Rennie and Turgeon, 2009; Slewinski and Braun, 2010).

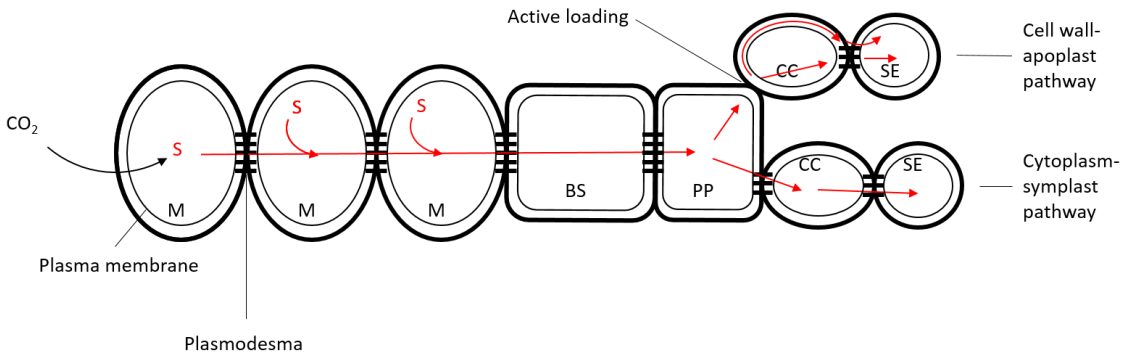

Figure 10. Schematic diagram of pathways of phloem loading in source leaves. In the totally symplastic pathway, sugars (S, red arrows) move from one cell to another in the plasmodesmata, all the way from the mesophyll (M) to the sieve elements (SE). In the partly apoplastic pathway, sugars enter the apoplast at some point. For simplicity, sugars are shown here entering the apoplast near the sieve element–companion cell complex, but they could also enter the apoplast earlier in the path and then move to the small veins. In any case, the sugars are actively loaded into the companion cells (CC) and sieve elements (SE) from the apoplast. Sugars loaded into the companion cells (CC) are thought to move through plasmodesmata into the sieve elements (SE). BS, bundle sheath. PP, phloem parenchyma.

For that reason, sucrose transporter proteins are not required to move sucrose across the plasma membrane in order to reach the collection phloem. However, also in symplasmic loading species, these transporters are still required for the recovery of sucrose leaking out along the transport phloem and are necessary to keep high the osmotic gradient (Minchin and Thorpe, 1987; Hafke et al., 2005; Bihmidine et al., 2013).

In the apoplasmic loading mechanism, sucrose move symplasmically through PD from M cells into the BS cell, and then into the PP cell (Russin et al., 1996; Haritatos et al., 2000; Ma et al., 2008). Then, sucrose takes the apoplasmic way, going in the extracellular space outside the symplasm, probably because of the paucity of PD connecting the CC-SE complex to the surrounding cells. Sucrose is exported by SWEET transporters into the BS-CC cell wall space or across the plasma membrane and is delivered in the apoplasm (Chen et al., 2012). Afterwards it is imported again into the plasma membrane of the CC-SE complex by sucrose trasporters (SUTs) and it moves again through PD into the ST for long distance transport to sink tissues (Slewinski et al., 2012; Baker et al., 2013). The importation of sucrose into the CC-SE complex requires energy because sucrose moves against its concentration gradient (Giaquinta et al., 1983). The lack of connectivity between STs and adjacent cells lead to achieve very high sucrose concentrations in STs, avoiding the backward spread of sugars via PD to reach an equilibrium (Rennie and Turgeon, 2009).

In polymer trapping phloem loading species, in addition to sucrose, other larger polymers are transported, such as raffinose and stachyose (Rennie and Turgeon, 2009). These molecules are synthesized in specialized CCs, called intermediate cells (ICs). Sucrose moves symplasmically from M to ICs, where it is converted into raffinose or stachyose, both too large to diffuse back, but still able to move via PD to the SE and to be transported long-distance in the ST sap.

The same plants can use different loading mechanism simultaneously, even within a single vein, or shift from one mechanism to another during development and/or in response to stress. However, a predominant phloem loading mechanism might be employed by a single plant species, and it could be used as a general reference mechanism for that species. For example, *Arabidopis thaliana* can be defined as an apoplasmic phloem loading species and this implies the presence of SWEETs and SUTs. In Arabidopsis SWEETs are encoded by a multi-gene family composed of 17 members (Chen et al., 2010). SWEETS

are a class of facilitate diffusers, with seven transmembrane domains, which can transport sugars across the plasma membrane down a concentration gradient (Chen et al., 2010). By subcellular localization studies eight of them have been demonstrated to be effectively plasma membrane proteins (Ge et al., 2000; Chu et al., 2006; Guan et al., 2008; Chen et al., 2010; Chen et al., 2012; Xuan et al., 2013). AtSWEET11 and AtSWEET12 are two closely related genes and are expressed in a subset of PP cells in Arabidopsis leaves (Chen et al., 2012). They were demonstrated to act as sucrose uniporters that reversibly transport sucrose (Chen et al., 2012). While the single mutants for *atsweet11* or *atsweet12* did not show a visible phenotype, the double mutants *atsweet11atsweet12* exhibited slower growth, mild leaf chlorosis and carbohydrate accumulation in leaves (Chen et al., 2012), suggesting a redundancy and confirming the importance of sucrose transport for the wellness of the entire plant.

SUTs possess 12 transmembrane domains and can form a pore that allows the transfer of sucrose through the plasma membrane (Lalonde et al., 2004; Sauer, 2007, Ayre, 2001; Geiger, 2011). SUTs function as sucrose/proton symporter that use the energy provided by the proton gradient generated across the membrane by H^+-ATPases to drive sucrose movement (Bush, 1990; Bush, 1993; Boorer et al., 1996; Zhou et al., 1997; Carpaneto et al., 2005; Gaxiola et al., 2007). Like SWEETs, SUTs are encoded by a multi-gene family (Aoki et al., 2003; Lalonde et al., 2004; Sauer, 2007; Braun and Slewinski, 2009; Doidy et al., 2012; Reinders et al., 2012) and they can be divided by phylogenetic analysis in multiple distinct clades (Aoki et al., 2003; Sauer, 2007; Braun and Slewinski, 2009; Reinders et al., 2012), confirmed by biochemical studies (Chandran et al., 2003; Carpaneto et al., 2005; Reinders et al., 2006, 2008, 2012). Apoplasmic phloem loading species, with mutations in phloem plasma-membrane SUT showed a stunted phenotype, chlorotic leaves with hyperaccumulation of starch and soluble sugars, altered biomass partitioning, and root growth and reproductive defects (Riesmeier et al., 1994; Bürkle et al., 1998; Gottwald et al., 2000; Hackel et al., 2006; Srivastava et al., 2008; Slewinski et al., 2009).

Once reached the sink tissues, sucrose and other organic compounds must be unloaded from the SE-CC complex. This can be done either symplasmically and/or apoplasmically into the surrounding cell wall matrix. Again, in the apoplasmic pathway, two classes of sugar transporters are involved in phloem unloading and post-phloem transport: sucrose effluxers that export sucrose in the apoplast and sucrose or hexose influxers that uptake

sugars in the sink cells, coupled with the H^+ gradient established through the activity of the plasma membrane H^+-ATPase. If sugars must be transported in the vacuole of the sink organ they must also cross the tonoplast. Since some transporters seem to be bidirectional, some of the transporters described for phloem loading could be involved in phloem unloading and the direction of the transport can depend upon the sucrose gradient, the pH and the membrane potential (Ayre, 2011). Sucrose can also be partially hydrolized in the apoplast, for example it can be converted by invertase (INV) in glucose and fructose, that can cross the membrane.

One of the major sink tissues in plant is developing seed. In Angiosperm seeds, the vascular bundles terminate in the maternal seed tissue, where the phloem unloading occurs and the filial tissues, namely the embryo and the endosperm, are isolated from the maternal tissue by an apoplasmic compartment (Stadler et al., 2005). Before and after crossing the apoplasmic compartment, the post-phloem sugar transport operates via a symplasmic pathway (Patrick, 1997). Hence, sugars must cross at least two plasma membranes during their movement from maternal to filial tissue (Weber et al., 2005), and this transition is accomplished by active transporters with an energy cost.

The plasticity of phloem unloading has been recently highlighted by the discovery of a dual switch in phloem unloading during ovule development in Arabidopsis (Werner et al., 2011). A symplasmic phloem pathway that drives sucrose into ovule primordia is shifted to an apoplasmic pathway when integuments are formed prior to flowering and is again switched to symplasmic unloading in the integuments following fertilization. The cause of the switch is unknown, but this developmental change in cellular route of assimilate transport resembles that in developing cotton fibres (Ruan et al., 2001; Ruan et al., 2004; Ruan et al., 2005). Overall, these observations suggest that symplasmic connectivity is highly regulated and varies not only between different sink types, but also between different developmental stages.

After phloem unloading, carbon can be used for different purposes: it can be accumulated in vacuoles as sucrose or exoses or in amyloplasts as starch or it can be used for respiration and growth. Sucrose can be either hydrolysed by INV into glucose and fructose, or degraded by sucrose synthase (Sus) into uridine-diphosphoglucose (UDP-Glc) and fructose. While both INV and Sus play an important signalling role in plant development (Ruan, 2012), INVs appear to play regulatory function in plant growth and development

(Ruan et al., 2009), whereas Sus is mainly involved in the biosynthesis of sugar polymers, including starch and cellulose, and in generation of energy (ATP) (Chourey et al., 1998; Coleman et al., 2009). In crop species, i.e. maize, mutation of one Sus, named SH1, disrupts endosperm cellularization, probably because of the reduction in the production of UDP-glucose required for cellulose biosynthesis, leading to a shrunken seed phenotype; whereas, loss of a second Sus, named Sus1, decreases starch accumulation in the endosperm (Chourey et al., 1998). In Arabidopsis, however, Sus does not appear to exert evident control over plant growth and development (Barratt et al., 2009), although the degree of reduction in Sus activity in the mutants analysed remains disputable (Baroja-Fernández et al., 2012).

The role of starch in Arabidopsis seed development

Arabidopsis seed development is defined by three phases: histodifferentiation, cell expansion and maturation/drying. The embryo sac undergoes a double fertilization event, by which a diploid embryo and a triploid endosperm are formed. In the first phase of development occurs the early morphogenesis, in which via several cell divisions, the embryo acquires the basic plant architecture. In the meanwhile, like in most angiosperms, Arabidopsis endosperm develops in two consecutive steps, an initial phase of free nuclear divisions without cytokinesis (syncytial phase) and a following cellularization (Costa et al., 2004), before being almost completely reabsorbed during maturation.

During this process, endosperm is progressively compartmentalized in three distinct domains that are likely to regulate the uptake of nutrients into the developing seed.

In the second phase of development, embryo cells expand and differentiate, while accumulating storage products as proteins, probably serving as nitrogen sources, and lipids, such as triacylglycerols (TAGs), glycerol esters and fatty acids, that serve as carbon reservoir supporting growth and metabolism of the young plant. In the third phase of development, the seed has reached the physiological maturity and, in some species, this coincides with rapid water loss to reach the maximum dry weight.

Fatty acids biosynthetic pathway is well understood in Arabidopsis seeds and involves different cellular compartments (Miquel and Browse, 1995). TAGs, are stored in cytosolic oily bodies that constitute about the 60% of the cell volume in mature embryo cotyledons (Mansfield and Briarty, 1992). Moreover, during maturation there is a preponderance of

mRNAs codifying for seed storage proteins (Heath et al., 1986; Pang et al., 1988). In addition to oils, glucose and fructose are present in the early stages of seed development but they gradually fade until seed reach the maturity (Focks and Benning, 1998). Also carbohydrates such as starch are transiently accumulated (Eastmond and Rawsthorne, 2000; Baud et al., 2002; Hills, 2004). Typically starch concentration decreases in the late stages of seed development and eventually disappear in mature seeds. In parallel with the decrease of starch, protein and oil contents increase (Baud et al., 2002; O'Neill et al., 2003; Andriotis et al., 2010).

Despite starch is not quantitatively relevant in mature seeds, in some developmental stages it represents an important fraction of the embryo weight. For example, in rape oilseeds the maximum starch content constitutes about the 8-10% of the dry weight (Silva et al., 1997; Eastmond and Rawsthorne, 2000) and the rate of accumulation is similar to that of seeds which store starch.

The role of starch in developing embryos of oilseed plants is not yet completely known, but there are hypotheses in this regard. First, it has been proposed that starch can serve in later stages of seed development as carbon storage for sugars and lipids biosynthesis, to feed the oxidative pentose phosphates pathway or to produce stachyose, a sugar that accumulates over exsiccation (Norton and Harris, 1975; Leprince et al., 1990). The progression of events during the maturation phase of the seed has been portrayed as a shift from starch to lipid storage (Eastmond and Rawsthorne, 2000; Schwender et al, 2003; Vigeolas et al., 2003; Lin et al., 2006; Musgrave at al., 2008). However, supposing that all the starch produced during seed development is degraded to give oil, it would not be sufficient to sustain the great overall oil production in the seed. Therefore, carbon and reductants necessary to produce oil, cannot entirely derive from starch. However, sucrose conversion in starch might be useful to recall other sugars in the seed, transforming the seed into a sink organ (Silva et al., 1997). In addition, to facilitate a carbon flux, i.e. from starch to lipid reserves, starch degradation and other storage compounds biosynthesis should occur at the same time and within the same cells, in the seed or in the embryo (Andriotis et al., 2010). Andriotis et al. (2010) demonstrated that, in Arabidopsis seeds, on the contrary, starch is accumulated in the testa in early developmental stages, whereas oil and proteins are produced in the embryo and later in the development. Moreover, in Arabidopsis embryo, the carbon flux that generates starch is greater and occurs over a

longer period along the seed axis (root-hypocotyl), rather than in cotyledons, which preferentially accumulate lipids. Mature Arabidopsis seed cotyledons contain about the 60% of the total oil content, whereas the seed axis only the 27% (Li et al., 2006). Thus the quantitative and temporal relationship between the flux of carbon to starch and the flux to oil were very different in different parts of the embryo. In general, these observations are consistent with the idea that starch act as a temporary carbon source in cells that are dividing or in the first stages of differentiation, where more energy is required to sustain fast metabolic changes rather than contribute to oil production. However, mutations affecting starch metabolism in Arabidopsis can lead to reduction in seed lipid content at maturity. Indeed, the starchless mutants lacking the plastidial PGM1 contain about the 40% less lipid than wild-type seeds (Periappuram et al., 2000) and *sex1* mutants, lacking GWD1 and unable to degrade starch (Yu e al., 2001), show 10 times more starch than wild-type seeds and 30% less lipid (Andriotis et al., 2010). Although these evidences seem to link starch metabolism and lipid accumulation, other observations seem to point in the opposite direction. In fact, in Arabidopsis and rape seeds, other disruptions of embryo starch metabolism, such as the loss of the sucrose synthases SUS2 and SUS3 or the reduction in the activity of ADP-Glc pyrophosphorylase, have no effect on the final lipid seed content (Barratt et al., 2009; Angeles-Núñez and Tiessen, 2010). As a consequence, the impact on seed oil content of mutation causing starch excess or starchless phenotypes can be explained considering the impaired seed lipid accumulation as an indirect effect of the altered maternal starch metabolism, rather than of the embryo itself. To assess this hypothesis, Andriotis et al. (2012) generated phenotypically wild-type plants bearing embryos defective in PGM1 and GWD1 gene and observed that, despite having disrupted starch metabolism, these embryos had wild-type lipid content at maturity, confirming that seed oil content is dependent on the night-time carbohydrate provision from the maternal plant to the reproductive structures. Moreover, the *gsl7* mutant lacking the glucan synthase-like 7 and defective in the phloem transport in the stem, showed impaired lipid accumulation in mature seeds (Andriotis et al., 2012).

As in leaves, starch synthesis in plastids of oilseed embryos, during the early-intermediate of cotyledons development, start from glucose 6-phosphate and pursues through the action of PGM, AGPase, SSs and BEs (Andriotis et al., 2010). In addition, starch degradation in the Arabidopsis seed seems to follow a pathway similar to that described for leaves at

night (Andriotis et al., 2010). Several mutations in enzymes necessary for normal starch breakdown in leaves impair seed starch turnover. As previously mentioned, the loss of GWD1 (in *sex1* mutants) reduces starch degradation rate in the testa and in the embryo at 12 DAF (Days After Flowering), when the starch content reach the greatest level (Andriotis et al., 2010). Thus, phosphorylation of the granule surface seems to have an important role in starch breakdown also in non-photosynthetic tissues as well as in leaves. Also the loss of SEX4 reduces the rate of starch loss in the testa, but without affecting starch turnover in the embryo (Andriotis et al., 2010). Thus, the importance of the phosphorylation/dephosphorylation cycle of starch granules in seeds appears unclear.

Beta-amylases are essential for normal starch degradation in both testa and embryo (Andriotis et al., 2010), whereas loss of the plastidial α-amylase, AMY3, or of the plastidial glucan phosphorylase, PHS1, has no effect (Fulton et al., 2008; Zeeman et al., 2004; Yu et al., 2005). Comparing mutants lacking of β-amylases, it appears that different the β-amylases have a different role on seed or on leaf starch breakdown. Whereas, mutants lacking BAM3 or BAM4 have reduced rate of starch degradation in leaves (Fulton et al., 2008), only the loss of BAM4 noticeably reduces the rate starch breakdown in seeds (Andriotis et al., 2010). Interestingly, BAM4 is reported to lack β-amylase activity, and it has been proposed to have a regulatory role through its interaction with other starch-degrading enzymes (Fulton et al., 2008). To further highlight the differences between leaves and seeds starch metabolism, the loss of the debranching enzyme ISA3, that is essential for starch degradation in leaves, has no effect on seed starch degradation, suggesting a possible role of the other plastidial debranching enzymes (ISA1, ISA2 and LDA) (Delatte et al., 2005; Wattebled et al., 2005; Streb et al., 2008).

Phosphorylation and its effects on starch structure

Since the early '900, potato starch was known to contain a certain amount of mono-esterified phosphate groups (Fernbach, 1904). Starch from almost all type of plant seems to be phosphorylated (Blennow et al., 2000a), and also glycogen (the starch analogous found in animals, fungi and bacteria) contains esterified-phosphate groups (Lomako et al., 1993). This suggests that phosphorylation is a general and well-preserved characteristic of reserve polysaccharide in all living organisms, even if phosphorylation levels change dramatically among species, organs and tissues. In Arabidopsis, storage starch has an intermediate degree of phosphorylation (a phosphorylated glucose unit every 1000) (Yu et al., 2001), whereas in cereal starch it is very low (one phosphate group every 10000 glucose unit) (Tabata et al., 1975; Blennow et al., 2000a) and in potato starch it is very high (one phosphorylated residue every 200-300 glucose unit) (Samec, 1914). Phosphorylation involves glucose residues belonging to both crystalline and amorphous region of starch granule, even if most of the phosphate groups are situated on the amylopectin (Samec, 1914; Blennow et al., 2000b). The phosphate groups are prevalently linked as monoesters at the C-6 position of the glucose residues (60-70%) while less than 30-40% of phosphoesterification occurs in C-3 position (Posternak, 1935; Hizukuri et al., 1970; Tabata and Hizukuri, 1971; Bay-Smidt et al., 1994). It is remarkable that in nature phosphorylation at the C-3 position seems to be only present in starch. Starch structure affects the phosphorylation process, since phosphate is prevalently found on the longer chains of amylopectin (30-100 glucose residues), but not at the reducing ends or close to the branch points (within 9 glucose residues from an α-1,6 linkage) (Takeda and Hizukuri, 1981; Takeda and Hizukuri, 1982; Blennow et al., 1998). The preferential modification of the long chains may explain the low phosphate content in secondary starch of cereal endosperm, which is mainly formed by low molecular weight chains (Blennow et al., 2002). However, it was demonstrated that branch points are important for phosphorylation, since amylopectin, but not amylose, is phosphorylated in plants (Mikkelsen et al., 2004).

A change in activity of starch synthases (SSs) or branching enzymes (BEs) can change amylopectin chain length and influence starch phosphorylation rate (Mikkelsen et al., 2004). On the contrary, changes in the phosphate content of starch do not modulate the activity of starch biosynthetic enzymes. In fact, phosphorylation does not affect the

branching pattern nor the chain length composition of amylopectin. Nevertheless, phosphorylation has an impact on starch structure: the presence of phosphate groups increases the hydration capacity of amylopectin chains and affects the viscosity of the jellified starch (Wiesenborn et al., 1994; Viskø-Nielsen et al., 2001). The study of these properties is of fundamental importance in exploitation of starch for industrial purposes, since its modification (i.e. phosphorylation) prevents crystallization during the processing steps and changes the consistency of the final product (Ellis et al., 1998).

Primary starch phosphorylation occurs both during synthesis that during degradation of the granule (Nielsen et al., 1994; Ritte et al., 2002a; Ritte et al., 2004). During synthesis, phosphorylation rate is constant, but in the dark, when starch degradation begins, the rate of phosphate incorporation increases (Ritte et al., 2002a; Ritte et al., 2004). There is not a net increase in starch phosphate content, since the phosphorylation and the removal of modified glucose chains cause a fast turnover (Ritte et al., 2002). Probably, starch phosphorylation during deposition is aimed to give a correct morphology to the granule: this modification can prevent interactions between amylose and amylopectin, which would increase structural instability of semi-crystalline regions (Blennow et al., 2002). It was shown that amylopectin crystalline region is made up by chains that form a compact structure of left-handed double helices, stabilized by hydrogen bonds between C-6 and C-2 atoms of glucose residues (Imberty et al., 1988). These double helices can crystallize in two principal different ways, the A-type (more dense) or B-type (more hydrated) crystalline polymorph. The free hydroxyl groups on C-3 and C-6 positions of glucose units are both located on the hydrophilic surface of the double helices and the phosphate groups can align or protrude from it (Fig. 11). This can affect the stability of the helices or their side-by-side packing and compromise the crystallinity of the starch.

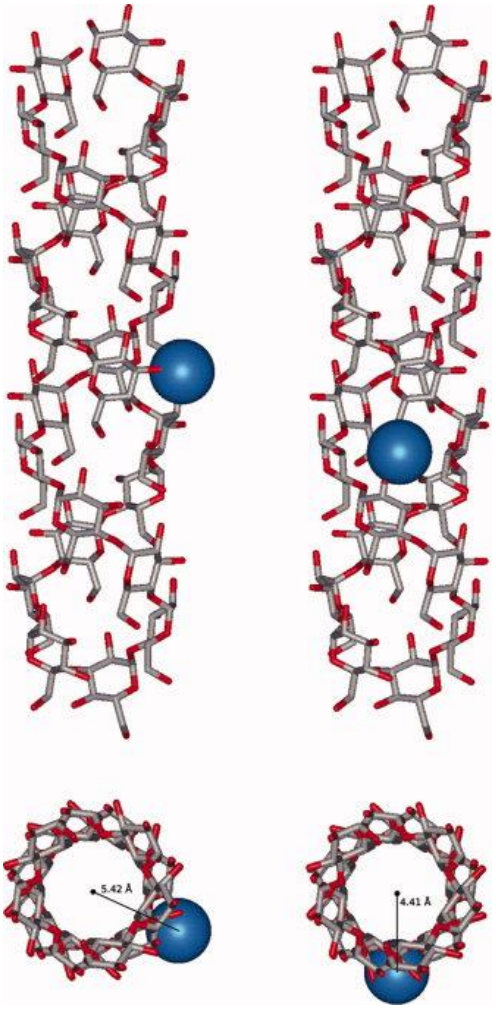

Figure 11. From Hansen et al. (2009), the structure of double helical amylopectin with an attached phosphate group, ignoring the effects of the glucosidic bond, with phosphate in the 3-position (left) and 6-position (right). The helical protrusion of the two phosphate groups by 5.42 Å and 4.41 Å is indicated on the figure.

However, whereas the C-6 phosphate is situated in the double-helix grooves and has a low steric hindrance, the C-3 hydroxyl groups protrude from the double-helical surface, determining a strong steric hindrance that notably affects the packing of the double helices (Blennow et al., 2002; Engelsen et al., 2003). Thus, it seems that the effects of phosphorylation on starch granule crystallinity mainly derive from the modification at the C-3 position of the glucose units, instead than from the phosphorylation at the C-6 position (O'Sullivan and Perez, 1999).

Starch phosphorylating enzymes

In 1998, for the first time, a protein (initially named R1) able to bind starch and to phosphorylate glycogen was identified in potato (Lorberth et al., 1998). Further analysis of R1 primary sequence highlighted a C-terminal sequence homology with bacterial phosphoenolpyruvate synthase (PPS; pyruvate, water dikinase; EC 2.7.9.2) and the pyruvate phosphate dikinase (PPDK; pyruvate, phosphate dikinase; EC 2.7.9.1) (Mikkelsen et al., 2004) The homologous region contains two highly conserved regions: a nucleotide binding domain (NBD) and, upstream, a 10-amino acids sequence containing the catalytic histidine (Yu et al., 2001). PPSs and PPDKs, acting as dikinases, catalyse the transfer of the β-phosphate group from ATP to pyruvate, with the simultaneous phosphorylation (by the γ-phosphate) of a molecule of water or phosphate, to generate orthophosphate or inorganic pyrophosphate.

Afterwards, it was demonstrated that the R1 enzyme phosphorylates starch with a reaction mechanism similar to that of PPSs and PPDKs and for this reason, in 2004, it was renamed GWD (Glucan, Water Dikinase; EC 2.7.9.4). Potato GWD antisense lines showed a decrease of about the 90% of starch-bound phosphate and a *sex* phenotype in leaves, as well as a reduction in "cold sweetening" (starch degradation occurring in response to low temperatures) of the potato tubers, suggesting that starch phosphorylation mediated by GWD was required for normal starch degradation (Lorberth et al., 1998; Viskø-Nielsen et al., 2001). Successively, by the means of potato GWD antibodies, homologous proteins were recognised in other plant species (Ritte et al., 2000), implying that this enzyme plays an important role over almost the entire plant kingdom.

Thus, according to the substrates and to the products of the reaction, three types of dikinases can be distinguished:

Group A (GWDs): ATP + α-glucan + H_2O → AMP + α-glucan-P + P_i

Group B (PPSs): ATP + pyruvate + H_2O → AMP + PEP + P_i

Group C (PPDKs): ATP + pyruvate + P_i → AMP + PEP + PP_i

Phylogenetically, dikinases with different functions, group into different clades or evolutionary branches (Fig. 12) (Mikkelsen et al., 2004).

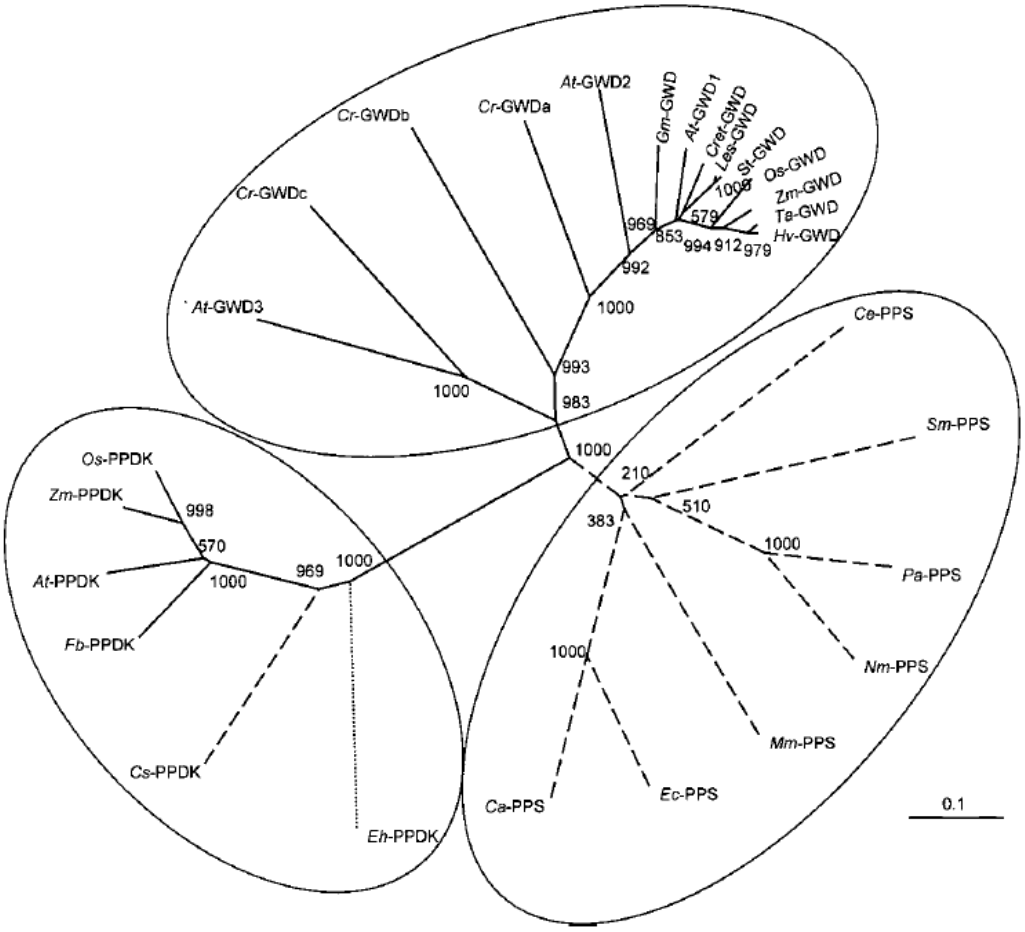

Figure 12. Phylogenetic tree, created by Mikkelsen et al. (2004) using Clustal X, of GWD family and PEP family proteins/ORFs (open reading frames) in the nucleotide-binding region. The consensus of the 1000 most likely trees created by the neighbour-joining method from bootstrapped data sets is showed. The number of bootstrap replicates is indicated next to each branch. The three dikinase clades or subgroups are circled. The scale indicates the average substitutions per site. Solid line, plant protein/ORF; dashed line, prokaryotic protein/ORF; dotted line, protist protein. The abbreviations and GenBank accession numbers of these dikinases are as follows. At -GWD1, Arabidopsis thaliana GWD1 (SEX1), accession no. AAG47821; At -GWD2, A. thaliana GWD homologue 2, accession no. AAO42141; At -GWD3, A. thaliana GWD homologue 3, accession no. NP198009; Cr -GWDa, Chlamydomonas reinhardtii GWD homologue a, accession no. BG857380; Cr-GWDb, C. reinhardtii GWD homologue b, accession no BF866967/AW661031; Cr -GWDc, C. reinhardtii GWD homologue c, genie 538.9 (C. reinhardtii Genome Release version 1.0, scaffold 538); Cret -GWD, Citrus reticulata (tangerine) GWD, accession no. AAM18228; Gm-GWD, Glycine max (soybean) GWD, accession no. AW133227/BI945390; Hv-GWD, Hordeum vulgare (barley) GWD, accession no. BU993123; Les-GWD, Lysopersicon esculentum (tomato) GWD, accession no. BE435569/AI489255; Os-GWD, Oryza sativa (rice) GWD, patent no. WO 00/28052A1; St -GWD, Solanum tuberosum (potato) GWD (R1), accession no. T07050; Ta-GWD, Triticum aestivum (wheat) GWD, accession no. CAC22583; Zm-GWD, Zea mays (maize) GWD, accession no. AY109804; At -PPDK, A. thaliana PPDK homologue, accession no. T01857; Cs-PPDK, Clostridium symbiosum PPDK, accession no. P22983; Fb -PPDK, Flaveria bidentis PPDK, accession no.

S56650; Os-PPDK, Oryza sativa (rice) PPDK, accession no. BAA22420; Eh-PPDK, Entamoeba histolytica PPDK, accession no. AAA18944; Zm-PPDK, Zea mays (maize) PPDK homologue, accession no. P11155; Ca-PPS, Clostridium acetobutylicum PPS, accession no. AAK78513; Ce-PPS, Corynebacterium efficiens PPS, accession no. NP_737171; Ec -PPS, Escherichia coli PPS, accession no. S20554; Mm-PPS, Methanococcus maripaludis PPS, accession no. AAD28736; Nm-PPS, Neisseria meningitidis PPS, accession no. NP_273662; Pa-PPS, Pseudomonas aeruginosa PPS, accession no. AAG05159; Sm-PPS, Staphylothermus marinus PPS, accession no. S51006.

The three clades shown in the figure 12, represent the three different reaction catalysed by the dikinases: the first group (B) is formed only by bacterial and archaea PPSs, the second one (C) is composed by PPDKs of plants, protist parasites and prokaryote, and the third group (A) includes only plant and algae GWDs.

Phylogenetic studies and alignments of conserved domains, including the Nucleotide Binding Domains (NBDs) and the regions containing the catalytic His, demonstrated that these three groups have a common origin and that GWDs family originated after the divergence of the plant kingdom. The conserved dikinase domain of GWDs has probably undergone to shuffling in the plant genome after the endosymbiotic event that led to the formation of chloroplasts from an ancestral cyanobacteria (Mikkelsen et al., 2004). Moreover, in the phylogenetic tree the NBD of GWDs seems evolutionary closer to that of prokaryotic PPSs than to PPDKs. This proximity based on the sequences is also reflected by the similarity in the dikinase catalytical mechanism of the two groups (Mikkelsen et al., 2004). Indeed, for both PPSs and GWDs, H_2O is the final acceptor of the γ-phosphate group of the ATP, whereas for PPDKs is P_i (Mikkelsen et al., 2004).

During PPSs and PPDKs activity, a phosphohistidine intermediate is formed. Initially, ATP interacts with the NBD of the enzyme, which get transiently autophosphorylated on the conserved His residue (Narindrasorasak and Bridger, 1977). Subsequently, when the enzyme interacts with the substrate, the β-phosphate group on the catalytic His is transferred to the pyruvate, generating phosphoenol pyruvate (PEP).

$$E^{-His} + AMP\text{-}P^{\beta}\text{-}P^{\gamma} + H_2O + pyruvate \rightarrow E^{-His\text{-}P^{\beta}} + P_i^{\gamma} + AMP + pyruvate$$

$$E^{-His\text{-}P^{\beta}} + P^{\gamma} + AMP + pyruvate \rightarrow E^{-His} + P_i^{\gamma} + AMP + P^{\beta}\text{-}pyruvate$$

Also for GWDs, the catalytic activity can be divided in two phases: the conserved histidine residue at position 992 undergoes autophosphorylation and mediates the phosphotransfer to the glucosyl residue, with an overall reaction mechanism that is very similar to that of PPSs and PPDKs (Mikkelsen et al., 2004).

$$GWD^{-His} + ATP + H_2O \rightarrow GWD^{-His\text{-}P} + P_i + AMP$$

$$GWD^{-His\text{-}P} + \alpha\text{-glucan} \rightarrow GWD^{-His} + \alpha\text{-glucan-P}$$

The substitution, by site-specific mutagenesis, of the catalytic His with an Alanine, showed that this residue plays an essential function, being the mutated enzyme devoid of phosphorylating activity (Mikkelsen et al., 2004). Potato GWD shows an optimum of activity at 35°C and pH 7 and is catalytically active as homodimer (Mikkelsen et al., 2004). The auto-phosphorylation does not affect the ability of the enzyme to dimerize (Mikkelsen et al., 2004). Moreover, in vitro studies demonstrated that the enzyme is preferentially active on long and ramified glucan chains (30-100 glucose residues) (Mikkelsen et al., 2004). This settle with the observation that amylopectin, and not amylose, is the main target of phosphorylation and that starches from cereal seeds, which have shorter amylopectin unit chains, are poorly phosphorylated (Ritte et al., 2000).

PPDKs have a multi-domain structure and the protein conformation changes during the two semi-reactions (Mikkelsen and Blennow, 2005). The coupling between the two distinct and separated binding sites (the ATP and the pyruvate binding sites) of PPDK is facilitated by the presence of a flexible domain containing the phospho-histidine. This flexible domain can be found alternatively in two different conformational states: adjacent to the NBD, where it can interact with ATP molecule, or near to the pyruvate-binding site (on which it can transfer the phosphate group). The auto-phosphorylation of the His residue can trigger the protein conformational change (Herzberger et al., 1996; Herzberger et al., 2002).

By proteolytic digestion and subsequent analysis of the fragments, it was demonstrated that GWD maintains this multi-domain organization and that possess also the flexible portion containing the phospho-histidine residue (Mikkelsen and Blennow, 2005). GWD was fragmented by proteolytic digestion and the resulting peptides were analysed by

microsequencing. These analyses highlighted that the protein was constituted by 5 domains of 37, 24, 21, 36 and 38 kDa (Fig. 13) (Mikkelsen and Blennow, 2005). In conjunction, GWD deletion mutants were generated to further investigate domain structure-function relationship.

The catalytic histidine, responsible of transfer of the phosphate group from ATP to starch, belongs to the 36 kDa domain, whereas the ATP binding domain is situated at the C-terminal portion of the 38 kDa domain. The glucan binding site is suggested to be part of the other 3 domains (24, 21 and 37 kDa) (Mikkelsen and Blennow, 2005). Interestingly, the ATP binding domain and the glucan binding domain are independent from each other, since the lack of one of them does not inhibit the activity of the remaining domain, and the truncated enzyme is still able to catalyse the corresponding semi-reaction (Mikkelsen and Blennow, 2005). The truncated enzyme formed by 36 and 38 kDa domains is still able to form the auto-phosphorylated intermediate but loses the ability to phosphorylate starch. This auto-phosphorylation, as for PPDKs, triggers the protein conformational changes. Thus, the domain containing the phospho-histidine residue is essential for the enzyme activity (Mikkelsen and Blennow, 2005)

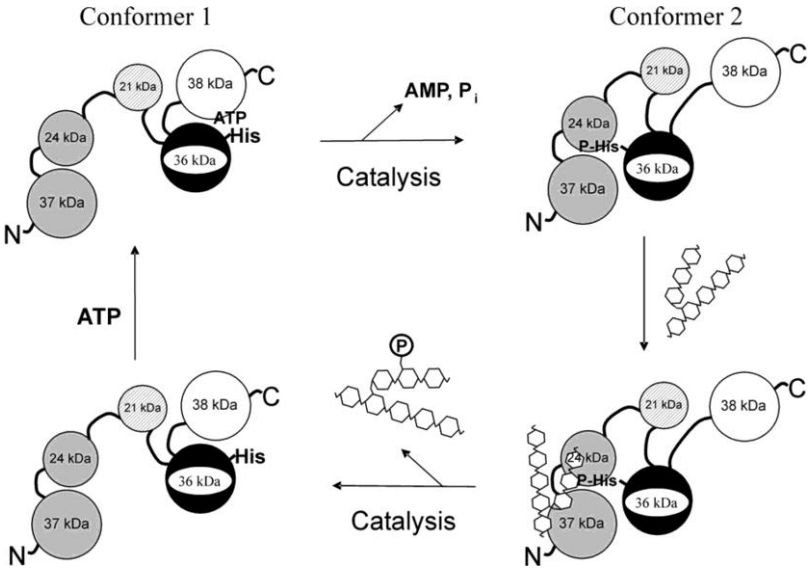

Figure 13. From Mikkelsen and Blennow (2005), hypothetical model illustrating the GWD catalytic cycle. Proteolytic fragments are represented as spatially separated structural domains connected by loops. GWD can bind ATP and autophosphorylate without the presence of the glucan substrate, then nucleotide substrate is shown to occur before binding of the glucan substrate, but the reverse situation or the simultaneous binding could possibly occur *in vivo*. To bind the ATP, GWD is considered to display the catalytic histidine domain spatially close to the ATP-binding site (conformer 1). Catalysis and

autophosphorylation induce a major conformational change (conformer 2), here illustrated as a rearrangement of the catalytic histidine domain, which allows the phosphohistidine to interact with the glucan-binding site. Once the glucan molecule has been bound, the second round of catalysis is initiated and the glucan substrate is phosphorylated. The enzyme then reverts to the initial conformational state (conformer 1) ready for another nucleotide molecule to bind. The ATP-binding site is shown to be located on the 38 kDa domain (white sphere), the catalytic histidine on the 36 kDa domain (black sphere), and the glucan-binding sites on the 37 and 24 kDa domains (grey spheres).

Since GWD is a chloroplastic protein involved in starch degradation, and considering that primary starch metabolism is highly correlated with photosynthesis, the existence of a regulation of the enzyme and of the process of starch phosphorylation linked with photosynthesis, can be hypotesized.

The light-dependent regulation is a mechanism that links the electron transport occurring during the photosynthesis with specific enzymatic activities, through the ferredoxin/thioredoxin system (Trx). Thioredoxins (Trxs) are small are small and ubiquitous disulfide/oxidoreductase proteins that, in the chloroplast, can modulate the activity of some enzyme by the reduction of regulatory disulfide bridges (Schürmann and Jacquot, 2000). Chloroplasts of higher plants contain four different types of Trxs (Meyer et al., 2002; Lemaire et al., 2003; Collin et al., 2004). Two of them, type *f* (Trx *f*) and type *m* (Trx *m*), that have different phylogenetic origins (Hartman et al., 1990), are involved in the control of carbon metabolism, with a certain substrate specificity (Schürmann and Jacquot, 2000; Baumann and Juttner, 2002; Schürmann, 2003). Mikkelsen and collaborators (2005) demonstrated that GWD interacts in vivo with Trxs and that is redox regulated. Both reduced Trx *f* and Trx *m*, at concentrations 3-fold lower compared to non-physiological reducing agents, activated GWD, even if Trx *f* was a more efficient activator in comparison to Trx *m* (Mikkelsen et al., 2005). On the contrary, using oxidised Trx *f* and *m* it was not possible to oxidize GWD. Therefore, other oxidants or other types of Trxs could mediate the in vivo oxidation of the protein. However, the protein oxidation led to an almost complete inactivation of the enzyme, which could be reverted by reduction (Mikkelsen et al., 2005). A more detailed analysis of the GWD primary sequence revealed a consensus sequence (CFATC), downstream the catalytic His residue, for the Trxs mediated regulation (Mikkelsen et al., 2005).

Many studies suggest that starch phosphorylation occur both during starch synthesis and degradation (Nielsen et al., 1994; Ritte et al., 2002; Ritte et al., 2004). However, phosphorylation rate is greater during dark period than in the light. How stated in the previous section, phosphate incorporation rate is stable during synthesis, but it is subjected to a rapid turnover during starch degradation (Ritte et al., 2004). Potato GWD is able to reversibly bind starch granules *in vitro*, and *in vivo* it can be found in the stroma under light conditions and not covalently bound to the starch surface when plant is kept in the dark (Ritte et al., 2000a). Thus, GWD can be found in a soluble or granule-bound state, depending on whether the plant is exposed to light or dark conditions (Ritte et al., 2000a; Mikkelsen et al., 2005). Given its redox regulation, GWD seems to be inactive when oxidized, condition occurring during darkness in the chloroplast. However, this seems counterintuitive since, during the dark period, the protein is found to be associated with starch granules and the phosphorylation rate increase.

***Arabidopsis thaliana* genome encodes three GWDs**

Glucan, water dikinases related proteins are widely distributed in photosynthetic eukaryotes. Potato GWD homologous has been found in many plant species, i.e. in sweet potato tubers, in corn and barley seeds, banana fruits (Ritte et al., 2000). GWDs are found also in algae: in *Ostreocuccus tauri* there are five dikinase isoenzymes and *Chlamydomonas reinhardtii* genome encodes for four isoforms of GWDs (Fettke et al., 2009). In Arabidopsis, three genes encode for the same number of enzymes belonging to the family of the glucan, water dikinases, named GWD1, GWD2 and PWD (Yu et al., 2001; Kötting et al, 2005; Baunsgaard et al., 2005; Glaring et al., 2007). The three gene products (as for all the other glucan, water dikinases identified till now) have a common structure, similar to that previously described for potato GWD: a nucleotide binding domain (NBD) at the C-terminal position, a short conserved sequence containing the catalytic histidine and a N-terminal starch binding domain (carbohydrate binding module, CBM) (Fettke et al., 2009).

Primary sequence alignments showed that CBM is present both in Arabidopsis α-amylase AMY3 and GWDs sequences. This domain, in GWD1 and AMY3, is composed by two repeated sequences (SBD1 and SBD2, Starch Binding Domains) of about 90 amino acids, with an homology between the two proteins respectively of the 31 and 25% (Yu et al.,

2005; Mikkelsen et al, 2006). On the contrary, PWD and GWD2 show a single copy of SBD (Yu et al., 2005).

Both GWD1 and PWD, but not GWD2, contain a chloroplast targeting sequence, in agreement with the involvement of GWD1 and PWD in chloroplast starch degradation (Glaring et al., 2007). Arabidopsis GWD1, as potato GWD, possess a consensus sequence that determine the specificity for Trx *f* mediated regulation and that is essential for Trx binding (Mikkelsen et al., 2005). Differently from GWD, the primary sequence of PWD does not contain this consensus region, nor does the protein seem to contain any disulfide bond, suggesting that it is not target of this type of regulation. As a consequence, PWD can presumably phosphorylate starch during the darkness, when Trxs are prevalently oxidised (Mikkelsen et al., 2005).

Unlike GWD1 and PWD, GWD2 seems to be localised in the cytosol (Glaring et al., 2007; Orzechowski, 2008). Also the expression of GWD2 gene is spatially and temporally different from that of GWD1 and PWD (Glaring et al., 2007). GWD2 is mainly expressed during plant senescence and in cells associated with the vascular tissue, consistently with the observation that *gwd2* mutants do not have a *sex* phenotype (Streb and Zeeman, 2012).

Glucan, water dikinase 1 (GWD1) of *Arabidopsis thaliana*

The *sex1* mutant of *Arabidopsis thaliana* was firstly isolated by iodine staining of leaves harvested after a period of darkness, searching for mutant plants unable to degrade starch at night (Caspar et al., 1991). Starch levels in these mutants were 5-folds higher than the highest levels observed in wild-type plants, with minor changes during the whole day (Tretheway and ap Rees, 1994). Further studies showed that *sex1* mutation mapped on the chromosome 1 and that the locus *sex1* codes for the GWD1 protein, an homologous of potato GWD also named R1 (66,3% of identity at nucleotide level; Yu et al., 2001). In Arabidopsis GWD1 is a monomer of 1399 amino acids, with a molecular weight of 156,5 kDa (Lorberth et al., 1998; Yu et al., 2001; Fettke et al., 2007). At the N-terminal part of Arabidopsis GWD1, a transit peptide of 75 amino acids targets the enzyme into the stroma (Mikkelsen et al., 2005). Like potato GWD, Arabidopsis enzyme has a multi-domain structure with a catalytic mechanism similar to that previously described (see Section

"Starch phosphorylating enzymes") and responsible of the phosphorylation in C-6 position of amylopectin (Ritte et al., 2006).

Phosphoglucan, water dikinase (PWD) of *Arabidopsis thaliana*

A gene on Arabidopsis chromosome 5 encodes for another chloroplastic isoform of GWD (Yu et al., 2001). Two groups independently discovered this second dikinase (Baunsgaard et al., 2005; Kötting et al., 2005). This GWD1 homologous was firstly named GWD3 and only later re-named PWD, because of its peculiar substrate specificity (Kötting et al., 2005). *PWD* gene encodes for a protein of 1196 amino acids with a monomeric molecular weight of 130 kDa and a 30% of sequence identity with Arabidopsis GWD1 (Fettke et al., 2009). The similarity with GWD1 is more pronounced at the C-terminal domain of the enzyme. On the contrary, the N-terminal region contains a single CBM, different from that of GWD1 and belonging to the family of CBM20 (Christiansen e al., 2009).

PWD protein is expressed in all starch containing tissues: roots, rosetta leaves, stems, flowers and siliquae (Baunsgaard et al., 2005).

PWD knockout plants synthesize less starch during the light period and degrade less starch during darkness with a consequent minor fluctuation of starch level during the day in comparison to wild-type plants (Baunsgaard et al., 2005). However, starch structure and distribution of chains of different length in the granule is not different from that of wild-type (Baunsgaard et al., 2005). As demonstrated both *in vivo* and *in vitro*, PWD catalyses the phosphorylate starch exclusively at the C-3 position of the glucose units and the phosphorylating activity of GWD1 is a fundamental prerequisite for PWD activity (Baunsgaard et al., 2015).

PWD and GWD1 proteins are co-expressed: their transcripts increase during a 8h light period, they pike 1h after of darkness and decrease over the dark period. Their transcription levels are co-regulated also in plants under different abiotic stress conditions (Baunsgaard et al., 2005). The dependence of the activity of PWD on pre-phosphorylated starch (Baunsgaard et al., 2005), the parallel transcriptional control of GWD1 and PWD genes (Baunsgaard et al., 2005) and the increase in GWD1 and PWD protein amounts found associated with the granule surface during starch degradation (Ritte et al., 2000a; Kötting et al., 2005), suggest the possible formation of enzymatic complexes, as already known for other starch metabolism related enzymes (See section "Hints on starch

metabolism regulation**”**). However, PWD does not require a direct interaction with GWD1 to phosphorylate starch. Then, the already existing phosphate in C-6 position may be a tag for the binding of PWD or it may trigger substrate conformational changes that are necessary for the activity of PWD (Kötting et al., 2005; Fettke et al., 2009). Plants lacking of PWD show a *sex* phenotype, proving that PWD mediated phosphorylation is important for starch metabolism and that the lack of PWD cannot be completely compensated by other enzymes. Since the PWD activity requires a previous step of starch phosphorylation given by GWD1, the absence of GWD1 abolishes also the PWD mediated phosphorylation. The *sex1* phenotype in GWD1 knockout plants is more severe and it is probably the result of the additional suppression of GWD1 and PWD activities (Kötting et al., 2005). The requirement of two sequential starch phosphorylation events suggests that phosphatesterification in C-3 position, and not the one in C-6, is the modification that trigger the initial attack of the granule by degrading enzymes. Indeed, starch double helices molecular modelling highlight that the phosphate groups bound in position C-3 protrude from the helices (Fig. 11), whereas the phosphates in C-6 position are buried. This can affect the bonds between glucose residues, the interactions of the double helices, the packing of the α-glucans and finally the way in which the surface of the granule is exposed to degradative enzymes (Hansen et al., 2009).

Glucan, water dikinase 2 (GWD2) of *Arabidopsis thaliana*

In Arabidopsis genome, on chromosome 4, was found a third sequence encoding for a third isoform of GWD, named GWD2. This protein is 1278 amino acid long; it has a 50% homology with GWD1 and a domain-structure more similar to that of GWD1 than that of PWD: it has the phospho-histidine conserved domain, the C-terminal NBD and two N-terminal tandem repeated SBDs, like GWD1 (Glaring et al., 2007).

Thanks to the presence of the starch binding domains, that are specific of enzymes involved in starch metabolism, it seems possible that GWD2 binds starch granules. Biochemical studies demonstrated that GWD2 is able to phosphorylate starch through a GWD1-like reaction and that the substrate specificity is similar to that of potato GWD (Ritte et al., 2002; Mikkelsen et al., 2004; Glaring et al., 2007). It does not need pre-phosphorylated starch, it displays a preference for long α-glucans and it exclusively phosphorylates on glucose C-6 atoms (Glaring et al., 2007). However, the absence of a

chloroplast-targeting signal and the lack of noticeable phenotypic traits in plants depleted of GWD2 suggests that GWD2 does not take part in the normal primary starch metabolism (Glaring et al., 2007). Moreover, GWD2 displays a precise and narrow expression profile, being mainly expressed in vascular tissues of leaves, stems, roots, flowers and siliques or in the later phase of plant development, just before the onset of senescence (Glaring et al., 2007). An unverified hypothesis suggests that, given the high age-dependency of GWD2 expression, the enzyme might be involved in the breakdown of starch or starch-like structures during the withdrawal of nutrients from the senescing leaf (Glaring et al., 2007). The existence of cytosolic starch degrading enzymes, such as GWD2 in companion cells or BAM5 that localizes in the phloem sieve elements, suggests an alternative polysaccharide degradation pathway (Glaring et al., 2007), facilitating the transport and availability of sugars through the phloem or preventing the build-up of such polymerized polysaccharides, that would impede flow through the sieve-plates (Wang et al., 1995). GWD2 can be transferred from the companion cells to the sieve elements via plasmodesmata by specific (selective) trafficking. As an alternative, the GWD2 encoding mRNA can be transported to the sieve elements, but it is unknown if once there it can give rise to any protein.

However, up to date no evidence has been found for the existence of large α-linked polysaccharides, other than starch, in phloem tissues, but cytosolic water-soluble heteroglycans (SHGs) have been identified in Arabidopsis (Fettke et al., 2005). SHGs may also be present in companion cells and phloem parenchyma cells, but there is no evidence supporting the requirement of water dikinase activity for their metabolism.

CHAPTER 1
New starch phenotypes produced by TILLING in barley

Pulished in 2014 by PLoS ONE 9(10): e107779; doi:10.1371/journal.pone.0107779

Francesca Sparla[1], Giuseppe Falini[2], Ermelinda Botticella[3], Claudia Pirone[1], Valentina Talamè[4], Riccardo Bovina[4], Silvio Salvi[4], Roberto Tuberosa[4], Francesco Sestili[3], Paolo Trost[1]

[1]Department of Pharmacy and Biotechnology FABIT, University of Bologna, Bologna, Italy

[2]Department of Chemistry "G. Ciamician", University of Bologna, Bologna, Italy

[3]Department of Agriculture, Forestry, Nature & Energy, University of Tuscia, Viterbo, Italy

[4]Department of Agricultural Sciences, University of Bologna, Bologna, Italy

Abstract

Barley grain starch is formed by amylose and amylopectin in a 1:3 ratio, and is packed into granules of different dimensions. The distribution of granule dimension is bimodal, with a majority of small spherical B-granules and a smaller amount of large discoidal A-granules containing the majority of the starch. Starch granules are semi-crystalline structures with characteristic X-ray diffraction patterns. Distinct features of starch granules are controlled by different enzymes and are relevant for nutritional value or industrial applications. Here, the Targeting-Induced Local Lesions IN Genomes (TILLING) approach was applied on the barley TILLMore TILLING population to identify 29 new alleles in five genes related to starch metabolism known to be expressed in the endosperm during grain filling: *BMY1* (*Beta-amylase 1*), *GBSSI* (*Granule Bound Starch Synthase I*), *LDA1* (*Limit Dextrinase 1*), *SSI* (*Starch Synthase I*), *SSIIa* (*Starch Synthase IIa*). Reserve starch of nine M3 mutant lines carrying missense or nonsense mutations was analysed for granule size, crystallinity and amylose/amylopectin content. Seven mutant lines presented starches with different features in respect to the wild-type: (i) a mutant line with a missense mutation in *GBSSI* showed a 4-fold reduced amylose/amylopectin ratio; (ii) a missense mutations in *SSI* resulted in 2-fold increase in A:B granule ratio; (iii) a nonsense mutation in *SSIIa* was associated with shrunken seeds with a 2-fold increased amylose/amylopectin ratio and different type of crystal packing in the granule; (iv) the remaining four missense mutations suggested a role of *LDA1* in granule initiation, and of *SSIIa* in determining the size of A-granules. We demonstrate the feasibility of the TILLING approach to identify new alleles in genes related to starch metabolism in barley. Based on their novel physicochemical

properties, some of the identified new mutations may have nutritional and/or industrial applications.

INTRODUCTION

Barley (*Hordeum vulgare* L.) is the fourth most important cereal crop both in terms of cultivated area and tonnage harvested; global production being mostly used as animal feed and for the malting industry (http://faostat.fao.org). Only 5% of the global production of barley is used as ingredients in food preparation, but nevertheless barley grains are a valuable functional food for the high content of soluble dietary fiber [1]. The recent assemblage of the sequence of the 5.1-Gb haploid genome of barley [2] further supports the role of barley as a model species for the Triticeae tribe, which includes very important crops such as wheat (bread and durum) and rye.

Mature barley grains typically contain 50–60% starch on a dry weight basis. Starch is synthesized and stored in granules composed of two types of D-glucose polymers, amylose and amylopectin. Amylose, generally accounting for about 25-30% of starch weight in barley, is essentially a linear polymer of D-glucose units linked by alpha-1,4-glucosidic bonds. The second polymer of starch, amylopectin, is highly branched because of the alpha-1,6-glucosidic bonds that connect short alpha-1,4 linear chains [3], [4], [5], [6], [7], [8], [9].

While most plants contain starch granules of similar size, the Triticeae endosperm presents two classes of starch granules characterized by different sizes and shapes [10], [11]. Most of the starch is stored in large A-granules, but small B-granules prevail in number. In barley, the diameter of A-granules ranges from 10 to 40 μm while B-granules are smaller than 10 μm [10]. Starch granules contain crystalline lamellae in which double helices, composed of parallel linear chains of amylopectin, interact among each other to form different types of crystal packing [3]. Crystalline lamellae are interspersed with amorphous lamellae in which amylopectin branches are concentrated. The exact location of amylose within the semicrystalline architecture of the starch granule is still unknown [9], but certainly amylose influences the global structure of starch granules. For example, starch granules of different composition are characterized by different types of X-ray diffraction patterns [3], [4], [8]. In cereals, the A-type crystal packing is predominant, while

the B-type crystallinity, typical of tuber starch, exists in smaller amounts. A third diffraction pattern, named V-type, is associated with lipid-amylose complexes and is little represented in native starches [3].

Both amylose/amylopectin ratios and the architecture of starch granules depend in a complex way on many different enzymes involved in starch metabolism [4], [5], [8], [9]. Biosynthesis of starch polymers in cereal grains strictly depends on the availability of ADP-glucose as a precursor for both amylose and amylopectin polymerization. Starting from ADP-glucose, a single enzyme, the granule-bound starch synthase I (GBSSI), is required for the synthesis of amylose. More complex is the biosynthetic pathway leading to amylopectin production as different classes of soluble starch synthases (SSs) and starch branching and debranching enzymes are required [5], [8], [9].

Starches with different amylose/amylopectin ratios have different properties that influence their possible use for either nutritional purposes or industrial transformations [6], [7], [9], [12], [13], [14]. In barley, mutants with 0-10% amylose (*waxy*) as well as mutants containing up to 70% amylose in the endosperm have been described [15], [16], [17]. Low-amylose starch displays higher freeze-thaw stability, an interesting property for food preparation [6]. On the other hand, high amylose starches have interesting nutritional properties due to their positive correlation with resistant starch. This starch fraction is highly resistant to human digestion in the small intestine and reaches the large bowel where it plays a role similar to dietary fiber. Consumption of high-amylose resistant starch is associated with several health benefits, including the prevention of colon cancer, type II diabetes, obesity and cardiovascular diseases [18], [19].

Starch granule size distribution is another important parameter that may affect technological properties and end-use of each particular type of starch [20]. Barley grains are largely used for malting and large A-granules are more readily attached by hydrolytic enzymes than small B-granules [10]. B-granules are apparently protected during malting by a heterogeneous matrix deriving from the grain (proteins and cell walls). As a result, a significant proportion of B-granules escapes degradation and causes several technological problems during beer production [21].

In a previous work using a TILLING strategy, novel allelic variants in genes involved in starch metabolism in barley seeds were identified [22]. Here we describe the starch phenotype of nine mutants carrying either missense or nonsense mutations in five starch-

related genes known to be expressed in the endosperm during grain filling: *BMY1* (beta-amylase 1), *GBSSI* (Granule Bound Starch Synthase I), *LDA1* (Limit Dextrinase 1), *SSI* (Starch Synthase I), *SSIIa* (Starch Synthase IIa). Seven mutant lines present starches with potentially interesting features for nutritional uses and/or industrial applications, including an altered amylose/amylopectin ratio or an unusually high percentage of A-granules or A-granules that are larger than in wild-type starch.

MATERIALS AND METHODS

TILLING analysis and plant materials

Details on the TILLING-based molecular screening for the five starch metabolism enzymes were reported in [22] and will only be summarized here. TILLMore is a chemically (sodium-azide, NaN_3) mutagenized barley population including 4,906 $M_{3:4}$ families [23]. TILLMore was screened using a standard TILLING protocol based on LI-COR vertical gel electrophoresis of PCR reactions obtained on 8X bulked genomic DNA samples. Genes tilled were *Beta-amylase 1* (*BMY1*), *Granule-Bound Starch Synthase I* (*GBSSI*), *Limit dextrinase 1* (*LDA1*), *Starch Synthase I* (*SSI*) and *Starch Synthase IIa* (*SSIIa*) (Table 1). For each mutant, plant materials phenotyped in this work were grains (kernels) of M_4 lines (three generations of selfing after mutation induction), which have been verified to be homozygous for the mutation (not shown).

Gene name	Mutant code	Genebank accession	Nucleotide change	Amino acid substitution	Seed and starch phenotype
Beta-amylase 1	2253-*BMY1*	EF175470	G2522A	D277N	Normal
	2682-*BMY1*	EF175470	G2944A	E348K	Normal
Granule-bound starch synthase I	1090-*GBSSI*	AB088761	G2306A	G493E	Low % amylose. Low % V-diffraction pattern
Limit dextrinase 1	905-*LDA1*	AF122050	G1528A	V270I	Low % A- granules
Starch synthase I	1132-*SSI*	AF234163	C5705T	T522I	High % A- granules
	1284-*SSI*	AF234163	G5666A	G509E	Low % A- granules. Large A-granules
	5850-*SSI*	AF234163	G6020A	G576D	High % A- granules. Small A-granules
Starch synthase IIa	1039-*SSIIa*	AY133251	G2453A	G678R	Small A-granules
	1517-*SSIIa*	AY133251	G2449A	W676*	Small and shrunken seeds. Low % total starch. High % amylose. High % V-diffraction pattern. Deformed granules

Table 1. List of TILLING mutant lines carrying either missense or nonsense mutations in five genes related to starch metabolism in barley grains that have been isolated as described in Bovina et al. [22] and phenotypically characterized in this work.

Mutant lines and cv. Morex were grown in open field following standard agronomic practice in 0.5-m long one-row plots (approx. 12 plants per plot) using a randomized design with two replicates. For each line, grains harvested (from all well-grown ears) from two replicates were bulked. The same experiment was carried out in two years. Grains from separated years constituted the biological replicates.

Starch extraction from barley grains

Starch was extracted by grinding the grains to a fine powder in a pepper mill. About 5 g of seeds, corresponding to about 100 seeds, were used for each line and for each biological replicate (except for line 1517-*SSIIa* for which 2.5 g of seeds were used). Starch grains were purified as described in [24]. Briefly, the powder was suspended in 70 ml Extraction Buffer (EB: 55 mM Tris-HCl, pH 6.8, 2.6% SDS, 10% glycerol, 2% ß-mercaptoethanol) and vigorously shaken for 48 h, replacing the EB solution every 24 h. Following the extraction, samples were washed three times in water and filtered through a nylon membrane (cut-off 100 µm) in order to eliminate debris. Filtered samples were spun down for 1 min at 10,000 g. Starch grains were resuspended in 25 ml acetone and spun down again. Once removed the supernatant, starch grains were air-dried under a chemical hood for about 48 h at room temperature.

SDS-PAGE analysis of starch granule proteins

Isolation and electrophoretic separation of starch granule proteins was carried out on mature seeds following the method reported by Zhao and Sharp [25] with some modifications, as reported by Mohammadkhani et al. [26]. Protein bands were visualized by silver staining.

Determination of total starch and amylose content

Total starch content was determined on whole flours using Megazyme Total Starch Assay Kit (Megazyme, Ireland). The relative content of amylose was determined using both the Amylose/Amylopectin assay kit (Megazyme, Ireland) following the manufacturer instructions, and by an iodometric assay as reported in Sestili et al. [27]. Three technical replicas were performed for each mutant and each type of measure. Total starch content

and relative amylose content (enzymatic method) were measured on two biological replicas.

Starch morphology

The morphology of starch samples was analyzed using a scanning electron microscopy (SEM) Hitachi S-4000. The samples were glued by a carbon type on an aluminum stub and gold coated (2 nm thick layer) before observations. For each sample two sets of 10 pictures at two magnifications (1000x and 2500x) were randomly collected. These two magnifications allowed a good estimation of the size of large and small granules. The granule size was estimated using the software ImageJ for image processing and analysis. The two main axes for each granule were recorded and 200-500 grains were measured for each sample. Percentage of granules with major axis lower than 8 µm (B-granules) was recorded in 10 pairs of pictures (at different magnification) for each genotype. Statistically significant differences between mutants and wild-type mean values were detected by Student's t-test ($P< 0.01$). The frequency analysis was carried out tacking classes of 2 µm.

Starch crystallinity

The X-ray powder diffraction patterns were recorded using a Philips X'Celerator diffractometer with Cu Ka radiation (l = 1.5418 Å) and equipped with a Ni filter. The samples were scanned for 2θ angles between 5º and 30º, with a resolution of 0.02º. The degree of crystallinity of samples was quantitatively estimated following the method of Nara and Komiya [28]. A smooth curve which connected peak baselines was computer-plotted on the diffraction patterns. The area above the smooth curve was taken to correspond to the crystalline portion, and the lower area between the smooth curve and a linear baseline which connected the two points of intensity at 2θ of 30° and 5°. The upper diffraction peak area and total diffraction area over the diffraction angle 5°–30° 2θ were integrated on X'Pert HighScore Plus software (PANalytical B.V. 2008). The ratio of upper area to total diffraction area was taken as the degree of crystallinity.

In the diffraction patterns only peaks associable to A-type and V-type crystallinities were detected. To estimate the relative amount of A-type and V-type crystallinities in the starch samples from the diffraction patterns, only well isolated diffraction peaks were considered. The one at 15.1° is diagnostic of the A-type crystallinity and the one at 19.7°

is diagnostic of the V-type one. These diffraction intensities has been normalized on the sum of their intensities.

RESULTS

TILLING molecular analysis

Molecular details about TILLING for five genes involved in starch metabolism were already reported in Bovina et al. [22] and will only be summarized here. TILLING was carried out in TILLMore, a TILLING population in the cultivar (cv.) Morex background which was chemically mutagenized using NaN_3 [23]. The analyses identified an allelic series for each of the genes examined with a total number of 29 mutations [22]. Seeds of nine mutant lines carrying either missense or nonsense mutations in the five genes analyzed (*BMY1 GBSSI*, *LDA1*, *SSI* and *SSIIa*) were phenotypically characterized in this study (Table 1).

Seeds of the mutant lines did not show any macroscopic differences in respect to Morex wild-type (wt) with the exception of the line 1517-*SSIIa* (*Starch Synthase IIa*) that showed shrunken kernels with an empty cavity inside (Figure 1). These seeds were also lighter than wild-type ones (3.6±0.3 vs. 4.9±0.1 g/100-kernels).

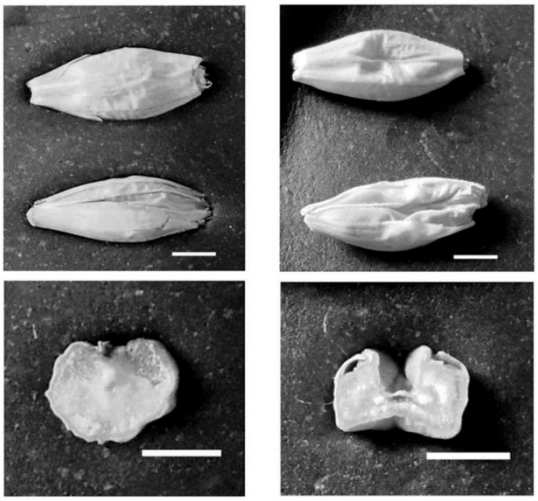

Figure 1. Seed morphology and transverse section of TILLING mutant line 1517-*SSIIa* (*Starch Synthase IIa*) (right) showing a shrunken phenotype, compared with cv. Morex wild-type (left). From top to bottom: adaxial and abaxial seed views, and seed cross section. White bars = 2 mm.

Total starch content

Total starch content was measured in whole flours obtained from two biological replicates for each of the nine mutant lines. The water content of the flours was very similar in all samples (≈9%, Table S1). Morex wt contained 43% starch on a fresh weight basis, but this value was diminished by one third in mutant 1517-*SSIIa* (27%, P<0.01; Table 2). In no other mutants the total starch content was significantly different to the wild-type value (P<0.05, n = 2).

	% starch		% amylose (enzymatic)		% amylose (colorimetric)	
Morex	42.5±1.3	(100)	32.3±3.2	(100)	33.4	(100)
2253-*BMY1*	47.7±2.7	(112)	31.9±1.9	(99)	34.0	(102)
2682-*BMY1*	46.2±0.6	(109)	34.4±0.9	(107)	29.0	(87)
1090-*GBSSI*	38.9±0.8	(92)	9.5±3.1 *	(29)	8.8	(26)
905-*LDA1*	44.2±0.5	(104)	31.0±2.2	(96)	30.8	(92)
1132-*SSI*	41.8±2.4	(98)	32.6±2.8	(101)	36.1	(108)
1284-*SSI*	40.6±1.1	(96)	34.5±1.0	(107)	35.9	(107)
5850-*SSI*	42.1±2.3	(99)	31.0±1.4	(99)	36.7	(110)
1039-*SSIIa*	43.1±2.1	(101)	34.9±0.7	(108)	36.4	(109)
1517-*SSIIa*	26.5±0.1 **	(62)	47.5±5.0 *	(147)	48.9	(146)

Total starch content is expressed as percentage of fresh weight (water content in flours was about 9%, with no significant differences among samples, see Table S1 in File S1). Amylose was detected either by enzymatic or colorimetric methods and it is expressed as a percentage of total starch. To facilitate comparisons, all values are also reported in brackets as percentage of the corresponding wild type value. Total starch and relative amylose content was determined on two biological replicates. Significant differences were detected by Student's t-test (P<0.05 = *; P<0.01 = **). For comparison, colorimetric analysis of amylose was performed on a single biological sample for each genotype, and data shown are means of 3 technical replicates (standard deviations were in all cases below 10% of the mean value).
doi:10.1371/journal.pone.0107779.t002

Table 2. Content of starch and amylose in seeds of TILLING mutant lines.

Amylose content

Whole flours from two biological replicates were also analysed for amylose content by enzymatic assay. For comparison, the relative content of amylose was also determined colorimetrically with similar results (Table 2). Wild-type starch contained 32% amylose and similar values were detected in seven over nine mutants (amylose/amylopectin ratio 0.47). However, mutant 1090-*GBSSI,* carrying a missense mutation in *Granule Bound Starch Synthase I*, contained only one third of the normal amylose content in its grain starch (9%, P<0.05; amylose/amylopectin ratio 0.10), and mutant 1517-*SSIIa,* carrying a nonsense mutation in *Starch Synthase IIa*, contained much more amylose than the wild-type (47%, P<0.05; amylose/amylopectin ratio 0.88; Table 2).

SDS-PAGE analysis

In order to assess whether the nine mutations identified had an effect on the electrophoretic protein profile typical of the starch granule proteins of barley, SDS-PAGE analysis was performed. With the exception of the lines 1517-*SSIIa* and 1284-*SSI*, all the mutants showed a profile identical to Morex wt, characterized by three major bands corresponding to SSIIa (overlapped with Starch Branching Enzyme II, SBEII), SSI and GBSSI [29] (Figure S1). The absence of the SSIIa enzyme was confirmed in the line 1517-*SSIIa*. Notably this mutant appeared to lack also SBEII and SSI isoforms. Moreover, although mutant 1284-*SSI* has no premature stop codon in the *SSI* gene, a drastic reduction of the SSI band was observed in starch granules (Figure 2).

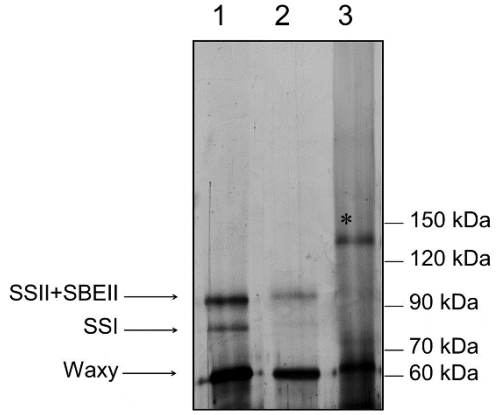

Figure 2. Electrophoretic separation (SDS–PAGE) of starch granule proteins extract from barley wild-type cv. Morex (1) and barley mutants 1284-*SSI* (2) and 1517-*SSIIa* (3). The bands corresponding to starch synthase II and starch branching enzyme II (SSII+SBEII), starch synthase I (SSI) and granule-bound starch synthase (GBSSI) are indicated. In lane 3, the high molecular weight band marked with an asterisk is probably due to impurities present in the starch preparation obtained from the shrunken seeds of line 1517-*SSIIa*. Molecular weight standard is schematically reported on the right.

Starch granules morphology

Starch extracts from wild-type and mutant grains were analysed by Scanning Electron Microscopy (SEM). With the exception of 1517-*SSIIa*, starch granules of all remaining samples were quite regularly shaped (Figure 3 and Figure S2). A quantitative analysis of granules dimensions was performed by collecting the length of the major and minor axis of 200-500 granules for each biological sample from their SEM digital images. Distribution of granule dimensions was clearly bimodal in all samples (Figure S2), with a major sub-population of small spherical granules (major axis <8 µm, B-granules), and a minor sub-population of larger discoid particles with a major axis varying between 8 and 30 µm (A-

granules). Distributions based on minor axis were qualitatively identical to those based on the major axis (not shown). Differently from all other mutants, starch of 1517-*SSIIa* contained irregularly shaped A-granules typically appearing like deflated spheres (Figure 3 and Figure S2 in File S1). B-granules were also irregular in shape and agglomerated. These features prevented a quantitative determination of A and B-type particles in 1517-*SSIIa* samples.

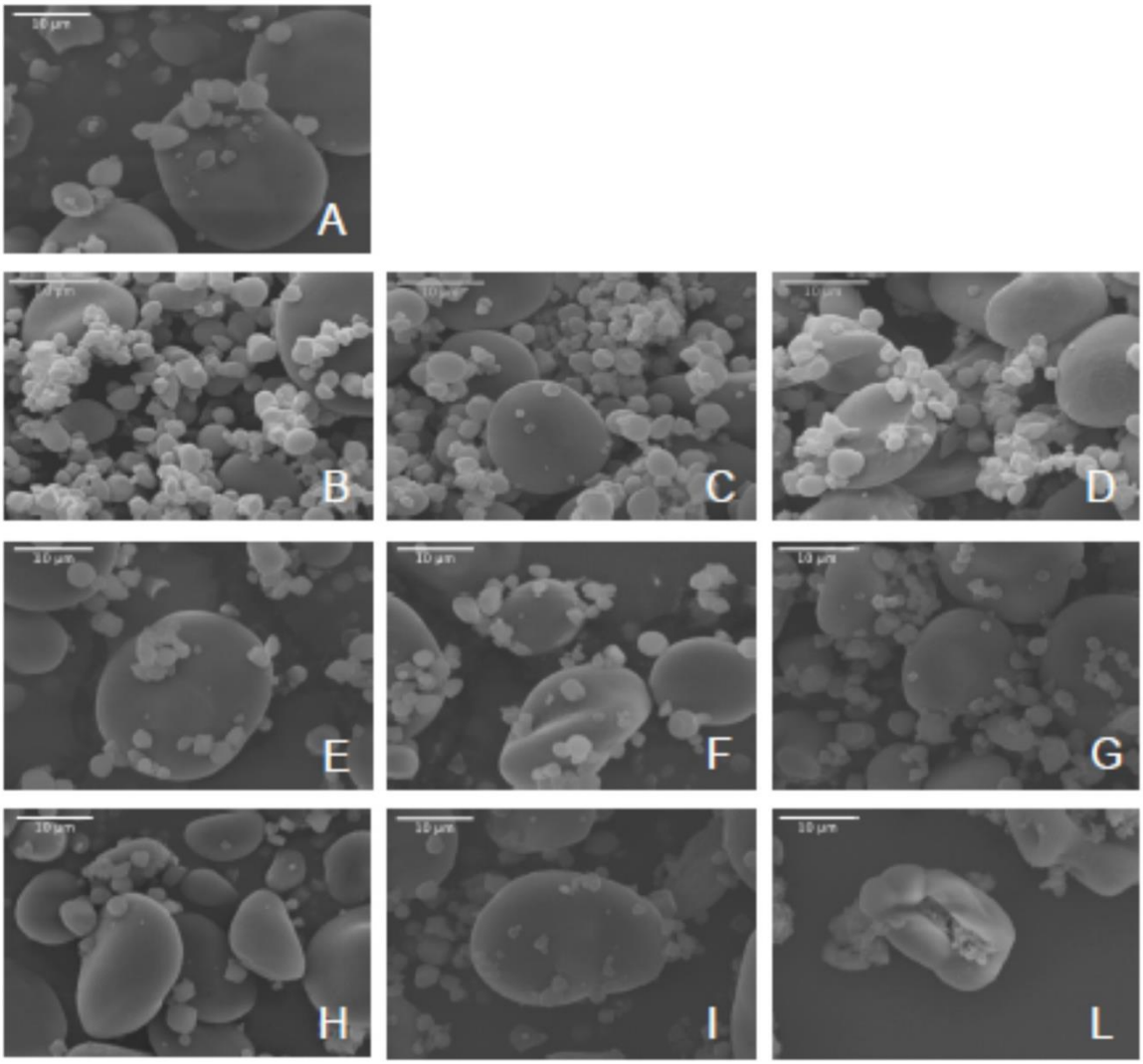

Figure 3. Scanning Electron Microscopy (SEM) analysis of starch granules from barley cv. Morex wild-type (A) and mutants 2253-*BMY1* (B), 2682-*BMY1* (C), 1090-*GBSSI* (D), 905-*LDA1* (E), 1132-*SSI* (F), 1284-*SSI* (G), 5850-*SSI* (H), 1039-*SSIIa* (I), 1517-*SSIIa* (L). Scale bar: 10 µm.

The percentage of B-granules (<8 µm) in wild-type purified starch was 73% (SD). A similar value was found in mutants of *BMY1*, *GBSSI* and *SSIIa* (Figure 4). In the four remaining mutants the percentage of B-granules differed significantly from the wild-type Morex

(P<0.01). B-granules were less abundant in two soluble starch synthase mutants, 1132-*SSI* (57%) and 5850-*SSI* (62%), but relatively more abundant in mutant 1284-*SSI* of the same gene (85%) and in mutant 905-*LDA1* of limit dextrinase I (85%) (Figure 4). All these four mutants contained missense mutations (Table 1).

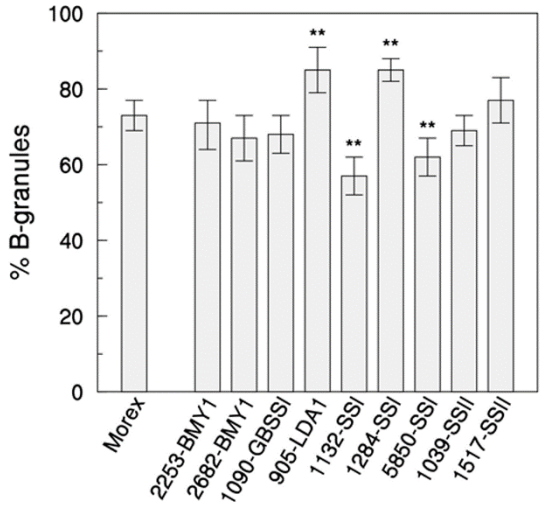

Figure 4. Percentage of B-type granules (diameter <8 µm) in grain starch of barley wild-type cv. Morex and mutant lines. Granules size distribution was determined on 10 couples of SEM images randomly collected for each genotype. Data shown are means ±SD (n = 10). Statistically significant differences between mutants and wild-type mean values were estimated by Student's t-test (P<0.01) and are highlighted by a double asterisk (**).

The average size of A- and B-granules in each sample was also analysed. In two mutants (5850-*SSI* and 1039-*SSIIa*, both missense mutations), A-type granules were significantly smaller (-25% major axis) than wt ones (17.1 µm) (Table 3; P<0.01). On the other hand, A-granules of 1284-*SSI* mutant were significantly larger (+15%) than wt ones. The average diameter of B-particles varied between 2.3 and 3.5 µm in all samples, with no significant differences between wt and mutants (Table 3). Interestingly, two missense mutants of *SSI* displayed symmetrical properties in A-granules size and frequency: in mutant 1284-*SSI* A-granules were larger but less abundant, while in mutant 5850-*SSI* they were relatively more numerous, but smaller in size (Table 3 and Figure 4).

	B-granules, major axis [µm]	A-granules, major axis [µm]
Morex	3.01±1.23	17.08±4.88
2253-*BMY1*	2.50±0.77	17.97±5.17
2682-*BMY1*	2.80±1.19	18.18±5.47
1090-*GBSSI*	2.26±0.86	16.49±7.24
905-*LDA1*	2.83±1.04	16.68±5.10
1132-*SSI*	3.45±1.09	17.70±4.38
1284-*SSI*	3.02±1.03	19.69±4.84 **
5850-*SSI*	3.38±1.86	13.15±3.41 **
1039-*SSIIa*	3.27±1.74	12.92±3.39 **
1517-*SSIIa*	Nd	Nd

Data are means ±SD of 200–500 granules measured for each genotype. Statistically significant differences as determined by Student's t-test are indicated (P<0.01 = **).
Nd, not determined (starch granules in 1517-*SSIIa* mutant were irregular in shape).
doi:10.1371/journal.pone.0107779.t003

Table 3. Length of major axis in A-type and B-type starch granules.

Crystallinity of starch granules

Crystallinity of starch granules was evaluated by X-ray powder diffraction. The crystallinity of wild-type starch was estimated as 29% and this value ranged between 26 and 33% in all mutants (Table 4), with no clear correlation between the degree of crystallinity and other phenotypic characters previously recorded. On the contrary, the type of crystallinity, as detected from the X-ray diffraction patterns, was more variable. In wild-type starch we estimated a large predominance of the A-type crystal pattern (81%), with a minor contribution of the V-type (Figure 5). No evidence for B-type crystallinity was obtained from diffraction patterns of wild-type and mutants. In most of the mutants, the type of crystallinity was similar to that observed in wild-type starch, *i.e.* 78-83% A-type and 17-22% V-type. Interestingly, however, in the low-amylose 1090-*GBSSI* mutant, crystallinity was almost exclusively of the A-type (92%) whereas in the high amylose 1517-*SSIIa* mutant crystallinity was prevalently of the V-type (76%) (Figure 5 and Table 4).

	% crystallinity	$I_{A\text{-}type}$	$I_{V\text{-}type}$
Morex	0.29	0.81	0.19
2253-BMY1	0.30	0.82	0.18
2682-*BMY1*	0.33	0.80	0.20
1090-*GBSSI*	0.26	0.92	0.08
905-*LDA1*	0.27	0.81	0.19
1132-*SSI*	0.28	0.79	0.21
1284-*SSI*	0.27	0.79	0.21
5850-*SSI*	0.27	0.80	0.20
1039-*SSIIa*	0.26	0.78	0.22
1517-*SSIIa*	0.29	0.24	0.76

These latter data represent a relative estimation of A-type and V-type crystallinity, respectively.
doi:10.1371/journal.pone.0107779.t004

Table 4. Percentage crystallinity and relative intensity of diffraction peaks at 15.1° and 19.7°.

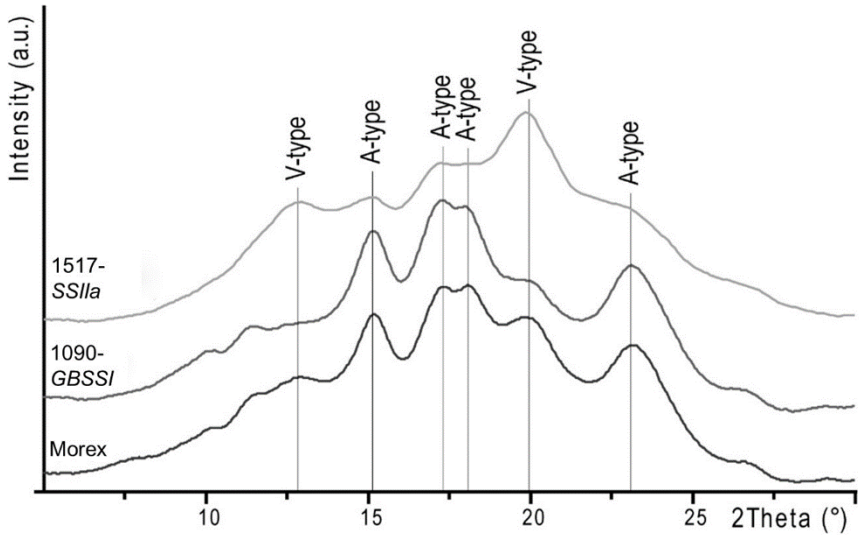

Figure 5. X-ray diffraction patterns of native starch extracts from barley wild-type cv. Morex (black) and mutants 1090-*GBSSI* (grey) and 1517-*SSIIa* (light grey). The characteristic peaks of the A-type and V-type polymorphs are indicated.

DISCUSSION

Starch structure and chemical composition are genetically determined by a large set of genes [5], [6], [8], [30] and the potential for obtaining different types of starch by screening natural or induced genetic variability is huge. TILLING provides a non-transgenic approach to explore this potential [7], [12], [22], [31], [32], [33], [34], [35], [36]. We exploited TILLING to identify and phenotypically characterize new alleles of five genes involved in grain starch metabolism of barley.

Granule bound starch synthase (*GBSSI*)

Granule-bound starch synthase I (*GBSSI*) [4] is specifically expressed in the endosperm of barley [30] where it is known to exert a tight control on the biosynthesis of amylose [37]. GBSSI is coded by the *waxy* locus and barley cultivars with altered GBSSI activity contain altered levels of amylose in grains, ranging between 0 and 41% of total starch [29]. Besides amylose, GBSSI is also involved in the synthesis of extra long glucan chains of amylopectin, such that also amylopectin may be modified in *waxy* mutants [38], [39], [40]. Low-amylose varieties can be used for food applications because of their peculiar starch features (low gelatinization temperature and retrogradation), that confer high freeze-thaw stability and anti-stailing properties to processed food [41], [42].

Here we report a new allele of *GBSSI* with a G493E point mutation. Grain starch of this mutant (1090-*GBSSI*) contains less than 10% amylose (vs. 30% of wild-type) and is thus defined low-amylose or near-waxy. Crystallinity of 1090-*GBSSI* starch was found to be largely A-type, with a minor contribution of the V-type pattern. A similar profile has been previously reported in low amylose barley [43], [44].

Plant starch synthases (both granule bound and soluble isoforms) are proteins of about 60-120 kDa that belong to the glycosyltransferase family GT-5 [4]. They typically contain a catalytic domain formed by two Rossman fold domains delimiting a deep cleft where the catalytic site is located (Figure 6). In plant starch synthases, the catalytic domain is often preceded by an N-terminal sequence of variable length and no clear function. The crystal structure of the catalytic domain of rice GBSSI [45] was used as a template to model barley GBSSI (the two proteins are 84% identical in amino acid sequence). According to the model, glycine-493 belongs to an alpha-helix of the second, C-terminal Rossman fold domain at approximately 10 Å from the ADP binding pocket [45] and 6 Å from the conserved STGGL motif suspected to be involved in catalysis and/or substrate binding [29].

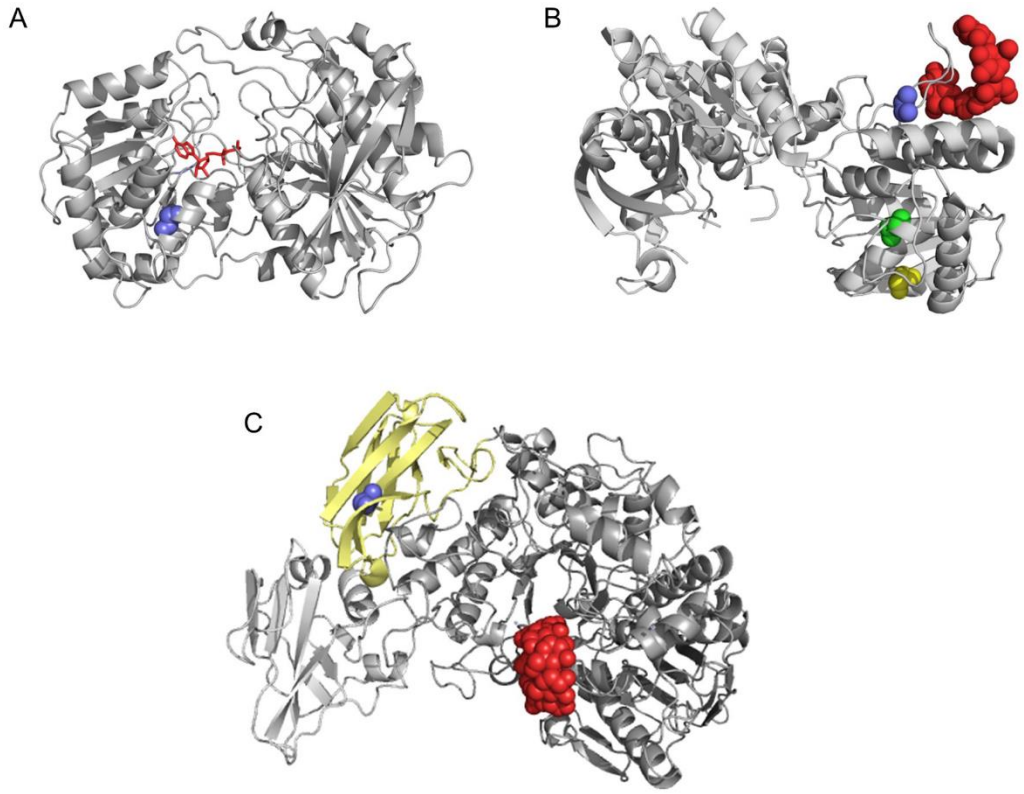

Figure 6. Localization of point mutations in the 3D structures of barley GBSSI, SSI and LDA1. A) Barley GBSSI was modelled by Swissmodel using the catalytic domain of wild-type rice GBSSI complexed with ADP as a template (pdb 3VUF). The two mature proteins are 84% identical in sequence. The main chain of glycine-493 is represented by blue spheres. In mutant 1090-*GBSSI,* glycine-493 is substituted by a glutamate (G493E). Co-crystallized ADP of the rice GBSSI structure (3VUF) is superimposed to highlight the adenine nucleotide binding site. B) Crystal structure of barley SSI, co-crystallized with a molecule of maltopentaose (red spheres) (pdb 4HLN). Main chain atoms of mutated residues are represented by coloured spheres: blue (G576D in mutant 5850-*SSI*), green (T522I in mutant 1132-*SSI*) and yellow (G509E in mutant 1284-*SSI*). C) Crystal structure of barley LDA1 (pdb 2X4B). The carbohydrate binding module CBM48 is coloured yellow. Residue no. 270 (blue spheres corresponding to main chain atoms) is part of the CBM48 domain. Mutant 905-*LDA1* carries a V270I mutation. A molecule of betacyclodextrine (red spheres) co-crystallized with the protein highlights the putative active site.

Several near-waxy cultivars are known in barley, all carrying a large deletion in the promoter region of the *GBSSI* gene that results in strongly diminished expression of the enzyme [29], [46]. Waxy cultivars with no detectable amylose are also known (e.g. cv. CDC Alamo and CDC Fibar) but they contain point mutations in the coding sequence that likely cause complete inactivation of the enzyme without drastically affecting the protein abundance in starch granules [29]. Interestingly, mutation G493E in 1090-*GBSSI* seems to

modulate, rather than inactivate, enzyme activity as demonstrated by the residual content of amylose (10%) detected in its starch. Moreover, this effect is obtained without altering protein expression, as suggested by the SDS-PAGE pattern identical to the wild-type. Indeed, mutation G493E may prove useful for the understanding the little known catalytic mechanism of GBSSI.

Limit dextrinase (*LDA1*)

Together with isoamylases (ISAs), limit dextrinases (LDAs, also known as pullulanases) constitute the set of starch debranching enzymes. The role of ISAs in removing excess branches of amylopectin formed by branching enzymes is well known [8]. In the absence of isoamylases, starch is synthesized in a highly branched form known as phytoglycogen [47]. Barley limit dextrinase is coded by a single gene (*LDA1*) and is apparently involved both in starch biosynthesis and degradation [48]. *In vivo*, the activity of LDA1 is regulated by a proteinaceous inhibitor LDI [49], and antisense transgenic barley with lower expression of LDI showed higher LDA1 activity and a lower percentage of B-granules (*i.e.* inhibition of granule initiation) and lower amylose/amylopectin ratio [50]. It was suggested that LDA, which is expressed when B-granules are formed, may play a role in reducing the amount of primers that allows the nucleation of small B-granules. In our study, we have found a mutant of *LDA1* (905-*LDA1*) with a higher percentage of small B-granules that further supports the role of this enzyme in starch granule initiation.

The tridimensional structure of barley *LDA1* has been solved [51]. The protein is made of four domains: the N-terminal domain, the CBM48 domain, the catalytic domain and the C-terminal domain. Valine-270 of *LDA1*, that in mutant 905-*LDA1* is substituted by a more bulky isoleucine, belongs to the carbohydrate binding module CBM48 and is located close to the interface with the catalytic domain (Figure 6). It is plausible that the substitution of valine in isoleucine (V270I) in the CBM48 domain may reduce the capability of the protein to bind glucans and in turn inhibit, albeit indirectly, its scavenging activity toward primers of granules nucleation. Consistently, starch of mutant 905-*LDA1* is formed by a larger number of granules (predominantly small B-granules) and the role of LDA1 in controlling granule nucleation is further supported.

Soluble starch synthase I (*SSI*)

In plants, soluble starch synthases are divided into four classes with different specificity (from *SSI* to *SSIV*), and some of them are represented by more than one isoform [4], [8], [9]. While *SSIV* is probably involved in starch granule initiation [52], *SSI* preferentially synthesize short glucan chains using short amylopectin chains as substrate [5], [8]. These short amylopectin chains may then be prolonged by *SSII* and *SSIII* [5], [8], but individual roles and cooperation between different starch synthases in building the starch granule are still undefined, in barley at least. Mutants in rice and wheat clearly suggest that the activity of the different starch synthases is not necessarily sequential and the lack of SSI may be partially compensated *in vivo* [8], [53], [54].

In cereals *SSI* is represented by a single isoform. We have analysed three missense mutations in *SSI* and all of them showed starch phenotypes consisting in modifications in either size or frequency of A- and B-granules. However, our results may appear contradictory: in fact two mutants showed a higher % of A-type granules (1132-*SSI* and 5850-*SSI*), while the third mutant had more B-type granules (1284-*SSI*). Morever, the A-granules of mutant 5850-*SSI* were more abundant but smaller in size and, symmetrically, the A-granules of mutant 1284-*SSI* were larger but less frequent. Only in mutant 1132-*SSI* the higher percentage of A-granules was not compensated by a reduction in size. The unexpected phenotypic difference between the three mutant lines may be due to currently unknown additional background mutations present in the genome of TILLMore mutant lines [23].

However, some hints could be obtained from the recently solved crystallographic structure of barley *SSI* [55] (Figure 6). The G576D substitution of mutant 5850-*SSI* is localized at the base of a loop involved in the formation of a high affinity binding site for maltooligosaccharides. This site is 30 Å away from the putative catalytic site, but is believed essential for colocalizing branched glucans and *SSI*, thereby favoring catalysis. Moreover, the starch phenotype associated to the G576D mutation (smaller A-granules) may suggest a role of this site in controlling the final size of large starch granules. The other two point mutations here described (Figure 6) are localized in regions of the protein not yet characterized, providing no suggestions to understand their role. Nevertheless, the high percentage of large A-granules in mutant 1132-*SSI* is interesting because this is a desirable trait for malting [10].

Initiation of A and B-granules are separated events, although little is known of the genetic control of this trait in Triticeae. In barley, A-granules are nucleated at 4–14 days post-anthesis, during endosperm cell division, while small B-granules are nucleated later, during endosperm cell growth [56]. A QTL controlling B-granules initiation was recently described in wild wheat Aegilops [10] and in Arabidopsis, SSIV is believed to positively regulate granule initiation [52]. Recently the suppression of *SSI* expression in wheat grains using RNAi technology led to the production of lines with a reduced proportion of B-granules [54]. All three *SSI* barley mutants analysed in this work showed an abnormal distribution between large and small granules. However, because of the complexity of our results, any conclusion about a possible role of SSI in granule initiation in barley is premature.

Soluble starch synthase IIa (*SSIIa*)

SSIIa is the major SS isoform of barley endosperm during grain filling [4]. Mutant *sex6* of barley cv. Himalaya has no *SSIIa* activity and produces shrunken kernels containing starch made of up to 70% amylose [15], [16]. *SSIIa* knock-out mutants are particularly interesting for industrial applications because of their higher level of amylose and resistant starch in the endosperm. Resistant Starch is associated with several human health benefits, including the prevention of the colon cancer, type-II diabetes and obesity [13], [19]. In this work, we identified a mutant line with A-granule of smaller size carrying a missense mutation (1039-*SSIIa*), and a *SSIIa* null mutant (1517-*SSIIa*) characterized by small/shrunken seeds and containing less starch with more amylose (48% of grain starch is made of amylose in this mutant). The SDS-PAGE analysis of starch extracted from 1517-*SSIIa* confirmed the absence of the protein *SSIIa*, together with *SBEII* and *SSI* isoforms. The simultaneous absence of *SSIIa*, *SBEII* and *SSI* in the starch granule was already observed in *SSIIa* mutants of barley, bread and durum wheat [14], [57], [58].

Starch crystallinity of 1517-*SSIIa* was largely characterized by a V-type diffraction pattern suggesting the formation of lipid-amylose complexes, similarly to those observed in the *sex6* mutant [15]. In the missense mutant 1039-*SSIIa*, in spite of the smaller size of A-granules, no other starch parameters including crystallinity were significantly affected. In barley endosperm, *SSIIa* was shown to extend short amylopectin glucan chains of 3-8 glucose units to chains of up to 35 units [15]. Consistently, the lack of *SSIIa* negatively

affects amylopectin synthesis, more than amylose synthesis [16], and mutant 1517-*SSIIa* is fully consistent with these results.

CONCLUSIONS

TILLING of five genes encoding enzymes involved in starch metabolism enabled us to identify seven new alleles that are associated with new starch phenotypes in terms of amylose/amylopectin ratio, or crystal packing, or distribution of A- and B-granules, or size of A-granules (Table 1). Our results confirmed the role played by granule-bound starch synthase (*GBSSI*) in controlling amylose biosynthesis and, conversely, the role played by soluble starch synthase IIa (*SSIIa*) in controlling amylopectin synthesis. Starch granule initiation appeared to be controlled by limit dextrinase (*LDA1*), and size of A-granules by starch synthases IIa. Thanks to their physical-chemical properties, these new alleles deserve further attention in order to investigate their possible interest in nutritional uses or industrial applications.

REFERENCES

1. Collins HM, Burton RA, Topping DL, Liao M-L, Bacic A, et al. (2010) Variability in fine structures of noncellulosic cell wall polysaccharides from cereal grains: potential importance in human health and nutrition. Cereal Chem 87: 272–282.
2. The International Barley Genome Sequencing Consortium (2012) A physical, genetic and functional sequence assembly of the barley genome. Nature 491: 711–716.
3. Buléon A, Colonna P, Planchot V, Ball S (1998) Starch granules: structure and biosynthesis. Int J Biol Macromol 23: 85-112.
4. Ball SG, Morell MK (2003) From bacterial glycogen to starch: understanding the biogenesis of the plant starch granule. Annu Rev Plant Biol 54: 207-233.
5. James MG, Denyer K, Myers A (2003) Starch synthesis in the cereal endosperm. Curr Opin Plant Biol 6: 215-222.
6. Jobling S (2004) Improving starch for food and industrial applications. Curr Opin Plant Biol 7: 210-218.
7. Morell MK, Myers AM (2005) Towards the rational design of cereal starches. Curr Opin Plant Biol 8: 204-210.

8. Jeon JS, Ryoo N, Hahn TR, Walia H, Nakamura Y (2010) Starch biosynthesis in cereal endosperm. Plant Physiol Bioch 48: 383-392.
9. Zeeman SC, Kossmann J, Smith AM (2010) Starch: its metabolism, evolution, and biotechnological modification in plants. Annu Rev Plant Biol 61: 209-234.
10. Mazanec K, Dycka F, Bobalova J (2011) Monitoring of barley starch amylolysis by gravitational field flow fractionation and MALDI-TOF MS. J Sci Food Agric 91: 2756–2761.
11. Howard T, Rejab NA, Griffiths S, Leigh F, Leverington-Waite M et al. (2011) Identification of a major QTL controlling the content of B-type starch granules in Aegilops. J Exp Bot 62: 2217-2228.
12. Slade AJ, Fuerstenberg SI, Loeffler D, Steine MN, Facciotti D (2005) A reverse genetic, nontransgenic approach to wheat crop improvement by TILLING. Nat Biotechnol 23: 75-81.
13. Bird AR, Vuaran MS, King RA, Noakes M, Keogh J et al. (2008) Wholegrain foods made from a novel high-amylose barley variety (Himalaya 292) improve indices of bowel health in human subjects. Brit J Nutr 99: 1032-1040.
14. Damiran D, Yu P (2010) Chemical profile, rumen degradation kinetics, and energy value of four hull-less barley cultivars: comparison of the zero-amylose waxy, waxy, high-amylose, and normal starch cultivars. J Agric Food Chem 58: 10553-10559.
15. Morel MK, Kosar-Hashemi B, Cmiel M, Samuel MS, Chandler P et al. (2003) Barley sex6 mutants lack starch synthase IIa activity and contain a starch with novel properties. Plant J 34: 173-185.
16. Li Z, Li D, Du X, Wang H, Larroque O et al. (2011) The barley amo1 locus is tightly linked to the starch synthase IIIa gene and negatively regulates expression of granule-bound starch synthase genes. J Exp Bot 62: 5217-5231.
17. Asare EK, Jaiswal S, Maley J, Båga M, Sammynaiken R et al. (2011) Barley grain constituents, starch composition, and structure affect starch in vitro enzymatic hydrolysis. J Agric Food Chem 59: 4743–4754.
18. Nugent AP (2005) Health properties of resistant starch. Nutrition Bulletin 30: 27–54.
19. Topping D (2007) Cereal complex carbohydrates and their contribution to human health. Trends Food Sci Technol 46: 220-229.
20. Dhital S, Shrestha AK, Hasjim J, Gidley MJ (2011) Physicochemical and structural properties of maize and potato starches as a function of granule size. J Agric Food Chem 59: 10151-10161.
21. MacGregor AW (1991) The effect of barley structure and composition on malt duality, in Proceedings of the European Brewery Convention Congress, Lisbon, Portugal, pp. 37–42.
22. Bovina R, Talamè V, Salvi S, Sanguineti MC, Trost P et al. (2011) Starch metabolism mutants in barley: a TILLING approach Plant Genetic Resources: Characterization and Utilization 9: 170–173.
23. Talamè V, Bovina R, Sanguineti MC, Tuberosa R, Lundqvist U et al. (2008) TILLMore, a resource for the discovery of chemically induced mutants in barley. Plant Biotechnol J 6: 477-485.
24. Kim K, Johnson W, Graybosch RA, Gaines CS (2003) Physicochemical properties and end-use quality of wheat starch as a function of waxy protein alleles. J Cereal Sci 37: 195-204.

25. Zhao XC, Sharp PJ (1996) An improved 1-D SDS-PAGE method for the identification of three bread wheat waxy proteins. J Cereal Sci 23: 191-193.
26. Mohammadkhani A, Stoddard FL, Marshall DR, Uddin MN, Zhao X (1999) Starch extraction and amylose analysis from half seeds. Starch/Stärke 51: 62-66.
27. Sestili F, Janni M, Doherty A, Botticella E, D'Ovidio R et al. (2010) Increasing the amylose content of durum wheat through silencing of the SBEIIa genes. BMC Plant Biol 10: 144.
28. Nara S, Komiya T (1983) Studies on the relationship between water-saturation state and crystallinity by the diffraction method for moistened potato starch. Starch/Stärke 35: 407–410.
29. Asare EK, Baga M, Rossnagel BG, Chibbar RN (2012) Polymorphism in the barley granule bound starch synthase 1 (gbss1) gene associated with grain starch variant amylose concentration. J Agric Food Chem 60: 10082-10092.
30. Radchuk VV, Borisjuk L, Sreenivasulu N, Merx K, Mock HP et al. (2009) Spatiotemporal profiling of starch biosynthesis and degradation in the developing barley grain. Plant Physiol 150: 190-204.
31. Sestili F, Botticella E, Bedo Z, Phillips A, Lafiandra D (2010) Production of novel allelic variation for genes involved in starch biosynthesis through mutagenesis. Molecular Breeding 25: 145-154.
32. Vriet C, Welham T, Brachmann A, Pike M, Pike J et al. (2010) A suite of Lotus japonicus starch mutants reveals both conserved and novel features of starch metabolism. Plant Physiol 154: 643-655.
33. Botticella E, Sestili F, Hernandez-Lopez A, Phillips A, Lafiandra D. High resolution melting analysis for the detection of EMS induced mutations in wheat SBEIIa genes. BMC Plant Biol. 10: 156.
34. Hazard B, Zhang X, Colasuonno P, Uauy C, Beckles DM et al. (2012) Induced mutations in the *starch branching enzyme II* (*SBEII*) genes increase amylose and resistant starch content in pasta wheat. Crop Sci 52: 1754–1766.
35. Slade AJ, McGuire C, Loeffler D, Mullenberg J, Skinner W et al. (2012) Development of high amylose wheat through TILLING. BMC Plant Biol 12: 69.
36. Bovina R, Brunazzi A, Gasparini G, Sestili F, Palombieri S et al. (2014) Development of a TILLING resource in durum wheat for reverse- and forward-genetics analyses. Crop & Pasture Science 65: 112–124.
37. Nelson OE, Rines HW (1962) The enzymatic deficiency in the waxy mutant of maize. Biochem Biophys Res Comm 9: 297–300.
38. Maddelein ML, Libessart N, Bellanger F, Delrue B, D'Hulst C et al. (1994) Toward an understanding of the biogenesis of the starch granule: determination of granule-bound and soluble starch synthase functions in amylopectin synthesis. J Biol Chem 269: 25150–25157.
39. Denyer K, Waite D, Edwards A, Martin C, Smith AM (1999) Interaction with amylopectin influences the ability of granule-bound starch synthase I to elongate malto-oligosaccharides. Biochem J 342: 647–653.
40. Yoo SH, Jane J-L (2002) Structural and physical characteristics of waxy and other wheat starches. Carbohydr Polym 49: 297-305.

41. Baik BK, Ullrich SE (2008) Barley for food: characteristics, improvement and renewed interest. J Cereal Sci 48: 233-242.
42. Howard TP, Fahy B, Leigh F, Howell P, Powell W et al. (2014) Use of advanced recombinant lines to study the impact and potential of mutations affecting starch synthesis in barley. J Cereal Sci 59: 196-202.
43. Waduge R, Hoover R, Vasanthan T, Gao J, Li J (2006) Effect of annealing on the structure and physicochemical properties of barley starches of varying amylose content. Food Res Int 39: 59–77.
44. Naguleswaran S, Vasanthan T, Hoover R, Bressler D (2013) The susceptibility of large and small granules of waxy, normal and high-amylose genotypes of barley and corn starches toward amylolysis at sub-gelatinization temperatures. Food Res Int 51: 771–782.
45. Momma M, Fujimoto Z (2012) Interdomain disulfide bridge in the rice granule bound starch synthase I catalytic domain as elucidated by X-ray structure analysis. Biosci Biotech Bioch 76: 1591-1595.
46. Patron NJ, Smith AM, Fahy BF, Hylton CM, Naldrett MJ et al. (2002) The altered pattern of amylose accumulation in the endosperm of low-amylose barley cultivars is attributable to a single mutant allele of granule-bound starch synthase I with a deletion in the 5'-non-coding region. Plant Physiol 130: 190-198.
47. Burton RA, Jenner H, Carrangis L, Fahy B, Fincher GB et al. (2002) Starch granule initiation and growth are altered in barley mutants that lack isoamylase activity. Plant J 31: 97–112.
48. Fujita N, Toyosawa Y, Utsumi Y, Higuchi T, Hanashiro I et al. (2009) Characterization of pullulanase (PUL)-deficient mutants of rice (Oryza sativa L.) and the function of PUL on starch biosynthesis in the developing rice endosperm. J Exp Bot 60: 1009-1023.
49. Huang Y, Cai S, Ye L, Han Y, Wu D et al. (2014) Genetic architecture of limit dextrinase inhibitor (LDI) activity in Tibetan wild barley. BMC Plant Biol 14: 117.
50. Stahl Y, Coates S, Bryce JH, Morris PC (2004) Antisense downregulation of the barley limit dextrinase inhibitor modulates starch granule size distribution, starch composition and amylopectin structure. Plant J 39: 599-611.
51. Vester-Christensen MB, Abou Hachem M, Svensson B, Henriksen A. (2010) Crystal structure of an essential enzyme in seed starch degradation: barley limit dextrinase in complex with cyclodextrins. J Mol Biol 403: 739-750.
52. Roldán I, Wattebled F, Mercedes Lucas M, Delvallé D, Planchot V et al. (2007) The phenotype of soluble starch synthase IV defective mutants of *Arabidopsis thaliana* suggests a novel function of elongation enzymes in the control of starch granule formation. Plant J 49: 492-504.
53. Fujita N, Yoshida M, Asakura N, Ohdan T, Miyao A et al. (2006) Function and characterization of starch synthase I using mutants in rice. Plant Physiol 140: 1070-1084.
54. McMaugh SJ, Thistleton JL, Anschaw E, Luo J, Konik-Rose C et al. (2014) Suppression of starch synthase I expression affects the granule morphology and granule size and fine structure of starch in wheat endosperm. J Exp Bot 65: 2189-2201.

55. Cuesta-Seijo JA, Nielsen MM, Marri L, Tanaka H, Beeren SR et al. (2013) Structure of starch synthase I from barley: insight into regulatory mechanisms of starch synthase activity. Acta Crystallogr D Biol Crystallogr 69: 1013-1025.
56. Jane J-L, Kasemsuwa T, Leas S, Ames IA, Zobel H et al. (1994) Anthology of starch granule morphology by scanning electron microscopy. Starch 46: 121-129.
57. Yamamori M, Fujita S, Hayakawa K, Matsuki J, Yasui T (2000) Genetic elimination of a starch granule protein, SGP-1, of wheat generates an altered starch with apparent high amylose. Theor Appl Genet 101: 21-29.
58. Lafiandra D, Sestili F, D'Ovidio R, Janni M, Botticella E et al. (2010) Approaches for the modification of starch composition in durum wheat. Cereal chem 87: 28-34.

SUPPORTING INFORMATION

	Water content (%)
Morex	8.78±1.10
2253-*BMY1*	9.16±1.48
2682-*BMY1*	7.59±1.63
1090-*GBSSI*	9.28±1.98
905-*LDA1*	9.69±1.20
1132-*SSI*	9.74±0.26
1284-*SSI*	10.26±1.44
5850-*SSI*	9.77±0.61
1039-*SSIIa*	9.97±1.55
1517-*SSIIa*	8.58±1.64

Table S1. Water content in whole flours of TILLING mutant lines. Dry weight was obtained after incubation of samples at 80°C for 24h. Data are means ± SD (n=4).

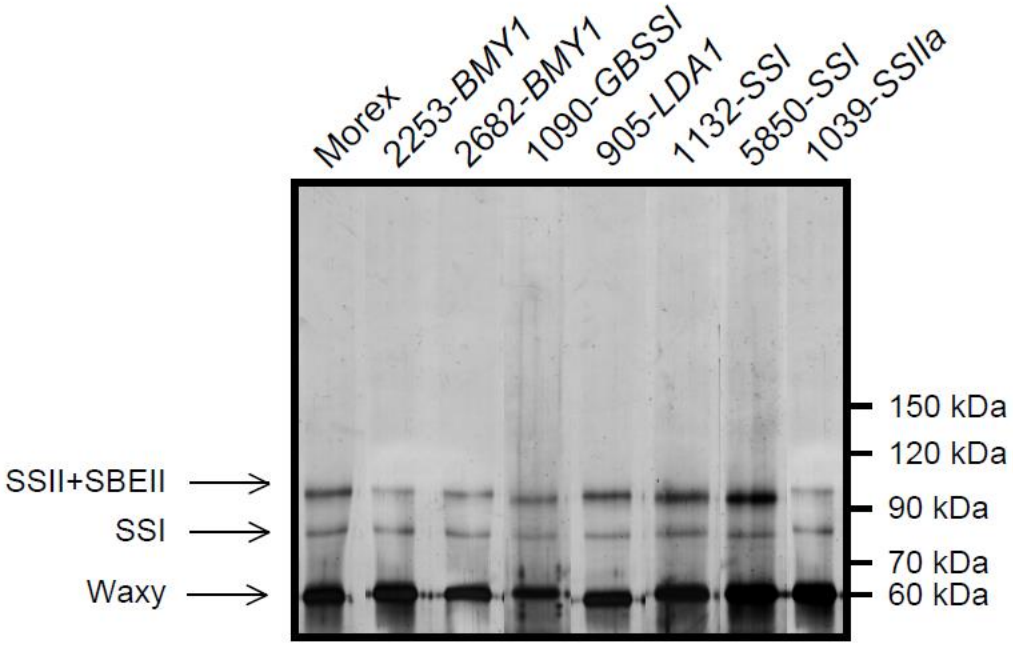

Figure S1. SDS–PAGE separation of starch protein extract from cv. Morex and barley mutants.

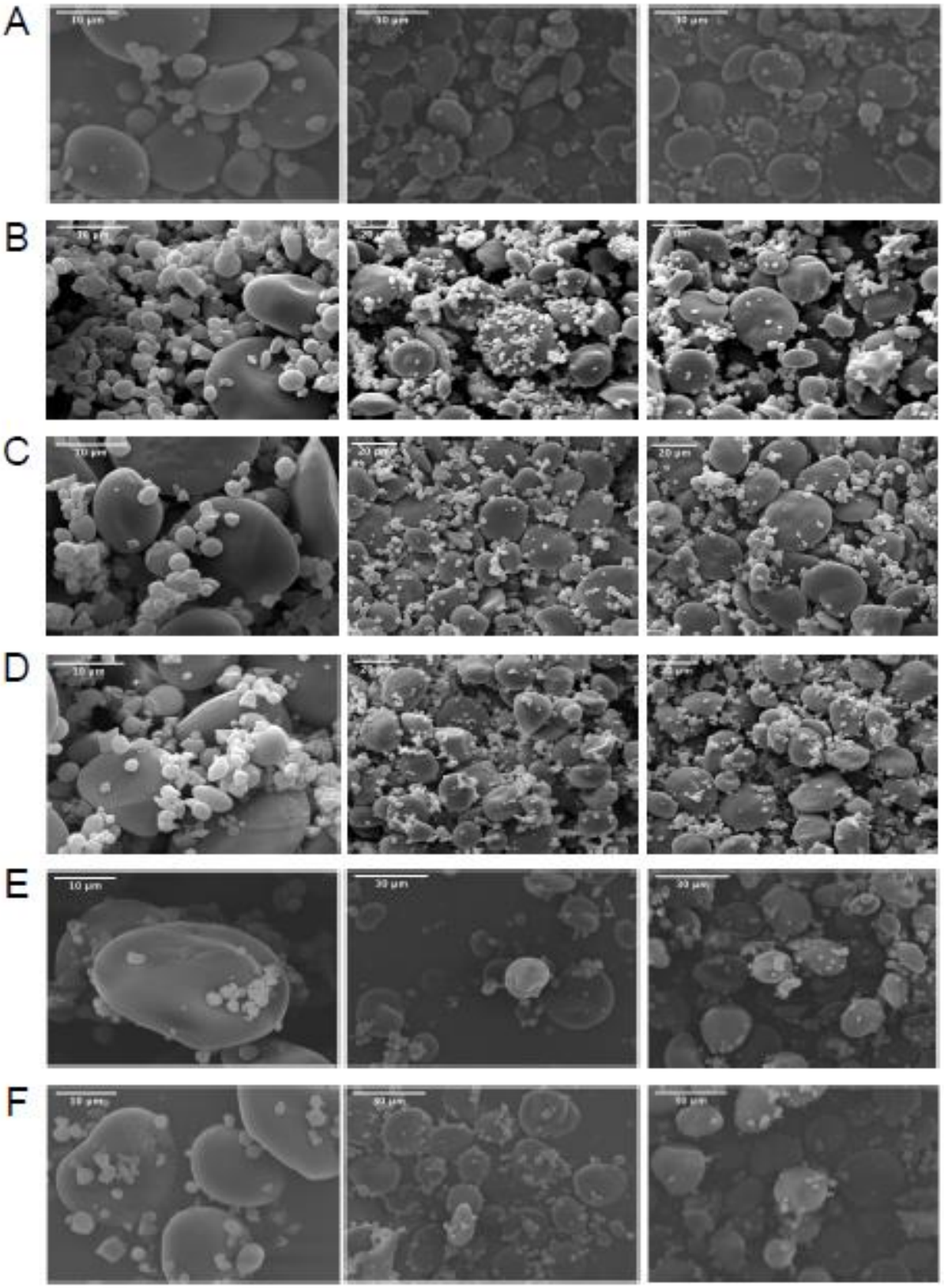
A
B
C
D
E
F

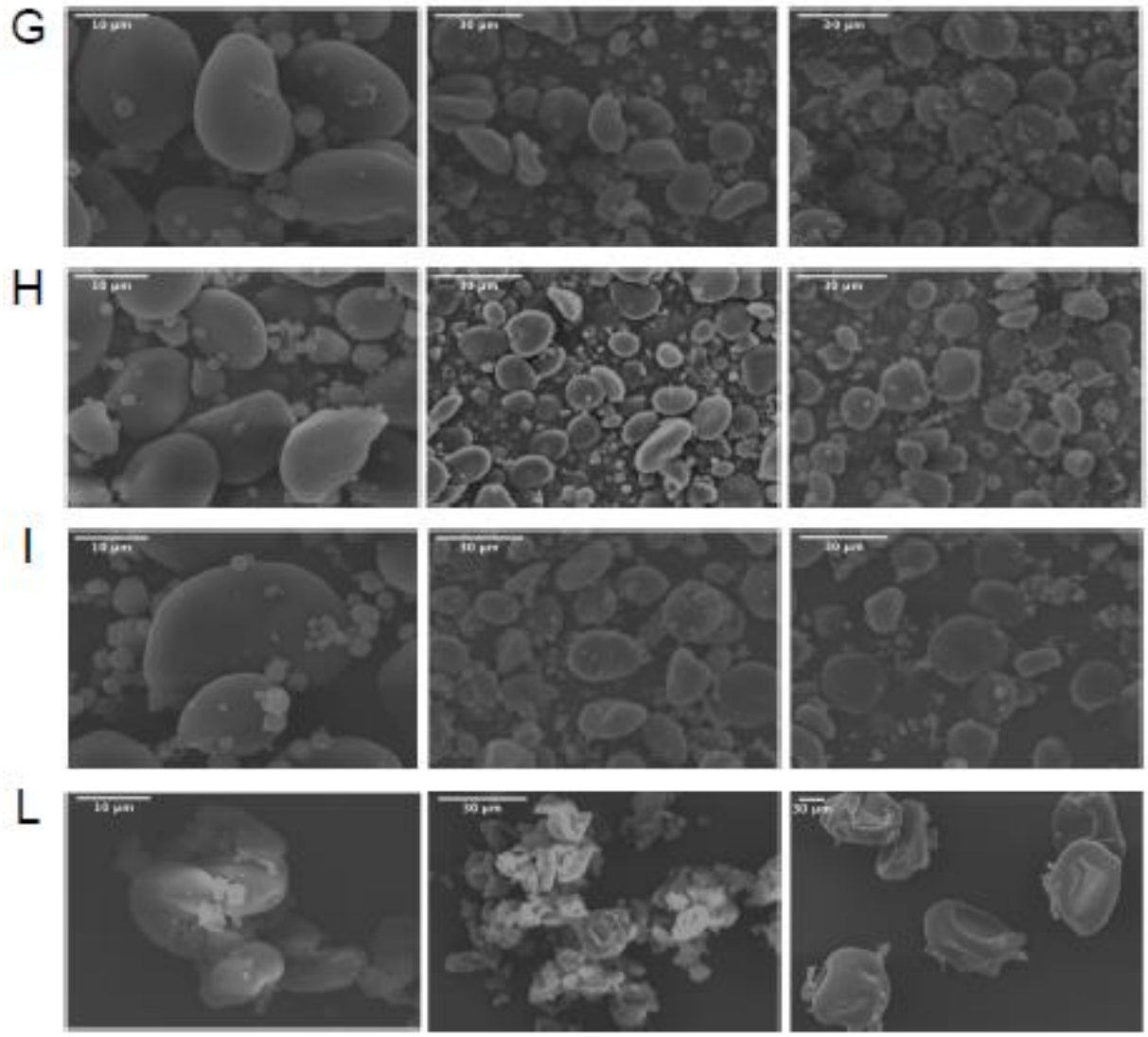

Figure S2. SEM analysis of starch granules from cv. Morex (A) and barely mutants 2253-*BMY1* (B), 2682-*BMY1* (C), 1090-*GBSSI* (D), 905-*LDA1* (E), 1132-*SSI* (F), 1284-*SSI* (G), 5850-*SSI* (H), 1039-*SSIIa* (I), 1517-*SSIIa* (L). Scale bars: 10, 20, and 30 µm.

CHAPTER 2

Starch phosphorylating enzymes are required for a proper development of Arabidopsis plants

Submitted to Plant Biology – Under review

Claudia Pirone[1], Ivan Gaiba[1], Alessio Adamiano[2], Paolo Trost[1], Francesca Sparla[1]

[1]Department of Pharmacy and Biotechnology FaBiT, University of Bologna, Via Irnerio 42, 40126 Bologna, Italy

[2]Department of Chemistry "G. Ciamician", University of Bologna, Via Selmi 2, 40126 Bologna, Italy

Abstract

The genome of *Arabidopsis thaliana* encodes two glucan, water dikinases, here reported as GWD1 and GWD2, and one phosphoglucan, water dikinase, named PWD. From a catalytic point of view, both GWDs and PWD destabilize the α-helices of starch granule, changing its physicochemical properties through the addition of phosphate groups to the amylopectin chains. Their activity is therefore necessary to the correct mobilization of transitory starch. Here we report that mutants lacking GWD1, GWD2 or PWD have an inefficient starch metabolism that afflicts plants growth and development, albeit to different extents. In comparison to wild-type, all mutants have seeds with a higher density, mainly ascribable to the decrease of lipids and to an increased accumulation of starch or seed coats. Apart from the *sex* phenotype characteristic of *gwd1* and *pwd1*, only *gwd1* appears to be clearly different from wild-type plants, in that it requires about 50% more time to reach the reproductive phase. As a consequence, the number of rosette leaves in *gwd1* is about 1.3 fold higher than in wild-type. The growth of mutants in continuous light do not fully revert the phenotype, suggesting that they do not suffer exclusively from carbon limitation. Considering that in *gwd1* the increase in biomass is associated with a small reduction of seeds productivity, this mutation could be of industrial interest providing plants with both good production of seeds and biomass. Moreover, the high accumulation of starch in leaves could increase the value of this raw material.

Structured abstract:

(1) Phosphoesterification of starch granules is of primary relevance in transitory starch

degradation.

(2) Single mutants lacking glucan, water dikinase 1 (GWD1), GWD2 or phosphoglucan, water dikinase (PWD) were compared with wild-type plants during their entire life cycle.

(3) All mutations altered plant development, albeit at different extent. Continuous low intensity light did not revert phenotypic traits, but conferred an identical behaviour among mutants but different from wild-type.

(4) Proper starch mobilization is not required for plant nutrition only. We suggest that starch accumulation above a threshold value could be integrated by hormone signals to drive the correct plant growth in respect to its energetic level.

INTRODUCTION

Atmospheric CO_2 is fixed into organic carbon skeletons by photosynthesis. Following the initial step of sugars production, sugars are partitioned to the non-photosynthetic tissues. Many studies reported that up to 80% of photosynthetic fixed carbon is exported from mature leaves to feed the heterotrophic tissues (Kalt-Torres *et al.* 1987; Komor 2000; Guo *et al.* 2002). Therefore, sink tissues are the primary consumers of newly fixed CO_2. However, the relationships between source and sink tissues are affected by many environmental and developmental factors, and a sink organ (e.g. seeds formation) can become a source (e.g. seed germination) depending on the developmental stage of the plant.

Photoassimilates divide into soluble sugars and insoluble starch with plant species dependent ratios (Zeeman & ap Rees 1999; Smith & Stitt 2007; Kölling *et al.* 2015). Although not the only one, sucrose is the most abundant sugar transported in the vascular system (Roitsch 1999; Braun *et al.* 2014; Osorio *et al.* 2014). As a consequence sucrose is somehow considered a shuttle molecule supplying sink tissues with carbon skeletons. Sucrose derives from a cytosolic pathway, consuming both the products of photosynthesis and the products of starch degradation.

Starch is the major non-structural carbohydrate in plants and usually the terms “storage” and “transitory” starch are used to distinguish between long- and short-term carbohydrate reservoirs, respectively. Albeit storage and transitory starch have the same biosynthetic pathway, their degradation occurs through two different mechanisms: α-

amylases are generally accepted as the major player in cereal endosperm mobilization being able to attack starch granule surface (Fincher 1989); on the contrary leaf starch degradation does not require any α-amylase activity (Yu *et al.* 2005) but an initial phosphorylation step is necessary to make starch surface accessible to a plethora of enzymes (Blennow *et al* 2000; Edner *et al*, 2007; Santelia *et al.* 2015). *GWD1* (At1g10760), *GWD2* (At4g24450) and *PWD* (At5g26570) are Arabidopsis genes encoding enzymes that catalyse starch phosphorylation. *In planta* starch phosphoesterification occurs only at the hydroxyl groups of the C-3 and C-6 of glucose molecules of the amylopectin (Blennow *et al.* 2002), the branched glucose polymer that constitutes about the 70-90% of starch granule (Ong *et al*. 1994; Roger & Colonna 1996). Phosphorylation at C-3 and C-6 hydroxyl groups of the glucose units has considerably different effect: while the C-6 bound phosphate does not severely affect starch granule crystallinity, C-3 modification significantly changes double-helix packing (O'Sullivan & Perez 1999; Blennow *et al.* 2002). Glucan, water dikinase (GWD) and phosphoglucan, water dikinase (PWD) catalyse the formation of glucosyl-phosphate esters by a dikinase mechanism (β-phosphate group of ATP is transferred to starch and the γ-phosphate group is transferred to water) (for a deep characterization of GWD catalytic mechanism see Hejazi *et al.* 2012). While GWDs transfer glucosyl residues at the C-6 position (Ritte *et al.* 2002), PWD transfers glucosyl residues at the C-3 position of an already phosphorylated amylopectin chain (Baunsgaard *et al.* 2005; Kötting *et al.* 2005). In Arabidopsis GWD1, GWD2 and PWD form a small protein family. Except for GWD2, GWD1 and PWD localize in chloroplast stroma (Ritte *et al.* 2000; Baunsgaard *et al.* 2005) where transitory starch is accumulated during the day. GWD2 is instead a cytosolic enzyme mainly expressed in the vascular tissues in age-dependent manner (Glaring *et al.* 2007). Several experimental evidences underline the requirement of GWD1 and PWD to ensure the proper rate of leaf starch degradation: plants lacking GWD1 are unable to degrade starch even after a prolonged dark period (Lorberth *et al.* 1998), and are therefore characterized by a strong starch excess (*sex*) phenotype. A less severe starch accumulation is typically associated to *pwd* mutants (Baunsgaard *et al.* 2005; Kötting *et al.* 2005). In agreement with its extra-plastidial localization *gwd2* knock out mutants do not show a *sex* phenotype (Glaring *et al.* 2007).

Several studies have been conducted on plants with altered expression of genes involved in starch metabolism (for a recent review see Lloyd & Kossmann 2015). However, much

attention has been placed on mutants strongly affected on their capacity to synthetize (i.e. starch-less phenotype, like *pgm* mutant) or to degrade starch (i.e. high-starch phenotype, like *sex1* mutant), while little attention has been paid to less severe mutations. Moreover, the data are often spotted throughout the literature and cover a single developmental stage or a specific organ. The aim of the present work is to study the phenotypic traits in single mutants lacking *GWD1*, *GWD2* and *PWD* genes during the entire life cycle and in different organs of *Arabidopsis thaliana*. While current knowledge of *gwd1* mutant is extensive, *pwd* is less characterized and nothing is known about *gwd2* mutant. For these reasons we intended to give an integrated overview of the phenotype of mutants.

MATERIALS AND METHODS

Genotype analysis

T-DNA lines were searched for insertions in At1g10760 (code for GWD1), At4g24450 (code for GWD2) and At5g26570 (code for PWD) genes. Stock seeds, were purchased from the European Arabidopsis Stock Centre (NASC, Nottingham, UK) (Table 1). Homozygous lines were selected by two independent PCR amplifications on genomic DNA extracted from 3/5 leaves of T3 plants. One PCR reaction was performed utilizing pairs of primers both specific for the gene under study, while a second PCR reaction was performed utilizing a gene-specific and a T-DNA left border primer (Table 1). Gene-specific primers were designed by T-DNA primer Design. PCR amplification was performed on a Biometra T-gradient thermocycler under the following conditions: 1) 5 min at 94°C, 2) 35 cycles of 30 sec at 93°C, 30 sec at 58°C and 1 min at 72°C. PCR products were separated on 0,8% TAE-agarose gel and visualized with ethidium bromide (Fig. 1). Twenty-40 plants were analyzed for each T-DNA line (Fig. 1). Seeds were collected only from homozygous lines. All experiments were carried out on T4 generation.

Gene	NASC code	Mutant	[1]LP (5'→3')	[2]RP (5'→3')	[3]LB (5'→3')
At1g10760	SAIL_165_B11	*gwd1*	CTGTTCTTGACAGAAGCCGAC	CAAAGAAATACTTGGAGGGGC	GCCTTTTCAGAAATGGATAAATAGCCTTGCTTCC
At5g26570	SALK_110814	*pwd*	GCTAGGGTAGCCACCGTAAAG	TCCGATATGTCCTTTTTCTGG	GCGTGGACCGCTTGCTGCAACT
At4g24450	SALK_152327C	*gwd2A*	AGACTCCTCCGTAGAAGCACC	GAAACTGGCGTTCTCAGATTG	GCGTGGACCGCTTGCTGCAACT
At4g24450	SALK_080260C	*gwd2B*	CAAATGTTCCGAATGGAAGAG	AGGTTATAAGAGCAGGGCCAG	GCGTGGACCGCTTGCTGCAACT

Table 1 - Index of Arabidopsis T-DNA mutants under study. Homozygous lines were identified through two independent PCR reactions performed on genomic DNA. Utilized pairs of primers were LP+RP and LB+RP. [1]LP: gene specific, left border primer; [2]RP: gene specific, right border primer; [3]LB: T-DNA specific, left border primer.

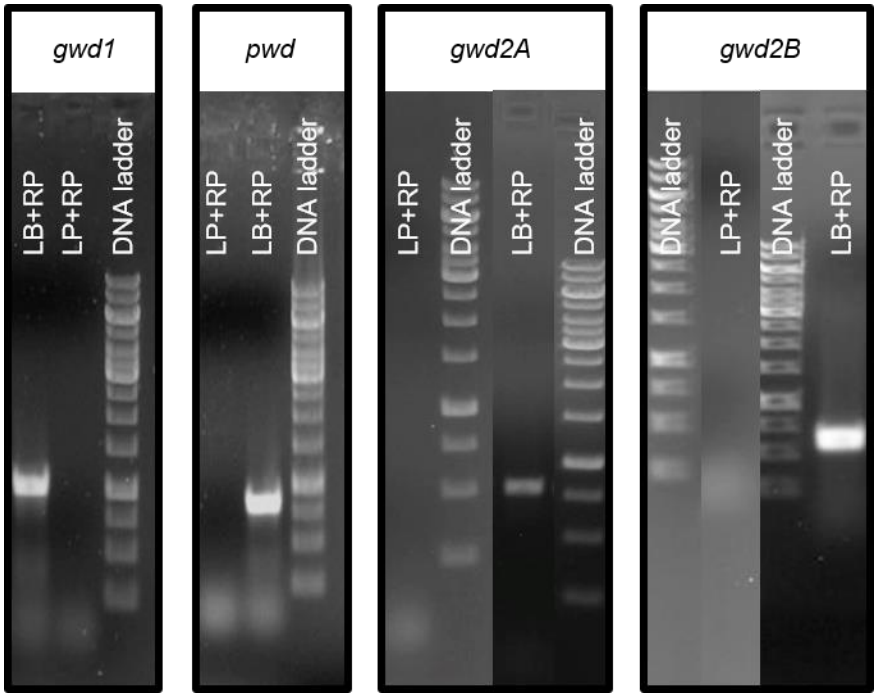

Figure 1 - PCR analyses were performed with 400 ng of DNA extracted from 30-day-old plants. Homozygous lines were selected using specific primers and 35 amplification cycles. Exclusively in homozygous lines, the pairs of primers LB+RP is expected to amplify a band of known length (typically around 300 bp) while on the same genome the pair LP+RP is expected unable to amplify. Representative results are reported.

Plant growth conditions

Wild-type and T-DNA Arabidopsis plants (ecotype Columbia) were grown on soil or on half-strength Murashige-Skoog medium (½MS-agar medium) (Micropoli), in a growth

chamber at 22°C either at a light intensity of 110 µmol photon m^{-2} s^{-1} for 12 hours per day or at a light intensity of 60 µmol photon m^{-2} s^{-1} for 24 hours per day. Seeds grown in ½MS-agar medium were sterilized with chlorine fumes for 5 hours, and then transferred onto square Petri dishes. Cold stratification of about 4 days in the dark was applied.

Phenotypic characterization

Leaves starch content was quantified from entire rosette of 31/35-day-old plants and measured as described in Smith & Zeeman (2006). Starch quantification was performed at 12 h light and 12 h dark on 4 independent biological replicas. The percentage of germination was calculated numbering seeds with radical protrusion after 72h of growth in respect to the total sowed seeds. The rate of primary root elongation was evaluated measuring the root length at regular intervals in the range of time between 2 and 7 days of growth. The flowering time was defined as the time required by the primary inflorescence to reach a height of 10 cm. The number of rosette leaves was assayed at the flowering time. The number of flowers, siliques and seeds pertain to the primary inflorescence only. The seeds density was evaluated by counting seeds able to cross 100%, 80% or 70% glycerol cushions after 15 min centrifugation at 13,000 rpm.

Quantification of starch, protein and lipids in seeds

For the quantification of seed proteins and seed starch content, about 30 mg of air-dried seeds were homogenized in a mortar at room temperature in the presence of 3 volume of Extraction Buffer (50 mM HEPES, 5 mM $MgCl_2$, pH 7.5, 1% Triton X-100, 15% glycerol, 2% SDS, 1 mM EDTA), carefully transferred into 1.5 ml tubes and centrifuged for 10 min at 13,000g. Supernatants were transferred into clean reaction tubes and used for protein quantification with bicinchoninic acid reagent (Sigma), according to the manufacturer's instructions. Pellets were washed once with 80% ethanol, three times with water and starch was quantified as described in Smith & Zeeman (2006). Total lipid quantification was performed gravimetrically as described in Wingenter *et al.* 2010 on 100 mg of mature and air-dried seeds for each genotype. Lipid composition was determined by means of silylation and GC-MS analysis as described in Torri *et al.* 2011.

RESULTS

Isolation of homozygous T-DNA lines and leaves starch quantification

Selection of homozygous lines with T-DNA insertion in *GWD1*, *PWD* and *GWD2* coding sequences were carried out by PCR experiments on genomic DNA. Two PCR amplifications with T-DNA and gene specific forward or reverse primers were performed (Tab. 1 and Fig. 1). Only for *GWD2* gene two independent T-DNA mutants were selected and named *gwd2*A and *gwd2*B. Generically *gwd2* will be used to comment on both the mutant lines *gwd2A* and *gwd2B*, given their similar behaviour. Leaves starch was quantified at the end of the day and at the end of the night and compared with that extracted from wild-type plants grown under the same conditions (Fig. 2). As expected from the absence of *GWD1* gene (Yu *et al.* 2001), starch content in *gwd1* mutant was 4.5 and 10 times higher than those measured in wild-type plants at 12h of light and 12h of dark, respectively. Such a severe starch excess (*sex*) phenotype was not evident in *pwd* mutant (Baunsgaard *et al.* 2005; Kötting *et al.* 2005), which appeared to be impaired mainly in starch degradation at night (Fig. 2). As previously reported (Glaring *et al.* 2007), the absence of a functionally active *GWD2* gene did not affect leaf starch content, whose concentrations were not statistically different from those of the wild-type (Fig. 2).

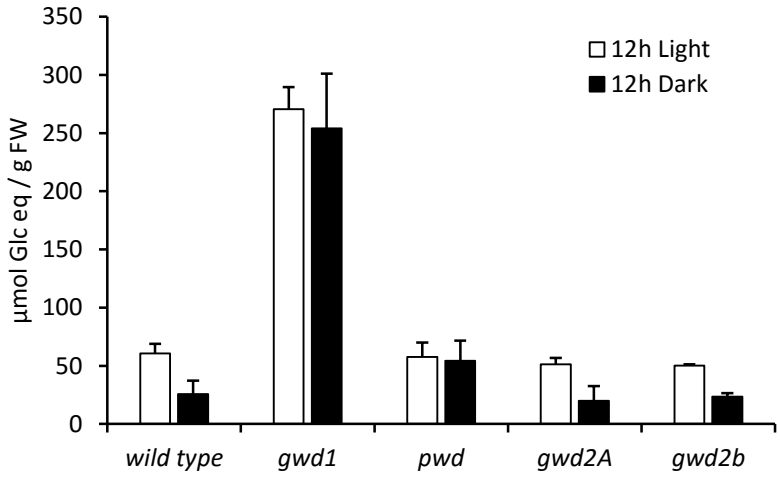

Figure 2 - Transitory starch content measured at the end of the light (12h Light) and at the end of the dark (12h Dark) period in wild-type and mutant plants, expressed as µmol of Glc equivalents/gram of fresh weight. Starch was extracted from entire rosette leaves of 31/35-day-old plants. Data are means ± SE (*n* = 4).

Seeds morphology and composition

As part of the phenotypic dissection, the effect on seeds of the T-DNA insertion in *GWD1*, *PWD* and *GWD2* genes, was evaluated weighting pools of 100 seeds collected from 31-52 different plants and no statistical differences were observed in comparison to wild-type seeds (Table 1). Seeds morphology was further analysed measuring length and width of 103-151 mature seeds collected from 10 different plants for each genotype (Table 2, Fig. 3). All seeds belonging to mutant genotypes were reduced in length in comparison to wild-type, while width was reduced in *gwd1* and *pwd* but not in mutants affecting *GWD2* gene. As a consequence, all mutated seeds were suggested to have a major density than wild-type. The hypothesis was confirmed measuring the seeds density on glycerol cushions. Three different glycerol concentrations were tested: 70%, 80% and 100% corresponding to densities of 1.181 g cm^{-3}, 1.208 g cm^{-3} and 1.261 g cm^{-3}, respectively. After centrifugation, the 32.2% of the *gwd1* seeds migrated to the bottom of the tube containing 100% glycerol while none of the wild-type seeds crossed the glycerol cushion; the 84.8% of *pwd1* seeds migrated to the bottom of the 80% glycerol cushion versus the 0.8% of wild-type seeds; and the 45.7% and 42.2% of *gwd2A* and *gwd2B,* respectively, seeds migrated to the bottom of the 70% glycerol cushion versus the 6.7% of wild-type seeds. Since the seed density depends on seed composition, the content of lipids, proteins and starch was evaluated in mature seeds of mutants and wild-type lines (Table 2). In agreement with the higher seed density of *gwd1*, *pwd* and *gwd2*, total lipids content (the lightest micro-components within seed) was statistically lowered in comparison to wild-type, albeit no differences in fatty acid composition were observed (Fig. 4). On the contrary, no statistical difference was observed in total proteins content among mutants and wild-type seeds, while only *gwd1* seeds showed a ~90-fold increase in starch (Table 2). Taking into account that in *pwd* and *gwd2A* mutants none of the seed components were increased, we can reasonably assume that their higher density was due to an increased seeds coat.

	Seed dimension			Seed composition		
	Weight• (mg)	Length (µm)	Width (µm)	Lipids (µg seed^{-1})	Proteins (µg seed^{-1})	Starch (ng seed^{-1})
wild-type	2.04 ± 0.07	511 ± 3.2	296 ± 1.7	4.70 ± 0.07	10.15 ± 1.05	5.06 ± 1.66
gwd1	1.94 ± 0.04	481 ± 3.9**	284 ± 1.9**	3.36 ± 0.22**	7.99 ± 0.26	434 ± 148**
pwd	1.80 ± 0.06	488 ± 3.7**	286 ± 1.7**	3.00 ± 0.29**	7.89 ± 0.13	11.58 ± 7.29
gwd2A	1.82 ± 0.06	483 ± 4.5**	296 ± 1.9	3.40 ± 0.08**	8.35 ± 0.65	7.14 ± 0.89
gwd2B	2.17 ± 0.10	474 ± 4.3**	291 ± 2.4	4.05 ± 0.14	9.47 ± 0.43	8.68 ± 5.46

•The seed weight is reported as the weight of 100 seeds.

Table 2 - Characterization of mature seeds collected from wild-type and mutant plants. Depending on the genotype, 31-52 pools composed of 100 seeds each were used to calculate seed weights. Seed length and width were measured on 102-151 seeds (depending on the genotype) collected from 10 single plants; values are means ± SE. Lipids, proteins and starch were quantified from mature seeds of wild-type and mutated lines; values are means ± SD (*n* = 3). Statistical analyses were performed using Student's t-test. **P ≤ 0.01.

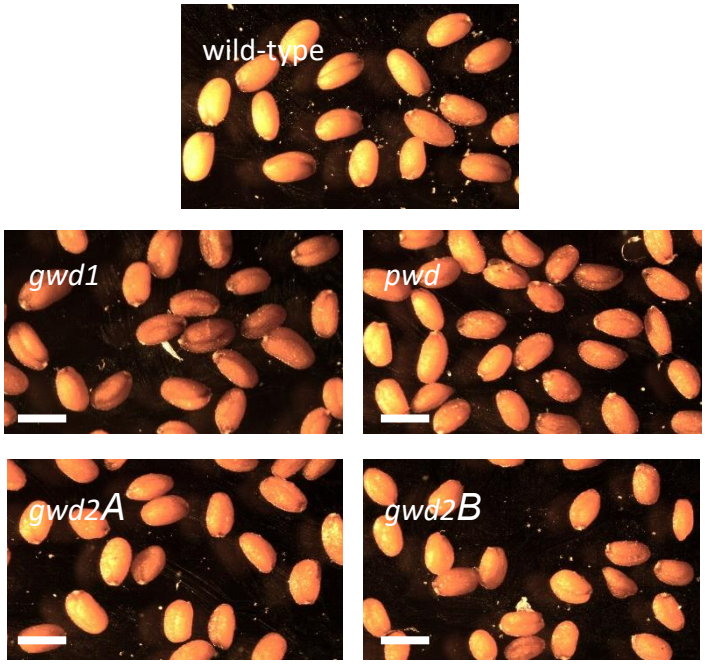

Figure 3 - Phenotypes of wild-type and T-DNA mutant seeds affected in starch phosphorylating enzymes. Batches of mature dry seeds were stereoscopically observed. Scale bar: 500 µm.

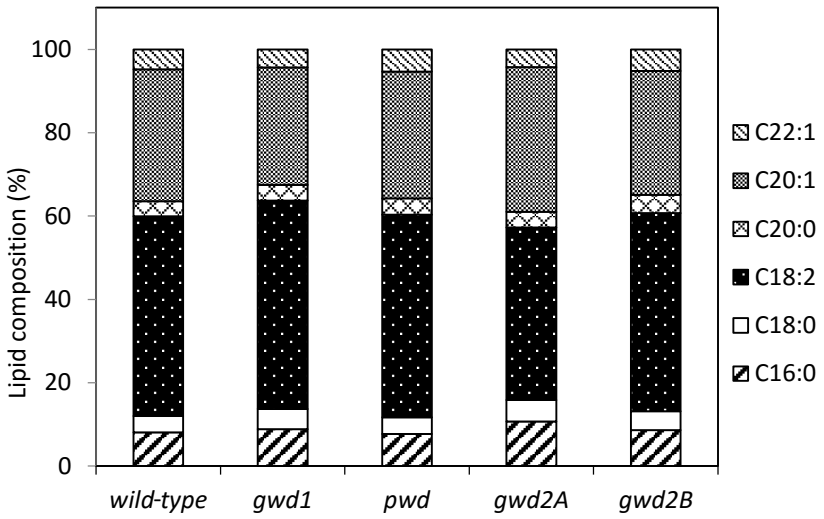

Figure 4 - Lipid composition of Arabidopsis seeds collected from wild-type and mutant plants.

Seed viability and rate of growth of primary root

As early phenotypic traits, seeds viability and rate of growth of primary root were evaluated. The former trait was measured as the percentage of seeds showing a radical protrusion after 72h of growth in respect to the total number of sowed seeds. The second trait was evaluated as the rate of primary root elongation within the range of linear growth phase (between 2 and 7 days). In agreement with the hypothesis of thicker coats that could make harder the radicle protrusion, the percentage of germination in *pwd* and *gwd2A* was statistically reduced in comparison to wild-type, while no statistically significant difference was observed comparing wild-type and *gwd1* samples (Table 3). Following germination, the minor lipid content measured in all mutant seeds (Table 2) could be responsible of the reduced rate of primary root elongation (Table 3). Moreover, the more severe reduction measured in *gwd1* mutants in respect to *pwd* and *gwd2A*, might be explained by the major impairment in transitory starch degrading pathway associated to this mutation. As the seedlings grow and acquire photosynthetic capacity, the inability to mobilize starch could strengthen the defect.

	Germination (%)	Growth rate (μm h^{-1})
wild-type	99.0 ± 0.2	175 ± 2
gwd1	97.9 ± 1.5	76 ± 1**
pwd	89.5 ± 4.9**	94 ± 3**
gwd2A	93.6 ± 3.1**	94 ± 3**
gwd2B	91.7 ± 7.2**	105 ± 3**

Table 3 - Seed viability and rate of primary root elongation. The percentage of germination was evaluated scoring the number of germinated seeds in respect to the number of sowed seeds. Four independent biological replicas, each of which composed by 30 mutated and 30 wild-type seeds sown on the same ½MS-agar plate, were scored. Data are means ± SE. Primary root elongation was obtained fitting data within the linear range of growth rate. Data are means ± SE of single seedlings (*n* = 49 ~ 100). Statistical analyses were performed using Student's t-test. **P ≤ 0.01.

Transition from vegetative to reproductive growth-phase and plant fitness

The effect of mutations on the transition from vegetative to reproductive growth was evaluated by measuring the days required to reach the flowering time, assessed when the primary inflorescence was 10 cm high. As shown in Table 4, as for wild-type plants about 70 days were necessary to reach the flowering time in both *pwd* and *gwd2A* mutants, while more than 100 days were required by *gwd1*. Once reached the flowering time, rosette leaves have been numbered (Table 4). Probably due to the prolonged vegetative phase, an increased number of rosette leaves was measured in *gwd1* mutant, while *pwd* and *gwd2A* showed a small but statistically significant decrease (Table 4).

	Flowering time (day)	Rosette leaf (number)
wild-type	69.6 ± 2.3	21.7 ± 0.8
gwd1	106.4 ± 2.3**	27.0 ± 0.6**
pwd	70.7 ± 2.4	18.9 ± 0.6**
gwd2A	72.6 ± 2.2	19.5 ± 0.5*
gwd2B	66.7 ± 2.2	20.7 ± 0.5

Table 4 - Time of flowering and number of rosette leaves in wild-type and mutated lines. Plants were grown under 12h light/ 12h dark cycle. Rosette growth rate was determined measuring the major diameter of the entire rosette, at different time points, during the linear growth phase, between the 13th and the 28th day of growth (n > 20). Time of flowering is defined by the length (10 cm) of the primary inflorescence (*n* > 90). The number of rosette leaves was assayed at the flowering time (*n* > 90). Data are means ± SE. Statistical analyses were performed using Student's t-test. **P ≤ 0.01; *P ≤ 0.05.

Exclusively on the primary inflorescence, the number of flowers, siliques, and seeds in *gwd1*, *pwd*, *gwd2A* and wild-type plants have been counted. Compared to wild-type, flowers, siliques and total seeds production were reduced in both *pwd* and *gwd2A* (Table 5). Interestingly, *gwd1* mutant characterized by most severe *sex* phenotype, did not show a reduced number of flowers and siliques, and the seeds production was less reduced than that observed in *pwd* and *gwd2* mutants (20% in *gwd1 v.s.* ~40% in *pwd* and *gwd2*) (Table 3).

	Flower	Silique	Seeds	Seeds per siliqua
		(number)		
wild-type	34.4 ± 1.4	25.7 ± 1.1	596 ± 30	24 ± 1
gwd1	32.8 ± 1.1	27.2 ± 0.9	477 ± 25**	18 ± 2**
pwd	22.9 ± 1.6**	14.5 ± 0.8**	349 ± 25**	23 ± 1
gwd2A	24.6 ± 1.4**	16.1 ± 0.8**	397 ± 23**	25 ± 3
gwd2B	28.3 ± 1.4**	17.0 ± 0.9**	355 ± 24 **	21 ± 1**

Table 5 - Number of flowers, siliques, seeds and seeds per silique in wild-type and mutated lines. Plants were grown under 12h light/ 12h dark cycle. Flowers, siliques and seed number pertain to the primary inflorescence ($n > 90$). Data are means ± SE. Statistical analyses were performed using Student's t-test. **P ≤ 0.01; *P ≤ 0.05.

Rescue by light

Some of the above-mentioned phenotypic traits were also analysed growing plants under continuous low intensity light. The purpose was to overcome the energy restriction that mutants unable to correctly degrade starch during the night might have experienced, without altering sugars ratio by the addition of exogenous sucrose. Despite continuous light exposure, wild-type plants did not achieve the same starch concentration of *gwd1* mutant, which showed a 7.8-fold higher starch content than wild-type suggesting that starch degradation is not solely restricted to dark period (Valerio *et al.* 2011; Zanella *et al.* 2016). Similarly, starch concentration in *pwd* and *gwd2* mutants was about twice to that of wild-type plants. As a consequence, *gwd2* mutant acquires a *sex* phenotype, not shown under growth condition of 12 hours per day (Fig. 2). Exposure to continuous light confers similar phenotypic traits to all mutants, although different from those of wild-type plants (Table 6). The rate of primary root elongation was approximately the 70% of wild-type, with a clear recovery in respect to those measured at 12 hours light cycle (Table 3). Compared to wild-type, the time required to reach the transition to reproductive phase was increased of about one week and accompanied by a greater number of rosette leaves (Table 4). Concerning the time necessary to the transition to reproductive phase, an opposite behaviour was observed in *gwd1* in respect to both *pwd* and *gwd2A* plants grown at 12 or 24 hours light. While continuous light reduces the time required by *gwd1* mutant, partially reverting the phenotype (Table 4 and Table 6), the same condition

revealed an unexpected phenotypic trait in *pwd* and *gwd2A*, that under 24h light delay their entrance in the reproductive phase (Table 4 and Table 6).

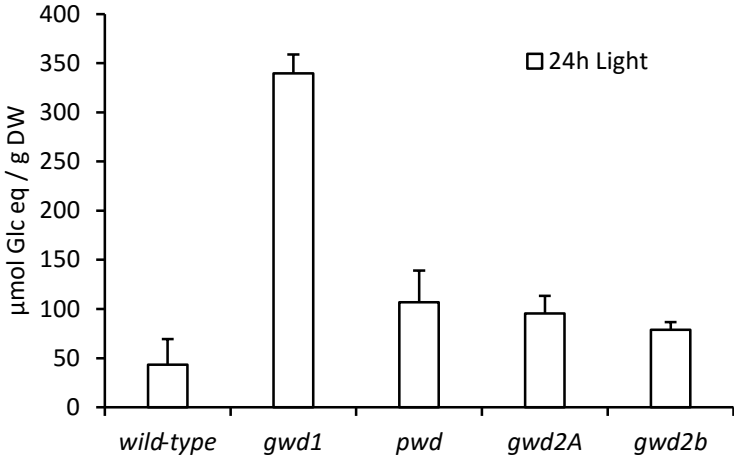

Figure 5 - Transitory starch content measured in wild-type and mutant plants kept under continuous light (24h Light), expressed as µmol of Glc equivalents/gram of dry weight. Starch was extracted from entire rosette leaves of 31/35-day-old plants. Data are means ± SE (*n* = 3).

	Root growth rate ($\mu m\ h^{-1}$)	Flowering time (day)	Rosette leaf (number)
wild-type	164 ± 2	48.5 ± 1.2	8.3 ± 0.2
gwd1	111 ± 6**	54.7 ± 1.4**	11.0 ± 0.3**
pwd	119 ± 6**	54.6 ± 1.0**	11.8 ± 0.3**
gwd2A	114 ± 6**	52.8 ± 0.9**	11.8 ± 0.4**
gwd2B	114 ± 5**	58.8 ± 1.3**	12.1 ± 0.5**

Table 6 - Rescue by light. Effects of the continuous low intensity light (60 µmol photon $m^{-2}\ s^{-1}$) on the rate of primary elongation (*n* = 30) and on the transition from vegetative to reproductive stage (*n* = 50). Data are means ± SE. Statistical analyses were performed using Student's t-test. **P ≤ 0.01.

DISCUSSION

Starch is a polymer of glucose that despite is simple composition has a tremendous relevance in almost all human fields, having both food and non-food applications (Zeeman

et al. 2010; Lloyd & Kossmann 2015). Plants accumulate starch in nearly all organs, albeit the lifetime of starch granules is very different depending on plant organs, tissues, developmental stages and environmental stimuli. Also starch morphology can be extremely various according to plant species (from spherical and discoidal in barley to polyhedral in rice) (Buléon *et al.* 1998; Wani *et al.* 2012; Sparla *et al.* 2014); nonetheless starch granules are always characterized by a strong stability. Presumably as a function of starch life time and localization, two main pathways of starch degradation are known: in cereal endosperm (long-term and extracellular starch storage) the endoamylolitic activity of α-amylases is required in its mobilization (Fincher 1989), while phosphoesterification at C-3 and C-6 positions of the glucose units is of primary relevance in the mobilization of short-life and intracellular starch granules (Blennow *et al.* 2000).

To evaluate the relative contribution of the three (phospho)glucan, water dikinases encoded by Arabidopsis genome, single mutants were analysed throughout their life cycle and compared with wild-type plants grown under the same conditions. As expected, the *sex* phenotype associated to leaves followed the relative contribution of the three enzymes to transient starch degradation in chloroplasts (Yu *et al.* 2001; Baunsgaard *et al.* 2005; Kötting *et al.* 2005; Glaring *et al.* 2007). In addition to leaves, transient accumulation of starch occurs in many other plant organs and tissues (e.g. stems, developing seeds, roots, flowers) (Caspar et al. 1991). Albeit Arabidopsis seeds store lipids and proteins up to 80% of the dry weight (Baud *et al.* 2002; O'Neill *et al.* 2003), small and transitory starch deposition occurs during the early phases of Arabidopsis seed development (Focks & Benning 1998; Baud *et al.* 2002; Andriotis *et al.* 2010). In agreement with previous works, wild-type mature seeds accumulated proteins and lipids over the 70% of the seeds weight, while in all analysed mutants the same components were only slightly higher than the 50%. Although the similar decrease in lipids content, only *gwd1* mutant showed a relevant starch accumulation (~90 fold higher then wild-type), constituting up to 5% of the seed weight. The appearance of a *sex* phenotype exclusively in *gwd1* seeds corroborates the hypothesis that transitory starch accumulation in seeds does not sustain lipids synthesis, rather confirms that an imbalance in the carbohydrate status (e.g. sucrose and glucose) might affect the storage pathways (Weber *et al.* 1997). Despite the different seeds composition, the percentage of germination in *gwd1* mutant was indistinguishable from that of wild-type seeds, being for both close to 100%. On the contrary *pwd1* and *gwd2*

showed a statistically relevant reduction in germination. At the present we are not able to explain such behaviour and several hypotheses can be postulated: (i) *GWD2* and *PWD* may have a predominant role in germination process (albeit not supported by *in silico* data); (ii) an altered carbohydrate status could act as developmental signal (iii) differently from *gwd1* seeds whose greater density can be ascribable to accumulation of starch, the higher density of *gwd2* and *pwd* seeds may reflect a thicker seed coat. For what we know, the latter case appears more reasonable considering that cellulose and hemicellulose are among the major sinks (Windsor *et al.* 2000). Therefore, we can assume that in absence of GWD1, carbohydrates deriving from mother plant are restrained into starch, while the absence of PWD or of GWD2 blocks them into the seed coats.

The rates of elongation of primary root underline how under a normal light/dark cycle all the three genes under study are required in sugars mobilization. While such a role was already observed on *gwd1* and *pwd* mutants (Yu *et al.* 2001; Baunsgaard *et al.* 2005; Kötting *et al.* 2005), here we show for the first time that also *GWD2* is necessary for a correct rate of root elongation, at least in the very early phase of growth. Interestingly, the reduction of primary root growth was not fully recovered under continuous light. The exposure to continuous low intensity light, flattens the phenotypic differences among the three mutants, that in any case still display a 30% reduction in the primary root elongation in comparison to wild-type. Similarly, the time required to reach the transition to reproductive phase and the number of rosette leaves at the flowering time clearly change in response to continuous light, conferring phenotypic traits different from those of wild-type but identical among all mutants. Recently it has been demonstrated that dwarfism characteristic of *gwd1* can be efficiently reverted by external application of gibberellin (GAs) (Paparelli *et al.* 2013). The Authors demonstrate that plants size depends from the synthesis of GAs, which in turn depend from how starch is efficiently mobilized during the night (Paparelli *et al.* 2013). Compared to wild-type, exposure to continuous light led to an increase in starch content, with the onset of *sex* phenotype even in *gwd2* mutant. Considering that wild-type plants never reach a starch concentration greater than those of mutants, an increase in starch turnover (intended as rate of synthesis and degradation) can be assumed. As a consequence of a compromised efflux route, mutants start to accumulate starch. Somehow perceived, the accumulation of starch could lead to a lower

synthesis of GAs or other plant hormones, with a consequent impairment in the development.

Fitness (evaluated as seed number) and plant productivity (evaluated as biomass production) are important traits for both agriculture and biotechnology purposes. Hence biomass and fitness of mutants were evaluated as number of rosette leaves, flowers, siliques and seeds pertaining to the primary inflorescence. Whereas *pwd* and *gwd2* mutants showed a decreased leaf, flower, silique and seed number, *gwd1* plants showed a biomass increase, an unchanged number of flowers and siliques but a minor number of seeds production with the consequent reduction of seeds per silique, in agreement with the previous observation that *gwd1* produce silique of smaller size in comparison to wild-type plants (Andriotis *et al.* 2012). Curiously plants grown under 12 hours of light require the same time to reach the transition to reproductive phase, with the only exception of *gwd1* mutant. Presumably, the about doubled time of flowering shown by *gwd1* is ascribable to the major impairment in leaves starch degradation compared to both wild-type, *pwd* and *gwd2* mutated plants. This prolonged time could be required by *gwd1* to reach a hypothetical energy threshold that allows the mutant to get into the reproductive phase. The gained source tissue (i.e. major leaf number) could properly respond to sink demand, as mirrored by the same number of flowers, silique and by the slight decrease in seeds production, compared to wild-type. On the contrary the mild or null *sex* phenotype characteristic of *pwd* and *gwd2* mutants, respectively, might allow them to reach the energy threshold at the same time of the wild-type plants. However, the minor development of the source tissue (i.e. minor leaf number) might not adequately respond to the demand of sink, with the consequent lower production of flowers, siliques and seeds. The onset of a *sex* phenotype under continuous low intensity light together with the onset of a common delay in the transition to the flowering time, strongly suggests that the ratio between starch and soluble sugars may somehow establish this hypothesized energy threshold.

The data presented in this study leads to the conclusion that phosphorylation events that drive starch degradation are not solely responsible to feed plants in absence of an active photosynthetic activity (i.e. during the night), but rather that a cross talk among starch, soluble sugars and hormones is required for a correct plant development.

REFERENCES

- Andriotis V.M.E., Pike M.J., Kular B., Rawsthorne S., Smith A.M. (2010) Starch turnover in developing oilseed embryos. *New Phytologist*, **187**, 791–804.
- Andriotis V.M.E., Pike M.J., Schwarz S.L., Rawsthorne S., Wang T.L., Smith A.M. (2012) Altered starch turnover in the maternal plant has major effects on Arabidopsis fruit growth and seed composition. *Plant Physiology*, **160**, 1175–1186.
- Baud S., Boutin J.-P., Miquel M., Lepiniec L., Rochat C. (2002) An integrated overview of seed development in Arabidopsis thaliana ecotype WS. *Plant Physiology and Biochemistry*, **40**, 151–160
- Baunsgaard L., Lutken H., Mikkelsen R., Glaring M.A., Pham T.T., Blennow A. (2005) A novel isoform of glucan, water dikinase phosphorylates pre-phosphorylated α-glucans and is involved in starch degradation in Arabidopsis. *The Plant Journal*, **41**, 595–605.
- Blennow A, Bay-Smidt A.M., Olsen C.E., Møller B.L. (2000) The distribution of covalently bound phosphate in the starch granule in relation to starch crystallinity. *International Journal of Biological Macromolecules*, **27**, 211–218.
- Blennow A., Engelsen S.B., Nielsen T.H., Baunsgaard L., Mikkelsen R. (2002) Starch phosphorylation: a new front line in starch research. *Trends in Plant Science*, **7**, 445–450.
- Braun D.M., Wang L., Ruan Y.L. (2014) Understanding and manipulating sucrose phloem loading, unloading, metabolism, and signalling to enhance crop yield and food security. *Journal of Experimental Botany*, **65**, 1713–1735.
- Buléon A., Colonna P., Planchota V., Ballb S. (1998) Starch granules: structure and biosynthesis. *International Journal of Biological Macromolecules*, **23**, 85–112.
- Caspar T., Lin T.P., Kakefuda G., Benbow L., Preiss J., Somerville C. (1991) Mutants of Arabidopsis with altered regulation of starch degradation. *Plant Physiology*, **95**, 1181–1188
- Edner C., Li J., Albrecht T., Mahlow S., Hejazi M., Hussain H., Kaplan F., Guy C., Smith S.M., Steup M., Ritte G. (2007) Glucan, water dikinase activity stimulates breakdown of starch granules by plastidial beta-amylases. *Plant Physiology*, **145**, 17–28.
- Fincher G.B. (1989) Molecular and cellular biology associated with endosperm mobilization in germinating cereal-grains. *Annual Review in Plant Physiology and Plant Molecular Biology* , **40**, 305–346.
- Focks N. & Benning C. (1998) wrinkled1: A novel, low-seed-oil mutant of Arabidopsis with a deficiency in the seed-specific regulation of carbohydrate metabolism. *Plant Physiology*, **118**, 91–101
- Glaring M.A., Zygadlo A., Thorneycroft D., Schulz A., Smith S.M., Blennow A., Baunsgaard L. (2007) An extra-plastidial alpha-glucan, water dikinase from Arabidopsis phosphorylates amylopectin in vitro and is not necessary for transient starch degradation. *Journal of Experimental Botany*, **58**, 3949–3960.
- Guo J., Jermyn W.A., Turnbull MH. (2002) Carbon assimilation, partitioning and export in mature cladophylls of two asparagus (*Asparagus officinalis*) cultivars with contrasting yield. *Physiol Plantarum*,

115, 362–369.

- Hejazi M., Steup M., Fettke J. (2012) The plastidial glucan, water dikinase (GWD) catalyses multiple phosphotransfer reactions. *FEBS Journal*, **279**, 1953–1966.
- Kalt-Torres W., Kerr P.S., Usuda H., Huber S.C. (1987) Diurnal changes in maize leaf photosynthesis. 1. Carbon exchange-rate, assimilate export rate, and enzyme-activities. *Plant Physiology*, **83**, 283–288.
- Komor E. (2000) Source physiology and assimilate transport: the interaction of sucrose metabolism, starch storage and phloem export in source leaves and the effects on sugar status in phloem. *Australian Journal of Plant Physiology*, **27**, 497–505.
- Kölling K., Thalmann M., Müller A., Jenny C., Zeeman S.C. (2015) Carbon partitioning in Arabidopsis thaliana is a dynamic process controlled by the plants metabolic status and its circadian clock. *Plant, Cell & Environment*, **38**, 1965–1979.
- Kötting O., Pusch K., Tiessen A., Geigenberger P., Steup M., Ritte G. (2005) Identification of a novel enzyme required for starch metabolism in Arabidopsis leaves. The phosphoglucan, water dikinase. *Plant Physiology*, **137**, 242–252.
- Lorberth R., Ritte G., Willmitzer L., Kossmann J. (1998) Inhibition of a starch-granule-bound protein leads to modified starch and repression of cold-induced sweetening. *Nature Biotechnology*, **16**, 473–477.
- Lloyd J.R. & Kossmann J. (2015) Transitory and storage starch metabolism: two sides of the same coin? *Current Opinion in Biotechnology*, **32**, 143–148.
- Ong M.H., Jumel K., Tokarczuk P.F., Blanshard J.M.V., Harding S.E. (1994) Simultaneous determinations of the molecular weight distributions of amyloses and the fine structures of amylopectins of native starches. *Carbohydrate Research*, **260**, 99–117
- Osorio S., Ruan Y.L., Fernie A.R. (2014) An update on source-to-sink carbon partitioning in tomato. *Frontiers in Plant Science*, 10.3389/fpls.2014.00516.
- O'Neill C.M., Gill S., Hobbs D., Morgan C., Bancroft I. (2003) Natural variation for seed oil composition in Arabidopsis thaliana. *Phytochemistry*, **64**, 1077–1090
- O'Sullivan A.C. & Perez S. (1999) The relationship between internal chain length of amylopectin and crystallinity in starch. *Biopolymers*, **50**, 381–390.
- Paparelli E., Parlanti S., Gonzali S., Novi G., Mariotti L., Ceccarelli N., van Dongen J.T., Kölling K., Zeeman S.C., Perata P. (2013) Nighttime sugar starvation orchestrates gibberellin biosynthesis and plant growth in Arabidopsis. *Plant Cell*, **25**, 3760–3769.
- Ritte G., Lloyd J.R., Eckermann N., Rottmann A., Kossmann J., Steup M. (2002). The starch-related R1 protein is an α-glucan, water dikinase. *Proceedings of the National* Academy of Sciences of the United States of America, 99, 7166–7171.
- Roger P. & Colonna P. (1996) Molecular weight distribution of amylose fractions obtained by aqueous leaching of corn starch. International Journal of Biological Macromolecules, **19**, 51–61.
- Roitsch T. (1999) Source-sink regulation by sugar and stress. *Current Opinion in Plant Biology*, **2**, 198–206.

- Santelia D., Trost P., Sparla F. (2015) New insights into redox control of starch degradation. *Current Opinion in Plant Biology*, **25**, 1–9.
- Smith A.M. & Stitt M. (2007) Coordination of carbon supply and plant growth. *Plant, Cell and Environment*, **30**, 1126–1149
- Smith A.M. & Zeeman S.C. (2006). Quantification of starch in plant tissues. *Nature Protocols,* **1**, 1342–1345.
- Sparla F., Falini G., Botticella E., Pirone C., Talamè V., Bovina R., Salvi S., Tuberosa R., Sestili F., Trost P. (2014) New starch phenotypes produced by TILLING in barley. *PLoS One*, **9**, e107779.
- Torri C., Samorì C., Adamiano A., Fabbri D., Faraloni C., Torzillo G. (2011) Preliminary investigation on the production of fuels and bio-char from Chlamydomonas reinhardtii biomass residue after bio-hydrogen production. *Bioresource Technology*, **102**, 8707–8713.
- Valerio C., Costa A., Marri L., Issakidis-Bourguet E., Pupillo P., Trost P., Sparla F. (2011) Thioredoxin-regulated beta-amylase (BAM1) triggers diurnal starch degradation in guard cells, and in mesophyll cells under osmotic stress. *Journal of Experimental Botany*, **62**, 545–555.
- Wani A.A., Singh P., Shah M.A., Schweiggert-Weisz U., Gul K., Wani I.A. (2012) Rice starch diversity: effects on structural, morphological, thermal, and physicochemical properties, *Comprehensive Reviews in Food Science and Food Safety*, **11**, 417–436.
- Weber H., Borisjuk L., Wobus U. (1997) Sugar import and metabolism during seed development. *Annual Review in Plant Physiology and Plant Molecular Biology*, **2**, 169–174.
- Windsor J.B., Symonds V.V., Mendenhall J., Lloyd A.M. (2000) Arabidopsis seed coat development: morphological differentiation of the outer integument. *Plant Journal*, **22**, 483–493.
- Wingenter K., Schulz A., Wormit A., Wic S., Trentmann O., Hoermiller I.I., Heyer A.G., Marten I., Hedrich R., Neuhaus H.E. (2010) Increased activity of the vacuolar monosaccharide transporter TMT1 alters cellular sugar partitioning, sugar signaling, and seed yield in Arabidopsis. *Plant Physiology*, **154**, 665–677.
- Yu T.S., Kofler H., Häusler R.E., Hille D., Flügge U.I., Zeeman S.C., Smith A.M., Kossmann J., Lloyd J., Ritte G., Steup M., Lue W.L., Chen J., Weber A. (2001) The Arabidopsis sex1 mutant is defective in the R1 protein, a general regulator of starch degradation in plants, and not in the chloroplast hexose transporter. *Plant Cell*, **13**, 1907–1918.
- Yu T.S., Zeeman S.C., Thorneycroft D., Fulton D.C., Dunstan H., Lue W.L., Hegemann B., Tung S.Y., Umemoto T., Chapple. A, Tsai D.L., Wang S.M., Smith A.M., Chen J., Smith S.M. (2005) α-Amylase is not required for breakdown of transitory starch in Arabidopsis leaves. *Journal of Biological Chemistry*, **280**, 9773–9779.
- Zanella M., Borghi G.L., Pirone C., Thalmann M., Pazmino D., Costa A., Santelia D., Trost P., Sparla F. (2016) β-amylase 1 (BAM1) degrades transitory starch to sustain proline biosynthesis during drought stress. *Journal of Experimental Botany*, 10.1093/jxb/erv572.
- Zeeman S.C. & ap Rees T. (1999) Changes in carbohydrate metabolism and assimilate export in starch-excess mutants of Arabidopsis. *Plant Cell Environment*, **22**, 1445–1453.

- Zeeman S.C., Kossmann J., Smith A.M. (2010) Starch: its metabolism, evolution, and biotechnological modification in plants. *Annual Review of Plant Biology*, **61**, 209–234.

CHAPTER 2

Starch phosphorylating enzymes are required for a proper development of Arabidopsis plants

ADDENDUM

Unpublished preliminary results

Claudia Pirone[1], Ivan Gaiba[1], Alessio Adamiano[2], Paolo Trost[1], Francesca Sparla[1]

[1]Department of Pharmacy and Biotechnology FaBiT, University of Bologna, Via Irnerio 42, 40126 Bologna, Italy

[2]Department of Chemistry "G. Ciamician", University of Bologna, Via Selmi 2, 40126 Bologna, Italy

MATERIALS AND METHODS

Lignin and cellulose staining

Rosette leaves of three 40-days plants from each genotype were harvested. After chlorophyll extraction with hot ethanol (80% [v/v]), on three leaves per plant lignin was stained with the phloroglucinol solution (1% phloroglucinol [w/v] in 6M HCl) and cellulose was stained with Congo-red (aqueous solution 1% [w/v]).

Stomatal aperture measurement

Analyses were performed on plants at the flowering time after 72 h of continuous light exposure. Abaxial epidermal peels were immediately placed on a microscope slide and observed with an image analyser-Axioplan microscope (Zeiss, Jena, Germany) connected to a Sony CCD-IRIS camera (SSC-M37CE, Sony, Japan). The captured images were then processed using ImageJ 1.48 for Windows. Stomata were randomly selected from the digital image collection, obtained from a set of leaves of 3-4 independently grown plants for both the wild-type and the mutants. Stomata apertures were calculated as the ratio between the width and length of the pore (an average of 100 stomatal apertures were analysed for each genotype).

Transpiration and carbon assimilation rates

Gas-exchange measurements were performed as described by Kölling et al., 2015, with an EGES-1 system (DMP Ltd, Switzerland). Custom-made chambers enclosing the whole

rosette were used. Chambers were connected to control unit, to IRGA (LI-7000, LI-COR Inc. USA), and to a Linux computer for data acquisition. The flow rate and the partial pressure of CO_2 and H_2O were kept under control both in incoming and outgoing. Gas exchange measurements were followed for 72h at flow of 200 µmol s^{-1}, air temperature of 20 °C and at a light intensity of 60 µmol photon m^{-2} s^{-1}. The incoming air was adjusted to a CO_2 concentration of 380–400 ppm and a relative humidity of 55–65%. The outgoing air of each chamber was measured for 360 s before the system switched to the next chamber. A dead time of 90 s was introduced after each switch to allow stabilization of the measurements. After the dead time, measurements were made every 2.5 s; every 60 s the average value was calculated and stored by the LabView application. The values for ΔCO_2, ΔH_2O, flow rate and the final fresh weight of the plant were used to calculate photosynthetic parameters. Each data point is the mean of measurements performed on four different plants.

RESULTS

Cellulose and lignin content

Cellulose production is one of the most carbon consuming processes in plants. Recently numerous observations support the view that photosynthesis, primary metabolism, and carbon sinks (e.g. lignin biosynthesis) are coordinated and that photosynthesis is partially regulated by the sink organs. Moreover, Rogers and colleagues (2005) showed that *sex1* mutants lacking of GWD1 exhibit reduced lignin accumulation. Similarly, changes in the activity of cellulose biosynthesis reduce the expression of genes involved in starch degradation and photosynthesis. In particular, the inhibition of cellulose biosynthesis redirects the metabolic flux from cell wall to starch (Wormit et al., 2012). To follow up on these observations, the content of lignin and cellulose was qualitatively evaluated in *gwd1*, *pwd* and *gwd2* mutant lines and compared to that of wild-type plants. At a glance, with our method, it was not possible to detect any differences between mutants and wild-type plants (data not shown). Further analysis, by means of more sensitive and quantitative methods, are therefore require to better assess lignin and cellulose content.

Transpiration rate and photosynthetic rate

In guard cells, mobilization of starch follows an opposite rhythm with respect to mesophyll cells. Namely, starch is present in darkness in almost all guard cells and is degraded during the first hours of light, presumably to provide carbon precursors needed for malate synthesis or sucrose accumulation (Horrer et al., 2016). Under standard growth conditions, BAM1 and AMY3 normally not required in nighttime starch breakdown in mesophyll cells, are involved in guard cell starch degradation (Valerio et al., 2011; Horrer et al., 2016). Differently from BAM1 and AMY3, to date there aren't studies highlighting phenotypic traits in guard cell of *gwd1*, *pwd* or *gwd2* plants.

To address the possible involvement of GWD1, PWD and GWD2 in stomata opening, mutants and wild-type plants were transferred to continuous low intensity light and the numbers of open stomata together with the size of pores were evaluated on epidermal peels. Albeit preliminary, the obtained data revealed a decreased number of open stomata in both *pwd* and *gwd2* mutants (Fig. 6) as well as a reduced size of the pores in comparison to wild-type and *gwd1* plants (Fig. 6).

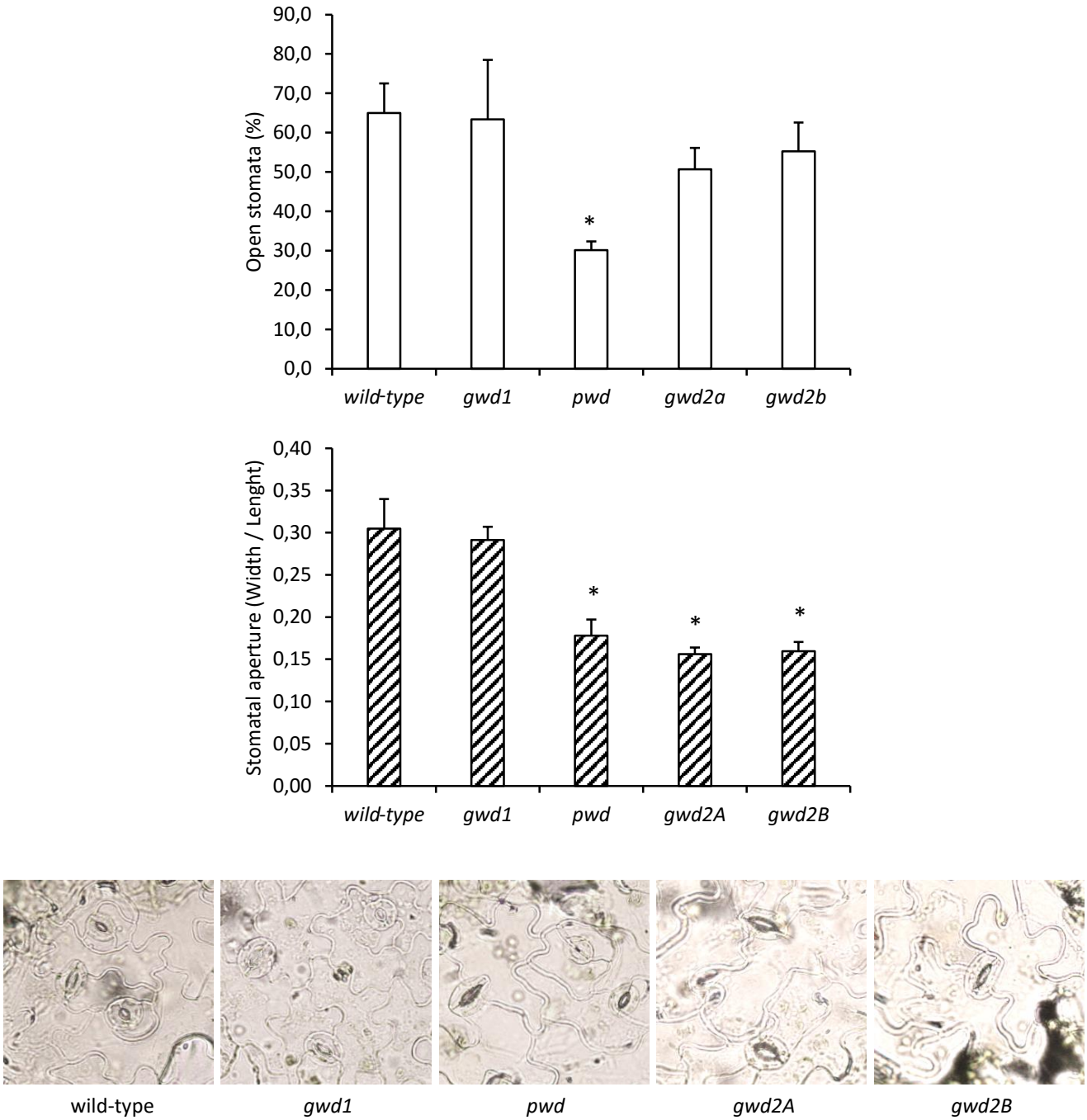

Figure 6 - Number of open stomata and stomatal aperture analysis performed on wild-type and mutant plants. Plants were grown on soil and transferred at the flowering time under continuous light. Leaves were collected after 72 h of light exposure. The number of open stomata was counted (upper graph). Stomatal aperture (middle graph) was determined as the ratio between width and length of the stomatal pore. Values are means ± SE (n > 150 guard cells). Lower panel, guard cells of wild-type and mutated plants. The same magnification was used. Statistical analyses were performed using Student's t-test. *P ≤ 0.05.

To better study the different role of *gwd1* and *pwd* in guard cells, gas exchanges experiments were performed in collaboration with Dr. D. Santelia (University of Zurich, CH) on *pwd*, *gwd1* and wild-type through the EGES-1 system (Kölling et al., 2015). This method allowed to calculate the net carbon assimilation/release (Fig. 7 and 8, lower panel), and the transpiration rate (Fig. 7 and 8, upper panel) of shoots of eight different plants at the same time (four wild-type and four mutants), monitoring for up to 72h plants response to continuous light.

In comparison to wild-type, *gwd1* mutants did not show any differences in transpiration and photosynthetic rates (Fig. 7), while *pwd* mutant showed a reduced transpiration (Fig. 8) rate and a consequent decrease in photosynthetic rate (Fig. 8), suggesting an involvement of the PWD protein in guard cell starch mobilization at least under continuous low intensity light.

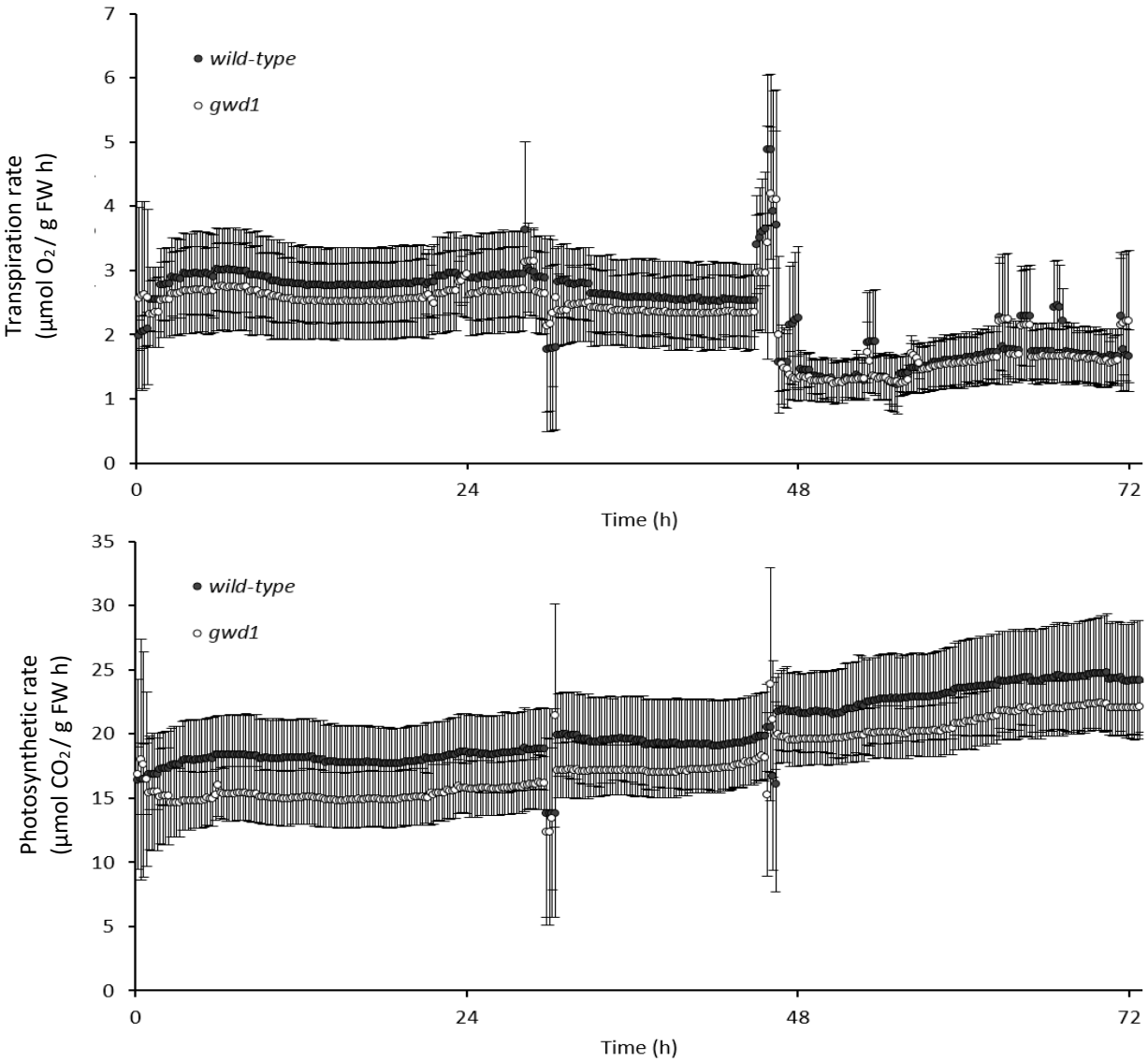

Figure 7 - Comparison of gas exchange measurements performed on wild-type (black dots) and *gwd1* (white dots) plants. Transpiration rate (upper panel) and photosynthetic rate (lower panel) were recorded over the 72 h of continuous light period.

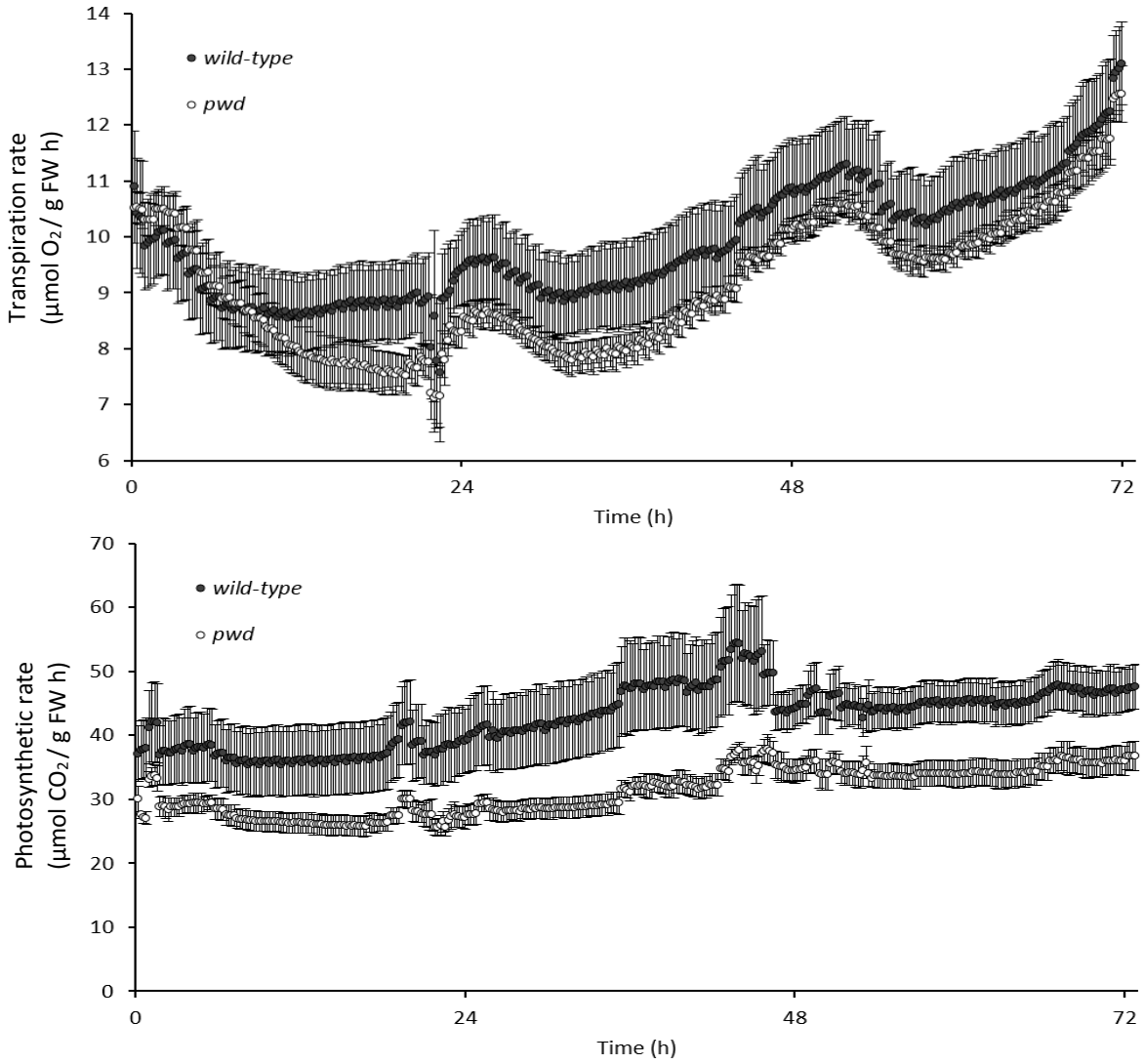

Figure 8 - Comparison of gas exchange measurements of wild-type (black dots) and *pwd* (white dots) plants recorded in parallel. The average measurements for transpiration rate (upper graph) and photosynthetic rate (lower graph) of four chambers per genotype are shown over a 72 h Light period.

DISCUSSION

In the case of continuous photosynthetic activity, stomata should be kept open to guarantee the appropriate gas exchanges, at the same time allowing water loss, which can become an issue for the plant, when exceeding the water uptake from the root. It was demonstrated that guard cell starch metabolism is necessary for stomatal aperture (Valerio et al., 2006; Hörrer et al., 2016). Then, in wild-type and mutant plants under continuous light the number of open stomata was assessed. Only the pwd plants showed

a difference for open stomata compared to wild-type. Indeed, the 70% of guard cells were found to be closed and the remaining 30% that were still open showed a significant decrease in stomata aperture. Indeed, *pwd* plants showed reduced transpiration and photosynthetic rates compared with wild-type plants, suggesting a role of PWD protein in guard cell starch metabolism under continuous light conditions. Further analyses are needed to assess the involvement of PWD in stomata starch degradation, such as starch quantification in guard cells of *pwd* mutant lines.

REFERENCES

Horrer D, Flütsch S, Pazmino D, Matthews JSA, Thalmann M, Nigro A, Leonhardt N, Lawson T, Santelia D (2016) Blue Light Induces a Distinct Starch Degradation Pathway in Guard Cells for Stomatal Opening. Curr Biol **26**: 362–370

Kölling K, Thalmann M, Müller A, Jenny C, Zeeman SC (2015) Carbon partitioning in Arabidopsis thaliana is a dynamic process controlled by the plants metabolic status and its circadian clock. Plant Cell Environ **38**: 1965–1979

Rogers LA, Dubos C, Cullis IF, Surman C, Poole M, Willment J, Mansfield SD, Campbell MM (2005) Light, the circadian clock, and sugar perception in the control of lignin biosynthesis. J Exp Bot **56**: 1651–1663

Valerio C, Costa A, Marri L, Issakidis-Bourguet E, Pupillo P, Trost P, Sparla F (2011) Thioredoxin-regulated beta-amylase (BAM1) triggers diurnal starch degradation in guard cells, and in mesophyll cells under osmotic stress. J Exp Bot **62**: 545–555

Wormit A, Butt SM, Chairam I, McKenna JF, Nunes-Nesi A, Kjaer L, O'Donnelly K, Fernie AR, Woscholski R, Barter MCL, et al (2012) Osmosensitive changes of carbohydrate metabolism in response to cellulose biosynthesis inhibition. Plant Physiol **159**: 105–117

CHAPTER 3

β-amylase 1 (BAM1) degrades transitory starch to sustain proline biosynthesis during drought stress

Published by Journal of Experimental Botany, 2016; doi: 10.1093/jxb/erv572

Martina Zanella[1,2], Gian Luca Borghi[1], Claudia Pirone[1], Matthias Thalmann[2], Diana Pazmino[2], Alex Costa[3], Diana Santelia[2], Paolo Trost[1] and Francesca Sparla[1,]

[1]Department of Pharmacy and Biotechnology FaBiT, University of Bologna, Via Irnerio 42, 40126 Bologna, Italy

[2]Institute of Plant Biology, University of Zürich, Zollikerstrasse 107, CH-8008 Zurich, Switzerland

[3]Department of Bioscience, University of Milan, Via Celoria 26, 20133 Milano, Italy

Abstract

During photosynthesis of higher plants, absorbed light energy is converted into chemical energy that, in part, is accumulated in the form of transitory starch within chloroplasts. In the following night, transitory starch is mobilized to sustain the heterotrophic metabolism of the plant. β-amylases are glucan hydrolases that cleave α-1,4-glycosidic bonds of starch and release maltose units from the non-reducing end of the polysaccharide chain. In Arabidopsis, nocturnal degradation of transitory starch involves mainly β-amylase-3 (BAM3). A second β-amylase isoform, β-amylase-1 (BAM1), is involved in diurnal starch degradation in guard cells, a process that sustains stomata opening. However, BAM1 also contributes to diurnal starch turnover in mesophyll cells under osmotic stress. With the aim of dissecting the role of β-amylases in osmotic stress responses in Arabidopsis, mutant plants lacking either BAM1 or BAM3 were subject to a mild (150mM mannitol) and prolonged (up to one week) osmotic stress. We show here that leaves of osmotically-stressed *bam1* plants accumulated more starch and fewer soluble sugars than both wild-type and *bam3* plants during the day. Moreover, *bam1* mutants were impaired in proline accumulation and suffered from stronger lipid peroxidation, compared with both wild-type and *bam3* plants. Taken together, these data strongly suggest that carbon skeletons deriving from BAM1 diurnal degradation of transitory starch support the biosynthesis of proline required to face the osmotic stress. We propose the transitory-starch/proline interplay as an interesting trait to be tackled by breeding technologies aiming to improve drought tolerance in relevant crops.

INTRODUCTION

Starch is a polymer of D-glucose and represents a convenient way to store carbohydrates as semi-crystalline and osmotically inert granules. The granules are mainly composed of a highly branched amylopectin polymer (70–90%), the remaining 10–30% being amylose which is much less branched (Denyer *et al.*, 2001; Zeeman *et al.*, 2002; Streb *et al.*, 2012). As a consequence of its structure, glucose units embedded in the starch granule may not be immediately available to satisfy the different demands of the organism when faced with an urgent request. The tight regulation of several enzymes involved in starch degradation seems consistent with the need to speed up the use of starch under particular conditions, i.e. under stress (Santelia *et al.*, 2015).

Two kinds of starch, structurally indistinguishable, are found in plants: secondary and transitory starch. This physiological distinction is mainly based on different storage organs and on different rates of synthesis and degradation (Smith *et al.*, 2005). Because of its commercial relevance, secondary starch has been extensively investigated, with the aim of creating new starch structures for industrial applications (Jobling, 2004; Santelia and Zeeman, 2011; Bahaji *et al.*, 2014). Conversely, the physiology of transitory starch has become a major topic of research only recently (Zeeman *et al.*, 2007; Stitt and Zeeman, 2012), with increasing evidence of the involvement of transitory starch metabolism in response to stress (Hummel *et al.*, 2010; Valerio *et al.*, 2011; Prasch *et al.*, 2015; Santelia *et al.*, 2015).

Due to their sessile nature, plants have to cope not only with rapid and daily environmental changes, but they must also balance the energy needed for growth with the energy required for stress responses. Starch biosynthesis is tightly correlated with photosynthesis, another process strongly affected by the environment. In the model plant *Arabidopsis thaliana*, half of the photoassimilates produced by the Calvin–Benson cycle during the day are typically exported to the cytosol to supply carbon skeletons for anabolic or catabolic processes, whereas the remaining half is retained in the chloroplast for transitory starch biosynthesis (Zeeman and ap Rees, 1999). Under normal growth conditions, the export of organic carbon is mediated by two different transport mechanisms which operate at different times of the diurnal cycle. During the day, photoassimilates mainly reach the cytosol via the triose phosphate/phosphate

translocator (TPT) (Flügge, 1999) whereas, during the night, β-maltose (the major product of starch degradation) and glucose are exported to the cytoplasm via the maltose (MEX1) (Nittylä *et al.*, 2004) and glucose (GLT and GT) (Cho *et al.*, 2011; Flügge *et al.*, 2011) transporters, respectively.

β-Amylases are the only enzymes that produce β-maltose, thereby connecting starch degradation in chloroplasts with sugar metabolism in the cytoplasm. Several β-amylases are encoded by the Arabidopsis genome (Lloyd *et al.*, 2005). BAM3 is a major, catalytically active β-amylase that is necessary for nocturnal starch degradation under physiological conditions. Conversely, BAM1 is little or not involved in this process (Fulton *et al.*, 2008; Kötting *et al.*, 2010). However, in response to drought or salt stress, BAM1 becomes a predominant β-amylase of leaves and is required for starch breakdown in mesophyll cells (Valerio *et al.*, 2011; Monroe *et al.*, 2014).

Water stress has severe negative impacts on plant growth and productivity (Cattivelli *et al.*, 2008; Rockström and Falkenmark, 2010; Osakabe *et al.*, 2014). A common trait of many plants affected by drought or salinity stress is the accumulation of osmoprotectants such as proline, glycine betaine, and sugar alcohols (Szabados and Savouré, 2009; Liang *et al.*, 2013). Proline accumulation occurs at very high levels when plants experience conditions of low water potential. Proline concentration can increase up to 100-fold compared with control conditions (Verbruggen and Hermans, 2008; Szabados and Savouré, 2009). However, proline not only functions as an osmoprotectant, but it can also scavenge reactive oxygen species (ROS) efficiently, thus protecting the cell from oxidative damage (Matysik *et al.*, 2002, Bartels and Sunkar, 2005).

In plants, proline synthesis occurs both in the cytosol and in the chloroplast, whereas degradation only occurs in mitochondria. Carbon skeletons for proline biosynthesis are provided by primary metabolism through the glutamate pool. Whether starch degradation is involved in this process is currently unknown.

To investigate the possible interplay between transitory starch and proline metabolism under drought stress, the response to 150mM mannitol treatments of two single T-DNA insertion mutants, *bam1* and *bam3*, and wild-type plants was studied and compared. The findings strongly suggest that, in the drought stress response of Arabidopsis, BAM1 and not BAM3 is the major player in starch degradation in the light, a metabolic pathway that

provides carbon skeletons for the biosynthesis of sucrose and proline to counteract both osmotic stress and oxidative damage.

MATERIALS AND METHODS

Plant material and growth conditions

Wild-type, T-DNAs, and *BAM1* promoter::GUS plants of *Arabidopsis thaliana* (ecotype Columbia, Col-0) were hydroponically grown at a constant temperature of 22 °C, under a 12/12h light/dark cycle with a photosynthetic photon flux density of 110 µmol m^{-2} s^{-1}, as described in Valerio *et al.* (2011). The GUS line and insertion sites of the T-DNA in *bam1* (SALK_039895) and *bam3* (CS92461) mutants had already been analysed (Fulton *et al.*, 2008; Valerio *et al.*, 2011).

Stress conditions

To analyse the response of Arabidopsis plants to drought further, previously tested conditions (300mM mannitol for up to 8h; Valerio *et al.*, 2011) were changed in order to obtain a mild (150mM mannitol) and prolonged (up to 7.5 d) osmotic stress. Mild osmotic stress was applied to 28/31-d-old plants (with 3/4 d of stratification time at 4 °C in darkness excluded), 1h after switching on the light. Treated plants were transferred to a freshly prepared hydroponic medium supplemented with 150mM mannitol. If not differently specified, plants were harvested either at the end of the light period (12h light) or at the end of the dark period (12h dark), every 12h for a maximum of 7.5d after the beginning of the treatment (DAT). Samples were immediately frozen in liquid nitrogen and stored at −80 °C for analysis.

GUS staining

Histochemical GUS staining was performed as described in Valerio *et al.* (2011). For each condition and for each time point, three independent transgenic plants were analysed. Control and treated (150mM mannitol) plants were collected every day during the experiment, always at the end of the 12h light period. Stained plants were examined by bright-field microscopy using a Nikon Eclipse 90-I microscope. The images show representative plants and leaves.

Determination of water loss

The loss of water from the leaves was determined as the ratio between the dry weight (DW) and the fresh weight (FW), measured on single plants collected after 12h of light and 12h of dark, under control or stress conditions, during a 6 d experiment. FW was scored immediately after excision and DW was determined after incubation at 80 °C for 24h. Five independent biological replicates were analysed.

Quantification of starch and soluble sugars

Quantification of starch and soluble sugars were carried out on whole rosette leaves of 3–5 plants for each experimental point. Starch was quantified on bleached leaves as described in Smith and Zeeman (2006). Quantification of sucrose, glucose, and maltose was performed as described in Egli *et al.* (2010) on freeze-dried supernatants obtained after extracting with 80% ethanol for 15min at 80 °C. Three independent biological replicas were analysed.

Lipid peroxidation assay

Oxidative damage was estimated by measuring total lipid peroxidation using the 2-thiobarbituric acid (TBA) assay, as described in Guidi *et al.* (1999). Briefly, about 200mg of leaves were powdered in liquid nitrogen, before being vigorously mixed with 3 vols of 0.1% (w/v) trichloroacetic acid (TCA). Samples were centrifuged and 0.5ml of each supernatant was transferred into a screw cap tube in the presence of 2.0ml 20% (w/v) TCA and 1.5 µl 0.5% (w/v) TBA. Following a 30min incubation at 90 °C, the reaction was stopped by placing the tubes in a bath of ice water. Samples were centrifuged and the absorbance of the supernatants was monitored at 532nm, subtracting the non-specific absorption at 600nm. The amount of MDA–TBA complex was calculated from the extinction coefficient $155 mM^{-1}$ cm^{-1}. Three independent biological replicas were analysed.

Proline quantification

Samples stored at −80 °C were ground in liquid nitrogen and the free proline content was measured as described by Bates *et al.* (1973). Briefly, 1.2ml of 3% 5-sulphosalicylic acid was added to 50mg of powdered leaves. Samples were centrifuged and appropriate

volumes of supernatant were transferred into clean tubes and brought to a final volume of 1ml with water, and then mixed with 1ml of glacial acetic acid and 1ml of 2.5% ninhydrin reagent Samples were incubated at 90 °C for 1h, cooled on ice, combined with an equal volume of toluene, and mixed vigorously. Following phase partitioning, the absorbance of the upper phase was monitored at 520nm. The calibration curve was prepared using different proline concentrations as standard. From 3–4 independent biological replicates were analysed.

RESULTS

Mild osmotic stress induces *BAM1* promoter activity

To understand the activation of *BAM1* in response to mild osmotic stress better, the activity of *GUS* in Arabidopsis plants stably transformed with the *BAM1* promoter controlling the GUS reporter gene (*BAM1promoter::GUS* plants) was examined. Adult plants were exposed to 150mM mannitol and collected every day for one week.

As previously reported in Valerio *et al.* (2011), in the absence of stress, GUS activity of *BAM1promoter::GUS* plants was mainly confined to guard cells (see Supplementary Fig. S1) and almost absent from mesophyll cells (Fig. 1, right panel). Under mild osmotic stress, a slight increase in the promoter activity of *BAM1* had already appeared at the beginning of the stress, albeit confined to leaf veins (Fig. 1A, B, left panel). Upon prolonged stress, GUS activity spread to mesophyll cells, first in young leaves and then throughout the whole rosette (Fig. 1C–E, left panel).

Fig. 1. Activity of BAM1promoter::GUS under control conditions and in response to 150mM mannitol treatment. Plants were grown under a 12/12h light/dark cycle and osmotic stress was applied 1h after the beginning of the light period. Plants were collected at the end of the light period. GUS activity was measured at 0.5 DAT (A); 1.5 DAT (B); 3.5 DAT (C); 6.5 DAT (D), and 7.5 DAT (E). Scale bar=1cm. Inset: magnification of a single leaf. Scale bar=0.5cm.

Water loss in response to stress

β-amylase 3 (BAM3) is the major isoform responsible for transitory starch degradation at night (Lao *et al.*, 1999; Fulton *et al.*, 2008). To get insights into the role of BAM1 in starch degradation in response to osmotic stress, *bam3* T-DNA mutant plants were also analysed. Dehydration rates of *bam1*, *bam3*, and wild-type plants in response to 150mM mannitol were determined (see Supplementary Fig. S2). The data obtained did not show statistically significant differences among the three genotypes, neither in response to stress nor in control conditions (see Supplementary Table S1 at *JXB* online). The similar decrease in water content observed in the three genotypes during the whole experiment, allows a comparison between genotypes of data expressed on a FW basis.

Starch content at the end of the light period

To investigate the involvement of BAM3- and BAM1-dependent starch degradation pathways in response to drought stress, the starch content was measured in leaves after 12h light, before and after the mannitol treatment (Fig. 2; see Supplementary Fig. S3).

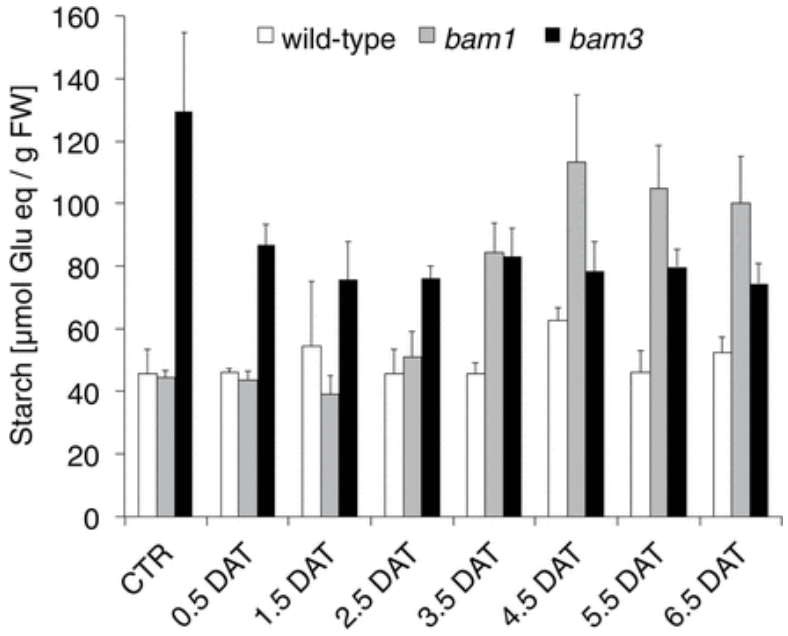

Fig. 2. Starch content in wild-type, *bam1*, and *bam3* plants measured after 12h of light in response to drought stress. Twenty-eight/31-d-old hydroponically grown plants were expose to 150mM mannitol 1h after switching on the light. Wild-type, *bam1*, and *bam3* plants were collected after 12h of light before and after mannitol treatment. Values are the means ±SD (*n*=3 independent biological replicates).

Consistent with the predominant role of BAM3 in transitory starch degradation (Fulton *et al.*, 2008), under control growth conditions *bam3* plants showed the well-known *s*tarch *ex*cess (*sex*) phenotype, characterized by small plants with a high starch content (~3-fold higher compared with wild-type plants) (Fig. 2). Conversely, compared with wild-type plants, *bam1* mutant plants did not show any significant change in starch concentration (Fig. 2; see Supplementary Table S2), again in agreement with the literature (Fulton *et al.*, 2008).

In response to osmotic stress, the ratio in starch content between *bam3* and wild-type samples suddenly decreased from ~3 (in the absence of mannitol) to ~2 (in the presence of mannitol), remaining roughly constant throughout the experiment (Fig. 2). On average, the amount of starch contained in *bam3* plants at the end of the day was reduced by ~50

µmol glucose equivalents g^{-1} FW as a consequence of the stress. Although with different timing, an opposite behaviour was observed in *bam1* plants. During the first three days of the experiment, starch content in *bam1* plants remained similar to the wild-type, but doubled wild-type levels from the fourth day onwards (Fig. 2). An average increase of ~50 µmol glucose equivalents g^{-1} FW was calculated.

Starch content at the end of the night period

To analyse the involvement of β-amylases on transitory starch turnover in response to drought further, the starch concentration was also measured at the end of the night period (12h dark), before and after mannitol treatment (Fig. 3). As expected, under control condition, wild-type and *bam1* plants did not differ in their starch content while *bam3* plants confirmed the *sex* phenotype (Fig. 3; see Supplementary Table S3) (Fulton *et al.*, 2008).

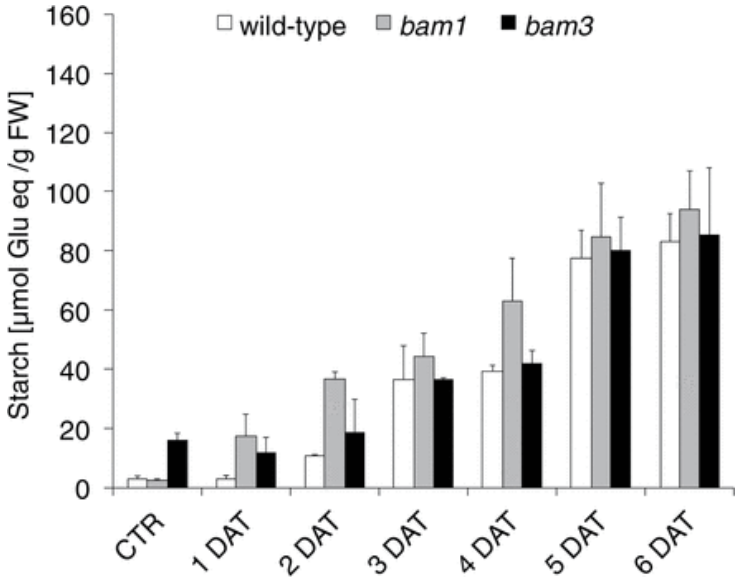

Fig. 3. Starch content in wild-type, *bam1*, and *bam3* plants after 12h of darkness in response to drought stress. Twenty-eight/31-d-old hydroponically grown plants were exposed to 150mM mannitol 1h after switching on the light. Wild-type, *bam1*, and *bam3* plants were collecte d after 12h of darkness before and after mannitol treatment. Values are the means ±SD (*n*=3 independent biological replicates).

High levels of starch were maintained in *bam3* mutants in the first two days of the experiment (Fig. 3). Conversely, *bam1* plants rapidly responded to 150mM mannitol with an increase in starch concentration that, within the first two days of the experiment, made

them closer to *bam3* than to wild-type plants. Later in the experiment (from 3–6 DAT) no significant differences were observed among the three genotypes in response to 150mM mannitol (Fig. 3).

Lipid peroxidation

A common effect of osmotic stress is the accumulation of free oxygen radicals (Aranjuelo *et al.*, 2011; Wilhelm and Selmar, 2011) leading to oxidation of unsaturated fatty acids and membrane damage (Hernandez *et al.*, 1993; Fadzilla *et al.*, 1997). Lipid peroxidation induced by osmotic stress was evaluated as the malondialdehyde (MDA) concentration on *bam1*, *bam3*, and wild-type plants treated with 150mM mannitol. The exposure to the osmotic stress increased the MDA concentration in all genotypes in a time-dependent manner (Fig. 4; see Supplementary Table S4). However, only *bam1* samples collected at 4.5 DAT showed a ~2-fold increase in MDA concentration compared with the wild-type, suggesting that BAM1 is an essential component of the Arabidopsis response to the oxidative damage caused by the osmotic stress.

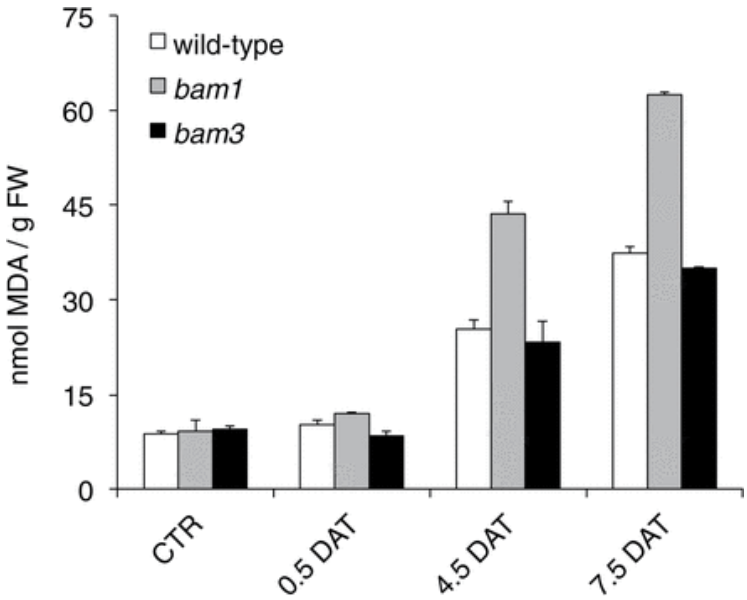

Fig. 4. Degree of lipid peroxidation in wild-type, *bam1*, and *bam3* plants exposed to osmotic stress. Lipid peroxidation was measured using the TBA assay in wild-type, *bam1*, and *bam3* plants before and after the 150mM mannitol treatment. Plants were collected after 12h light and different lengths of treatment. Values are the means ±SD (*n*=3 independent biological replicates).

Proline content

Proline is considered a compatible osmolyte and its accumulation in response to different stresses has been reported in several plant species (Szabados and Savouré, 2009). In order to test whether proline accumulation in osmotically stressed Arabidopsis plants might depend on the activity of β-amylases, the proline concentration was measured in rosette leaves of wild-type, *bam1*, and *bam3* plants subject to 150mM mannitol treatments (Fig. 5). In the absence of stress, similar proline concentrations (~0.67 μμmol g^{-1} FW) were measured in the three genotypes and no significant differences were observed until 2.5 DAT (Fig. 5; see Supplementary Table S5). At 3.5 DAT, both *bam1* and *bam3* mutants showed less proline accumulation with respect to the wild-type. However, at later time points, only the *bam1* mutant showed a limited accumulation of proline, while *bam3* plants recovered the same proline concentration as wild-type plants (Fig. 5).

Interestingly at 6.5 DAT, the lower proline content of the *bam1* mutant with respect to the wild-type (and *bam3* plants) corresponded to ~37 μmol proline g^{-1} FW (Fig. 5). Considering that the same mutant at the same time point accumulated a surplus of ~48 μmol glucose equivalents g^{-1} FW (Fig. 2), it seems reasonable that impaired starch degradation was the reason for the failure in proline accumulation.

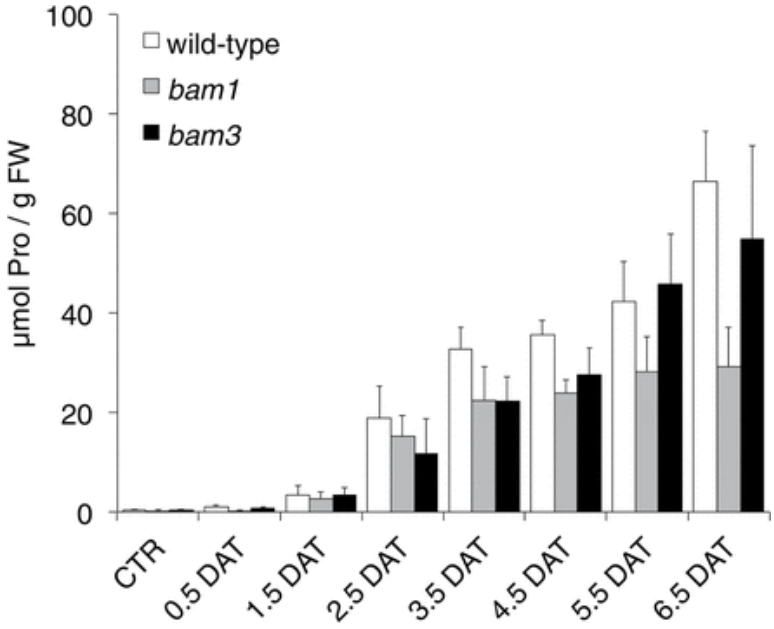

Fig. 5. Proline content in wild-type, *bam1*, and *bam3* plants in response to drought stress. Proline concentration was measured in whole rosettes of 28/31-d-old wild-type, *bam1*, and *bam3* plants. Plants

were collected after 12h of light before and after 150mM mannitol treatment. Values are the means ±SD (*n*=3–4 independent biological replicates).

Soluble sugars

Sucrose, maltose, and glucose concentrations were measured in wild-type, *bam1*, and *bam3* plants in response to 150mM mannitol both after 12h of light and after 12h of dark (Fig. 6; see Supplementary Table S6). Under control conditions, the concentration of soluble sugars in all genotypes at the end of the day or at the end of the night, resembled the values already reported in the literature (Fulton *et al.*, 2008; Hummel *et al.*, 2010). Glucose was higher than sucrose, which was much higher than maltose, and all three sugars appeared to be more concentrated at the end of the night.

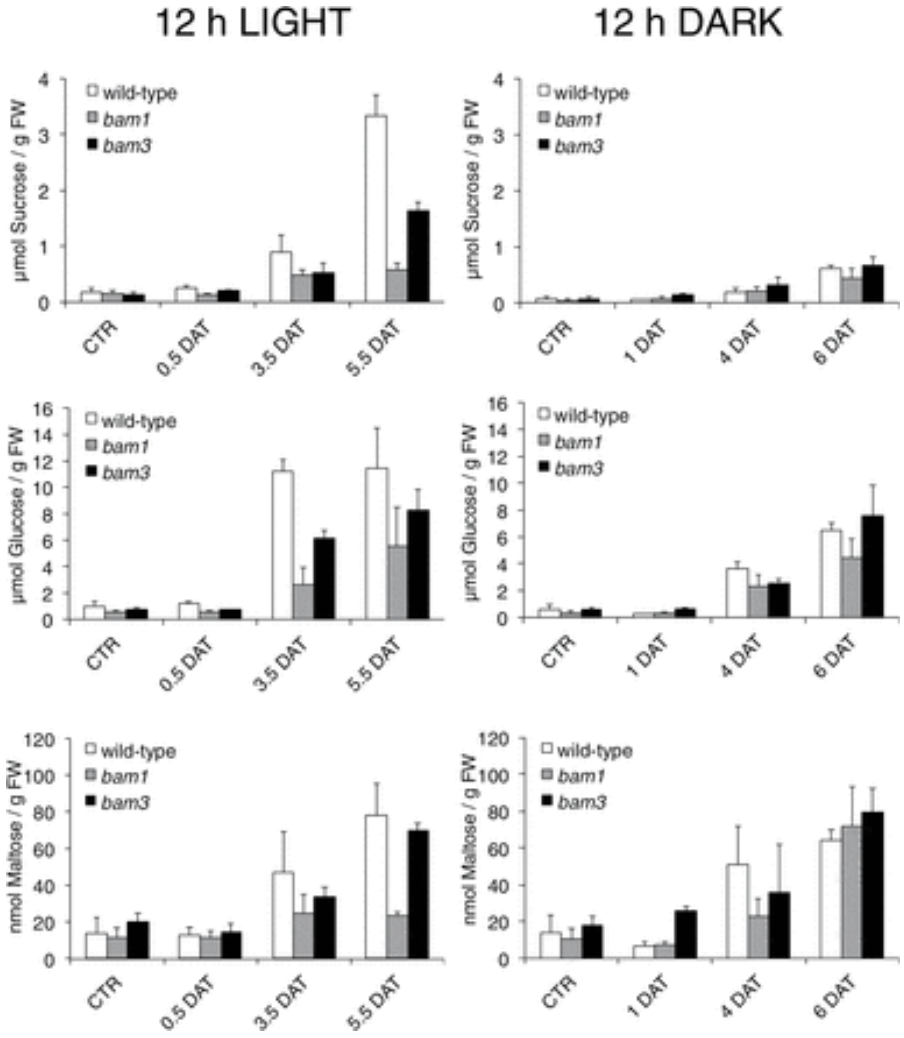

Fig. 6. Sucrose, glucose, and maltose content in wild-type, *bam1*, and *bam3* plants measured after 12h of light and aftert 12h of darkness in response to drought stress. Hydroponically grown Arabidopsis plants

were exposed to 150mM mannitol 1h after switching on the light. Whole rosettes of wild-type, *bam1*, and *bam3* plants were collected after 12h of light (left panels) and 12h of darkness (right panels) before and after 150mM mannitol treatment. Values are the means ±SD (*n*=3 independent biological replicates).

Similar to what was observed for transitory starch (Fig. 3), during the osmotic stress experiment, soluble sugar concentrations measured at the end of the night were essentially similar among the genotypes (Fig. 6, right panels), with the only exception being maltose in the *bam3* mutant at 1 DAT, which was more concentrated than in the wild-type (Fulton *et al.*, 2008). By contrast, at the end of the day, *bam1* plants showed a general decrease in sucrose, glucose, and maltose concentrations with respect to both wild-type and *bam3* plants (Fig. 6, left panels). By comparison with wild-type plants at 5.5 DAT, the absence of BAM1 led to a decrease of ~2.8 μmol sucrose g^{-1} FW, ~5.9 μmol glucose g^{-1} FW, and ~55 nmol of maltose g^{-1} FW.

DISCUSSION

Plants are sessile organisms with a metabolism that essentially depends on light and needs to be continuously adapted to environmental changes. A fundamental aspect of this adaptation consists of the circadian cycles of diurnal synthesis and nocturnal degradation of transitory starch that allow plants to harmonize with the natural rhythm of light availability (Stitt and Zeeman, 2012). Nocturnal degradation of transitory starch sustains basal metabolism and the reallocation of organic carbon in the absence of an external input of energy. On top of that, under stress conditions, plants need to redirect transitory carbon fluxes in order to fuel stress responses, a decision that often implies detrimental effects on growth. As far as transitory starch is concerned, its degradation and use of the resulting carbon units for stress responses involve a large set of enzymes, including β-amylases.

With the aid of *bam3* and *bam1* knock-out mutants (Fulton *et al.*, 2008; Valerio *et al.*, 2011), we have investigated the relative contribution of BAM1 and BAM3 to transitory starch degradation in response to mild and prolonged osmotic stress. BAM3 is required for nocturnal starch degradation under physiological conditions (Fulton *et al.*, 2008), while BAM1 is dispensable for transitory starch degradation in the absence of stress, but is

activated by drought stress at the transcriptional level and post-translationally activated by reduced thioredoxins (Sparla *et al.*, 2006; Valerio *et al.*, 2011). Under control growth conditions, the rosette leaves of *bam3* mutants contained high levels of starch during the whole day, which were always higher than the wild-type plants. Under osmotic stress, the starch levels of *bam3* plants suddenly decreased, particularly during the light and became closer to wild-type levels. Different from *bam3*, under control growth conditions, the levels of leaf starch in *bam1* mutants were similar to the wild-type plants, in agreement with the notion that BAM1 is confined to guard cells until plants start to flower (Valerio *et al.*, 2011; Prasch *et al.*, 2015). However, in response to osmotic stress, BAM1 also appears in mesophyll cells and the starch content in *bam1* mutants increased, particularly so at the end of the light and after several days of stress. In conclusion, a mild, prolonged osmotic stress caused a decrease in daylight starch in plants with no BAM3 and, conversely, an increase in daylight starch in plants with no BAM1, suggesting that BAM1 is involved in daylight starch degradation upon stress. This hypothesis fits with both the induction of the BAM1 promoter by the osmotic stress and the redox regulation of BAM1 that favours its activity in the light (Sparla *et al.*, 2006; Valerio *et al.*, 2011).

Plants have evolved several different mechanisms to respond to limited water availability and proline accumulation has long been reported to be a part of the drought-stress response (Szabados and Savouré, 2009). The main pathway of proline biosynthesis derives from glutamic acid and it can occur both in the cytosol and the chloroplast. Under stress conditions, however, the plastidial pathway of proline biosynthesis may prevail as a result of the re-localization of Δ^1-pyrroline-5-carboxylate synthetase (P5CS1) into chloroplasts (Székely *et al.*, 2008). P5CS1 catalyses the limiting step of proline biosynthesis and its role in proline accumulation in water-stressed plants is recognized (Székely *et al.*, 2008). Although each of the three genotypes investigated in our study (*bam1*, *bam3*, and Col-0) accumulated proline under osmotic stress, the proline concentration of *bam1* mutants did not reach the same levels as those reached by wild-type and *bam3* plants. The lack of adequate proline accumulation in *bam1* mutants correlated with a more severe oxidative stress in these plants, as judged by the extent of lipid peroxidation. Moreover, lower proline levels in *bam1* plants went together with lower concentrations of sucrose, glucose, and maltose and, as discussed above, higher levels of starch. Following several days of stress, the starch content in *bam1* plants at the end of the phototosynthetic period

exceeded wild-type levels by about 50 µmol glucose equivalents g^{-1} FW. To put this value into context, proline accumulation in these same plants and under the same conditions was lower than in wild-type plants by 37 µmol g^{-1} FW, while soluble sugars (sucrose and glucose) decreased by 12 µmol hexoses g^{-1} FW. Based on these numbers, the reason why *bam1* plants had less proline and soluble sugars upon stress may well be that the carbon skeletons required to make these osmolytes are stuck into starch granules and, as such, are not available. Since BAM1 is suggested to play a role in starch degradation under these conditions, it makes sense that its absence has more dramatic effects during the day, when BAM1 is redox-activated and P5CS1 is sufficiently concentrated (Hayashi *et al.*, 2000; Székely *et al.*, 2008) to catalyse the metabolic flux leading to proline.

Although the whole pathway connecting the degradation of transitory starch with the biosynthesis of proline still remains to be discovered, the results presented here strongly suggest a link between these two metabolic pathways and suggest a role for BAM1 in this context. Our results suggest that a mild osmotic stress stimulates starch turnover in the light through the activation of BAM1, both at the transcriptional and post-translational level. Indeed, BAM1 activity is strictly redox-regulated and, since it requires thioredoxin f to be highly reduced, BAM1 is predicted to be more active under photosynthetic conditions (Sparla *et al.*, 2006). Based on correlative observations, we propose that maltose derived from BAM1 degradation of starch upon stress sustains the biosynthesis of proline (and soluble sugars) thereby alleviating the oxidative stress. Since water availability is a major constraint for modern agriculture, the efforts in selecting crops with better water use efficiency should take into account this link between starch and proline metabolism.

LITERATURE

Aranjuelo I, Molero G, Erice G, Avice JC, Nogués S. 2011. Plant physiology and proteomics reveals the leaf response to drought in alfalfa (*Medicago sativa* L.). Journal of Experimental Botany 62, 111-123.

Bahaji A, Li J, Sánchez-López ÁM, Baroja-Fernández E, Muñoz FJ, Ovecka M, Almagro G, Montero M, Ezquer I, Etxeberria E, Pozueta-Romero J. 2014. Starch biosynthesis, its regulation and biotechnological approaches to improve crop yields. Biotechnology Advances 32, 87-106.

Bartels D and Sunkar R. 2005. Drought and salt tolerance in plants. Critical Reviews in Plant Sciences 24, 23-58.

Bates IS, Waldren RP, Teare ID. 1973. Rapid determination of free proline for water stress studies. Plant Soil 39, 205-207.

Cattivelli L, Rizza F, Badeck F-W, Mazzucotelli E, Mastrangelo AM, Francia E, Marè C, Tondelli A, Stanca AM. 2008. Drought tolerance improvement in crop plants: An integrated view from breeding to genomics. Field Crops Research 105, 1-14.

Cho MH, Lim H, Shin DH, Jeon JS, Bhoo SH, Park YI, Hahn TR. 2011. Role of the plastidic glucose translocator in the export of starch degradation products from the chloroplasts in *Arabidopsis thaliana*. New Phytologist 190, 101-112.

Denyer K, Johnson P, Zeeman SC, Smith AM. 2001. The control of amylose synthesis. Journal of Plant Physiology 158, 479-487.

Egli B, Kölling K, Köhler C, Zeeman SC, Streb S. 2010. Loss of cytosolic phosphoglucomutase compromises gametophyte development in Arabidopsis. Plant Physiology 154, 1659-1671.

Fadzilla NM, Finch RP, Burdon RH. 1997. Salinity, oxidative stress and antioxidant responses in shoot cultures of rice. Journal of Experimental Botany 48, 325-331.

Flügge U-I. 1999. Phosphate translocators in plastids. Annual Review of Plant Physiology and Plant Molecular Biology 50, 27-45.

Flügge U-I, Häusler RE, Ludewig F, Gierth M. 2011. The role of transporters in supplying energy to plant plastids. Journal of Experimental Botany 62, 2381-2392.

Fulton DC, Stettler M, Mettler T, Vaughan CK, Li J, Francisco P, Gil M, Reinhold H, Eicke S, Messerli G, Dorken G, Halliday K, Smith AM, Smith SM, Zeeman SC. 2008. Beta-AMYLASE4, a noncatalytic protein required for starch breakdown, acts upstream of three active beta-amylases in Arabidopsis chloroplasts. Plant Cell 20, 1040-1058.

Guidi L, Bongi G, Ciompi S, Soldatini GF. 1999. In *Vicia faba* leaves photoinhibition from ozone fumigation in light precedes a decrease in quantum yield offunctional PSII centres. Journal of Plant Physiology 154, 167-172.

Hayashi F, Ichino T, Osanai M, Wada K. 2000. Oscillation and regulation of proline content by P5CS and ProDH gene expressions in the Light/Dark cycles in *Arabidopsis thaliana* L. Plant Cell Physiolgy 41, 1096-1101.

Hernandez JA, Corpass FJ, Gomez M, del Rio LA, Sevilla F. 1993. Salt-induced oxidative stress mediated by active oxygen species in pen leaf mitochondria. Physiologia Plantarum 89, 103-110.

Hummel I, Pantin F, Sulpice R, Piques M, Rolland G, Dauzat M, Christophe A, Pervent M, Bouteillé M, Stitt M, Gibon Y, Muller B. 2010. Arabidopsis plants acclimate to water deficit at low cost through changes of carbon usage: an integrated perspective using growth, metabolite, enzyme, and gene expression analysis. Plant Physiology 154, 357-372.

Jobling S. 2004. Improving starch for food and industrial applications. Current Opinion in Plant Biology 7, 210-218.

Kötting O, Kossmann J, Zeeman SC, Lloyd JR. 2010. Regulation of starch metabolism: the age of enlightenment? Current Opinion in Plant Biology 13, 321-328.

Lao NT, Schoneveld O, Mould RM, Hibberd JM, Gray JC, Kavanaugh TA. 1999. An Arabidopsis gene encoding a chloroplast targeted ß-amylase. Plant Journal 20, 519-525.

Liang X, Zhang L, Natarajan SK, Becker DF. 2013. Proline mechanisms of stress survival. Antioxidant Redox Signalling 19, 998-1011.

Lloyd JR, Kossmann J, Ritte G. 2005. Leaf starch degradation comes out of the shadows. Trends in Plant Science 10, 130-137.

Matysik J, Alia, Bhalu B, Mohanty P. 2002. Molecular mechanisms of quenching of reactive oxygen species by proline under stress in plants. Current Science 82, 525-532.

Monroe JD, Storm AR, Badley EM, Lehman MD, Platt SM, Saunders LK, Schmitz JM, Torres CE. 2014. beta-Amylase1 and beta-amylase3 are plastidic starch hydrolases in Arabidopsis that seem to be adapted for different thermal, pH, and stress conditions. Plant Physiology 166, 1748-1763.

Nittylä T, Messerli G, Trevisan M, Chen J, Smith AM, Zeeman SC. 2004. A previously unknown maltose transporter essential for starch degradation in leaves. Science 303, 87-89.

Osakabe Y, Osakabe K, Shinozaki K, Tran LS. 2014. Response of plants to water stress. Frontiers in Plant Science, doi: 10.3389/fpls.2014.00086.

Prasch CM, Ott KV, Bauer H, Ache P, Hedrich R, Sonnewald U. 2015. ß-amylase1 mutant Arabidopsis plants show improved drought tolerance due to reduced starch breakdown in guard cells. Journal of Experimental Botany 66, 6059-6067.

Rockström J and Falkenmark M. 2010. Semiarid crop production from a hydrological perspective: gap between potential and actual yields. Critical Reviews in Plant Sciences 19, 319-346.

Santelia D and Zeeman SC. 2011. Progress in Arabidopsis starch research and potential biotechnological applications. Current Opinion in Biotechnology 22, 271-280.

Santelia D, Trost P, Sparla F. 2015. New insights into redox control of starch degradation. Current Opinion in Plant Biology 25, 1-9.

Smith AM and Zeeman SC. 2006. Quantification of starch in plant tissues. Nature Protocols 1, 1342-1345.

Smith AM, Zeeman SC, Smith SM. 2005. Starch degradation. Annual Review of Plant Biology 56, 73-98.

Sparla F, Costa A, Lo Schiavo F, Pupillo P, Trost P. 2006. Redox regulation of a novel plastid-targeted beta-amylase of Arabidopsis. Plant Physiololgy 141, 840-850.

Stitt M and Zeeman SC. 2012. Starch turnover: pathways, regulation and role in growth. Current Opinion in Plant Biology 15, 282-292.

Streb S, Eicke S, Zeeman SC. 2012. The simultaneous abolition of three starch hydrolases blocks transient starch breakdown in Arabidopsis. Journal of Biological Chemistry 287, 41745-41756.

Szabados L and Savouré A. 2009. Proline: a multifunctional amino acid. Trends in Plant Science 15, 89-97.

Székely G, Abrahám E, Cséplo A, Rigó G, Zsigmond L, Csiszár J, Ayaydin F, Strizhov N, Jásik J, Schmelzer E, Koncz C, Szabados L. 2008. Duplicated P5CS genes of Arabidopsis play distinct roles in stress regulation and developmental control of proline biosynthesis. Plant Journal 53, 11-28.

Valerio C, Costa A, Marri L, Issakidis-Bourguet E, Pupillo P, Trost P, Sparla F. 2011. Thioredoxin-regulated beta-amylase (BAM1) triggers diurnal starch degradation in guard cells, and in mesophyll cells under osmotic stress. Journal of Experimental Botany 62, 545-555.

Verbruggen N and Hermans C. 2008. Proline accumulation in plants: a review. Amino Acids 35, 753-759.

Wilhelm C and Selmar D. 2011. Energy dissipation is an essential mechanism to sustain the viability of plants: the physiological limits of improved photosynthesis. Journal of Plant Physiology 168, 79-87.

Zeeman SC, Tiessen A, Pilling E. 2002. Starch synthesis in Arabidopsis. Granule synthesis, composition, and structure. Plant Physiology 129, 516-529.

Zeeman SC and ap Rees T. 1999. Changes in carbohydrate metabolism and assimilate partitioning in starch-excess mutants of Arabidopsis. Plant Cell Environment 22, 1445-1453.

Zeeman SC, Smith SM, Smith AM. 2007. The diurnal metabolism of leaf starch. Biochemical Journal 401, 13

SUPPLEMENTARY INFORMATION

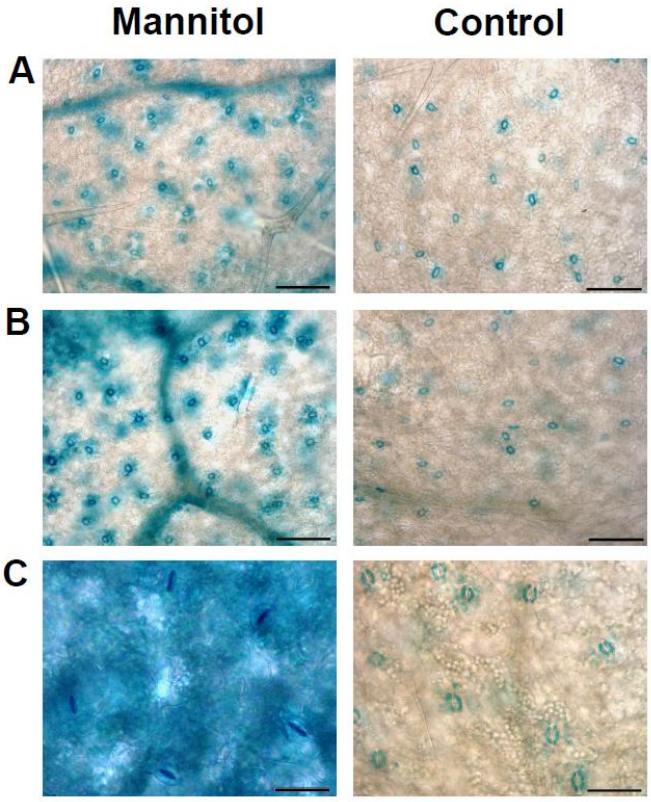

Figure S1: Activity of BAM1promoter::GUS under control conditions and in response to 150 mM mannitol. Plants were grown under 12 h light/ 12 h dark cycle and osmotic stress was applied 1 h after the beginning of light period. Plants were collected at the end of the light period. GUS activity was measured at 0.5 DAT, panel A; 1.5 DAT, panel B; 6.5 DAT, panel C. Scale bar = 100 µm.

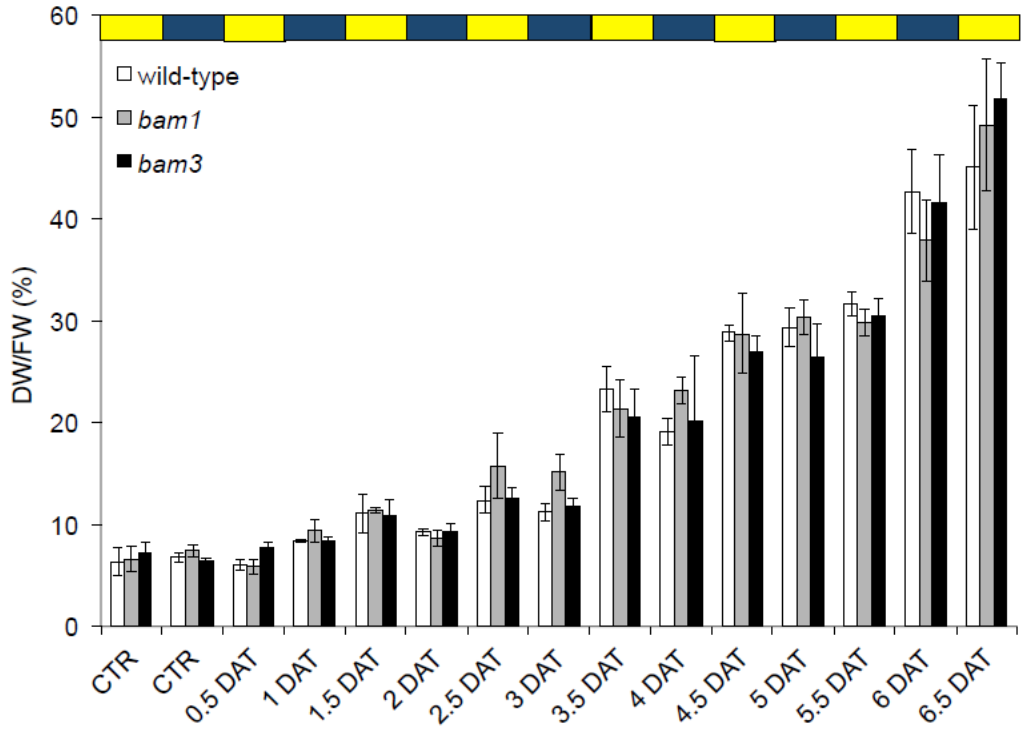

Figure S2: Loss of water in wild-type, *bam1* and *bam3* plants exposed to 150 Mm mannitol. Water loss was estimated as the percentage of the ratio between dry weight (DW) and fresh weight (FW) of the whole rosette of wild-type, *bam1* and *bam3* plants. Plants were collected at 12 h of light and 12 h of dark under control and at increasing time of stress. Values are the means ± SD of five independent biological replicas.

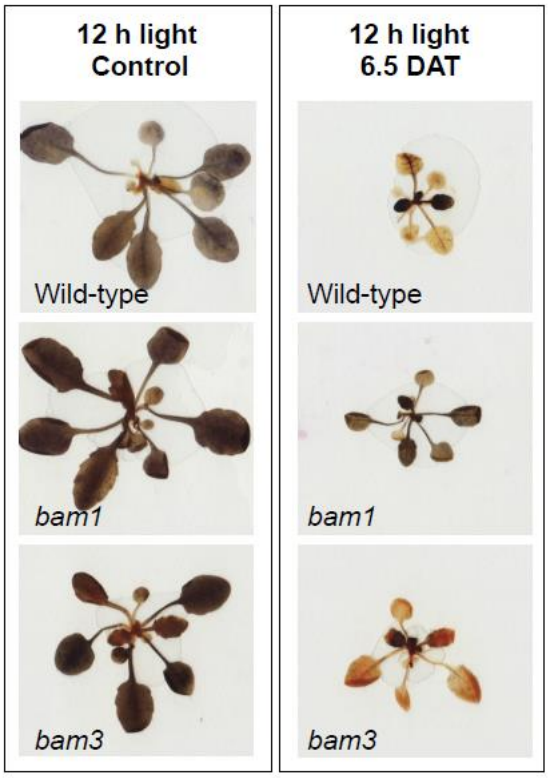

Figure S3: Starch content in wild-type, *bam1* and *bam3* plants qualitatively evaluated with Lugol staining. Thirty-d-old plants were collected at the end of the light period (12 h light) under control (left panel) or in response to mannitol treatment (right panel).

	bam1	*bam3*
CTR 12 L	0.7560	0.2656
CTR 12 D	0.0992	0.2527
0.5 DAT	0.6168	0.0013
1 DAT	0.0635	0.6080
1.5 DAT	0.6861	0.1011
2 DAT	0.2050	0.9505
2.5 DAT	0.0672	0.7540
3 DAT	0.0019	0.3327
3.5 DAT	0.2465	0.1234
4 DAT	0.0011	0.7270
4.5 DAT	0.9761	0.3938
5 DAT	0.0544	0.1256
5.5 DAT	0.5310	0.2726
6 DAT	0.0959	0.7033
6.5 DAT	0.3328	0.0649

Supplementary Table S1. p-value obtained from Student's t-tests performed on loss of water, estimated as the percentage of the ratio between dry weight and fresh weight of the whole rosette in response to drought stress in *bam1* and *bam3* mutants and compared with wild-type samples (Figure S2). Control samples were collected at the end of the light (12 L) and at the end of the dark (12 D) periods. CTR=control; DAT=day after treatment.

	bam1	*bam3*
CTR	0.7823	0.0053
0.5 DAT	0.2608	0.0005
1.5 DAT	0.2906	0.1954
2.5 DAT	0.4426	0.0035
3.5 DAT	0.0024	0.0025
4.5 DAT	0.0163	0.0618
5.5 DAT	0.0027	0.0031
6.5 DAT	0.0067	0.0090

Supplementary Table S2. p-value obtained from Student's t-tests performed on starch concentration quantified at 12 h of light in response to drought stress in *bam1* and *bam3* mutants and compared with wild-type samples (Fig. 2). CTR=control; DAT=day after treatment.

	bam1	*bam3*
CTR	0.7239	0.0009
1 DAT	0.0273	0.0415
2 DAT	0.0000	0.2800
3 DAT	0.3768	0.9859
4 DAT	0.0510	0.4054
5 DAT	0.5801	0.7747
6 DAT	0.3241	0.8917

Supplementary Table S3. p-value obtained from Student's t-tests performed on starch concentration quantified at 12 h of dark in response to drought stress in *bam1* and *bam3* mutants and compared with wild-type samples (Fig. 3). CTR=control; DAT=day after treatment.

	bam1	*bam3*
CTR	0.5398	0.0498
0.5 DAT	0.0264	0.0783
4.5 DAT	0.0002	0.3886
7.5 DAT	0.0007	0.0625

Supplementary Table S4. p-value obtained from Student's t-tests performed on degree of lipid peroxidation determined at 12 h of light in response to drought stress in *bam1* and *bam3* mutants and compared with wild-type samples (Fig. 4). CTR=control; DAT=day after treatment.

	bam1	*bam3*
CTR	0.6736	0.9898
0.5 DAT	0.0477	0.4345
1.5 DAT	0.6412	0.9250
2.5 DAT	0.4628	0.2639
3.5 DAT	0.0178	0.0136
4.5 DAT	0.0033	0.0683
5.5 DAT	0.0478	0.5668
6.5 DAT	0.0052	0.3592

Supplementary Table S5. p-value obtained from Student's t-tests performed on proline concentration quantified at 12 h of light in response to drought stress in *bam1* and *bam3* mutants and compared with wild-type samples (Fig. 5). CTR=control; DAT=day after treatment.

	Sucrose		Glucose		Maltose	
	bam1	*bam3*	*bam1*	*bam3*	*bam1*	*bam3*
CTR 12 L	0.6426	0.4945	0.1249	0.3231	0.7692	0.3382
0.5 DAT 12 L	0.0174	0.3848	0.0061	0.0126	0.7395	0.7074
3.5 DAT 12 L	0.1083	0.1524	0.0006	0.0011	0.1842	0.3693
5.5 DAT 12 L	0.0002	0.0017	0.0746	0.1891	0.0055	0.4432
CTR 12 D	0.4273	0.7277	0.3874	0.9541	0.6086	0.6026
1 DAT 12 D	0.1079	0.0027	0.0664	0.0003	0.7142	0.0005
4 DAT 12 D	0.9369	0.2815	0.0892	0.0341	0.0958	0.4676
6 DAT 12 D	0.1730	0.5704	0.0802	0.2191	0.5797	0.1248

Supplementary Table S6. p-value obtained from Student's t-tests performed on sucrose, glucose and maltose concentrations quantified at 12 h of light (12 L) and 12 h of dark (12 D) in response to drought stress in *bam1* and *bam3* mutants and compared with wild-type samples (Fig. 6). CTR=control; DAT=day after treatment.

CHAPTER 4

BAM1 and AMY3, two redox sensitive enzymes involved in Arabidopsis starch degradation, are target of glutathionylation

Unpublished results

Claudia Pirone[1], Gian Luca Borghi[1], Paolo Trost[1], Diana Santelia[2], Francesca Sparla[1]

[1]Department of Pharmacy and Biotechnology FaBiT, University of Bologna, Via Irnerio 42, 40126 Bologna, Italy

[2]Institute of Plant Biology, University of Zürich, Zollikerstrasse 107, CH-8008 Zurich, Switzerland

Abstract

Arabidopsis genome encodes for nine β-amylases (BAM1-9) and for three α-amylases (AMY1-3), respectively exo- and endo- hydrolases involved in starch degradation. Among them only 4 β-amylases (BAM1-4) and one α-amylase (AMY3) are found to be chloroplastic (Yu et al., 2005; Zeeman et al., 2010; Glaring et al., 2011). Despite being active amylases, plants depleted of AMY3 or BAM1 proteins can degrade starch efficiently in standard growth conditions (Yu et al., 2005; Kaplan and Guy, 2005; Kötting et al., 2009). However, when other starch-degrading enzymes are missing the lack of AMY3 and BAM1 enhance the starch excess (*sex*) phenotype, pointing to their involvement in this process (Fulton et al., 2008). BAM1 and AMY3 appear to synergistically degrade starch *in vitro* (Seung at al., 2013) and, *in vivo*, their role in diurnal starch degradation in guard cells has been highlighted (Valerio et al., 2011; Prasch et al., 2015; Horrer et al., 2016). In addition,, BAM1 is known to be involved in starch degradation in mesophyll cells in response to osmotic stress (Valerio et al., 2011; Zanella et al., 2016). Similarly, also the transcriptional levels of AMY3 increase during drought stress, suggesting the involvement of both the enzymes in the onset to the stress response (Santelia D., personal communication). Another behavioral similarity between BAM1 and AMY3 is their thioredoxin-dependent redox-regulation. For what we know, BAM1 and AMY3 are the only members of their protein family whose activity is inhibited by the formation of a disulfide bridge with a midpoint redox potential at pH 7.0 of -302 mV and at pH 7.9 of -329 mV, respectively (Sparla et al., 2006; Seung at al., 2013). As a consequence, BAM1 and AMY3 seem to be part of a diurnal starch degradation pathway that occurs in specialized cell types, as guard cells, or under stress conditions.

In the last decade, glutathionylation has emerged as an alternative redox post-translational modification (PMT) consisting in the formation of a mixed disulfide between a protein cysteine residue and a glutathione molecule, occurring prevalently under oxidative stress (Zaffagnini et al., 2012b). This reversible modification has been shown to have different roles, like the protection of protein thiols from irreversible oxidation, but also protein redox regulation and signaling (Zaffagnini et al., 2012b). To analyze the susceptibility of *Arabidopsis thaliana* BAM1 (AtBAM1) and AMY3 (AtAMY3) to glutathionylation, both the enzymes have been recombinant expressed, purified and their activities have been assayed in presence of hydrogen peroxide (H_2O_2) with or without reduced glutathione (GSH). Both the enzymes were inhibited by the different treatments, although the inhibition rates were slower in presence of GSH. Moreover, the addition of reduced DTT to oxidized samples fully reverted the enzyme activities only when H_2O_2 treatment was performed in presence of GSH, strongly suggesting that both AtBAM1 and AtAMY3 were glutathionylated. This hypothesis was confirmed by western blot and mass spectrometry analyses. For a better comprehension of the molecular mechanism of glutathionylation and to identify target cysteine residues, all the Cys to Ser variants both of AtBAM1 and AtAMY3 were incubated with BioGSSG and analysed by western blotting using anti-biotin antibodies, without providing an unequivocal result. However, it was shown that pre-oxidized AtBAM1 could no more undergo glutathionylation. Thus, generation of the disulfide bond in AtBAM1 prevents the formation of mixed disulfide with glutathione, probably because of the involvement of the same cysteines residues. Assuming so, the opposite mechanism can be hypothesized and glutathionylation might interfere with or prevent AtBAM1 switch-off caused by the formation of the intra-molecular disulfide bond. The same seems not to be true for AtAMY3, since pre-oxidized enzyme is still target of glutathionylation.

Taken together, these data suggest a role of glutathionylation in protecting AtBAM1 and AtAMY3 from fast and irreversible oxidation under oxidative stress conditions.

INTRODUCTION

Starch is a glucose polymer that accumulates in plastids of higher plants as insoluble and crystalline granules. For simplicity, starches can be classified as transitory (or primary) and storage (secondary) starch. Despite displaying the same structure and sharing a common biosynthetic pathway, transitory starch and storage starch are degraded by a different set of enzymes (Smith et al., 2005). As suggested by the name, storage starch is typically found in storage organs, such as seeds or tubers, and it is remobilized in response to internal stimuli to support specific phases of growth (e.g. germination). In contrast, primary starch is transiently stored in chloroplasts of autotrophic tissues and, under normal growth conditions, is synthesized during the day and degraded during the following night to supply energy for plant metabolism in absence of light. Moreover, primary starch can be degraded in the light to cope with abiotic and biotic stress, supplying energy and carbon required to meet specific demands of the cells (Valerio et al., 2011; Zanella et al., 2016). Primary starch accumulates also in the chloroplasts of specialized cells of the plant, e.g. guard cells (Smith et al., 2005; Prasch et al., 2015; Horrer et al., 2015). Through the stomatal pore, guard cells exchange gases (i.e. CO_2 and H_2O) with the external environment. In these cells, starch metabolism is reverted, following an opposite rhythm compared to mesophyll cells. Starch is mobilized in the light period to produce malate and sucrose that contribute to increase guard cell osmolality, turgor and stomatal opening (Vavasseur and Raghavendra, 2005; Lawson et al., 2014).

In higher plants, chloroplasts are the site of oxygenic photosynthesis. During this process, electrons ripped from water are donated to ferredoxin (Fdx), which function as a mobile electron carrier that distributes electrons to indirectly produce NADPH or to supply other specific processes located in the stroma, such as reactions involved in chloroplast redox regulation (Schürmann and Buchanan, 2008). In this case, electrons are transferred from Fdx to thioredoxyns (Trxs) via Fdx-Trx-reductase (FTR) (Schürmann and Buchanan, 2008). Moreover, oxygenic photosynthesis release oxygen. Therefore, in chloroplasts, due to the high-energy exposure and to the inevitable leakage of electrons from the electron-transfer reactions, O_2 can undergo a stepwise reduction that lead to production of highly reactive oxygen species (ROS) (Foyer and Harbinson, 1994; Foyer, 1997). ROS include free

radicals such as superoxide anion ($O_2^{\bullet -}$), hydroxyl radical ($^{\bullet}OH$), as well as non-radical molecules like hydrogen peroxide (H_2O_2), singlet oxygen ($^1O_2$), and so forth (Sharma et al., 2012). While at low concentrations ROS play important roles in cell signalling (i.e. H_2O_2 is an essential signal that mediates ABA-induced stomatal closure), at high concentrations ROS are extremely harmful molecules that tend to uncontrollably oxidize different types of cellular components (Wang and Song, 2008; Sharma et al., 2012). When the level of ROS exceeds the defence mechanisms, a cell is said to be in a state of "oxidative stress". The balance by which ROS will act as damaging or signalling molecule is subtle and depends on the rate of their production and scavenging. Although ROS are unavoidable by-products of photosynthesis, many environmental stresses (drought, salinity, chilling, metal toxicity, UV-B radiation, pathogens attack) enhance generation of ROS in plants (for reviews see: Cruz de Carvalho, 2008; Sharma et al, 2012; Suzuki et al., 2012). Therefore, plants have developed sets of enzymatic and non-enzymatic antioxidative systems to detoxify excess ROS, to prevent and repair oxidative damage and maintain redox homeostasis (Shigeoka et al., 2002; Mittler et al., 2004; Foyer and Shigeoka, 2011).

Due to their physicochemical properties, cysteine residues may perceive alterations in cellular oxidant levels as well as changes in the redox environment. The oxidative modifications of selected protein cysteines, affecting single or double thiol groups, can be used in chloroplast metabolic regulation (Geigenberger et al., 2005; Glaring et al., 2012; Geigenberger and Fernie, 2014; Santelia et al., 2015). These redox sensitive cysteines are often characterized by lower pK_a values (Roos et al., 2013) compared to the pK_a values of insensitive ones (typically ranging between 8–9), which result in their deprotonation under physiological pH conditions, generating thiolate anions ($-S^-$) that exhibit much higher reactivity than their protonated thiol (-SH) counterparts (Winterbourn and Hampton, 2008) (Fig. 1). The reactivity of the thiolate anions also depends on the local protein environment, and currently there is no accurate way to predict their reactivity (Randall et al., 2013). In the presence of oxidants, thiolate anions rapidly form sulfenic acids (-SOH), which are important intermediates in the thiol oxidation process (Kettenhofen and Wood, 2010; Lo Conte and Carroll, 2013). Sulfenic acids generally rapidly react with nearby thiol groups (Poole et al., 2004) to form intra- or intermolecular disulfide bonds (-S–S-), or with non-protein thiols such as glutathione (GSH or GSSG) to form mixed disulfide bonds (-S–SG) (see below) (Fig. 1). Further oxidation of sulfenic acid

leads to sulfinic acid (-SO_2H) and sulfonic acid (-SO_3H) formation, which are typically irreversible oxidation processes (Fig. 1) (Santelia et al., 2015). Most oxidative thiol modifications are reduced by thioredoxins (Trxs) (Berndt et al., 2007; Lu and Holmgren, 2014), which use direct thiol-disulfide reactions to reduce back disulfide bonds (Fig.1), while glutaredoxins (GRXs) restore enyme activity removing single thiol modification, such as S-glutathionylation (Meyer et al., 2012).

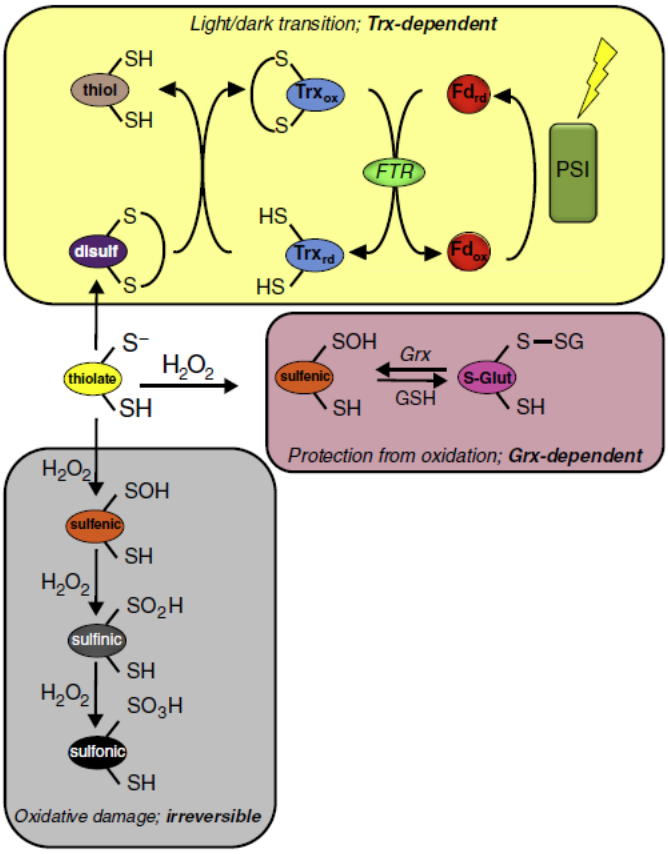

Figure 1 - From Santelia et al. (2015), schematic overview of major oxidative thiol modifications in redox regulated enzymes of chloroplast stroma. Cysteines by low pKa values, namely "reactive cysteines", at physiological pH are prevalently found in the highly reactive thiolate anion form (–S^-; yellow oval) rather than in their thiol form (–SH). The thiolate anion leads either to the formation of a disulfide bond (S–S; violet oval) or in presence of hydrogen peroxide (H_2O_2), to the formation of sulfenic acid (R–SOH; orange oval). The disulfide bond, can be indirectly reduced back by light, through the ferredoxin/thioredoxin system (pathway depicted within the yellow box). Alternatively, in the presence of hydrogen peroxide (H_2O_2) sulfenic acid can be further oxidised to to sulfinic (R–SO_2H; grey oval) and sulfonic acids (R–SO_3H; black oval), two hyperoxidized forms that irreversibly damage the enzymes (pathway depicted within the grey box). However, in presence of reduced glutathione (GSH), sulfenic acid can also form a mixed disulfide with glutathione (S-glut; pink oval), a modification that can be removed by glutaredoxin (Grx), restoring the

enzyme activity (pathway depicted within the pink box). Abbreviations: PSI, photosystem I (green square); Fd_{ox}, oxidized ferredoxin (red circle); Fd_{rd}, reduced ferredoxin (red circle); FTR, ferredoxin:thioredoxin reductase (green oval); Trx_{rd}, reduced thioredoxin (blue oval); Trx_{ox}, oxidized thioredoxin (blue oval).

Redox control based on thiol-reactivity of the Calvin-Benson cycle enzymes is well characterized, and provide an excellent link between the two phases of the photosynthesis, the light and the carbon reactions (Schürmann and Buchanan, 2008). In most species, including Arabidopsis, about half of the photoassimylates produced during the day by photosynthesis are transiently stored in chloroplast as primary starch (Zeeman and ap Rees, 1999). The major steps in primary starch metabolism has been elucidated and the key genes/proteins identified (Zeeman et al., 2010) (Fig.2).

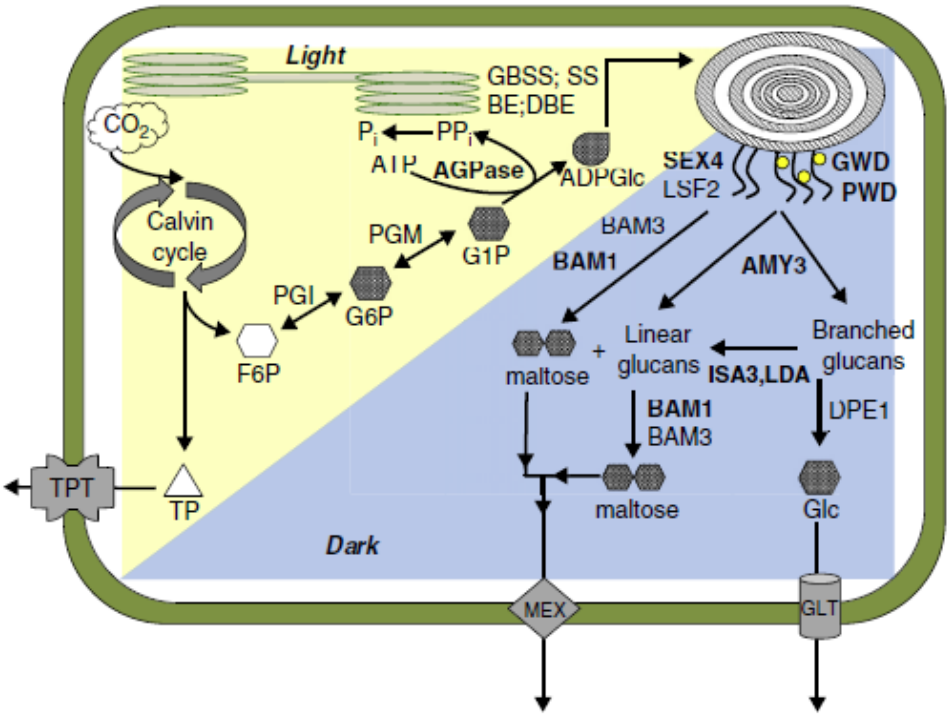

Figure 2 - Schematic representation of Arabidopsis transitory starch synthesis and degradation pathways (Santelia et al., 2015). During the day, photoassimilates are exported to the cytosol as triose phosphates (TP), via the triose-phosphate transporter (TPT), to sustain sucrose biosynthesis, while the remaining fixed carbon is converted into transitory starch. The first irreversible step of starch biosynthesis is the formation of ADP-glucose (ADPGlc) through the bond of an ATP molecule to glucose-1-phosphate (G1P), with the concomitant release of inorganic pyrophosphate (PPi), hydrolyzed to inorganic phosphate (Pi). G1P is produced by phosphoglucomutase (PGM) from glucose-6-phosphate (G6P), which in turn is the product of fructose-6-phosphate (F6P) transformation mediated by phosphoglucose isomerase (PGI). Granule-bound starch synthase (GBSS), starch synthases (SS), branching enzymes (BE) and debranching enzymes (DBE) are all involved in the correct formation of highly compacted starch granules. During the following night, starch

is degraded. Glucan, water dikinase (GWD) and phosphoglucan, water dikinase (PWD) phosphorylate external layers of the starch granule (phosphate is represented by yellow circles), making starch accessible to hydrolytic enzymes. Phosphate from starch and glucans oligosaccharides is subsequently removed by phosphoglucan phosphatases starch excess 4 (SEX4) and Like SEX4 isoform 2 (LSF2). These phosphorylation and dephosphorylation events are necessary for starch remobilization. The hydrolytic action of β-amylases (BAM3 and BAM1) on linear polyglucans, shorten the chains releasing β-maltose units that are exported to the cytosol via maltose transporter (MEX). Alfa-Amylase 3 (AMY3) specifically hydrolyzes α-1,4 internal glicoside linkages in starch. The two DBE isoamylase 3 (ISA3) and limit dextrinase 1 (LDA1) take part in starch degradation by removing the branch points which otherwise would limit the activity of β-amylases. The disproportionating enzyme (DPE1) releases glucose that can be transported to cytoplasm via glucose transporter (GLT). Enzymes target of redox modifications are highlighted in bold.

Moreover, it has been shown that primary starch synthesis and degradation are tightly and reciprocally coordinated and correlated with other metabolic pathways of the central metabolism, such that early depletion of starch at dusk or abnormal accumulation of starch during the day strongly affect metabolism and growth (Gibon et al., 2004; Gibon et al., 2009; Graf et al., 2010; Scialdone et al., 2013; Kölling et al., 2015). Indeed, starch turnover and carbon allocation for plant growth are dependent of both light-dark cycles and the biological clock (Stitt and Zeeman, 2012).

Recently, redox regulation of enzymes involved in the primary starch metabolism has begun to be investigated and the activity of many of them have been demonstrated to be affected by reducing or oxidizing conditions, indicating that they may be regulated by the redox potential of the plastid stroma. Much research has focused on the control of AGPase, the first enzyme on the committed pathway of starch synthesis. AGPase is rapidly activated upon illumination by reduction of an intermolecular disulfide bond between the Cys residues joining the two small subunits of this heterotetrameric enzyme (Hendriks et al., 2003; Thormählen et al., 2013). In addition, redox activation of AGPase is also promoted by sugars, regardless of light (Hendriks et al., 2003; Kolbe et al., 2005; Thormählen et al., 2013). Reductive activation of AGPase in non-photosynthetic tissues or in nocturnal leaves requires alternative systems of electron transfer linked to NADPH generated from sugars, rather than to photoreduced Fdx. This can be accomplished by the plastid NADPH-dependent thioredoxin reductase (NTRC) (Serrato et al., 2004; Michalska et al., 2009). This is a bimodular protein containing both a NADPH dependent thioredoxin

reductase (NTR) and a Trx domain on a single polypeptide (Serrato et al., 2004; Pascual et al., 2011). Thus, the role of redox regulation spread beyond the mere adjustment of metabolic pathways in response to light/dark cycle. In addition to AGPase, reductive activation by thiol/disulfide modulation has also been shown, by means of comprehensive *in vitro* studies, for other enzymes involved in the pathway of starch synthesis downstream of AGPase, such as SS1, SS3, SBE2, ISA1, ISA2 (Glaring et al., 2012). This enables redox regulation mediated by Trxs to coordinate the supply and the use of ADPGlc for starch synthesis, linking external factors such as light and sucrose to the activation of the whole pathway.

There are also evidences of redox regulation for starch degrading enzymes. In Arabidopsis, leaf starch breakdown begins with a primary event of phosphorylation followed by a subsequent dephosphorylation of the starch granule (reviewed by Pérez and Bertoft, 2010; Silver et al., 2014). Three enzymes involved in this starch phosphate metabolism, the (phospho)glucan, water dikinases (GWD and PWD) and the phosphoglucan phosphatase SEX4, contain redox sensitive cysteines. However, only GWD and SEX4 seem to be affected by the redox potential *in vitro*, being activated under reducing conditions (Mikkelsen et al., 2005; Sokolov et al., 2006; Silver et al., 2014). Given that starch degradation was shown to occur during the night and that the chloroplast stroma is generally considered to be a more reducing environment during the day (i.e. when photosynthetic process is active), such regulation seems counter-intuitive. However, the midpoint redox potential of GWD is very high ($E_{m,\ 7.9}$ of -310 for GWD of Solanum tuberosum), making a strict control of its enzymatic activity by changes in redox potential unlikely (Mikkelsen et al., 2005). Moreover, redox regulation of GWD on nocturnal starch degradation seems not to play an important role *in vivo* (Skeffington et al., 2014). On the contrary, GWD appears also to be implicated in starch synthesis during the day, and in agreement with that, it seems that starch phosphorylation is greater in plants grown under continuous light, rather than in a light-dark cycle (Hejazi et al., 2014). SEX4, as other members of the protein tyrosine phosphatase (PTP) superfamily, has a conserved catalytic cysteine with a very low pK_a value (Sokolov et al., 2006; Silver et al., 2014). Then, a disulfide bridge, acting as a redox dependent switch between the catalytic cysteine (residue 198) and the nearby cysteine (residue 130), is formed (Silver et al., 2014). SEX4 seems to be more active in the light, given that Trxs can reactivate the oxidized form of

the enzyme *in vitro*, again contrasting with the observed starch excess (*sex*) phenotype of the *sex4* mutants (Silver et al., 2013). Given that starch phosphorylation seems to occur also during the day, SEX4 may function in light conditions to reduce the excess of bound phosphate promoting the elongation of glucan chains (Ritte et al., 2004; Hejazi et al., 2014; Santelia et al., 2015).

Also isoamylase 3 (ISA3), limit dextrinase (LDA) and debranching enzymes (DBEs), all involved in starch degradation through the removal of branched points from glucan polymers, are redox sensitive (Schindler et al., 2001; Delatte et al., 2006; Repellin et al., 2008; Glaring et al., 2012). LDA is activated upon reduction by thiol compounds such as dithiothreitol and GSH, but a specific activation mediated by Trxs has not been documented (Schindler et al., 2001). Moreover, spinach LDA1 has an acidic pH optimum and no activity above pH 7. GSH mediated activation of LDA1 broadens the pH activity curve towards less acidic pH values, but LDA1 still seems more prone to function in chloroplast in the dark than in the light (Schindler et al., 2001). Given that GSH concentration does not change in function of the light/dark conditions, LDA activity *in vivo* is probably mainly regulated by pH. The following step of starch degradation requires the action of amylases, enzymes able to cleave α-1,4 glucose bonds of starch (reviewed by Zeeman et al., 2010). *Arabidopsis thaliana* genome encodes for 9 β-amylases (BAM1-9) and 3 α-amylases (AMY1-3) (Zeeman et al., 2010). Only 4 of the 9 β-amylases (BAM1-4) and one α-amylase (AMY3) have been found to be chloroplastic proteins (Yu et al., 2005; Sparla et al., 2006; Fulton et al., 2008; Glaring et al., 2011). β-amylases are exo-acting enzymes able to hydrolyze α-1,4 bonds and are responsible for the release of maltose units from the non-reducing end of polyglucans, like starch, in the chloroplast stroma. Conversely, α-amylases are endo-acting enzymes that hydrolyses α-1,4 linkages in starch to produce small linear and branched soluble glucans.

In current starch degradation model, BAM3 plays the major role in transitory starch degradation at night (Lao et al., 1999; Fulton et al., 2008), whereas BAM1 was shown to be involved in diurnal starch degradation in mesophyll cells under osmotic stress conditions (Valerio et al., 2011; Prasch et al., 2015; Zanella et al., 2016) and was found to be essential, together with AMY3, for diurnal starch breakdown in guard cells, to sustain stomatal opening (Valerio et al., 2011; Prasch et al., 2015; Horrer et al., 2016). Consistently, inactive BAM1 bears a disulfide bridge ($E_{m,7.0}$ of -302 mV), presumably

between cysteine residues 32 and 470, which is rapidly reduced by Trxs *in vitro* (Sparla et al., 2006). No experimental evidence supports redox regulation of BAM3 activity. However, modelling of BAM3 protein does not exclude the possibility of disulfide bridges formation (Glaring et al., 2012). In addition to the redox control, BAM1 and BAM3 display other different biochemical properties (Monroe et al., 2014). While BAM3 has an acidic pH optimum and a preference for lower temperatures, favouring its activity in nighttime starch degradation, BAM1 is more active at higher pH and temperature values, justifying its predominant role in daytime stress responses (Monroe et al., 2014). Similar to BAM1, also AMY3 is redox regulated via a disulfide bridge between cysteine residues 499 and 587 with a midpoint redox potential at pH 7.9 of -329 mV, and the inactive oxidized form of the enzyme can be reactivated by reduced Trx (Seung et al., 2013). The broad pH optimum of AMY3 (centred at pH 7.5) and the Trx-mediated regulation suggest that its activity may be promoted during the day, similarly to BAM1 (Seung et al., 2013). Although *amy3* mutants have no *sex* phenotype, the combined loss of AMY3 together with other enzymes involved in starch degradation results in a more severe *sex* phenotype (Kötting et al., 2005; Streb et al., 2012). Moreover, *amy3* mutants synthesize the same starch amount than wild-type (Yu et al., 2005). Thus, is difficult that the activity of AMY3 can fit in starch biosynthetic pathway. In addition, it was demonstrated that AMY3 works synergistically with BAM1 *in vitro* to efficiently degrade starch and that AMY3 expression, like BAM1, is increased during stress (Seung et al., 2013). While cysteine 587 is conserved among α-amylases, cysteine 499 is specific for AMY3 and also cysteine 32 and 499 of BAM1 are not conserved in BAM3 or in other β-amylases (Sparla et al., 2006; Seung et al., 2013), suggesting that redox sensitivity is not a common feature of endo or exo-amylases, but rather a specific additional regulatory trait required in starch metabolism in different conditions, tissues or species.

Glutathione (γ-l-glutamyl-l-cysteinylglycine) is a small tripeptide constituting the major thiol-based redox buffer of plant cells. In the cytosol and most organelles, glutathione concentration reaches the order of millimolar (Foyer and Noctor, 2005; Rouhier et al., 2008; Krueger et al., 2009; Queval et al., 2011). In the stroma of chloroplasts, under non-stress conditions, glutathione is found prevalently in its reduced form (GSH), because the levels of the oxidized form (GSSG) are kept to a minimum by NADPH-dependent glutathione reductase (Foyer and Noctor, 2011). GSH is involved in detoxification of ROS

through the ascorbate–glutathione cycle (Asada, 2006). In addition, glutathione can reversibly form a mixed disulfide with reactive and accessible protein cysteines. This post-translational modification, named protein glutathionylation, has been extensively studied in mammalian cells (Mieyal et al., 2008; Shelton and Mieyal, 2008; Dalle-Donne et al., 2009; Xiong et al., 2011) and is emerging as an important additional mechanism of redox regulation in plants. Glutathionylation is generally promoted by ROS (Zaffagnini et al., 2012b). Indeed, although glutathionylation *in vitro* can be obtained via direct reaction with GSSG, the major mechanism of protein glutathionylation *in vivo* is based on a primary oxidation of protein thiols to sulfenic acids (–SOH) caused by hydrogen peroxide, followed by the formation of a mixed disulfide (–SSG) with reduced glutathione (GSH) (Zaffagnini et al., 2012b). Thus, glutathionylation may prevent irreversible over-oxidation of cysteine residues to sulfinic ($–SO_2H$) and sulfonic forms ($–SO_3H$). While glutathionylation occurs through a non-enzymatic mechanism *in vivo*, the regeneration of reduced thiols (namely deglutathionylation) also depends on GSH but requires the involvement of small oxidoreductases belonging to the thioredoxin superfamily and known as glutaredoxins (GRXs) (Rouhier et al., 2008; Zaffagnini et al., 2012b). Besides protection of protein thiols against over-oxidation, gluathionylation is involved in the regeneration mechanisms of specific antioxidant enzymes such as peroxiredoxins and methionine sulfoxide reductases (Zaffagnini et al., 2012b) and in most cases gluathionylation has a modulatory function on the activity of target proteins (Zaffagnini et al., 2012b). From several proteomic analyses, many chloroplastic proteins involved in carbon assimilation pathway seem to undergo glutathionylation under artificially imposed oxidative stress conditions (Ito et al., 2003; Dixon et al., 2005; Zaffagnini et al., 2012a; Michelet et al., 2008; Gao et al., 2009a) suggesting a global regulatory role of this modification.

Given that AMY3 and BAM1 are the only redox regulated amylases in Arabidopsis and that they seem to work synergistically in daytime transitory starch breakdown in guard cells or during stress responses, they might be part of an alternative starch degradation pathway occurring in specialized cells and/or under stress conditions. Moreover, it seems reasonable to hypothesize that they may undergo alternative redox post-translational modification or protective mechanism, such as glutathionylation, to modulate their activity. The purpose of the present work was thus to investigate the behaviour of *Arabidopsis thaliana* BAM1 (AtBAM1) and AMY3 (AtAMY3) enzymes under oxidative

conditions in order to assess the relationships between oxidants, gluathionylation and enzyme activities.

EXPERIMENTAL PROCEDURES

In silico analysis of α- and β-amylases

The amino acid sequences of *Arabidopsis thaliana* β-amylase 1 (At3g23920; AtBAM1), *Arabidopsis thaliana* β-amylase 3 (At4g17090; AtBAM3) and sweet potato (*Ipomoea batata*) β-amylase (IbBMY1) were aligned with Clustal Omega (Sievers et al., 2011). Similarly, primary sequences of *Arabidopsis thaliana* α-amylase 3 (At1g69830; AtAMY3), *Arabidopsis thaliana* α-amylase 1 (At4g25000; AtAMY1) and barley (*Hordeum vulgare*) α-amylase type A isozyme (HvAMY1) were compared by alignment with Clustal Omega (Sievers et al., 2011). The presence of signal peptides and potential cleavage sites was predicted by ChloroP (Emanuelsson et al., 1999) and SignalP (Petersen et al., 2011). The three dimensional model of AtBAM1 was made using Swiss-Model workspace (http://swissmodel.expasy.org/workspace) based on the known structure of barley (*Hordeum vulgare*) β-amylase (PDB code 1B1Y; Mikami et al., 1999). The structure was generated with the Swiss-PDB viewer software.

Cloning, expression, and purification of AtBAM1 and AtAMY3 proteins

Two different constructs coding for the mature form of AtBAM1 were used. One construct was made into the pET28a(+) (Novagen) expression vector putting in frame the cDNA for AtBAM1 with an His-Tag and a thrombine cleavage site at the 5’ end of the AtBAM1 coding sequence, as described in Sparla et al. 2006. The second construct was kindly provided by Dr. Diana Santelia (University of Zurich) and was made into the pET21a(+) (Novagen) expression vector. In this second construct the thrombine cleavage site followed by a His-Tag was put in frame at the 3’ end of the cDNA for AtBAM1. AtBAM1 was expressed and purified as described in Sparla et al. (2006). AtAMY3 cloning, expression and purification were performed as previously described by Seung et al., 2013. Point mutations in the AtBAM1 and AtAMY3 genes were generated according to Sparla et al. (2006) and Seung et al. (2013). Commercial IbBMY1 protein was purchased by Sigma-Aldrich.

Enzyme activity assays and oxidative treatments

Redox modulation of wild-type proteins and mutated forms of AtBAM1 and AtAMY3 was assayed measuring the enzyme activities after 1 h incubation at 25°C of pure enzymes in 100 mM Tricine-NaOH, pH 7.9 in absence (control) or in presence (treated samples) of different oxidizing agents such as 0.1 mM and 0.5 mM H_2O_2; 25 µM $CuCl_2$; 20 mM oxidized DTT; 1 mM GSSG and 0.5 mM H_2O_2 plus 2.5 mM GSH. In order to test the reversibility of the oxidative treatments, treated samples were incubated for 30 min at 25 °C with 80mM reduced DTT. After treatments, the enzyme activities were measured with the artificial substrates *p*-nitrophenyl maltopentaoside (PNPG3) and *p*-nitrophenyl maltoheptaoside (BPNPG7) for β- and α-amylase activities, respectively, diluting the samples and following the manufacturer instructions (Megazyme, Ireland).

The kinetics of inactivation of AtBAM1 and AtAMY3 were performed incubating at 25°C the pure recombinant enzymes in 100mM Tricine-NaOH, pH 7.9 in absence (control) or in presence (treated samples) of 0.5 mM H_2O_2 and 0.5 mM H_2O_2 plus 2.5 mM GSH. At different time points, aliquots of incubated samples were diluted and their activities were measured as described above.

Biotinylation of GSSG

Biotinylated oxidized glutathione (BioGSSG) was prepared mixing under mild alkaline conditions (50 mM KPi buffer, pH 7.2), the water-soluble biotinylation reagent, EZ-Link Sulfo-NHS-Biotin (Thermo Fisher Scientific), with oxidized glutathione. Specifically, 50 µl of 48 mM EZ-Link Sulfo-NHS-Biotin were added to 50 µl of 32 mM GSSG. The mixture was incubated 1 h at room temperature. After incubation, any remaining biotinylation reagent was quenched by the addition of 35 µl of 0.6 M NH_4HCO_3 buffer.

Biotinylated GSSG assay

Reduced and oxidized AtBAM1 was obtained incubating pure enzyme in presence of 80 mM reduced or oxidized DTT for 16-18h at 4° C. Oxidized AtAMY3 was obtained incubating the enzyme in presence of 40 mM oxidized DTT for 16-18h at 4° C. Following incubation, DTTs were removed by NAP-5 columns (GE-Healthcare) pre-equilibrated in 100 mM Tricine-NaOH, pH 7.9. Reduced and oxidized forms of AtBAM1 and AtAMY3, were incubated in the presence of 2 mM BioGSSG at 25°C. After 1 h incubation, half of the

BioGSSG-treated sample was treated with 80 mM reduced DTT for 30 min to assess the reversibility of the reaction, while the second half was transferred into a tube containing SDS-loading buffer 1X without reducing agent and in presence of 100 mM iodoacetamide (IAM) and 20 mM n-ethilmaleimide (NEM). Control samples were incubated with 100 mM IAM and 20 mM NEM for 30 min in the dark at 25°C before of a second incubation at 25°C for 1 h in the presence of 2 mM BioGSSG. After incubation, protein samples were further divided and loaded on two denaturating non-reducing SDS-PAGE (12,5% poly-acrylamide) gels. One gel was analysed by Coomassie staining while the second gel was transferred to a nitrocellulose membrane and analysed by Western blot using monoclonal anti-biotin antibodies diluted 1:3800. Secondary antibodies diluted 1:2000 and peroxidase-conjugated were used for the detection by enhanced chemiluminescence (Durrant, 1990)

ESI-ToF mass spectrometry

Reduced AtBAM1 and AtAMY3 were incubated for 1 h at 25 °C in the presence of 1 mM GSSG, and desalted with NAP-5 columns in 100 mM Tricine-NaOH pH 7.9, before being analysed by ESI-ToF mass spectrometry (MS) at the Functional Genomics Center Zürich. In order to test the reversibility of the treatment, GSSG-treated samples were desalted in 100 mM Tricine-NaOH pH 7.9 and incubated with 10 mM reduced DTT for additional 2 h at 25 °C. After reduction, samples were desalted with NAP-5 columns and then analysed by ESI-ToF MS at the Functional Genomics Center Zürich.

Determination of cysteines pk_a of AtBAM1 and AtAMY3

Iodoacetamide (IAM) can form covalent adducts with sulfhydryl groups by nucleophilic substitution. The reaction is pH-dependent and specific for thiols. Since thiols react with IAM in their unprotonated form ($-S^-$), this reagent is most frequently used to identify the cysteines pK_a, also referred to as “reactive cysteines” (Paulsen and Carroll, 2013). Typically, the activity of the protein is inhibited when IAM reacts with catalytic residues.

The pH-dependence of the inactivation of AtBAM1 and AtAMY3 by IAM was carried out as described in Bedhomme et al. (2012). Briefly, the recombinant proteins, respectively in 10 mM MES (pH 6.5) or in 10 mM Tricine-NaOH (pH 7.9) were incubated with or without 375 µM IAM (corresponding to a ~10-fold excess of akylating reagent over the –SH groups) for 20 min in different buffers with a pH range from 4 to 10. After incubation, activities

were determined as described above (see Section "Enzyme activity assays and oxidative treatments"). The residual activity expressed as a percentage of maximal activity was plotted against pH, and the pK_a value was calculated by fitting the experimental data to a derivation of Henderson–Hasselbalch equation (Bedhomme et al., 2012).

RESULTS

Sequence analysis of *Arabidopsis thaliana* BAM1

Multiple sequence alignments indicate that *Arabidopsis thaliana* BAM1 (AtBAM1) shares the 55% of identity with Arabidopsis BAM3 (AtBAM3), the 47% with sweet potato BMY1 (IbBMY1), the 48,2% with barley (*Hordeum vulgare)* BMY1 (HvBMY1) and 26,5% of identity with *Bacillus cereus* β-amylase (BcSpoII), in agreement with phylogenetic analysis demonstrating that AtBAM1 and AtBAM3 fall in the same β-amylase subfamily, but different from that of of the other proteins (Fulton et al., 2008). Arabidopsis BAM1 and BAM3 localize in the chloroplast stroma (Sparla et al. 2006; Lao et al., 1999), while IbBMY1 account for about 5% of the total soluble protein of tuberous roots of sweet potato (Nakamura et al., 1991) and does not show transit peptide for plastid localization, rather contains a putative signal peptide for secretory pathway, as well as BcSpoII (Fig. 3). Reactive cysteine residues are particularly important because of their ability to sense and transduce changes in redox status caused by the presence of oxidised thiols and by ROS production. AtBAM1 possesses eight cysteine residues, while AtBAM3, IbBMY1, HvBMY1 and BcSpoII have respectively seven, six, five and three cysteine residues in the mature peptide. Only three AtBAM1 cysteine residues (Cys148, 261 and 399) are present also in the other proteins (except than Cys261 that is not conserved in BcSpoII) and a fourth one (Cys413) is conserved only in AtBAM3 (Fig. 3).

Differently from many other β-amylases characterized by a monomeric structure, IbBMY1 was found to be a tetramer, however its tetrameric structure was not relevant for the catalysis but rather has a stabilization effect on the overall structure of the enzyme (Balls et al., 1984). The structures of IbBMY1, HvBMY1 and BcSpoII have been solved by X-ray crystallography (Balls et al., 1948; Cheong et al., 1995; Mikami et al. 1999a; Mikami et al. 1999b; Oyama et al., 2003) allowing the identification of the substrate binding pocket and of the active sites. A reactive cysteine, in its thiolate anion form, can form a disulfide bond

with another resolving cysteine, if proximal, or with glutathione, depending on its accessibility (Klomsiri et al., 2011).

Since the crystal structure of AtBAM1 is not available, to determine cysteines accessibility and proximity, a homology model based on the deposited barley β-amylase structure (Mikami et al., 1999b) was built, since the two enzymes share a greater identity based on the primary sequence (Supplementary information, Fig. S1). The N-terminal domain of AtBAM1 containing Cys32 is not conserved, but Cys470 seems situated in a flexible C-terminal loop. Nevertheless, Cys506 seems to be located at the very end of a C-terminal loop, and seems to be more accessible and exposed to the solvent than Cys470, making Cys506 an alternative candidate for disulfide bond formation. None of these cysteine residues (Cys32, 470, 506) of AtBAM1 are conserved in AtBAM3 or IbBMY1.

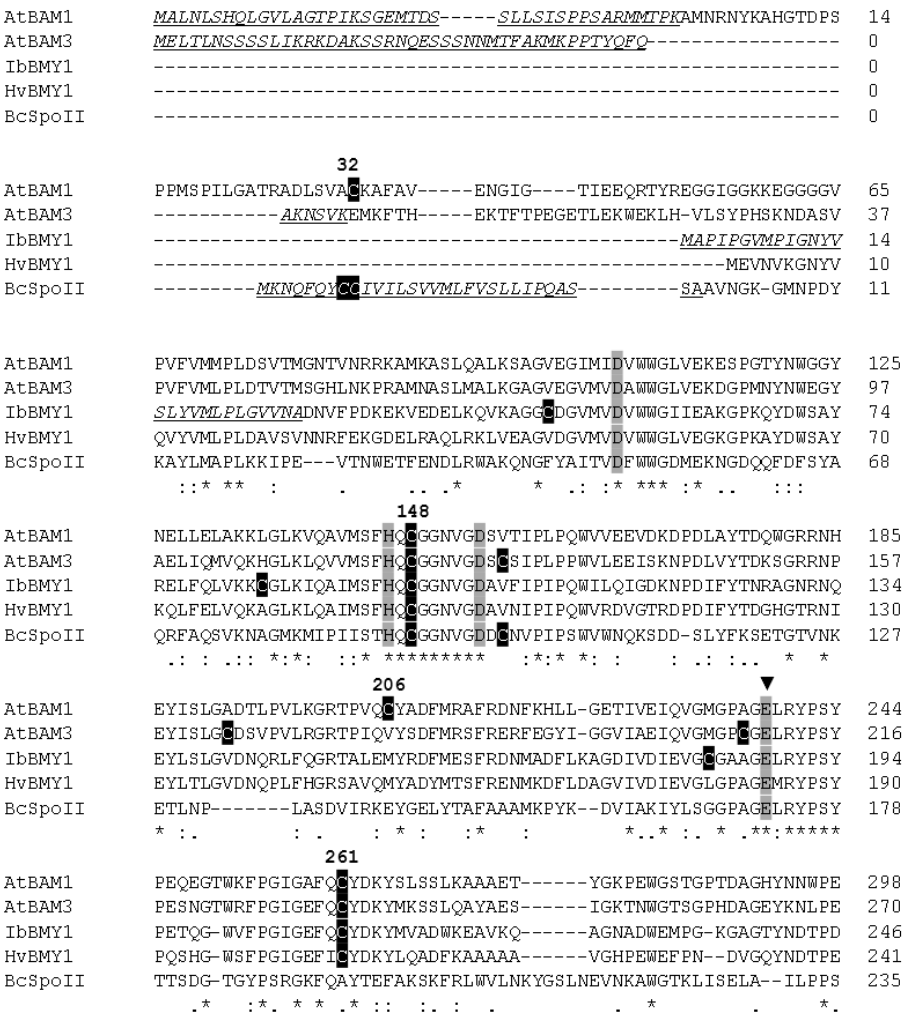

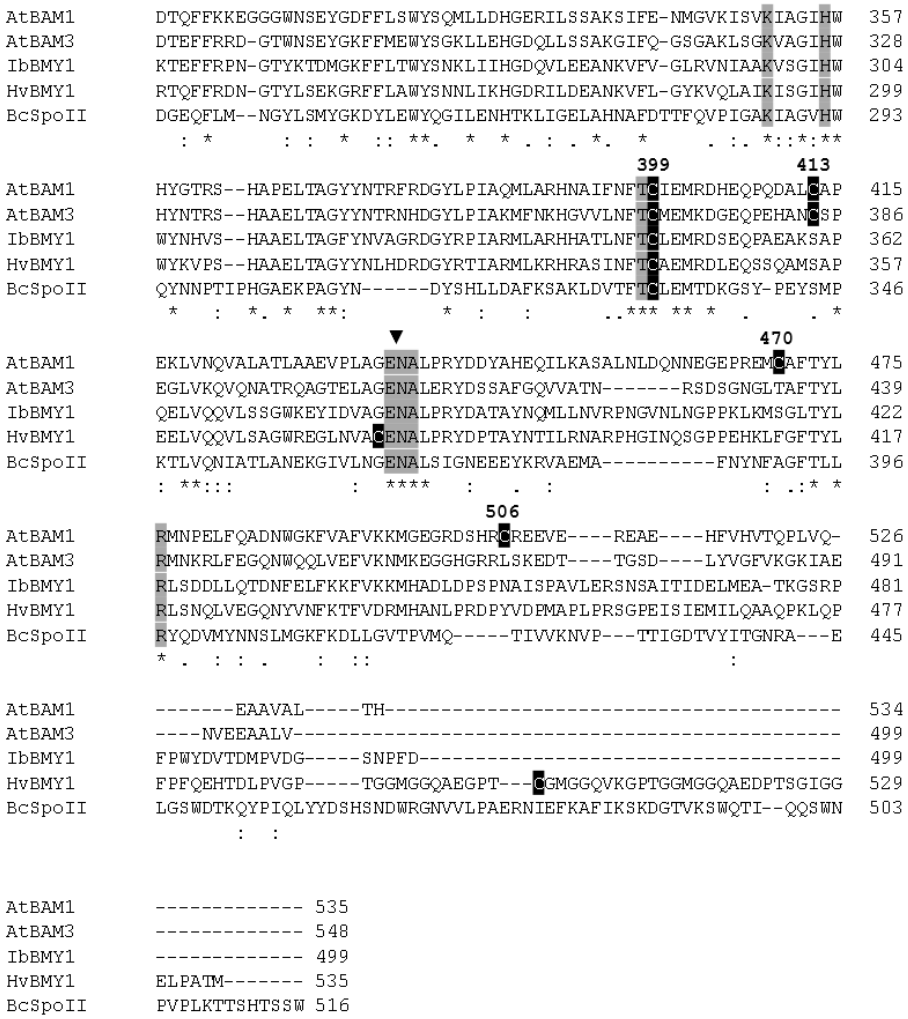

Figure 3 - Multiple alignment of precursors of *Arabidopsis thaliana* BAM1 (At3g23920, AtBAM1), *Arabidopsis thaliana* BAM3 (At4g17090, AtBAM£), Ipomoea batatas BMY1 (IbBMY1), *Hordeum vulgare* BMY1 (HvBMY1) and *Bacillus cereus* β-amylase (BcSpoII). Transit peptides of AtBAM1 and AtBAM3 as predicted by ChloroP (Emanuelsson et al., 1999), signal peptide of IbBMY1 as predicted by SignalP (Petersen et al., 2011) and signal peptide of BcSpoII (Nanmori et al., 1993) are underlined and italics on top of the figure. The cysteines are on black field. Catalytic (indicated by an arrow, ▼) and substrate binding conserved amino acids are highlighted in grey. The size of the proteins is given in amino acids and numeration for AtBAM1, AtBAM3 and BcSpoII starts from the first predicted residue of mature proteins. Only residues of AtBAM1 are numbered above the alignment. Identical (*), conserved (:) and semiconserved (.) residues are indicated below the alignment.

The sensitivity to oxidizing conditions is not a common feature of all β-amylases

Given that we were not able to obtain recombinant AtBAM3, the redox behaviour of AtBAM1 was compared to that of the commercial enzyme IbBMY1. Despite their high

amino acidic identity (47%), the effects of the tested oxidizing conditions were completely different. Contrary to AtBAM1, the activity of IbBMY1 was totally unaffected by incubation with 20 mM oxidized DTT, suggesting the absence of a regulatory disulfide bridge in the sweet potato enzyme (Fig. 4). To further investigate the sensibility of the two enzymes to oxidative conditions, both AtBAM1 and IbBMY1 were incubated in presence of 0.5 mM H_2O_2 and 25 µM $CuCl_2$, which are respectively a physiologically relevant molecule and powerful oxidant. As reported in Fig. 4, IbBMY1 activity was not inhibited by oxidative treatments, while the same treatments strongly inhibited AtBAM1 activity. Moreover, AtBAM1 activity was inhibited in a time and dose dependent manner by H_2O_2 (Supplementary information, Fig. S3). Interestingly, both H_2O_2- and $CuCl_2$-dependent inhibition were fully reverted by reduced DTT, suggesting the transition of the thiol groups belonging to catalytically or regulative cysteine residues to the sulfenic form (-SOH), instead of the transition to sulfinic (-SO_2H) or sulfonic forms (-SO_3H), which are known as irreversible forms of oxidized cysteine.

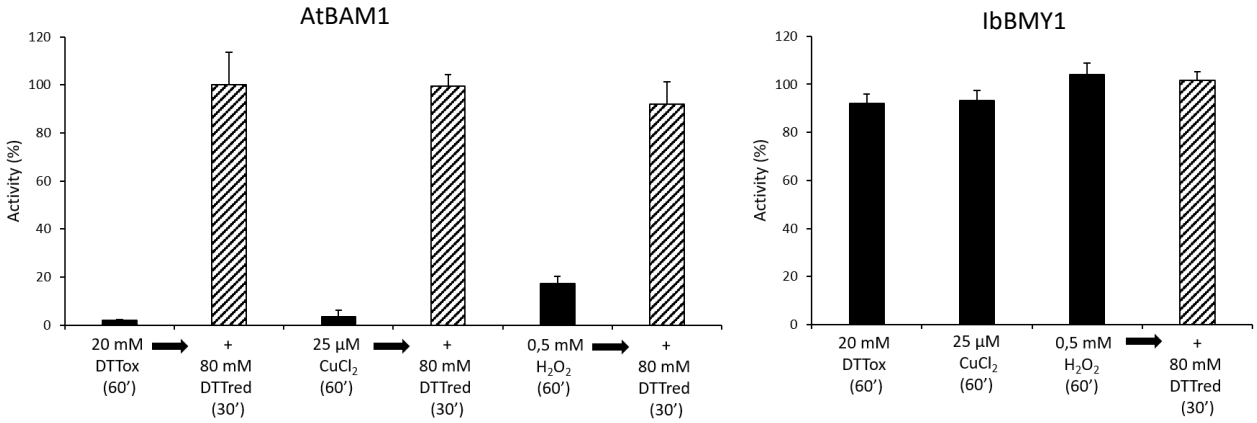

Figure 4 - Sensitivity of AtBAM1 (left panel) and IbBMY1 (right panel) to different oxidant treatments. Purified recombinant AtBAM1 and commercially available IbBMY1 were incubated with Tricine buffer as control or exposed to 20 mM DTTox, 25 µM $CuCl_2$ or 0,5 mM H_2O_2 (black bars) for 1 hour at 25°C prior to activity assay. Activity was measured with the artificial substrate PNPG3 (Sparla et al., 2006). Activity is given as a percentage of the fully active form. The reversibility of the inactivation was assessed by 30 min incubation with 80 mM DTTred (stripe pattern bars). Values represent the mean ± S.D. (n > 3).

Arabidopsis thaliana BAM1 is a possible target of glutathionylation

Protein glutathionylation has emerged as a novel redox post-translational modification with a regulatory and protective role, occurring prevalently under stress conditions (Zaffagnini et al., 2012b). Despite its sensitivity to H_2O_2, AtBAM1 is preferentially involved

in starch degradation under stress condition (Valerio et al., 2011). Therefore, a possible effect of glutathionylation on AtBAM1 activity was assayed (Fig. 5). To this purpose, the kinetic of inhibition of AtBAM1 performed in the presence of 0.5 mM H_2O_2 plus 2.5 mM GSH was compared with that obtained incubating the enzyme with 0.5 mM H_2O_2 alone. Even if GSH can act as a scavenger for H_2O_2, the kinetic of inhibition of AtBAM1 in presence of H_2O_2 plus GSH was much slower than that obtained by H_2O_2 alone (Fig. 5), suggesting a possible role of glutathionylation in preventing irreversible oxidation of cysteine residues.

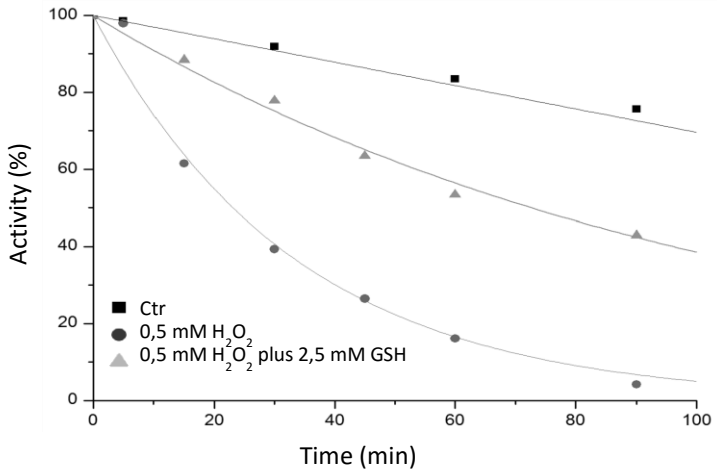

Figure 5 - Kinetics of inactivation of AtBAM1 by H_2O_2 and H_2O_2 plus GSH. AtBAM1 was incubated with Tricine buffer (Ctr), 0,5 mM H_2O_2 alone or 0,5 mM H_2O_2 plus 2,5 mM GSH. AtBAM1 activity was measured at different time points with the artificial substrate PNPG3 (Sparla et al., 2006). Activity is given as a percentage of the fully active form (n =3; data are means ± S.D. < 10% for each data point, not shown).

To better explore this hypothesis, AtBAM1 was incubated for 1 hour in the presence of 1 mM GSSG (Fig. 6). Interestingly the resulted ~30% of inhibition could have been completely reverted by reduced DTT (Fig. 6). Similarly, 1h incubation of AtBAM1 with 0.5 mM H_2O_2 plus 2.5 mM GSH resulted in a decrease of protein activity, again fully reverted by a subsequent incubation with reduced DTT (Fig. 6). Taken together these results strongly suggest that glutathione might react with AtBAM1, probably inducing the

formation of a mixed disulfide bridge between a cysteine residue and one molecule of glutathione.

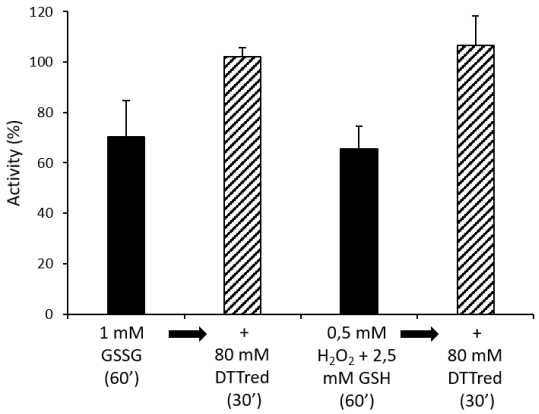

Figure 6 - Sensitivity of AtBAM1 to glutathionylation. Purified recombinant AtBAM1 was incubated with Tricine buffer as control or exposed to 1 mM GSSG or to 0,5 mM H_2O_2 plus 2,mM GSH (black bars) for 1 hour at 25°C prior to activity assay. The reversibility of the inactivation was assessed by 30 min incubation with 80 mM DTTred (stripe pattern bars). Activity was measured with the artificial substrate PNPG3 (Sparla et al., 2006). Activity is given as a percentage of the fully active form. Values represent the mean ± S.D. (*n* = 4).

Sequence analysis of *Arabidopsis thaliana* AMY3

Alfa-amylases can be classified into three subfamilies according to their subcellular localization and gene structure (Stanley et al., 2002). Family one of α-amylases are characterized by having a signal peptide that targets the protein to the secretory pathway (Fig. 7). Cereal grain amylases are classified within this family, and due to their pivotal role in the endosperm during mobilization of starch, much work on plant α-amylases has focused on this family. Among family one, barley (*Hordeum vulgare* L.) α-amylase 1 (HvAMY1) is one of the most thoroughly described and represents one of the few for which crystal structure is available (Robert et al., 2003). In *Arabidopsis*, three genes encode α-amylase-like proteins (Yu et al., 2005), one isoform for each family. Arabidopsis α-amylase 1 (AtAMY1; At4g25000 gene) belongs to family one of α-amylases and was suggested to accumulate in the apoplast of leaves during senescence or after biotic or abiotic stress, with the possible function of starch degradation after cell death (Doyle et al., 2007). Indeed, AtAMY1 show a signal peptide that allows protein secretion (Fig 7). Family two of α-amylases has largely unknown functions and its members have no

predicted targeting peptide, therefore they are thought to localize into the cytoplasm. Family three of α-amylases has been shown to participate in leaf starch breakdown (Kötting et al., 2009) and are characterized by a large N-terminal extension, typically 400–500 amino acids in length, which contains a predicted chloroplast transit peptide and tandem carbohydrate-binding modules. Alfa-amylase isozyme 3 from *Arabidopsis thaliana* (AtAMY3) belong to this family and shows these characteristics. In fact, AtAMY3 has a chloroplast transit peptide and localize in the chloroplast (Yu et al., 2005; Glaring et al., 2011) (Fig. 7). Moreover, AtAMY3 has two tandem N-terminal starch-binding domains belonging to the carbohydrate-binding module family 45 (CBM45; Cantarel et al., 2009) (Fig. 7), with a high sequence similarity to those found in the starch phosphorylating enzyme α-glucan, water dikinase (GWD) (Mikkelsen et al., 2006; Glaring et al., 2011), which would enable interaction with the starch granule surface (Yu et al., 2005; Glaring et al., 2011). The two CBM45 domains in AtAMY3 are separated by a linker of approximately 50 amino acids (Fig. 7). Each domain contains five aromatic amino acids (Fig. 7) that are widely conserved across all species (Glaring et al., 2011).

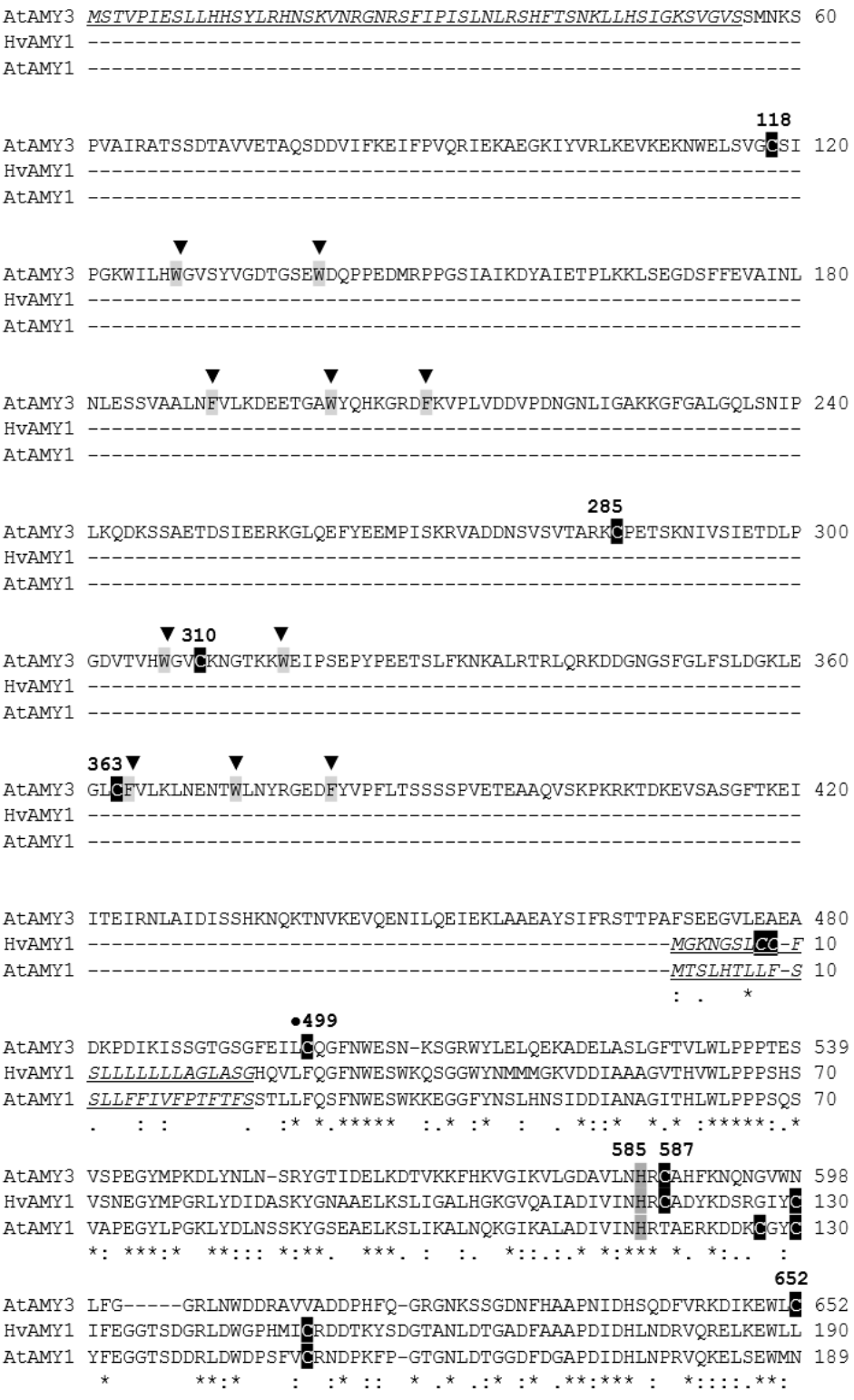
AtAMY3 MSTVPIESLLHHSYLRHNSKVNRGNRSFIPISLNLRSHFTSNKLLHSIGKSVGVSSMNKS 60
HvAMY1 ----------
AtAMY1 ----------
118
AtAMY3 PVAIRATSSDTAVVETAQSDDVIFKEIFPVQRIEKAEGKIYVRLKEVKEKNWELSVGCSI 120
HvAMY1 ----------
AtAMY1 ----------
AtAMY3 PGKWILHWGVSYVGDTGSEWDQPPEDMRPPGSIAIKDYAIETPLKKLSEGDSFFEVAINL 180
HvAMY1 ----------
AtAMY1 ----------
AtAMY3 NLESSVAALNFVLKDEETGAWYQHKGRDFKVPLVDDVPDNGNLIGAKKGFGALGQLSNIP 240
HvAMY1 ----------
AtAMY1 ----------
285
AtAMY3 LKQDKSSAETDSIEERKGLQEFYEEMPISKRVADDNSVSVTARKCPETSKNIVSIETDLP 300
HvAMY1 ----------
AtAMY1 ----------
310
AtAMY3 GDVTVHWGVCKNGTKKWEIPSEPYPEETSLFKNKALRTRLQRKDDGNGSFGLFSLDGKLE 360
HvAMY1 ----------
AtAMY1 ----------
363
AtAMY3 GLCFVLKLNENTWLNYRGEDFYVPFLTSSSSPVETEAAQVSKPKRKTDKEVSASGFTKEI 420
HvAMY1 ----------
AtAMY1 ----------
AtAMY3 ITEIRNLAIDISSHKNQKTNVKEVQENILQEIEKLAAEAYSIFRSTTPAFSEEGVLEAEA 480
HvAMY1 ----------MGKNGSLCC-F 10
AtAMY1 ----------MTSLHTLLF-S 10
499
AtAMY3 DKPDIKISSGTGSGFEILCQGFNWESN-KSGRWYLELQEKADELASLGFTVLWLPPPTES 539
HvAMY1 SLLLLLLLAGLASGHQVLFQGFNWESWKQSGGWYNMMMGKVDDIAAAGVTHVWLPPPSHS 70
AtAMY1 SLLFFIVFPTFTFSSTLLFQSFNWESWKKEGGFYNSLHNSIDDIANAGITHLWLPPPSQS 70
585 587
AtAMY3 VSPEGYMPKDLYNLN-SRYGTIDELKDTVKKFHKVGIKVLGDAVLNHRCAHFKNQNGVWN 598
HvAMY1 VSNEGYMPGRLYDIDASKYGNAAELKSLIGALHGKGVQAIADIVINHRCADYKDSRGIYC 130
AtAMY1 VAPEGYLPGKLYDLNSSKYGSEAELKSLIKALNQKGIKALADIVINHRTAERKDDKCGYC 130
652
AtAMY3 LFG-----GRLNWDDRAVVADDPHFQ-GRGNKSSGDNFHAAPNIDHSQDFVRKDIKEWLC 652
HvAMY1 IFEGGTSDGRLDWGPHMICRDDTKYSDGTANLDTGADFAAAPDIDHLNDRVQRELKEWLL 190
AtAMY1 YFEGGTSDDRLDWDPSFVCRNDPKFP-GTGNLDTGGDFDGAPDIDHLNPRVQKELSEWMN 189

Figure 7 - Sequence alignment of AtAMY3, HvAMY1 and AtAMY1 precursors were created using UniProt Knowledgebase Align (http://www.uniprot.org/align). The alignment shows the chloroplast transit peptide (italic and underlined) in AtAMY3 and the signal peptides (italic and underlined) in AtAMY1 and HvAMY1. The five residues of each of the two N-terminal CBM45 domains of AtAMY3 are highlighted in light grey and indicated by an arrow (▼). The size of the proteins is given in amino acids. Beginning of AtAMY3 conserved C-terminal domain is announced by a dot (●). The numbering of amino acids includes transit peptide and signal peptides. Only residues of AtAMY3 are numbered above the alignment. All cysteines are given in black field, while other important residues are shown in dark grey field. Identical (*), conserved (:) and semiconserved (.) residues are indicated below the alignment.

AtAMY3 show a 45,7% of sequence identity with HvAMY1 and a slightly lower value (43,6%) with AtAMY1 protein (Larkin et al., 2007). In turn, HvAMY1 and AtAMY1 show about the 57% of sequence identity (Larkin et al., 2007). However, AtAMY3 C-terminal domain, responsible of catalysis, is well conserved. Within the catalytic domain, the HvAMY1 aspartic acid residue 204, essential for the activity, is conserved in AtAMY3 (Asp666), as in AtAMY1 (Asp203) (Seung et al., 2013).

Arabidopsis AMY3 sequence show 9 cysteine residues. Of these residues, four (Cys118, Cys285, Cys310, and Cys363) are located in the N-terminal extension and five (Cys499, Cys587, Cys652, Cys743, and Cys832) in the α-amylase domain (Fig. 7). Seung and collaborators (2013) demonstrated that the enzyme was redox regulated at physiological

relevant redox potentials via a disulfide exchange. Specifically, the enzyme was found to be active when reduced and inactive when oxidized, in concomitance with the formation of a disulfide bridge between residues Cys499 and Cys587, that probably alters the tertiary structure of the protein in a way that blocks the active site (Brandes et al., 1996; Silver et al., 2013). Indeed, Cys587 is highly conserved among α-amylases and in HvAMY1 has been previously shown to be important for catalysis (Mori et al., 2001). Moreover, Cys587 is in close proximity to the active site and is located two residues away from His585 of AtAMY3, which aligns with His117 of HvAMY1 (corresponding to His93 in mature protein) and functions as a transition state stabilizer, which substitution causes a sharp decrease in protein activity (Søgaard et al., 1993). The close proximity of AtAMY3 Cys587 and of Cys 499 to the active site may explain why those two site-directed mutants were less active or almost completely inactive, respectively (Seung et al., 2013). Other site-directed AtAMY3 mutants with low activities included cysteine to serine substitution of residue 285 or 652, suggesting they may also contribute to the activity or to the stability of the protein. Interestingly, Cys499 is generally conserved in AMY3 sequences of other organisms (Seung et al, 2013). AMY3 sequences in which Cys499 is not conserved, mostly show a leucine residue at this position and another additional cysteine residue 11 amino acids upstream, which is not usually present and may be an alternative partner cysteine for a disulfide bridge (Seung et al., 2013). HvAMY1 and AtAMY1 do not show any cysteine residue corresponding to Cys499 of AtAMY3 nor any upstream additional cysteine, suggesting that those proteins are not likely to be redox regulated by the formation of a disulfide bridge (Fig. 7).

Oxidative treatments on AtAMY3

As for AtBAM1, also AtAMY3 displayed an unusually redox behaviour for an enzyme that should be involved in transitory starch degradation at night (Seung et al., 2013). AtAMY3 has been reported to be reversible inactivated by $CuCl_2$ treatment, activated by reduced Trxs and able to form a regulatory disulfide bridge with a midpoint redox potential of -329 mV between cysteine residues 499 and 587 (Seung et al., 2013). Moreover, as for AtBAM1, these peculiar redox properties are not found in all α-amylases, since HvAMY1 was completely insensitive to redox treatments (Seung et al., 2013).

In addition to the similar redox behaviour, it has been demonstrated that AtBAM1 and AtAMY3 work synergistically to degrade starch *in vitro* (Seung et al., 2013) and more recently both enzymes have been found in chloroplast stroma of guard cells where participating in transitory starch degradation to sustain stomatal aperture (Valerio et al., 2011; Prasch et al., 2015; Horrer et al., 2016). Also the expression pattern of AtAMY3 is different from that expected for a protein involved in nocturnal starch degradation, being induced by stress condition such as cold shock (Kaplan and Guy, 2005). Taken together, these data strongly suggest a possible "minor" pathway of starch degradation occurring in specialized cells and/or under stress conditions, involving AtBAM1 and AtAMY3 that are not essential for nighttime transitory starch breakdown under normal growth conditions, as witnessed by the absence of a *sex* phenotype in mutants lacking of AtBAM1 or AtAMY3 (Yu et al., 2005; Kaplan and Guy, 2005; Kötting et al., 2009).

For this reason, the behaviour of AtAMY3 to H_2O_2 treatments was studied (Fig. 8 and Fig. S4, supplementary information). After one hour of incubation with 0.1 mM and 0.5 mM H_2O_2, AtAMY3 activity was measured by the artificial substrate BPNPG7. As reported in Fig. 8, AtAMY3 activity was reversibly inhibited in a dose dependent manner by H_2O_2.

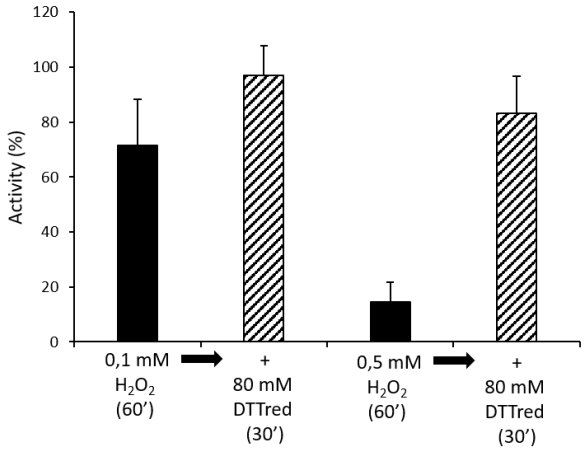

Figure 8 - Sensitivity of AtAMY3 to different concentrations of H_2O_2. Purified recombinant AtAMY3 was incubated in Tricine buffer (as control) or exposed to 0.1 and 0.5 mM H_2O_2 (black bars) for 1 hour at 25°C prior to assay the activities. Activity is expressed as percentage of control sample. The reversibility of the inhibition was assessed by 30 min incubation with 80 mM reduced DTT (stripe pattern bars). Activity was measured with the artificial substrate BPNPG7 (Seung et al., 2013). Values represent the mean ± S.D. (*n* = 3).

To study the possible involvement of a glutathionylation event on AtAMY3, the effect of 1 mM GSSG and 0.5 mM H_2O_2 plus 2.5 mM GSH was tested on the pure enzyme (Fig. 9). Interestingly while GSSG treatment caused a 40% inhibition of the enzyme activity, fully revertible by reduced DTT, the treatment performed in the presence of H_2O_2 plus GSH was without effect on the enzyme activity (Fig. 9).

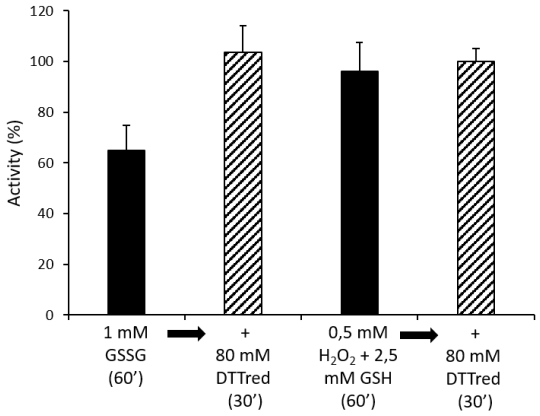

Figure 9 - Sensitivity of AtAMY3 to glutathionylation. Purified recombinant AtAMY3 was incubated with Tricine buffer as control or exposed to 1 mM GSSG or to 0,5 mM H_2O_2 plus 2,5 mM GSH (black bars) for 1 hour at 25°C prior to activity assay. The reversibility of the inactivation was assessed by further 30 min incubation with 80 mM DTTred (stripe pattern bars). Activity was measured with the artificial substrate BPNPG7 (Seung et al., 2013). Activity is given as a percentage of the fully active form. Values represent the mean ± S.D. (*n* = 3).

To better analyse the effect of H_2O_2 plus GSH on AtAMY3 activity, a time course experiment was performed (Fig. 10). Albeit GSH is a physiological ROS scavenger, able to lower the amounts of H_2O_2 in the sample, with the concomitant production of GSSG, the amounts of oxidant in the reaction mixture should be still sufficient to oxidize the enzyme. Interestingly, in the presence of GSH the inhibitory effect of H_2O_2 was completely abolished, leaving an enzyme as active as the control sample (Fig. 10).

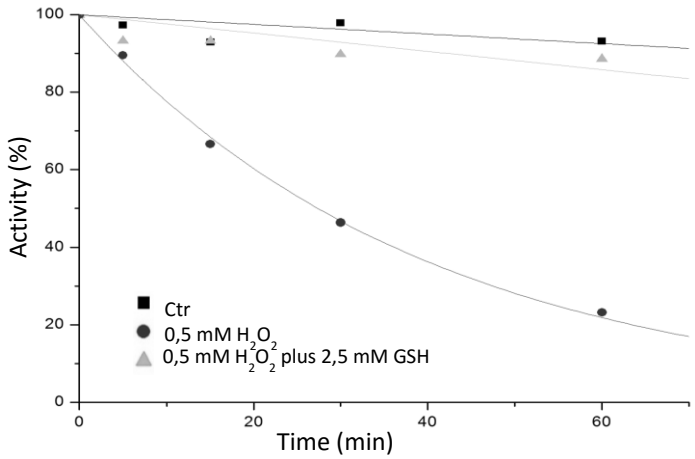

Figure 10 - Kinetics of inactivation of AtAMY3 by H_2O_2 and H_2O_2 plus GSH. AtAMY3 was incubated with tricine buffer (Ctr), 0,5 mM H_2O_2 alone or 0,5 mM H_2O_2 plus 2,5 mM GSH. AtAMY3 activity was measured at different time points with the artificial substrate BPNPG7 (Seung et al., 2013). Activity is given as a percentage of the fully active form (n =2; data are means ± S.D. < 10% for each data point, not shown).

Actually, the different behaviour of AtAMY3 to GSSG and H_2O_2 plus GSH treatments is difficult to explain. GSSG is also known to promote the formation of disulfide bonds in target proteins (Cumming et al., 2004; Chakravarthi et al., 2004). Then, inhibition of AtAMY3 measured after GSSG incubation might be due to a dithiol/disulfide exchange, whereas the absence of inhibition after incubation with H_2O_2 plus GSH might be ascribed to the glutathionylation of AtAMY3. Further experiments are required to address the question.

Both AtBAM1 and AtAMY3 are glutathionylated

The effect of biotin-conjugated GSSG (BioGSSG) was tested on recombinant proteins AtBAM1, AtAMY3 and on the commercial enzyme IbBMY1 (Fig. 11). The glutathionylated state of BioGSSG-treated AtBAM1 and AtAMY3 was clearly revealed by the reaction with anti-biotin antibodies (Fig. 11). The signal was both reversed by reduced DTT, underlining the reversibility and the specificity of the reaction, and prevented by alkylation. On the contrary, under the same condition that leads to glutathionylation of AtAMY3 and AtBAM1, the lack of signal for IbBMY1 revealed that the protein is not glutathionylated.

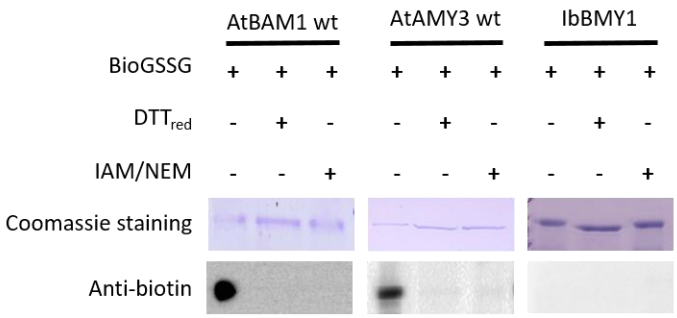

Figure 11 - Analysis of AtBAM1, AtAMY3 and IbBMY1 glutathionylation with biotin-conjugated GSSG (BioGSSG). The proteins were incubated with BioGSSG (2 mM, 1h) with or without a pre-incubation with 100 mM IAM and 20 mM NEM. The reversibility of the reaction was assessed by treatment with 80 mM DTTred (30 min for BAM1 and 1h for AMY3) performed on half of the non-alkylated sample incubated with BioGSSG. Proteins were separated by non-reducing SDS-PAGE and transferred to nitrocellulose membrane for western blotting analysis with anti-biotin antibodies.

In order to confirm the glutathionylated state of AtBAM1 and AtAMY3, MS analysis (ESI-ToF) was performed on both proteins. The MS spectra of GSSG treated enzymes showed two sharp peaks (Fig. 12, left panels): one corresponding to the molecular mass of AtBAM1 (60542.0 Da) or AtAMY3 (96813.5 Da) and the second one corresponding to the glutathionylated forms (60847.0 Da and 97123.5 Da, for AtBAM1 and AtAMY3, respectively). The presence of peaks corresponding to the unmodified proteins, suggest that the incubation conditions were not saturating. In addition, AtBAM1 spectrum showed another peak corresponding to a mass increase of 610 Da, presumably ascribable to a double glutathionylated enzyme (a theoretical increment mass of 305 Da is expected for each glutathione molecule bound to the target protein). In agreement with a reversible modulation of the enzyme activities and with the BioGSSG assay, in both samples a single peak appeared following treatment with reduced DTT (Fig. 12, right panels). These data clearly indicate that in the presence of GSSG both enzymes are reversibly glutathionylated.

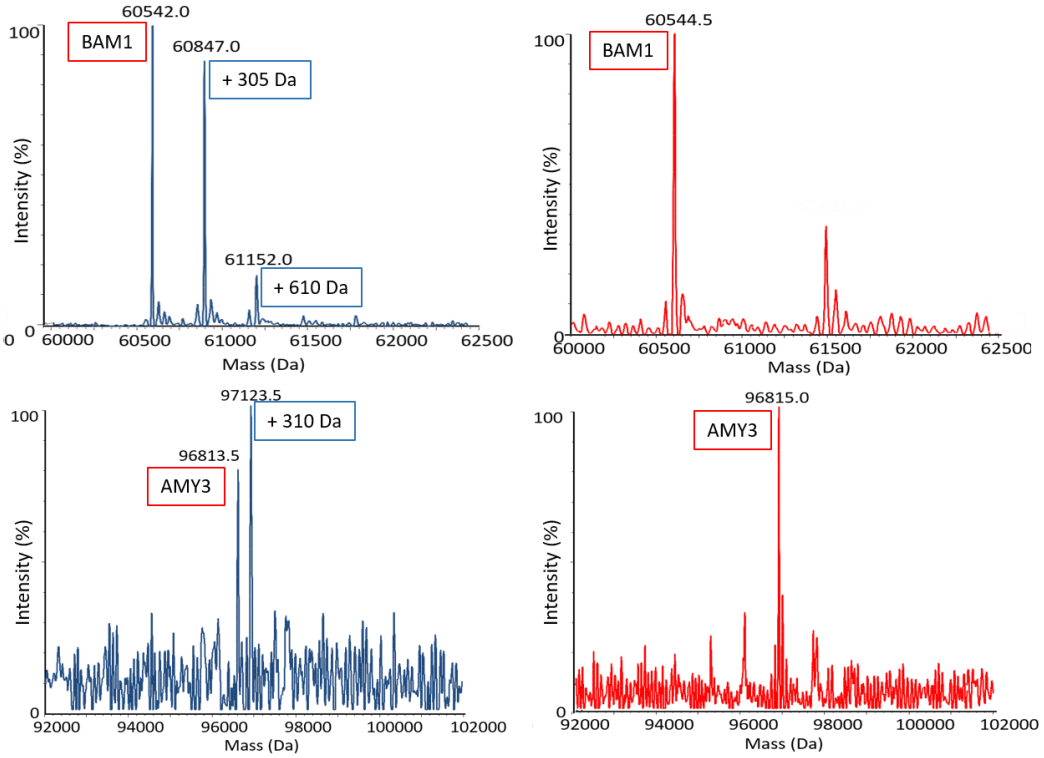

Figure 12 - Analysis of AtBAM1 and AtAMY3 glutathionylation by ESI-MS analysis. Mass spectra of GSSG treated (1h, 1mM) recombinant AtBAM1 (upper panels) and AtAMY3 (lower panels) were performed before (red line) and after (blue line) treatment with 10mM dithiothreitol (DTTred) (2h). Measurement accuracy: ±5 Da.

Attempt to identify cysteine residues that are target of glutathionylation in AtBAM1 and AtAMY3

AtBAM1 and AtAMY3 contain at least two redox reactive cysteine residues involved in the formation of the regulatory disulfide bridge (Sparla et al., 2006; Seung et al., 2013) which could be target of glutathionylation. In our hands, AtBAM1 oxidation mediated by oxidized DTT prevented BioGSSG dependent glutathionylation (Fig. 13), suggesting that the modified cysteine residues may be the ones involved in disulfide bridge formation. However, AtBAM1 double mutant C32S C470S, lacking Cys32 and Cys470, that are proposed as one of the possible couple of cysteine involved in disulfide bond (Sparla et al., 2006), is still glutathionylated in the presence of BioGSSG (Fig. 13). This behaviour might be explained by a possible conformational change that could occur in response to the formation of the regulatory disulfide bridge between Cys32 and Cys470 and that would make inaccessible a third putative cysteine residue. Alternatively to this hypothesis

and more simply, the regulatory disulfide bridge could occur between Cys32 and Cys506, the second couple of cysteines proposed to be involved in the regulation of AtBAM1 (Sparla et al., 2006).

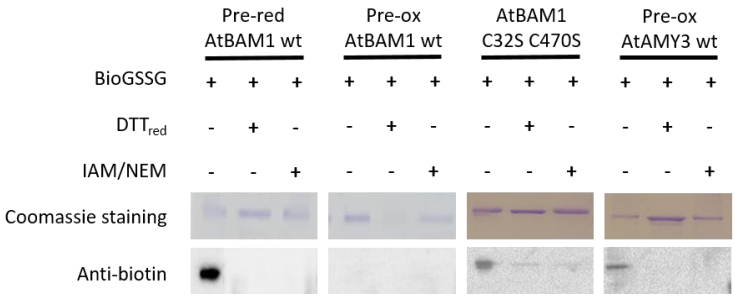

Figure 13 - Glutathionylation analysis of pre-oxidized and pre-reduced AtBAM1, double mutant AtBAM1 C32S C470S and pre-oxidized AtAMY3 with biotin-conjugated GSSG (BioGSSG). AtBAM1 was incubated over night with 80 mM DTTox or DTTred at 4°C and then buffer exchanged. AtAMY3 was incubated over night with 40 mM DTTox at 4° C and then buffer exchanged. Subsequently, the analyses were performed as described in Fig. 11.

In agreement with ESI-MS analysis that suggested the bond of two GSH molecules, all AtBAM1 single mutants were glutathionylated by BioGSSG (Fig. 14).

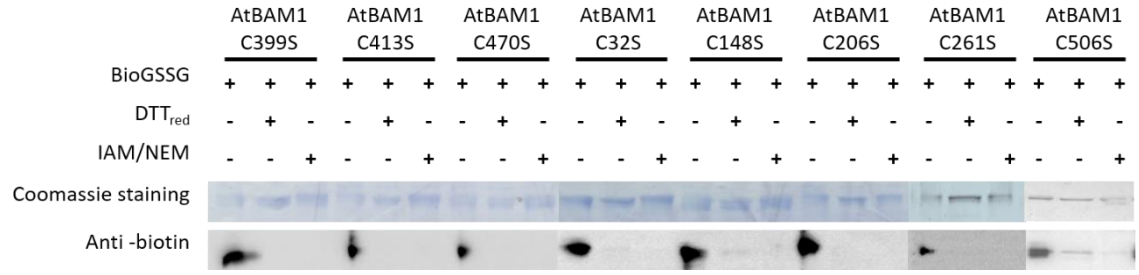

Figure 14 - Glutathionylation analysis of AtBAM1 mutants with biotin-conjugated GSSG (BioGSSG). All AtBAM1 Cys to Ser mutants were analysed as described in Fig. 11.

Differently from AtBAM1, pre-oxidized AtAMY3 still reacted with BioGSSG (Fig. 13), suggesting that the modification might occur on a cysteine residue not involved in disulfide bridge formation (namely Cys499 and Cys587, Seung et al., 2013) or that the protein was not completely oxidated. In order to identify the Cys residue target of glutathionylation, considering that ESI-MS analysis showed that glutathionylation

occurred on a single cysteine residue (Fig. 13), all Cys to Ser single mutants of AtAMY3 were analysed by BioGSSG (Fig. 15). Against all odds, all AtAMY3 Cys to Ser variants formed a mixed disulfide bridge with BioGSSG (Fig. 15). Such a result is difficult to explain without assuming that the mutation of the target cysteine residue in AtAMY3 may change the conformation of the protein or modify the molecular environment around a usually non-modified cysteine residue, making it more prone to glutathionylation.

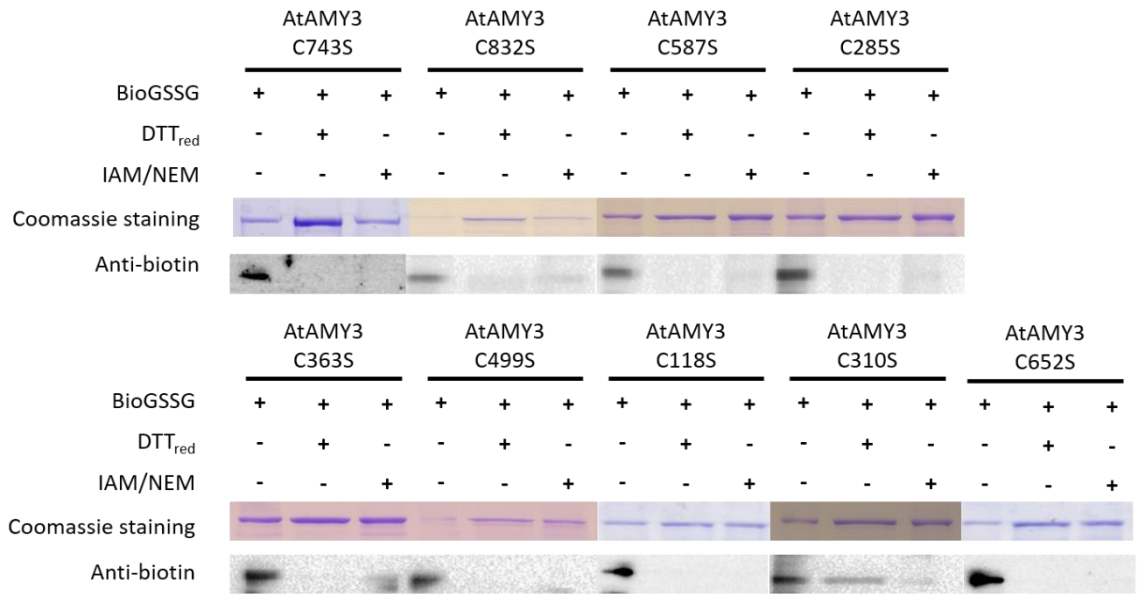

Figure 15 - Glutathionylation analysis of AtAMY3 mutants with biotin-conjugated GSSG (BioGSSG). All AtAMY3 Cys to Ser mutants were analysed as described in Fig. 11.

H_2O_2-dependent oxidation and sensitivity to glutathionylation of AtBAM1 single mutants C32S, C470S, C506S

Since it is known that, under oxidizing conditions, Cys32 of AtBAM1 can form a disulfide bridge with another cysteine residue suggested to be Cys470 or Cys506 (Sparla et al., 2006), the sensitivity to H_2O_2 and H_2O_2 plus GSH was measured in wild-type AtBAM1 and in the three single mutants C32S, C470S and C506S (Fig. 16 and Fig. 17), with the aim of identify the cysteines target of glutathionylation. Moreover, these three cysteine residues are of particular interest because they were the only cysteines to seem solvent accessible (supplementary information, Fig. S1) and non-conserved (Fig. 3) in redox-insensitive and non-glutathionylated IbBMY1.

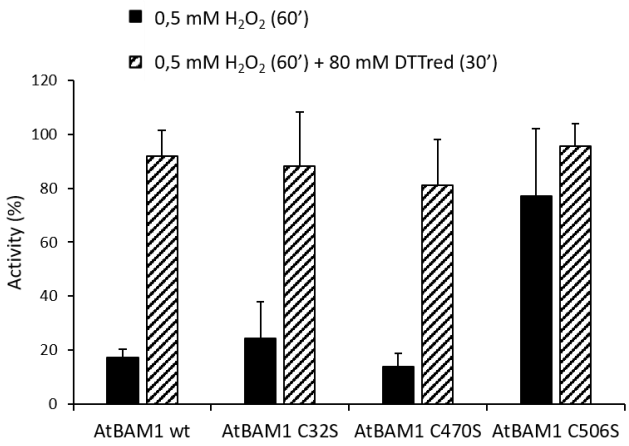

Figure 16 - Sensitivity of AtBAM1 wild-type and C32S, C470S, C506S to H_2O_2. Purified recombinant AtBAM1 single mutant proteins were incubated with tricine buffer as control or exposed to 0,5 mM H_2O_2 (black bars) for 1 hour at 25°C prior to activity assay. The reversibility of the inactivation was assessed by 30 min incubation with 80 mM DTTred (stripe pattern bars). Activity was measured with the artificial substrate PNPG3 (Sparla et al., 2006). Activity is given as a percentage of the fully active form. Values represent the mean ± S.D. (n > 3).

As reported in Fig. 16, H_2O_2 treatment inhibited AtBAM1 activity at the same extent in both wild-type protein and C32S, C470S mutants, while the lack of Cys506 gave rise to an enzyme insensitive to H_2O_2 treatment, suggesting a possible role of Cys506 as a sensor or mediator of protein oxidation. C506S mutant also showed a slight decrease in protein specific activity compared to wild-type AtBAM1 (Supplementary information, Table S1) suggesting a possible involvement of Cys506 in the catalytic mechanism. However, more analyses are required to assess this hypothesis.

Because through BioGSSG was not possible to discriminate without any doubt which residues were responsible of AtBAM1 glutathionylation, AtBAM1 C32S, C470S, C506S sensitivity to glutathionylation mediated by H_2O_2 plus GSH was assessed (Fig. 17).

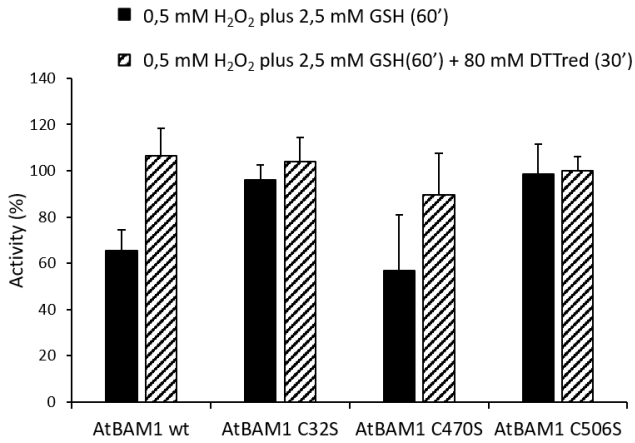

Figure 17 - Sensitivity of AtBAM1 wild-type and C32S, C470S, C506S to glutathionylation. Purified recombinant AtBAM1 was incubated with Tricine buffer as control or exposed to 0,5 mM H_2O_2 plus 2,mM GSH (black bars) for 1 hour at 25°C prior to activity assay. The reversibility of the inactivation was assessed by 30 min incubation with 80 mM DTTred (stripe pattern bars). Activity was measured with the artificial substrate PNPG3 (Sparla et al., 2006). Activity is given as a percentage of the fully active form. Values represent the mean ± S.D. (n = 4).

Unlike wild-type protein and C470S mutant, both C32S and C506S were insensitive to glutathionylation mediated by H_2O_2 plus GSH, suggesting that Cys32 and Cys506 might be the targets of glutathionylation. This finding is also consistent with both data obtained by ESI-MS analysis that suggested multiple glutathionylation sites on AtBAM1 (Fig. 12) and with BioGSSG assay performed on single mutants (Fig. 14).

Determination of pK_a values for AtBAM1 and AtAMY3

At present it is unclear what feature better contributes to the sensitivity of a cysteinyl residues to S-glutathionylation. The reaction rate of most protein cysteines with ROS and/or GSH is too slow to be of physiological relevance. This situation changes drastically when cysteine is in its thiolate anion ($-S^-$) form (Dalle-Donne et al., 2007). The pK_a value of a cysteine represents pH value at which a cysteine residue is in equilibrium between its thiol (-SH) and thiolate ($-S^-$) forms. Typically, unreactive cysteines show a pK_a value around 8.5 or 8.6. The formation of a cysteine thiolate anion which can react to form a mixed disulfide with GSH or with a second cysteine residue to form a protein disulfide (Rhee et al, 2000; Cumming et al., 2004), occurs only in unusual microenvironments in which the nearby amino acid residues significantly lower the pK_a through electrostatic interactions.

Consequently, at pH ~7, a thiol with a pK_a value below 7 will exist mostly in its reactive thiolate form.

IAM is a strong alkylating agent able to bind cysteine residues, inhibiting protein activity if these cysteine residues are somehow involved in the catalytic process. Since IAM preferentially reacts with thiolate anion, pK_a of catalytic relevant cysteines can be assessed by measuring the pH dependence of IAM inactivation. Both AtBAM1 and AtAMY3 were therefore treated with IAM at different pH value and their activities were compared to those measured at the same pH value but in absence of the alkylating reagent. The curves obtained plotting the percentage of inhibition in function of pH values show sigmoidal trends with a single inflection point corresponding to a pK_a 8.3 for AtBAM1 and of 7.2 for AtAMY3 (Fig. 18).

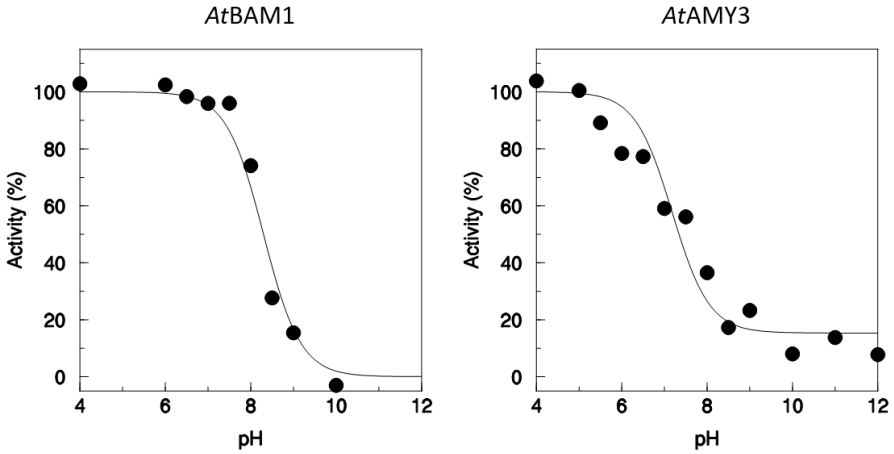

Figure 18 - Determination of the pK_a value of the active-site cysteine residue of AtBAM1 and AtAMY3. Enzymes were incubated with 0.375 mM IAM at different pH values for 20 min at room temperature and activity was determined. After incubation, the percentage of the remaining activity at each pH was determined by comparing the activity of the enzyme incubated with and without IAM. Results are means ±S.D. < 10% for each data point, not shown (n = 2). The pK_a value was obtained by non-linear regression using an adaptation of the Henderson–Hasselbalch equation (Bedhomme et al., 2012).

Concerning AtBAM1, the obtained pKa value was too high to suggest that the cysteine residues involved in the post translational modifications (both disulfide bridge formation and glutathionylation) might be involved even in the catalysis. On the contrary, the pK_a value measured for AtAMY3 was compatible with the hypothesis that at least one cysteine residue might be involved both in the catalysis and in the redox regulation. Indeed, it has been demonstrated that Cys587 of AtAMY3, that can form the regulatory disulfide bridge

with Cys499 under oxidizing conditions, is also required for the catalysis (Seung et al., 2013). Hence, Cys587 is a possible candidate target for glutathionylation, despite seeming not particularly accessible or exposed to the solvent (see Supplementary Fig. S2). Although low pK_a of a protein thiol provides a useful guide to its reactivity, this is not a generalizable rule. In fact, in addition to reactivity (which depends in turn on the pK_a of the thiol), other factors can contribute to the sensitivity of a given cysteinyl residue to protein glutathionylation, whether solvent accessibility, but also the microenvironment surrounding the target cysteine or a combination of these effects (Winterbourn and Hampton, 2008; Reddie and Carrol, 2008; Dalle-Donne et al., 2009).

DISCUSSION

Beside link the photosynthetic electron transport with the Calvin-Benson cycle enzymes (Buchanan and Balmer, 2005; Schürmann and Buchanan, 2008; König et al., 2012), chloroplast-target thioredoxins can also modulate the activity of several proteins belong to different pathways, including enzymes involved in starch metabolism (Santelia et al., 2015). This fine regulation appears to be essential to modulate enzyme activity in response to light condition. Despite their role in transitory starch degradation, typically occurring in the dark (i.e. oxidizing condition), AtBAM1 and AtAMY3 are subjected to thiol-based redox regulation being activated by reduced thioredoxins (Sparla et al., 2006; Seung et al., 2013). Till now, AtBAM1 and AtAMY3 are the only members of their protein family whose activity is inhibited by the formation of a disulfide bridge with a midpoint redox potential at pH 7.0 of -302 mV and at pH 7.9 of -329 mV, respectively (Sparla et al., 2006; Seung at al., 2013). As a consequence, AtBAM1 and AtAMY3 appear more reasonably belonging to a diurnal starch degradation pathway that occurs in specialized cell types, as guard cells, or under stress conditions (Valerio et al., 2011; Seung et al., 2013; Horrer et al., 2016; Zanella et al., 2016). In chloroplast stroma, stress conditions are often accompanied by the formation of reactive oxygen species (ROS), including H_2O_2, which can oxidize protein cysteine residues damaging also in irreversible manner, enzyme activity (Quan et al., 2008). To protect themself from irreversible oxidation, reactive cysteine residues can undergo to glutathionylation. As a consequence, glutathionylation has emerged as a novel redox post-translational modification occurring under stress

conditions and suggested to be mediated by H_2O_2 (Rouhier et al., 2008; Zaffagnini et al., 2012b). While glutathionylation is supposed to be a non-enzymatic reaction *in vivo*, deglutathionylation involves NADPH, glutathione reductase, reduced glutathione (GSH) and glutaredoxins (GRXs) (Zaffagnini et al., 2012b).

Proteomic analyses did not detect AtBAM1 and AtAMY3 as target of H_2O_2–dependent oxidation or as target of glutathionylation (Gao et al., 2009b; Muthuramalingam et al., 2013; Waszczak et al., 2014). This can be due to the low amount of both enzymes under experimental tested conditions (Muthuramalingam et al., 2013; Waszczak et al., 2014), to the use of dark-grown cells or of different photosynthetic model organisms, such as *Chlamydomonas reinhardtii* (Gao et al., 2009b).

In order to study the sensibility of AtBAM1 and AtAMY3 to oxidation, both enzymes were recombinant expressed and purified before analyse *in vitro* the effect of H_2O_2–treatment on their activities, measured with the artificial substrates PNPG3 and BPNPG7, respectively. Both AtBAM1 and AtAMY3 activities were inhibited by H_2O_2–treatments in a time- and dose-dependent manner (Fig. 4 and S2; Fig. 8 and S3). Interestingly the inhibition rates were significantly reduced (for AtBAM1) and even completely suppressed (for AtAMY3) when the treatments were performed in the presence of H_2O_2 plus GSH (Fig. 5 and 10). Since it has been suggested that *in vivo* glutathionylation events are mainly triggered by a first oxidation of the reactive cysteine residue to sulfenic form, followed by the formation of a mixed disulfide with GSH (Zaffagnini et al., 2012b; Fig. 1), the obtained data strongly suggest that both AtBAM1 and AtAMY3 might be target of such modification. As a consequence of being glutathionylated both AtBAM1 and AtAMY3 remain active. However, since the simultaneous presence of GSH and H_2O_2 in the samples might lower H_2O_2 concentration, reducing the effect of the oxidant, oxidative susceptibility of AtBAM1 and AtAMY3 was tested with different oxidants, such as $CuCl_2$ and GSSG (Fig. 4, 6 and 9). All oxidative treatments inhibited both AtBAM1 and AtAMY3 activities, underlining their propensity to be reversibly oxidized, as demonstrated by the recovery of the enzyme activities following the addition of reduced DTT to treated samples (Fig. 4, 6, 8 and 9). Taken together these results strongly suggest that both AtBAM1 and AtAMY3 are prone to glutathionylation.

AtBAM1 and AtAMY3 glutathionylation by means of biotinylated GSSG was confirmed through western blotting (Fig. 11). Moreover, glutathionylation mediated by GSSG was

assessed by ESI mass spectrometry for both AtBAM1 and AtAMY3 (Fig. 12). Albeit the enzymes were treated for 1 hour with 1 mM GSSG, both ESI-MS spectra still showed a peak corresponding to the unmodified proteins (Fig. 12), suggesting that GSSG-mediated glutathionylation is a slow process or that GSSG treatment can be resolved by the formation of an inter-molecular disulfide bonds that can not be detected by ESI-MS analysis. Further analyses are needed to verify these hypotheses. In addition, ESI-MS analysis suggested a possible double glutationylation for AtBAM1 (Fig. 12). In order to verify this result, all the Cys to Ser variants of AtBAM1 were incubated with BioGSSG and analysed by western blot (Fig 14). As expected, all AtBAM1 single mutants were found to be glutathionylated confirming the hypothesis of a double glutathionylation event. On the contrary, ESI-MS analysis on GSSG-treated AtAMY3 pointed toward glutathionylation of a single cysteine residue. To confirm this result, all the Cys to Ser variants of AtAMY3 were incubated with BioGSSG and analysed through western blot using anti-biotin antibodies. Surprisingly, all the mutants resulted to form a mixed disulfide bond with BioGSSG. This result might be explained assuming that the mutation of the target cysteine residue in AtAMY3 may change the conformation of the protein or modify the molecular environment around a usually non-modified cysteine residue, making it more prone to glutathionylation.

Sparla and collaborators (2006) reported that the activity of AtBAM1 is regulated through the formation of a disulfide bridge between the cysteine residue 32 and a second cysteine. Looking at the biochemical behaviour of the single mutants and comparing the primary amino acid sequences of redox and non-redox sensitive β-amylases, the Authors suggested as possible partners of Cys32 the cysteines 470 or the 506. *In silico* analysis performed to create a structural model of AtBAM1 based on the crystal structure of barley β-amylase, confirmed that both Cys470 and Cys506 are accessible and exposed to the solvent. (Fig. S1). Since the oxidation of AtBAM1 through the formation of the regulatory disulfide bridge prevent BioGSSG-mediated glutathionylation (Fig. 13), and considering that BioGSSG signal was still visible in the double mutant C32S C470S (Fig. 13), it appears more reasonable to suppose that the Cys506 could be the second regulatory residue. Also the activities of the wild-type enzyme and those of the single mutants C32S, C470S and C506S measured in presence of H_2O_2 plus GSH strongly support the hypothesis that Cys32

and Cys506 might be the targets of glutathionylation, being the only mutants insensitive to glutathionylation (Fig. 17).

Comparison of the amino acid sequence of bacterial and plant β-amylases revealed a 30% homology, with several highly conservative regions (Nomura et al., 1995). *Bacillus cereus* β-amylase has 3 cysteine residues (Cys91, Cys99 and Cys331). Two of these cysteines (Cys91 and Cys331) pertain to conserved sequence regions of bacterial and plant β-amylases and correspond to Arabidopsis BAM1 Cys148 and Cys399 (Fig. 3). In *Bacillus cereus* β-amylase, these two residues are situated in the active cleft of the enzyme, near to the substrate binding site (Nomura et al., 1995). However, Cys331 seems to be of prominent importance in catalytic activity (Nomura et al., 1995), whereas Cys91 can form a structural disulfide bond with Cys99, which is not conserved in AtBAM1 and IbBMY1, but is present in AtBAM3. The curve obtained plotting the percentage of AtBAM1 inhibition mediated by the alkylant agent IAM in function of pH values, shows sigmoidal trend with a single inflection point corresponding to a pK_a value of 8.3 (Fig. 18). Thus, the pK_a value obtained for AtBAM1 was too high for a residue involved in redox regulation and might be ascribable to Cys399, which is probably involved in the catalytic mechanism. On the other hand, Cys32 and Cys506 seem to be involved in redox regulation but not in catalysis (Tab. S1), and the lack of Cys506 gave rise to an enzyme insensitive to H_2O_2 treatment (Fig. 16), suggesting a possible role of Cys506 as a sensor or mediator of protein oxidation. Thus, it is possible to hypotesize a protective role of glutathionylation on Cys32 and Cys506 aimed to prevent fast or irreversible oxidation of the protein and to modulate enzyme activity.

Unlike AtBAM1, the pK_a value measured for AtAMY3 was more acidic (pK_a 7.2). Since in illuminated chloroplasts the pH value of the stroma is close to 8.0 (Heldt et al., 1973; Werdan et al., 1975), it is reasonable to assume that the same cysteine residue of AtAMY3 might be involved both in the catalysis and in the redox regulation. The finding that Cys499 and Cys587 are responsible of the regulatory disulfide bridge (Seung et al., 2013) together with catalytic role of Cys587 in HvAMY1 (Mori et al., 2001), strongly point toward Cys587 as target of glutathionylation. However, pre-oxidized AtAMY3, in which disulfide bond formation was promoted, was still glutathionylated (Fig. 13), thus reasonably leading to exclude Cys499 and Cys587 from being target of this modification. However, is also possible that the oxidizing pre-treatment (16-18 h in the presence of 40 mM DTTox) was

not sufficient to get a completely oxidised sample, leaving the question unsolved. Then, further investigations are needed to determine which cysteine residues undergo glutathyionylation in AtAMY3. In any case, glutathionylation seems to prevent protein inhibition mediated by H_2O_2.

It was shown that both AtBAM1 an AtAMY3 work synergistically *in vitro* to degrade starch (Seung et al., 2013) and that AtBAM1 and AtAMY3 expression seem to be promoted in illuminated mesophyll cells of plants under stress conditions (Sparla et al., 2006; Valerio et al., 2011; Dr. Santelia, personal comunication). Hence, is possible to imagine that AtBAM1 and AtAMY3, which are not required for nighttime transitory starch degradation (Yu et al., 2005; Fulton et al., 2008), can be part of a minor pathway of starch breakdown occurring by light under stress conditions. In the proposed model (Fig. 19), under oxidative stress conditions, H_2O_2 production could inhibit enzyme activity. However, H_2O_2 also promote glutathionylation of both enzymes preventing their fast and irreversible oxidation and allows them to keep on degrading starch. Furthermore, glutathionylation can be seen as an additional means to modulate protein activity to prevent premature exhaustion of plant starch reserves. Indeed, it is known that plants control the rate of storage and consumption of their reserves to avoid the risk of starvation (Gibon et al., 2004; Gibon et al., 2009; Graf et al., 2010; Scialdone et al., 2013; Kölling et al., 2015).

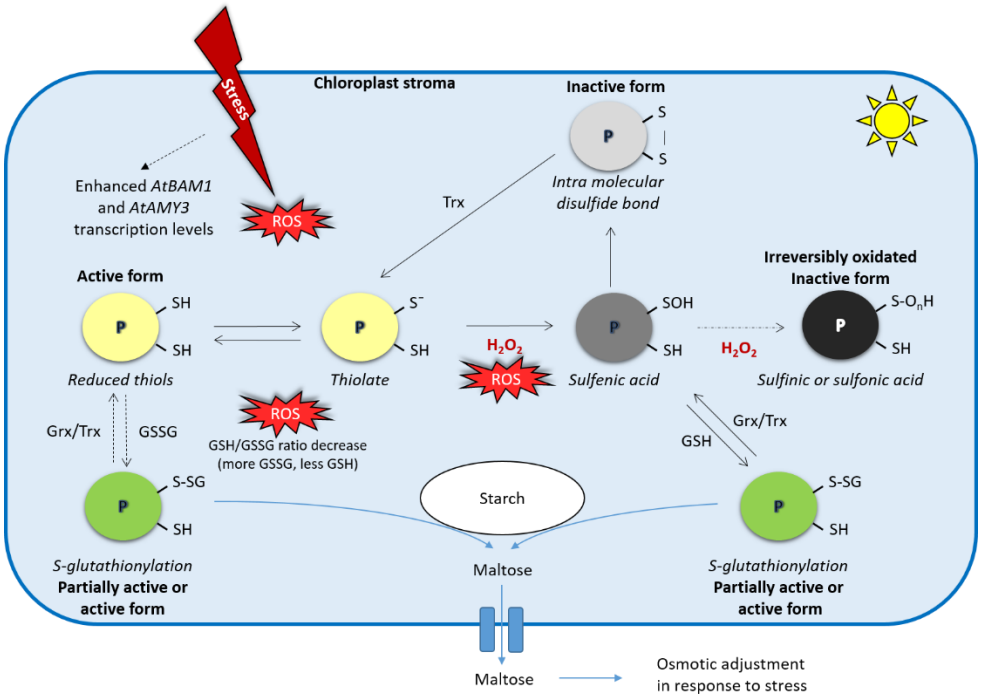

Figure 19 – Schematic model of glutathionylation effects on AtBAM1 or AtAMY3 proteins (represented the P letter at the center of different color spheres) and of the role of the modification in illuminated mesophyll cells under stress conditions. When stress occurs, both AtBAM1 and AtAMY3 expression is promoted and ROS (i.e. H_2O_2) production increases. In turn, H_2O_2 production causes oxidation and inactivation (light grey sphere, intra-molecular disulfide bond formation; dark grey sphere, sulfenic acid formation; black sphere, irreversibly oxidated protein due to the formation of sulfinic or sulfonic acids) of both AtBAM1 and AtAMY3. However, the proteins are required to degrade transitory starch. AtBAM1 can produce osmolytes (maltose) necessary to counteract the stress through osmotic adjustments. On the other side, H_2O_2 production can promote glutathionylation either increasing the amounts of oxidized glutathione (GSSG) or triggering the formation of sulfenic acid forms of cysteine residues that can subsequently react with GSH (that is normally present in the chloroplast at millimolar concentration) to form a mixed disulfide bond. Glutathionylated proteins are active, albeit AtBAM1 activity seem to be reduced compared with the non-modified form. In this way, AtBAM1 and AtAMY3 can still degrade transitory starch. Moreover, glutathionylation can be reverted by Trxs or Grxs and proteins can be reactivated. AtBAM1 and AtAMY3 are not required for normal transitory starch degradation during the day, then when the stress ceases, protein levels may decrease back again.

REFERENCES

Asada K (2006) Production and scavenging of reactive oxygen species in chloroplasts and their functions. Plant Physiology **141**: 391–396

Balls AK, Walden MK, Thompson RR (1948) A crystalline β-amylase from sweet potatoes. J Biol Chem **173**: 9–19

Bedhomme M, Adamo M, Marchand CH, Couturier J, Rouhier N, Lemaire SD, Zaffagnini M, Trost P (2012) Glutathionylation of cytosolic glyceraldehyde-3-phosphate dehydrogenase from the model plant *Arabidopsis thaliana* is reversed by both glutaredoxins and thioredoxins in vitro. Biochem J **445**: 337–347

Berndt C, Lillig CH, Holmgren A (2007) Thiol-based mechanisms of the thioredoxin and glutaredoxin systems: implications for diseases in the cardiovascular system. Am J Physiol Heart Circ Physiol **292**: H1227–1236

Brandes HK, Larimer FW, Hartman FC (1996) The molecular pathway for the regulation of phosphoribulokinase by thioredoxin f. J Biol Chem **271**: 3333–3335

Buchanan BB, Balmer Y (2005) Redox regulation: a broadening horizon. Annual Review of Plant Biology **56**: 187–220

Cantarel BL, Coutinho PM, Rancurel C, Bernard T, Lombard V, Henrissat B (2009) The Carbohydrate-Active EnZymes database (CAZy): an expert resource for Glycogenomics. Nucl Acids Res **37**: D233–D238

Chakravarthi S, Jessop CE, Bulleid NJ (2006) The role of glutathione in disulphide bond formation and endoplasmic-reticulum-generated oxidative stress. EMBO Rep **7**: 271–275

Cheong CG, Eom SH, Chang C, Shin DH, Song HK, Min K, Moon JH, Kim KK, Hwang KY, Suh SW (1995) Crystallization, molecular replacement solution, and refinement of tetrameric β-amylase from sweet potato. Proteins **21**: 105–117

Cruz de Carvalho MH (2008) Drought stress and reactive oxygen species. Plant Signal Behav **3**: 156–165

Cumming RC, Andon NL, Haynes PA, Park M, Fischer WH, Schubert D (2004) Protein disulfide bond formation in the cytoplasm during oxidative Stress. J Biol Chem **279**: 21749–21758

Dalle-Donne I, Rossi R, Colombo G, Giustarini D, Milzani A (2009) Protein S-glutathionylation: a regulatory device from bacteria to humans. Trends in Biochemical Sciences **34**: 85–96

Dalle-Donne I, Rossi R, Giustarini D, Colombo R, Milzani A (2007) S-glutathionylation in protein redox regulation. Free Radical Biology and Medicine **43**: 883–898

Delatte T, Umhang M, Trevisan M, Eicke S, Thorneycroft D, Smith SM, Zeeman SC (2006) Evidence for distinct mechanisms of starch granule breakdown in plants. J Biol Chem **281**: 12050–12059

Dixon DP, Skipsey M, Grundy NM, Edwards R (2005) Stress-induced protein S-glutathionylation in arabidopsis. Plant Physiology **138**: 2233–2244

Doyle EA, Lane AM, Sides JM, Mudgett MB, Monroe JD (2007) An α-amylase (At4g25000) in Arabidopsis leaves is secreted and induced by biotic and abiotic stress. Plant, Cell & Environment **30**: 388–398

Durrant I (1990) Light-based detection of biomolecules. Nature **346**: 297–298

Emanuelsson O, Nielsen H, von Heijne G (1999) ChloroP, a neural network-based method for predicting chloroplast transit peptides and their cleavage sites. Protein Sci **8**: 978–984

Foyer CH (1997) Oxygen metabolism and electron transport in photosynthesis. Cold Spring Harbor Monograph Archive **34**: 587–621

Foyer CH, Harbinson J (1994) Oxygen metabolism and the regulation of photosynthetic electron transport. *In* Causes of photooxidative stress and amelioration of defense systems in plants. Londres, GBR: CRC press: 1–42

Foyer CH, Noctor G (2005) Redox homeostasis and antioxidant signaling: a metabolic interface between stress perception and physiological responses. Plant Cell **17**: 1866–1875

Foyer CH, Noctor G (2011) Ascorbate and glutathione: the heart of the redox hub. Plant Physiology **155**: 2–18

Foyer CH, Shigeoka S (2011) Understanding oxidative stress and antioxidant functions to enhance photosynthesis. Plant Physiol **155**: 93–100

Fulton DC, Stettler M, Mettler T, Vaughan CK, Li J, Francisco P, Gil M, Reinhold H, Eicke S, Messerli G, et al (2008) β-amylase 4, a noncatalytic protein required for starch breakdown, acts upstream of three active β-amylases in Arabidopsis chloroplasts. Plant Cell **20**: 1040–1058

Gao X-H, Bedhomme M, Michelet L, Zaffagnini M, Lemaire SD (2009a) Glutathionylation in photosynthetic organisms - Chapter 12. Advances in Botanical Research **52**: 363–403

Gao X-H, Bedhomme M, Veyel D, Zaffagnini M, Lemaire SD (2009b) Methods for analysis of protein glutathionylation and their application to photosynthetic organisms. Mol Plant **2**: 218–235

Geigenberger P, Fernie AR (2014) Metabolic control of redox and redox control of metabolism in plants. Antioxid Redox Signal **21**: 1389–1421

Geigenberger P, Kolbe A, Tiessen A (2005) Redox regulation of carbon storage and partitioning in response to light and sugars. J Exp Bot **56**: 1469–1479

Gibon Y, Bläsing OE, Palacios-Rojas N, Pankovic D, Hendriks JHM, Fisahn J, Höhne M, Günther M, Stitt M (2004) Adjustment of diurnal starch turnover to short days: depletion of sugar during the night leads to a temporary inhibition of carbohydrate utilization, accumulation of sugars and post-translational activation of ADP-glucose pyrophosphorylase in the following light period. The Plant Journal **39**: 847–862

Gibon Y, Pyl E-T, Sulpice R, Lunn JE, Höhne M, Günther M, Stitt M (2009) Adjustment of growth, starch turnover, protein content and central metabolism to a decrease of the carbon supply when Arabidopsis is grown in very short photoperiods. Plant, Cell & Environment **32**: 859–874

Glaring MA, Baumann MJ, Hachem MA, Nakai H, Nakai N, Santelia D, Sigurskjold BW, Zeeman SC, Blennow A, Svensson B (2011) Starch-binding domains in the CBM45 family – low-affinity domains from glucan, water dikinase and α-amylase involved in plastidial starch metabolism. FEBS Journal **278**: 1175–1185

Glaring MA, Skryhan K, Kötting O, Zeeman SC, Blennow A (2012) Comprehensive survey of redox sensitive starch metabolising enzymes in *Arabidopsis thaliana*. Plant Physiol Biochem **58**: 89–97

Graf A, Schlereth A, Stitt M, Smith AM (2010) Circadian control of carbohydrate availability for growth in Arabidopsis plants at night. Proc Natl Acad Sci U S A **107**: 9458–9463

Hejazi M, Mahlow S, Fettke J (2014) The glucan phosphorylation mediated by α-glucan, water dikinase (GWD) is also essential in the light phase for a functional transitory starch turn-over. Plant Signal Behav **9**: e28892

Heldt WH, Werdan K, Milovancev M, Geller G (1973) Alkalization of the chloroplast stroma caused by light-dependent proton flux into the thylakoid space. Biochim Biophys Acta **314**: 224–241

Hendriks JHM, Kolbe A, Gibon Y, Stitt M, Geigenberger P (2003) ADP-glucose pyrophosphorylase is activated by posttranslational redox-modification in response to light and to sugars in leaves of Arabidopsis and other plant species. Plant Physiol **133**: 838–849

Horrer D, Flütsch S, Pazmino D, Matthews JSA, Thalmann M, Nigro A, Leonhardt N, Lawson T, Santelia D (2016) Blue light induces a distinct starch degradation pathway in guard cells for stomatal opening. Curr Biol **26**: 362–370

Ito H, Iwabuchi M, Ogawa K (2003a) The sugar-metabolic enzymes aldolase and triose-phosphate isomerase are targets of glutathionylation in *Arabidopsis thaliana*: detection using biotinylated glutathione. Plant Cell Physiol **44**: 655–660

Ito H, Iwabuchi M, Ogawa K (2003b) The sugar-metabolic enzymes aldolase and triose-phosphate isomerase are targets of glutathionylation in *Arabidopsis thaliana*: detection using biotinylated glutathione. Plant and Cell Physiology **44**: 655–660

Kaplan F, Guy CL (2005) RNA interference of Arabidopsis β-amylase 8 prevents maltose accumulation upon cold shock and increases sensitivity of PSII photochemical efficiency to freezing stress. Plant J **44**: 730–743

Kettenhofen NJ, Wood MJ (2010) Formation, reactivity, and detection of protein sulfenic acids. Chem Res Toxicol **23**: 1633–1646

Klomsiri C, Karplus PA, Poole LB (2011) Cysteine-based redox switches in enzymes. Antioxid Redox Signal **14**: 1065–1077

Kolbe A, Tiessen A, Schluepmann H, Paul M, Ulrich S, Geigenberger P (2005) Trehalose 6-phosphate regulates starch synthesis via posttranslational redox activation of ADP-glucose pyrophosphorylase. Proc Natl Acad Sci USA **102**: 11118–11123

Kölling K, Thalmann M, Müller A, Jenny C, Zeeman SC (2015) Carbon partitioning in *Arabidopsis thaliana* is a dynamic process controlled by the plants metabolic status and its circadian clock. Plant Cell Environ **38**: 1965–1979

König J, Muthuramalingam M, Dietz K-J (2012) Mechanisms and dynamics in the thiol/disulfide redox regulatory network: transmitters, sensors and targets. Curr Opin Plant Biol **15**: 261–268

Kötting O, Pusch K, Tiessen A, Geigenberger P, Steup M, Ritte G (2005) Identification of a novel enzyme required for starch metabolism in Arabidopsis leaves. The phosphoglucan, water dikinase. Plant Physiol **137**: 242–252

Kötting O, Santelia D, Edner C, Eicke S, Marthaler T, Gentry MS, Comparot-Moss S, Chen J, Smith AM, Steup M, et al (2009) Starch-exchess 4 is a laforin-like phosphoglucan phosphatase required for starch degradation in *Arabidopsis thaliana*. Plant Cell **21**: 334–346

Krueger S, Niehl A, Lopez M, Steinhauser D, Donath A, Hildebrandt T, Romero LC, Hoefgen R, Gotor C, Hesse H (2009) Analysis of cytosolic and plastidic serine acetyltransferase mutants and subcellular metabolite distributions suggests interplay of the cellular compartments for cysteine biosynthesis in Arabidopsis. Plant, Cell and Environment **32**: 349–367

Lao NT, Schoneveld O, Mould RM, Hibberd JM, Gray JC, Kavanagh TA (1999) An Arabidopsis gene encoding a chloroplast-targeted β-amylase. The Plant Journal **20**: 519–527

Larkin MA, Blackshields G, Brown NP, Chenna R, McGettigan PA, McWilliam H, Valentin F, Wallace IM, Wilm A, Lopez R, et al (2007) Clustal W and Clustal X version 2.0. Bioinformatics **23**: 2947–2948

Lawson T, Simkin AJ, Kelly G, Granot D (2014) Mesophyll photosynthesis and guard cell metabolism impacts on stomatal behaviour. New Phytol **203**: 1064–1081

Lo Conte M, Carroll KS (2013) The redox biochemistry of protein sulfenylation and sulfinylation. J Biol Chem **288**: 26480–26488

Lu J, Holmgren A (2014) The thioredoxin antioxidant system. Free Radic Biol Med **66**: 75–87

Magrane M, Consortium U (2011) UniProt Knowledgebase: a hub of integrated protein data. Database **2011**: bar009

Michalska J, Zauber H, Buchanan BB, Cejudo FJ, Geigenberger P (2009) NTRC links built-in thioredoxin to light and sucrose in regulating starch synthesis in chloroplasts and amyloplasts. Proc Natl Acad Sci USA **106**: 9908–9913

Michelet L, Zaffagnini M, Vanacker H, Le M, Marchand C, Schroda M, Lemaire SD, Decottignies P (2008) In vivo targets of S-thiolation in *Chlamydomonas reinhardtii*. Journal of Biological Chemistry **283**: 21571–21578

Mieyal JJ, Gallogly MM, Qanungo S, Sabens EA, Shelton MD (2008) Molecular mechanisms and clinical implications of reversible protein S-glutathionylation. Antioxidants and Redox Signaling **10**: 1941–1988

Mikami B, Adachi M, Kage T, Sarikaya E, Nanmori T, Shinke R, Utsumi S (1999a) Structure of raw starch-digesting Bacillus cereus beta-amylase complexed with maltose. Biochemistry **38**: 7050–7061

Mikami B, Yoon HJ, Yoshigi N (1999b) The crystal structure of the sevenfold mutant of barley β-amylase with increased thermostability at 2.5 A resolution. J Mol Biol **285**: 1235–1243

Mikkelsen R, Mutenda KE, Mant A, Schürmann P, Blennow A (2005) α-Glucan, water dikinase (GWD): A plastidic enzyme with redox-regulated and coordinated catalytic activity and binding affinity. PNAS **102**: 1785–1790

Mikkelsen R, Suszkiewicz K, Blennow A (2006) A novel type carbohydrate-binding module identified in α-glucan, water dikinases is specific for regulated plastidial starch metabolism. Biochemistry **45**: 4674–4682

Mittler R, Vanderauwera S, Gollery M, Van Breusegem F (2004) Reactive oxygen gene network of plants. Trends Plant Sci **9**: 490–498

Monroe JD, Storm AR, Badley EM, Lehman MD, Platt SM, Saunders LK, Schmitz JM, Torres CE (2014) β-amylase 1 and β-amylase 3 are plastidic starch hydrolases in Arabidopsis that seem to be adapted for different thermal, pH, and stress conditions. Plant Physiol **166**: 1748–1763

Mori H, Bak-Jensen KS, Gottschalk TE, Motawia MS, Damager I, Møller BL, Svensson B (2001) Modulation of activity and substrate binding modes by mutation of single and double subsites +1/+2 and -5/-6 of barley α-amylase 1. Eur J Biochem **268**: 6545–6558

Muthuramalingam M, Matros A, Scheibe R, Mock H-P, Dietz K-J (2013) The hydrogen peroxide-sensitive proteome of the chloroplast in vitro and in vivo. Front Plant Sci **4**: 54

Nakamura K, Ohto MA, Yoshida N, Nakamura K (1991) Sucrose-induced accumulation of β-amylase occurs concomitant with the accumulation of starch and sporamin in leaf-petiole cuttings of sweet potato. Plant Physiol **96**: 902–909

Nanmori T, Nagai M, Shimizu Y, Shinke R, Mikami B (1993) Cloning of the β-amylase gene from *Bacillus cereus* and characteristics of the primary structure of the enzyme. Appl Environ Microbiol **59**: 623–627

Nomura K, Yoneda I, Nanmori T, Shinke R, Morita Y, Mikami B (1995) The role of SH and S-S groups in *Bacillus cereus* β-Amylase. J Biochem **118**: 1124–1130

Oyama T, Miyake H, Kusunoki M, Nitta Y (2003) Crystal structures of beta-amylase from *Bacillus cereus* var mycoides in complexes with substrate analogs and affinity-labeling reagents. J Biochem **133**: 467–474

Pascual MB, Mata-Cabana A, Florencio FJ, Lindahl M, Cejudo FJ (2011) A comparative analysis of the NADPH thioredoxin reductase C-2-Cys peroxiredoxin system from plants and cyanobacteria. Plant Physiol **155**: 1806–1816

Paulsen CE, Carroll KS (2013) Cysteine-mediated redox signaling: chemistry, biology, and tools for discovery. Chem Rev **113**: 4633–4679

Pérez S, Bertoft E (2010) The molecular structures of starch components and their contribution to the architecture of starch granules: A comprehensive review. Starch/Stärke **62**: 389–420

Petersen TN, Brunak S, von Heijne G, Nielsen H (2011) SignalP 4.0: discriminating signal peptides from transmembrane regions. Nat Meth **8**: 785–786

Poole LB, Karplus PA, Claiborne A (2004) Protein sulfenic acids in redox signaling. Annu Rev Pharmacol Toxicol **44**: 325–347

Prasch CM, Ott KV, Bauer H, Ache P, Hedrich R, Sonnewald U (2015) β-amylase 1 mutant Arabidopsis plants show improved drought tolerance due to reduced starch breakdown in guard cells. J Exp Bot **66**: 6059–6067

Quan L-J, Zhang B, Shi W-W, Li H-Y (2008) Hydrogen peroxide in plants: a versatile molecule of the reactive oxygen species network. J Integr Plant Biol **50**: 2–18

Queval G, Jaillard D, Zechmann B, Noctor G (2011) Increased intracellular H_2O_2 availability preferentially drives glutathione accumulation in vacuoles and chloroplasts. Plant, Cell and Environment **34**: 21–32

Randall LM, Ferrer-Sueta G, Denicola A (2013) Peroxiredoxins as preferential targets in H_2O_2-induced signaling. Meth Enzymol **527**: 41–63

Reddie KG, Carroll KS (2008) Expanding the functional diversity of proteins through cysteine oxidation. Current Opinion in Chemical Biology **12**: 746–754

Repellin A, Båga M, Chibbar RN (2008) In vitro pullulanase activity of wheat (*Triticum aestivum* L.) limit-dextrinase type starch debranching enzyme is modulated by redox conditions. Journal of Cereal Science **47**: 302–309

Rhee SG, Bae YS, Lee SR, Kwon J (2000) Hydrogen peroxide: a key messenger that modulates protein phosphorylation through cysteine oxidation. Science's STKE. doi: 10.1126/stke.2000.53.pe1

Ritte G, Scharf A, Eckermann N, Haebel S, Steup M (2004) Phosphorylation of transitory starch is increased during degradation. Plant Physiol **135**: 2068–2077

Robert X, Haser R, Gottschalk TE, Ratajczak F, Driguez H, Svensson B, Aghajari N (2003) The structure of barley α-amylase isozyme 1 reveals a novel role of domain C in substrate recognition and binding: a pair of sugar tongs. Structure **11**: 973–984

Roos G, Foloppe N, Messens J (2013) Understanding the pK_a of redox cysteines: the key role of hydrogen bonding. Antioxid Redox Signal **18**: 94–127

Rouhier N, Lemaire SD, Jacquot J-P (2008) The role of glutathione in photosynthetic organisms: emerging functions for glutaredoxins and glutathionylation. Annual Review of Plant Biology **59**: 143–166

Santelia D, Trost P, Sparla F (2015) New insights into redox control of starch degradation. Current Opinion in Plant Biology **25**: 1–9

Schindler I, Renz A, Schmid FX, Beck E (2001) Activation of spinach pullulanase by reduction results in a decrease in the number of isomeric forms. Biochim Biophys Acta **1548**: 175–186

Schürmann P, Buchanan BB (2008) The ferredoxin/thioredoxin system of oxygenic photosynthesis. Antioxid Redox Signal **10**: 1235–1274

Scialdone A, Mugford ST, Feike D, Skeffington A, Borrill P, Graf A, Smith AM, Howard M (2013) Arabidopsis plants perform arithmetic division to prevent starvation at night. eLife. doi: 10.7554/eLife.00669

Serrato AJ, Pérez-Ruiz JM, Spínola MC, Cejudo FJ (2004) A novel NADPH thioredoxin reductase, localized in the chloroplast, which deficiency causes hypersensitivity to abiotic stress in *Arabidopsis thaliana*. J Biol Chem **279**: 43821–43827

Seung D, Thalmann M, Sparla F, Abou Hachem M, Lee SK, Issakidis-Bourguet E, Svensson B, Zeeman SC, Santelia D (2013) *Arabidopsis thaliana* AMY3 is a unique redox-regulated chloroplastic α-amylase. J Biol Chem **288**: 33620–33633

Sharma P, Jha AB, Dubey RS, Pessarakli M (2012) Reactive oxygen species, oxidative damage, and antioxidative defense mechanism in plants under stressful conditions. Journal of Botany **2012**: e217037

Shelton MD, Mieyal JJ (2008) Regulation by reversible S-glutathionylation: molecular targets implicated in inflammatory diseases. Molecules and Cells **25**: 332–346

Shigeoka S, Ishikawa T, Tamoi M, Miyagawa Y, Takeda T, Yabuta Y, Yoshimura K (2002) Regulation and function of ascorbate peroxidase isoenzymes. J Exp Bot **53**: 1305–1319

Sievers F, Wilm A, Dineen D, Gibson TJ, Karplus K, Li W, Lopez R, McWilliam H, Remmert M, Söding J, et al (2011) Fast, scalable generation of high-quality protein multiple sequence alignments using Clustal Omega. Mol Syst Biol **7**: 539

Silver DM, Kötting O, Moorhead GBG (2014) Phosphoglucan phosphatase function sheds light on starch degradation. Trends Plant Sci **19**: 471–478

Silver DM, Silva LP, Issakidis-Bourguet E, Glaring MA, Schriemer DC, Moorhead GBG (2013) Insight into the redox regulation of the phosphoglucan phosphatase SEX4 involved in starch degradation. FEBS J **280**: 538–548

Skeffington AW, Graf A, Duxbury Z, Gruissem W, Smith AM (2014) Glucan, water dikinase exerts little control over starch degradation in Arabidopsis leaves at night. Plant Physiol **165**: 866–879

Smith AM, Zeeman SC, Steven M (2005) Starch degradation. Annu Rev Plant Biol **56**: 73–98

Søgaard M, Kadziola A, Haser R, Svensson B (1993) Site-directed mutagenesis of histidine 93, aspartic acid 180, glutamic acid 205, histidine 290, and aspartic acid 291 at the active site and tryptophan 279 at the raw starch binding site in barley alpha-amylase 1. J Biol Chem **268**: 22480–22484

Sokolov LN, Dominguez-Solis JR, Allary A-L, Buchanan BB, Luan S (2006) A redox-regulated chloroplast protein phosphatase binds to starch diurnally and functions in its accumulation. Proc Natl Acad Sci USA **103**: 9732–9737

Sparla F, Costa A, Lo Schiavo F, Pupillo P, Trost P (2006) Redox regulation of a novel plastid-targeted β-amylase of Arabidopsis. Plant Physiol **141**: 840–850

Stanley D, Fitzgerald AM, Farnden KJF (2002) Characterisation of putative α-amylases from apple (*Malus domestica*) and *Arabidopsis thaliana*. Biologia **5**: 137–148

Stitt M, Zeeman SC (2012) Starch turnover: pathways, regulation and role in growth. Curr Opin Plant Biol **15**: 282–292

Streb S, Eicke S, Zeeman SC (2012) The simultaneous abolition of three starch hydrolases blocks transient starch breakdown in Arabidopsis. J Biol Chem **287**: 41745–41756

Suzuki N, Koussevitzky S, Mittler R, Miller G (2012) ROS and redox signalling in the response of plants to abiotic stress. Plant, Cell & Environment **35**: 259–270

Thormählen I, Ruber J, von Roepenack-Lahaye E, Ehrlich S-M, Massot V, Hümmer C, Tezycka J, Issakidis-Bourguet E, Geigenberger P (2013) Inactivation of thioredoxin f1 leads to decreased light activation of ADP-glucose pyrophosphorylase and altered diurnal starch turnover in leaves of Arabidopsis plants. Plant Cell Environ **36**: 16–29

Valerio C, Costa A, Marri L, Issakidis-Bourguet E, Pupillo P, Trost P, Sparla F (2011) Thioredoxin-regulated β-amylase (BAM1) triggers diurnal starch degradation in guard cells, and in mesophyll cells under osmotic stress. J Exp Bot **62**: 545–555

Vavasseur A, Raghavendra AS (2005) Guard cell metabolism and CO_2 sensing. New Phytol **165**: 665–682

Wang P, Song C-P (2008) Guard-cell signalling for hydrogen peroxide and abscisic acid. New Phytol **178**: 703–718

Waszczak C, Akter S, Eeckhout D, Persiau G, Wahni K, Bodra N, Van Molle I, De Smet B, Vertommen D, Gevaert K, et al (2014) Sulfenome mining in *Arabidopsis thaliana*. Proc Natl Acad Sci USA **111**: 11545–11550

Weise SE, Schrader SM, Kleinbeck KR, Sharkey TD (2006) Carbon balance and circadian regulation of hydrolytic and phosphorolytic breakdown of transitory starch. Plant Physiol **141**: 879–886

Werdan K, Heldt HW, Milovancev M (1975) The role of pH in the regulation of carbon fixation in the chloroplast stroma. Studies on CO_2 fixation in the light and dark. Biochim Biophys Acta **396**: 276–292

Winterbourn CC, Hampton MB (2008) Thiol chemistry and specificity in redox signaling. Free Radic Biol Med **45**: 549–561

Xiong Y, Uys JD, Tew KD, Townsend DM (2011) S-glutathionylation: from molecular mechanisms to health outcomes. Antioxidants and Redox Signaling **15**: 233–270

Yoshida N, Nakamura K (1991) Molecular cloning and expression in *Escherichia coli* of cDNA encoding the subunit of sweet potato beta-amylase. J Biochem **110**: 196–201

Yu T-S, Zeeman SC, Thorneycroft D, Fulton DC, Dunstan H, Lue W-L, Hegemann B, Tung S-Y, Umemoto T, Chapple A, et al (2005) α-Amylase Is Not Required for Breakdown of Transitory Starch in Arabidopsis Leaves. J Biol Chem **280**: 9773–9779

Zaffagnini M, Bedhomme M, Groni H, Marchand CH, Puppo C, Gontero B, Cassier-Chauvat C, Decottignies P, Lemaire SD (2012a) Glutathionylation in the photosynthetic model organism *Chlamydomonas reinhardtii*: a proteomic Survey. Mol Cell Proteomics **11**: M111.014142

Zaffagnini M, Bedhomme M, Lemaire SD, Trost P (2012b) The emerging roles of protein glutathionylation in chloroplasts. Plant Sci **185-186**: 86–96

Zanella M, Borghi GL, Pirone C, Thalmann M, Pazmino D, Costa A, Santelia D, Trost P, Sparla F (2016) β-amylase 1 (BAM1) degrades transitory starch to sustain proline biosynthesis during drought stress. J Exp Bot erv572

Zeeman SC, Kossmann J, Smith AM (2010) Starch: its metabolism, evolution, and biotechnological modification in plants. Annual Review of Plant Biology **61**: 209–234

Zeeman SC, ap Rees T (1999) Changes in carbohydrate metabolism and assimilate export in starch-excess mutants of Arabidopsis. Plant, Cell & Environment **22**: 1445–1453

SUPPLEMENTARY INFORMATION

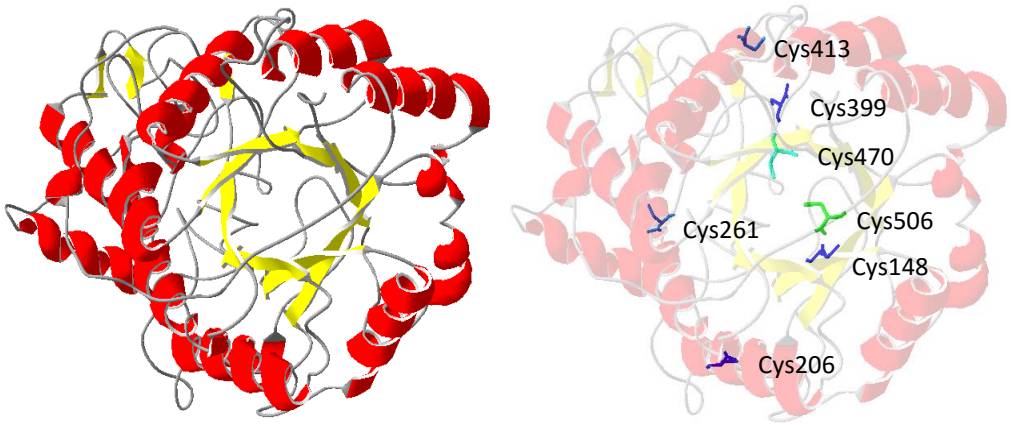

Figure S1 – Three dimensional model of *Arabidopsis thaliana* BAM1 (left panel) and accessibility of the cys residues (right panel). The model was made using Swiss-Model workspace (http://swissmodel.expasy.org/workspace) based on the known structure of barley (*Hordeum vulgare)* β-amylase (PDB code 1B1Y; Mikami et al., 1999). The structure was generated with the Swiss-PDB viewer software. Red: α-eliches; yellow: β-sheets; grey: loops. The sequence of BAM1 includes eight cysteines (Cys32, Cys148, Cys206, Cys261, Cys399, Cys413, Cys470, Cys506). Here, only seven are shown since the homology model of BAM1 based on the structure of barley β-amylase started at Gly61. Each cysteine is colored by its relative accessibility, from dark blue (completely buried) to red (amino-acids with at least 75% of their relative surface accessibility accessible). Cys470 and Cys506 is situated on a loop, proving to be easily accessible and exposed.

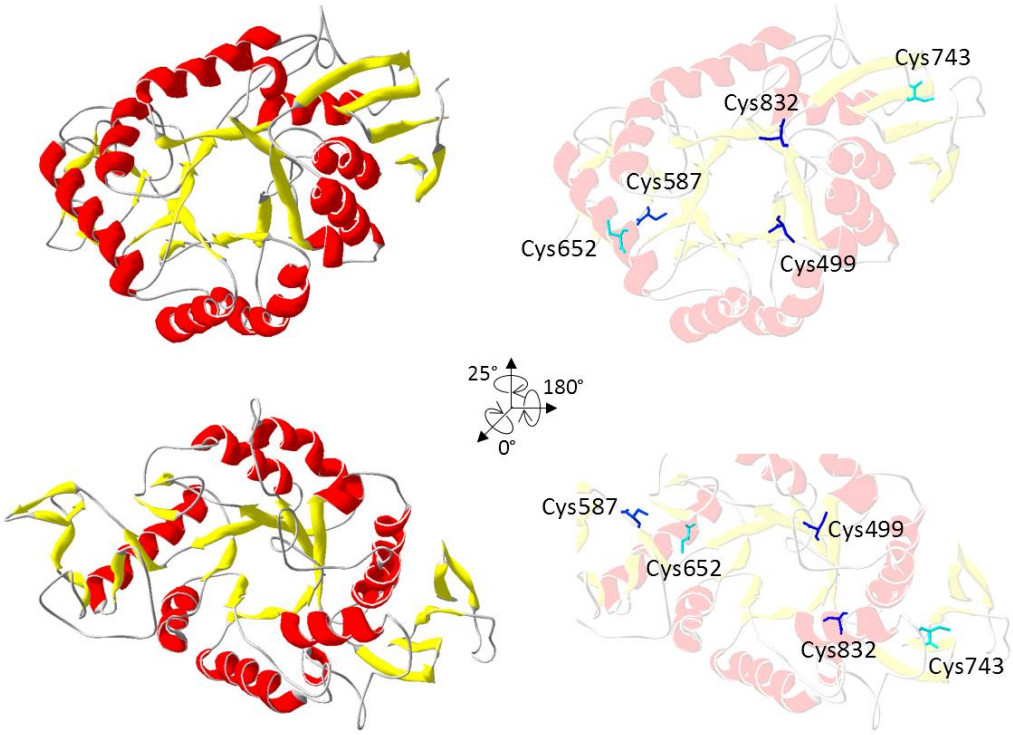

Figure S2 – Three dimensional model of *Arabidopsis thaliana* AMY3 (left panels) and accessibility of the cys residues (right panels). The model was made using Swiss-Model workspace (http://swissmodel.expasy.org/workspace) based on the known structure of barley (*Hordeum vulgare)* α-amylase isozyme 1 (HvAMY1, PDB code 3BSG; Nielsen et al., 2008). The structure was generated with the Swiss-PDB viewer software. Red: α-eliches; yellow: β-sheets; grey: loops. The sequence of AMY3 includes nine cysteines. Here, only five (Cys499, Cys587, Cys652, Cys743, Cys832) are shown since the homology model of AtAMY3 based on the structure of barley α-amylase started at Glu496. Each cysteine is colored by its relative accessibility, from dark blue (completely buried) to red (amino-acids with at least 75% of their relative surface accessibility accessible).

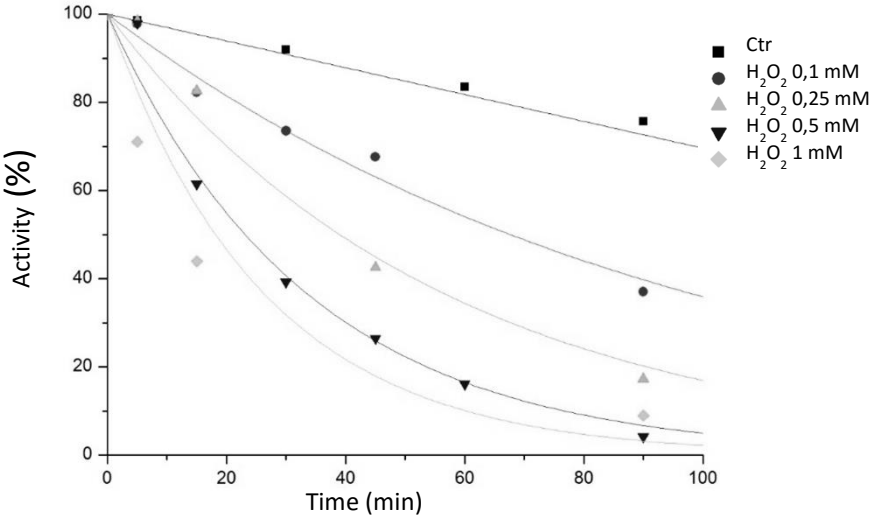

Figure S3 – Kinetics of inactivation of AtBAM1 performed at different concentrations of H_2O_2. AtBAM1 was incubated in 100 mM Tricine-NaOH buffer, pH 7.9 in absence (control) or in presence of different H_2O_2 concentrations. Activity was measured at different time points with the artificial substrate PNPG3. Activity is given as a percentage of the fully active form.

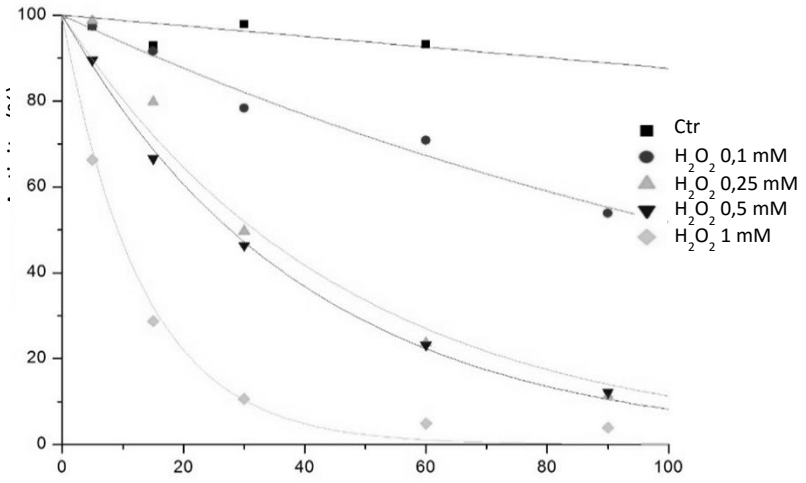

Figure S4 – Kinetics of inactivation of AtAMY3 performed at different concentrations of H_2O_2. AtAMY3 was incubated in 100 mM Tricine-NaOH buffer in absence (control) or in presence of different H_2O_2 concentrations. Activity was measured at different time points with the artificial substrate BPNPG7. Activity is given as a percentage of the fully active form.

	Specific activity (μmol min^{-1} $μg^{-1}$)
AtBAM1 wild-type (*n* = 5)	676,5 ± 142,6
AtBAM1 C32S (*n* = 2)	627,1 ± 0,3
AtBAM1 C470S (*n* = 1)	975,1 ± n.d
AtBAM1 C506S (*n* = 2)	550,4 ± 36.1

Table S1 – Specific activity of AtBAM1 wild-type protein and mutants C32S, C470S, C506S. Activity was measured after 60 min of incubation at 25° C with the artificial substrate B-PNPG3. Data are means ± S.D.

GENERAL INTRODUCTION REFERENCES

Alcázar-Alay SC, Meireles MAA, Alcázar-Alay SC, Meireles MAA (2015) Physicochemical properties, modifications and applications of starches from different botanical sources. Food Science and Technology (Campinas) **35**: 215–236

Alexander RD, Morris PC (2006) A proteomic analysis of 14-3-3 binding proteins from developing barley grains. Proteomics **6**: 1886–1896

Andriotis VME, Pike MJ, Kular B, Rawsthorne S, Smith AM (2010) Starch turnover in developing oilseed embryos. New Phytologist **187**: 791–804

Andriotis VME, Pike MJ, Schwarz SL, Rawsthorne S, Wang TL, Smith AM (2012) Altered starch turnover in the maternal plant has major effects on Arabidopsis fruit growth and seed composition. Plant Physiol **160**: 1175–1186

Angeles-Núñez JG, Tiessen A (2010) Arabidopsis sucrose synthase 2 and 3 modulate metabolic homeostasis and direct carbon towards starch synthesis in developing seeds. Planta **232**: 701–718

Aoki N, Hirose T, Scofield GN, Whitfeld PR, Furbank RT (2003) The sucrose transporter gene family in rice. Plant Cell Physiol **44**: 223–232

Ayre BG (2011) Membrane-transport systems for sucrose in relation to whole-plant carbon partitioning. Mol Plant **4**: 377–394

Badenhuizen N (1969) The biosynthesis of starch granules in higher plants. New york: Appleton-Century-Crofts 1–115

Baker RF, Slewinski TL, Braun DM (2013) The Tie-dyed pathway promotes symplastic trafficking in the phloem. Plant Signaling & Behavior **8**: e24540

Ballicora MA, Frueauf JB, Fu Y, Schürmann P, Preiss J (2000) Activation of the potato tuber ADP-glucose pyrophosphorylase by thioredoxin. J Biol Chem **275**: 1315–1320

Ball S, Guan HP, James M, Myers A, Keeling P, Mouille G, Buléon A, Colonna P, Preiss J (1996) From glycogen to amylopectin: a model for the biogenesis of the plant starch granule. Cell **86**: 349–352

Ball SG, Morell MK (2003) From bacterial glycogen to starch: understanding the biogenesis of the plant starch granule. Annu Rev Plant Biol **54**: 207–233

Baroja-Fernández E, Muñoz FJ, Li J, Bahaji A, Almagro G, Montero M, Etxeberria E, Hidalgo M, Sesma MT, Pozueta-Romero J (2012) Sucrose synthase activity in the sus1/sus2/sus3/sus4 Arabidopsis mutant is sufficient to support normal cellulose and starch production. PNAS **109**: 321–326

Barratt DHP, Derbyshire P, Findlay K, Pike M, Wellner N, Lunn J, Feil R, Simpson C, Maule AJ, Smith AM (2009) Normal growth of Arabidopsis requires cytosolic invertase but not sucrose synthase. PNAS **106**: 13124–13129

Baud S, Boutin J-P, Miquel M, Lepiniec L, Rochat C (2002) An integrated overview of seed development in Arabidopsis thaliana ecotype WS. Plant Physiology and Biochemistry **40**: 151–160

Baumann U, Juttner J (2002) Plant thioredoxins: the multiplicity conundrum. Cell Mol Life Sci **59**: 1042–1057

Baunsgaard L, Lütken H, Mikkelsen R, Glaring MA, Pham TT, Blennow A (2005) A novel isoform of glucan, water dikinase phosphorylates pre-phosphorylated α-glucans and is involved in starch degradation in Arabidopsis. The Plant Journal **41**: 595–605

Bay-Smidt AM, Wischmann B, Olsen CE, Nielsen TH (1994) Starch bound phosphate in potato as studied by a simple method for determination of organic phosphate and 31P-NMR. **46**: 167–172

Beck E, Ziegler P (1989) Biosynthesis and degradation of starch in higher plants. Annual Review of Plant Physiology and Plant Molecular Biology **40**: 95–117

Berg JM, Tymoczko JL, Stryer L (2002) Complex carbohydrates are formed by linkage of monosaccharides. Biochemistry. 5th edition. New York: W H Freeman; 2002. Section 11.2

Bihmidine S, Hunter CT, Johns CE, Koch KE, Braun DM (2013) Regulation of assimilate import into sink organs: update on molecular drivers of sink strength. Front Plant Sci **4**: 177

Blanshard JMV (1987) Starch granule structure and function. Starch properties and potential, critical reports on applied chemistry, Galliard T. John Wiley & Sons, pp 16–54

Blanshard JMV, Bates DR, Muhr AH, Worcester DL, Higgins JS (1984) Small-angle neutron scattering studies of starch granule structure. Carbohydrate Polymers **4**: 427–442

Blauth SL, Kim K-N, Klucinec J, Shannon JC, Thompson D, Guiltinan M (2002) Identification of Mutator insertional mutants of starch-branching enzyme 1 (sbe1) in *Zea mays* L. Plant Mol Biol **48**: 287–297

Blauth SL, Yao Y, Klucinec JD, Shannon JC, Thompson DB, Guilitinan MJ (2001) Identification of Mutator insertional mutants of starch-branching enzyme 2a in corn. Plant Physiol **125**: 1396–1405

Blennow A, Bay-Smidt AM, Olsen CE, Møller BL (2000a) The distribution of covalently bound phosphate in the starch granule in relation to starch crystallinity. Int J Biol Macromol **27**: 211–218

Blennow A, Bay-Smidt AM, Wishmann B, Olsen CE, Moller B (1998) The degree of starch phosphorylation is related to the chain length distribution of the neutral and the phosphorylated chains of amylopectin. Carbohydr Res **307:**45–54

Blennow A, Engelsen SB, Munck L, Møller BL (2000b) Starch molecular structure and phosphorylation investigated by a combined chromatographic and chemometric approach. Carbohydrate Polymers **41**: 163–174

Blennow A, Nielsen TH, Baunsgaard L, Mikkelsen R, Engelsen SB (2002) Starch phosphorylation: a new front line in starch research. Trends Plant Sci **7**: 445–450

Boorer KJ, Loo DDF, Frommer WB, Wright EM (1996) Transport mechanism of the cloned potato H+/sucrose cotransporter StSUT1. J Biol Chem **271**: 25139–25144

Bozonnet S, Jensen MT, Nielsen MM, Aghajari N, Jensen MH, Kramhøft B, Willemoës M, Tranier S, Haser R, Svensson B (2007) The "pair of sugar tongs" site on the non-catalytic domain C of barley α-amylase participates in substrate binding and activity. FEBS J **274**: 5055–5067

Braun DM, Slewinski TL (2009) Genetic control of carbon partitioning in grasses: roles of sucrose transporters and Tie-dyed loci in phloem loading. Plant Physiol **149**: 71–81

Bryant DA, Frigaard N-U (2006) Prokaryotic photosynthesis and phototrophy illuminated. Trends in Microbiology **14**: 488–496

Buléon A, Colonna P, Planchot V, Ball S (1998) Starch granules: structure and biosynthesis. International Journal of Biological Macromolecules **23**: 85–112

Bürkle L, Hibberd JM, Quick WP, Kühn C, Hirner B, Frommer WB (1998) The H+-sucrose cotransporter NtSUT1 is essential for sugar export from tobacco leaves. Plant Physiol **118**: 59–68

Burrell MM (2003) Starch: the need for improved quality or quantity—an overview. J Exp Bot **54**: 451–456

Burton RA, Bewley JD, Smith AM, Bhattacharyya MK, Tatge H, Ring S, Bull V, Hamilton WD, Martin C (1995) Starch branching enzymes belonging to distinct enzyme families are differentially expressed during pea embryo development. Plant J **7**: 3–15

Burton RA, Jenner H, Carrangis L, Fahy B, Fincher GB, Hylton C, Laurie DA, Parker M, Waite D, van Wegen S, et al (2002) Starch granule initiation and growth are altered in barley mutants that lack isoamylase activity. Plant J **31**: 97–112

Bush DR (1990) Electrogenicity, pH-dependence, and stoichiometry of the proton-sucrose symport. Plant Physiol **93**: 1590–1596

Bush DR (1993) Proton-coupled sugar and amino acid transporters in plants. Annual Review of Plant Physiology and Plant Molecular Biology **44**: 513–542

Bustos R, Fahy B, Hylton CM, Seale R, Nebane NM, Edwards A, Martin C, Smith AM (2004) Starch granule initiation is controlled by a heteromultimeric isoamylase in potato tubers. Proc Natl Acad Sci USA **101**: 2215–2220

Cairns AJ, Pollock CJ, Gallagher JA, Harrison J (2000) Fructans: Synthesis and Regulation. *In* RC Leegood, TD Sharkey, S Caemmerer, eds, Photosynthesis: Physiology and Metabolism. Springer Netherlands, Dordrecht, pp 301–320

Carpaneto A, Geiger D, Bamberg E, Sauer N, Fromm J, Hedrich R (2005) Phloem-localized, proton-coupled sucrose carrier ZmSUT1 mediates sucrose efflux under the ocntrol of the sucrose gradient and the proton motive force. J Biol Chem **280**: 21437–21443

Caspar T, Huber SC, Somerville C (1985) Alterations in growth, photosynthesis, and respiration in a starchless mutant of *Arabidopsis thaliana* (L.) deficient in chloroplast phosphoglucomutase activity. Plant Physiol **79**: 11–17

Caspar T, Lin TP, Kakefuda G, Benbow L, Preiss J, Somerville C (1991) Mutants of Arabidopsis with altered regulation of starch degradation. Plant Physiol **95**: 1181–1188

Chandran D, Reinders A, Ward JM (2003) Substrate specificity of the *Arabidopsis thaliana* sucrose transporter AtSUC2. J Biol Chem **278**: 44320–44325

Chatterton NJ, Silvius JE (1980) Photosynthate partitioning into leaf starch as affected by daily photosynthetic period duration in six species. Physiologia Plantarum **49**: 141–144

Chatterton NJ, Silvius JE (1979) Photosynthate partitioning into starch in soybean leaves. I. Effects of photoperiod versus photosynthetic period duration. Plant Physiol **64**: 749–753

Cheng J, Khan MA, Qiu W-M, Li J, Zhou H, Zhang Q, Guo W, Zhu T, Peng J, Sun F, et al (2012) Diversification of genes encoding granule-bound starch synthase in monocots and dicots is marked by multiple genome-wide duplication events. PLoS ONE **7**: e30088

Chen L-Q, Hou B-H, Lalonde S, Takanaga H, Hartung ML, Qu X-Q, Guo W-J, Kim J-G, Underwood W, Chaudhuri B, et al (2010) Sugar transporters for intercellular exchange and nutrition of pathogens. Nature **468**: 527–532

Chen L-Q, Qu X-Q, Hou B-H, Sosso D, Osorio S, Fernie AR, Frommer WB (2012) Sucrose efflux mediated by SWEET proteins as a key step for phloem transport. Science **335**: 207–211

Chia T, Thorneycroft D, Chapple A, Messerli G, Chen J, Zeeman SC, Smith SM, Smith AM (2004) A cytosolic glucosyltransferase is required for conversion of starch to sucrose in Arabidopsis leaves at night. Plant J **37**: 853–863

Cho M-H, Lim H, Shin DH, Jeon J-S, Bhoo SH, Park Y-I, Hahn T-R (2011) Role of the plastidic glucose translocator in the export of starch degradation products from the chloroplasts in *Arabidopsis thaliana*. New Phytol **190**: 101–112

Chourey PS, Taliercio EW, Carlson SJ, Ruan Y-L (1998) Genetic evidence that the two isozymes of sucrose synthase present in developing maize endosperm are critical, one for cell wall integrity and the other for starch biosynthesis. Mol Gen Genet **259**: 88–96

Christiansen C, Hachem MA, Glaring MA, Viksø-Nielsen A, Sigurskjold BW, Svensson B, Blennow A (2009) A CBM20 low-affinity starch-binding domain from glucan, water dikinase. FEBS Letters **583**: 1159–1163

Chu Z, Yuan M, Yao J, Ge X, Yuan B, Xu C, Li X, Fu B, Li Z, Bennetzen JL, et al (2006) Promoter mutations of an essential gene for pollen development result in disease resistance in rice. Genes Dev **20**: 1250–1255

Coleman HD, Yan J, Mansfield SD (2009) Sucrose synthase affects carbon partitioning to increase cellulose production and altered cell wall ultrastructure. PNAS **106**: 13118–13123

Collin V, Lamkemeyer P, Miginiac-Maslow M, Hirasawa M, Knaff DB, Dietz K-J, Issakidis-Bourguet E (2004) Characterization of plastidial thioredoxins from Arabidopsis belonging to the new y-type. Plant Physiol **136**: 4088–4095

Comparot-Moss S, Kötting O, Stettler M, Edner C, Graf A, Weise SE, Streb S, Lue W-L, MacLean D, Mahlow S, et al (2010) A putative phosphatase, LSF1, is required for normal starch turnover in Arabidopsis leaves. Plant Physiol **152**: 685–697

Costa LM, Gutièrrez-Marcos JF, Dickinson HG (2004) More than a yolk: the short life and complex times of the plant endosperm. Trends Plant Sci **9**: 507–514

Craig J, Lloyd JR, Tomlinson K, Barber L, Edwards A, Wang TL, Martin C, Hedley CL, Smith AM (1998) Mutations in the gene encoding starch synthase II profoundly alter amylopectin structure in pea embryos. Plant Cell **10**: 413–426

Crevillén P, Ballicora MA, Mérida A, Preiss J, Romero JM (2003) The different large subunit isoforms of *Arabidopsis thaliana* ADP-glucose pyrophosphorylase confer distinct kinetic and regulatory properties to the heterotetrameric enzyme. J Biol Chem **278**: 28508–28515

Crevillén P, Ventriglia T, Pinto F, Orea A, Mérida A, Romero JM (2005) Differential pattern of expression and sugar regulation of *Arabidopsis thaliana* ADP-glucose pyrophosphorylase-encoding genes. J Biol Chem **280**: 8143–8149

Critchley JH, Zeeman SC, Takaha T, Smith AM, Smith SM (2001) A critical role for disproportionating enzyme in starch breakdown is revealed by a knock-out mutation in Arabidopsis. Plant J **26**: 89–100

Crumpton-Taylor M, Grandison S, Png KMY, Bushby AJ, Smith AM (2012) Control of starch granule numbers in Arabidopsis chloroplasts. Plant Physiol **158**: 905–916

Dauvillée D, Colleoni C, Mouille G, Morell MK, d'Hulst C, Wattebled F, Liénard L, Delvallé D, Ral JP, Myers AM, et al (2001) Biochemical characterization of wild-type and mutant isoamylases of Chlamydomonas reinhardtii supports a function of the multimeric enzyme organization in amylopectin maturation. Plant Physiol **125**: 1723–1731

Davis JP, Supatcharee N, Khandelwal RL, Chibbar RN (2003) Synthesis of novel starches in planta: opportunities and challenges. Starch/Stärke **55**: 107–120

Davies HV (1990) Carbohydrate metabolism during sprouting. American Potato Journal **67**: 815–827

Davies HV, Ross H (1984) The pattern of starch and protein degradation in tubers. **27**: 373–381

Davies HV, Ross HA (1987) Hydrolytic and phosphorolytic enzyme activity and reserve mobilisation in sprouting tubers of potato (*Solanum tuberosum* L.). Journal of Plant Physiology **126**: 387–396

Deiting U, Zrenner R, Stitt M (1998) Similar temperature requirement for sugar accumulation and for the induction of new forms of sucrose phosphate synthase and amylase in cold-stored potato tubers. Plant, Cell & Environment **21**: 127–138

Delatte T, Trevisan M, Parker ML, Zeeman SC (2005) Arabidopsis mutants Atisa1 and Atisa2 have identical phenotypes and lack the same multimeric isoamylase, which influences the branch point distribution of amylopectin during starch synthesis. Plant J **41**: 815–830

Delatte T, Umhang M, Trevisan M, Eicke S, Thorneycroft D, Smith SM, Zeeman SC (2006) Evidence for distinct mechanisms of starch granule breakdown in plants. J Biol Chem **281**: 12050–12059

Delvallé D, Dumez S, Wattebled F, Roldán I, Planchot V, Berbezy P, Colonna P, Vyas D, Chatterjee M, Ball S, et al (2005) Soluble starch synthase I: a major determinant for the synthesis of amylopectin in *Arabidopsis thaliana leaves*. Plant J **43**: 398–412

Denyer K a. y., Johnson P, Zeeman S, Smith AM (2001) The control of amylose synthesis. Journal of Plant Physiology **158**: 479–487

Doidy J, van Tuinen D, Lamotte O, Corneillat M, Alcaraz G, Wipf D (2012) The *Medicago truncatula* sucrose transporter family: characterization and implication of key members in carbon partitioning towards arbuscular mycorrhizal fungi. Mol Plant **5**: 1346–1358

Dumez S, Wattebled F, Dauvillee D, Delvalle D, Planchot V, Ball SG, D'Hulst C (2006) Mutants of Arabidopsis lacking starch branching enzyme II substitute plastidial starch synthesis by cytoplasmic maltose accumulation. Plant Cell **18**: 2694–2709

Eastmond PJ, Rawsthorne S (2000) Coordinate changes in carbon partitioning and plastidial metabolism during the development of oilseed rape embryos. Plant Physiol **122**: 767–774

Edner C, Li J, Albrecht T, Mahlow S, Hejazi M, Hussain H, Kaplan F, Guy C, Smith SM, Steup M, et al (2007) Glucan, water dikinase activity stimulates breakdown of starch granules by plastidial β-amylases. Plant Physiol **145**: 17–28

Eichelmann H, Laisk A (1994) CO_2 uptake and electron transport rates in wild-type and a starchless mutant of *Nicotiana sylvestris* (the role and regulation of starch synthesis at saturating CO_2 concentrations). Plant Physiol **106**: 679–687

Ekkehard Neuhaus H, Stitt M (1990) Control analysis of photosynthate partitioning: Impact of reduced activity of ADP-glucose pyrophosphorylase or plastid phosphoglucomutase on the fluxes to starch and sucrose in *Arabidopsis thaliana* (L.) Heynh. Planta **182**: 445–454

Ellis RP, Cochrane MP, Dale MFB, Duffus CM, Lynn A, Morrison IM, Prentice RDM, Swanston JS, Tiller SA (1998) Starch production and industrial use. J Sci Food Agric **77**: 289–311

Emes MJ, Bowsher CG, Hedley C, Burrell MM, Scrase-Field ESF, Tetlow IJ (2003) Starch synthesis and carbon partitioning in developing endosperm. J Exp Bot **54**: 569–575

Engelsen SB, Madsen AØ, Blennow A, Motawia MS, Møller BL, Larsen S (2003) The phosphorylation site in double helical amylopectin as investigated by a combined approach using chemical synthesis, crystallography and molecular modeling. FEBS Lett **541**: 137–144

Evert RF (1982) Sieve-tube structure in relation to function. BioScience **32**: 789–795

Fannon JE, Hauber RJ, BeMiller JN (1992) Surface pores of starch granules. Cereal Chem **69**: 284–288

Fernbach A (1904) Some observations on the composition of potato starch. C R Hebd D Seances D Acad D Sci **138**: 428–430

Fettke J, Chia T, Eckermann N, Smith A, Steup M (2006) A transglucosidase necessary for starch degradation and maltose metabolism in leaves at night acts on cytosolic heteroglycans (SHG). Plant J **46**: 668–684

Fettke J, Eckermann N, Tiessen A, Geigenberger P, Steup M (2005) Identification, subcellular localization and biochemical characterization of water-soluble heteroglycans (SHG) in leaves of *Arabidopsis thaliana* L.: distinct SHG reside in the cytosol and in the apoplast. Plant J **43**: 568–585

Fettke J, Hejazi M, Smirnova J, Höchel E, Stage M, Steup M (2009) Eukaryotic starch degradation: integration of plastidial and cytosolic pathways. J Exp Bot erp054

Fincher GB (1989) Molecular and cellular biology associated with endosperm mobilization in germinating cereal grains. Annual Review of Plant Physiology and Plant Molecular Biology **40**: 305–346

Flügge U-I (1999) Phosphate translocators in plastids. Annual Review of Plant Physiology and Plant Molecular Biology **50**: 27–45

Flügge U-I, Häusler RE, Ludewig F, Gierth M (2011) The role of transporters in supplying energy to plant plastids. J Exp Bot **62**: 2381–2392

Focks N, Benning C (1998) wrinkled1: a novel, low-seed-oil mutant of Arabidopsis with a deficiency in the seed-specific regulation of carbohydrate metabolism. Plant Physiol **118**: 91–101

Fondy BR, Geiger DR, Servaites JC (1989) Photosynthesis, carbohydrate metabolism, and export in *Beta vulgaris* L. and *Phaseolus vulgaris* L. during square and sinusoidal light regimes. Plant Physiol **89**: 396–402

Frandsen TP, Lok F, Mirgorodskaya E, Roepstorff P, Svensson B (2000) Purification, enzymatic characterization, and nucleotide sequence of a high-isoelectric-point α-glucosidase from barley malt. Plant Physiol **123**: 275–286

French D (1984) *In* Whistler RL, BeMiller JN, Pashalls EF, Eds. Starch: chemistry and technology. Academic Press, 2nd edn. New York

French D (1973) Chemical and physical properties of starch. J Anim Sci **37**: 1048–1061

Fritzius T, Aeschbacher R, Wiemken A, Wingler A (2001) Induction of ApL3 expression by trehalose complements the starch-deficient Arabidopsis mutant adg2-1 lacking ApL1, the large subunit of ADP-glucose pyrophosphorylase. Plant Physiol **126**: 883–889

Fu H, Subramanian RR, Masters SC (2000) 14-3-3 proteins: structure, function, and regulation. Annu Rev Pharmacol Toxicol **40**: 617–647

Fujita N, Yoshida M, Asakura N, Ohdan T, Miyao A, Hirochika H, Nakamura Y (2006) Function and characterization of starch synthase I using mutants in rice. Plant Physiol **140**: 1070–1084

Fulton DC, Stettler M, Mettler T, Vaughan CK, Li J, Francisco P, Gil M, Reinhold H, Eicke S, Messerli G, et al (2008) Beta-AMYLASE4, a noncatalytic protein required for starch breakdown, acts upstream of three active β-amylases in Arabidopsis chloroplasts. Plant Cell **20**: 1040–1058

Fu Y, Ballicora MA, Leykam JF, Preiss J (1998) Mechanism of reductive activation of potato tuber ADP-glucose pyrophosphorylase. J Biol Chem **273**: 25045–25052

Gallant D, Guilbot A (1971) Artefacts during preparation of sections of starch-granules. Studies under light and electron microscope. Starch/Stärke **23**: 244–250

Gallant DJ, Bouchet B, Baldwin PM (1997) Microscopy of starch: evidence of a new level of granule organization. Carbohydr polym **32**: 177–191

Gaxiola RA, Palmgren MG, Schumacher K (2007) Plant proton pumps. FEBS Lett **581**: 2204–2214

Geigenberger P (2011) Regulation of starch biosynthesis in response to a fluctuating environment. Plant Physiol **155**: 1566–1577

Geigenberger P, Kolbe A, Tiessen A (2005) Redox regulation of carbon storage and partitioning in response to light and sugars. J Exp Bot **56**: 1469–1479

Geiger D (2011) Plant sucrose transporters from a biophysical point of view. Mol Plant **4**: 395–406

Geiger DR, Servaites JC (1994) Diurnal regulation of photosynthetic carbon metabolism in C3 plants. Annual Review of Plant Physiology and Plant Molecular Biology **45**: 235–256

Gentry MS, Dowen RH, Worby CA, Mattoo S, Ecker JR, Dixon JE (2007) The phosphatase laforin crosses evolutionary boundaries and links carbohydrate metabolism to neuronal disease. J Cell Biol **178**: 477–488

George GM, van der Merwe MJ, Nunes-Nesi A, Bauer R, Fernie AR, Kossmann J, Lloyd JR (2010) Virus-induced gene silencing of plastidial soluble inorganic pyrophosphatase impairs essential leaf anabolic pathways and reduces drought stress tolerance in Nicotiana benthamiana. Plant Physiol **154**: 55–66

Gérard C, Colonna P, Buléon A, Planchot V (2002) Order in maize mutant starches revealed by mild acid hydrolysis. Carbohydrate Polymers **48**: 131–141

Ge YX, Angenent GC, Wittich PE, Peters J, Franken J, Busscher M, Zhang LM, Dahlhaus E, Kater MM, Wullems GJ, et al (2000) NEC1, a novel gene, highly expressed in nectary tissue of *Petunia hybrida*. Plant J **24**: 725–734

Giaquinta RT (1983) Phloem loading of sucrose. Annual Review of Plant Physiology **34**: 347–387

Gibon Y, Bläsing OE, Palacios-Rojas N, Pankovic D, Hendriks JHM, Fisahn J, Höhne M, Günther M, Stitt M (2004) Adjustment of diurnal starch turnover to short days: depletion of sugar during the night leads to a temporary inhibition of carbohydrate utilization, accumulation of sugars and post-translational activation of ADP-glucose pyrophosphorylase in the following light period. The Plant Journal **39**: 847–862

Gidley MJ (1987) Factors affecting the crystalline type (AC) of native starches and model compounds: a rationalisation of observed effects in terms of polymorphic structures. Carbohydrate Research **161**: 301–304

Glaring MA, Skryhan K, Kötting O, Zeeman SC, Blennow A (2012) Comprehensive survey of redox sensitive starch metabolising enzymes in Arabidopsis thaliana. Plant Physiol Biochem **58**: 89–97

Glaring MA, Zygadlo A, Thorneycroft D, Schulz A, Smith SM, Blennow A, Baunsgaard L (2007) An extra-plastidial α-glucan, water dikinase from Arabidopsis phosphorylates amylopectin in vitro and is not necessary for transient starch degradation. J Exp Bot **58**: 3949–3960

Gómez-Casati DF, Iglesias AA (2002) ADP-glucose pyrophosphorylase from wheat endosperm. Purification and characterization of an enzyme with novel regulatory properties. Planta **214**: 428–434

Gottwald JR, Krysan PJ, Young JC, Evert RF, Sussman MR (2000) Genetic evidence for the in planta role of phloem-specific plasma membrane sucrose transporters. PNAS **97**: 13979–13984

Graf A, Schlereth A, Stitt M, Smith AM (2010) Circadian control of carbohydrate availability for growth in Arabidopsis plants at night. PNAS **107**: 9458–9463

Graf A, Smith AM (2011) Starch and the clock: The dark side of plant productivity. Trends in Plant Science **16**: 169–175

Guan H, Li P, Imparl-Radosevich J, Preiss J, Keeling P (1997) Comparing the properties of *Escherichia coli* branching enzyme and maize branching enzyme. Arch Biochem Biophys **342**: 92–98

Guan Y-F, Huang X-Y, Zhu J, Gao J-F, Zhang H-X, Yang Z-N (2008) RUPTURED POLLEN GRAIN1, a member of the MtN3/saliva gene Family, is crucial for exine pattern formation and cell integrity of microspores in Arabidopsis. Plant Physiol **147**: 852–863

Hackel A, Schauer N, Carrari F, Fernie AR, Grimm B, Kühn C (2006) Sucrose transporter LeSUT1 and LeSUT2 inhibition affects tomato fruit development in different ways. Plant J **45**: 180–192

Hädrich N, Hendriks JHM, Kötting O, Arrivault S, Feil R, Zeeman SC, Gibon Y, Schulze WX, Stitt M, Lunn JE (2012) Mutagenesis of cysteine 81 prevents dimerization of the APS1 subunit of ADP-glucose pyrophosphorylase and alters diurnal starch turnover in Arabidopsis thaliana leaves. Plant J **70**: 231–242

Hafke JB, Amerongen J-K van, Kelling F, Furch ACU, Gaupels F, Bel AJE van (2005) Thermodynamic battle for photosynthate acquisition between sieve tubes and adjoining parenchyma in transport phloem. Plant Physiol **138**: 1527–1537

Hansen PI, Spraul M, Dvortsak P, Larsen FH, Blennow A, Motawia MS, Engelsen SB (2009) Starch phosphorylation--maltosidic restrains upon 3'- and 6'-phosphorylation investigated by chemical synthesis, molecular dynamics and NMR spectroscopy. Biopolymers **91**: 179–193

Haritatos E, Medville R, Turgeon R (2000) Minor vein structure and sugar transport in *Arabidopsis thaliana*. Planta **211**: 105–111

Hartman H, Syvanen M, Buchanan BB (1990) Contrasting evolutionary histories of chloroplast thioredoxins f and m. Mol Biol Evol **7**: 247–254

Heath JD, Weldon R, Monnot C, Meinke DW (1986) Analysis of storage proteins in normal and aborted seeds from embryo-lethal mutants of Arabidopsis thaliana. Planta **169**: 304–312

Hejazi M, Fettke J, Kötting O, Zeeman SC, Steup M (2010) The Laforin-like dual-specificity phosphatase SEX4 from Arabidopsis hydrolyzes both C6- and C3-phosphate esters introduced by starch-related dikinases and thereby affects phase transition of alpha-glucans. Plant Physiol **152**: 711–722

Hendriks JHM, Kolbe A, Gibon Y, Stitt M, Geigenberger P (2003) ADP-glucose pyrophosphorylase is activated by posttranslational redox-modification in response to light and to sugars in leaves of Arabidopsis and other plant species. Plant Physiol **133**: 838–849

Hennen-Bierwagen TA, Lin Q, Grimaud F, Planchot V, Keeling PL, James MG, Myers AM (2009) Proteins from multiple metabolic pathways associate with starch biosynthetic enzymes in high molecular weight complexes: a model for regulation of carbon allocation in maize amyloplasts. Plant Physiol **149**: 1541–1559

Hennen-Bierwagen TA, Liu F, Marsh RS, Kim S, Gan Q, Tetlow IJ, Emes MJ, James MG, Myers AM (2008) Starch biosynthetic enzymes from developing maize endosperm associate in multisubunit complexes. Plant Physiol **146**: 1892–1908

Herzberg O, Chen CCH, Liu S, Tempczyk A, Howard A, Wei M, Ye D, Dunaway-Mariano D (2002) Pyruvate site of pyruvate phosphate dikinase: crystal structure of the enzyme-phosphonopyruvate complex, and mutant analysis. Biochemistry **41**: 780–787

Herzberg O, Chen CC, Kapadia G, McGuire M, Carroll LJ, Noh SJ, Dunaway-Mariano D (1996) Swiveling-domain mechanism for enzymatic phosphotransfer between remote reaction sites. PNAS **93**: 2652–2657

Hills MJ (2004) Control of storage-product synthesis in seeds. Curr Opin Plant Biol **7**: 302–308

Hizukuri S (1986) Polymodal distribution of the chain lengths of amylopectins, and its significance. Carbohydrate Research **147**: 342–347

Hizukuri S, Tabata S, Nikuni Z (1970) Studies on starch phosphate. Part 1. Estimation of glucose-6-phosphate residues in starch and the presence of other bound phosphate(s). Starch Starke **22**: 330–343

Howard T, Rejab NA, Griffiths S, Leigh F, Leverington-Waite M, Simmonds J, Uauy C, Trafford K (2011) Identification of a major QTL controlling the content of B-type starch granules in Aegilops. J Exp Bot **62**: 2217–2228

Horrer D, Flütsch S, Pazmino D, Matthews JSA, Thalmann M, Nigro A, Leonhardt N, Lawson T, Santelia D (2016) Blue light Induces a distinct starch degradation pathway in guard cells for stomatal opening. Current Biology **26**: 362–370

Huber SC (2007) Exploring the role of protein phosphorylation in plants: from signalling to metabolism. Biochem Soc Trans **35**: 28–32

Huber SC, Bickett DM (1984) Evidence for control of carbon partitioning by fructose 2,6-bisphosphate in spinach leaves. Plant Physiol **74**: 445–447

Hussain H, Mant A, Seale R, Zeeman S, Hinchliffe E, Edwards A, Hylton C, Bornemann S, Smith AM, Martin C, et al (2003) Three isoforms of isoamylase contribute different catalytic properties for the debranching of potato glucans. Plant Cell **15**: 133–149

Iglesias AA, Barry GF, Meyer C, Bloksberg L, Nakata PA, Greene T, Laughlin MJ, Okita TW, Kishore GM, Preiss J (1993) Expression of the potato tuber ADP-glucose pyrophosphorylase in *Escherichia coli*. J Biol Chem **268**: 1081–1086

Imberty A, Chanzy H, Pérez S, Buléon A, Tran V (1988) The double-helical nature of the crystalline part of A-starch. J Mol Biol **201**: 365–378

James MG, Denyer K, Myers AM (2003) Starch synthesis in the cereal endosperm. Curr Opin Plant Biol **6**: 215–222

James MG, Robertson DS, Myers AM (1995) Characterization of the maize gene sugary1, a determinant of starch composition in kernels. Plant Cell **7**: 417–429

Jane J-L, Kasemsuwan T, Leas S, Zobel H, Robyt JF (1994) Anthology of starch granule morphology by scanning electron microscopy. Starch/Stärke **46**: 121–129

Jane J-L, Xu, A, Radosavljevic M, Seib PA (1992) Location of amylose in normal starch granules. I. Susceptibility of amylose and amylopectin to cross linking reagent. Cereal Chem **69**: 405–409

Jeon J-S, Ryoo N, Hahn T-R, Walia H, Nakamura Y (2010) Starch biosynthesis in cereal endosperm. Plant Physiol Biochem **48**: 383–392

Jobling S (2004) Improving starch for food and industrial applications. Current Opinion in Plant Biology **7**: 210–218

Jones G, Whelan WJ (1969) The action pattern of D-enzyme, a transmaltodextrinylase from potato. Carbohydrate Research **9**: 483–490

Kaplan F, Guy CL (2005) RNA interference of Arabidopsis β-amylase 8 prevents maltose accumulation upon cold shock and increases sensitivity of PSII photochemical efficiency to freezing stress. Plant J **44**: 730–743

Kasemsuwan T, Jane J-L (1994) Location of amylose in normal starch granules. II. Locations of phosphodiester cross linking revealed by phosphorus-31 nuclear magnetic resonance. Cereal Chem **71**: 282–287

Kleczkowski LA (1994) Glucose activation and metabolism through UDP-glucose pyrophosphorylase in plants. Phytochemistry **37**: 1507–1515

Kleczkowski LA, Villand P, Preiss J, Olsen OA (1993) Kinetic mechanism and regulation of ADP-glucose pyrophosphorylase from barley (Hordeum vulgare) leaves. J Biol Chem **268**: 6228–6233

Kolbe A, Tiessen A, Schluepmann H, Paul M, Ulrich S, Geigenberger P (2005) Trehalose 6-phosphate regulates starch synthesis via posttranslational redox activation of ADP-glucose pyrophosphorylase. Proc Natl Acad Sci USA **102**: 11118–11123

Kötting O, Kossmann J, Zeeman SC, Lloyd JR (2010) Regulation of starch metabolism: the age of enlightenment? Current Opinion in Plant Biology **13**: 321–329

Kötting O, Pusch K, Tiessen A, Geigenberger P, Steup M, Ritte G (2005) Identification of a novel enzyme required for starch metabolism in Arabidopsis leaves. The phosphoglucan, water dikinase. Plant Physiol **137**: 242–252

Kötting O, Santelia D, Edner C, Eicke S, Marthaler T, Gentry MS, Comparot-Moss S, Chen J, Smith AM, Steup M, et al (2009) STARCH-EXCESS4 is a laforin-like phosphoglucan phosphatase required for starch degradation in Arabidopsis thaliana. Plant Cell **21**: 334–346

Kristensen M, Lok F, Planchot V, Svendsen I, Leah R, Svensson B (1999) Isolation and characterization of the gene encoding the starch debranching enzyme limit dextrinase from germinating barley. Biochim Biophys Acta **1431**: 538–546

Kubo A, Colleoni C, Dinges JR, Lin Q, Lappe RR, Rivenbark JG, Meyer AJ, Ball SG, James MG, Hennen-Bierwagen TA, et al (2010) Functions of heteromeric and homomeric isoamylase-type starch-debranching enzymes in developing maize endosperm. Plant Physiol **153**: 956–969

Lalonde S, Tegeder M, Throne-Holst M, Frommer WB, Patrick JW (2003) Phloem loading and unloading of sugars and amino acids. Plant, Cell & Environment **26**: 37–56

Lalonde S, Wipf D, Frommer WB (2004) Transport mechanisms for organic forms of carbon and nitrogen between source and sink. Annu Rev Plant Biol **55**: 341–372

Lao NT, Schoneveld O, Mould RM, Hibberd JM, Gray JC, Kavanagh TA (1999) An Arabidopsis gene encoding a chloroplast-targeted β-amylase. The Plant Journal **20**: 519–527

Lee S-K, Hwang S-K, Han M, Eom J-S, Kang H-G, Han Y, Choi S-B, Cho M-H, Bhoo SH, An G, et al (2007) Identification of the ADP-glucose pyrophosphorylase isoforms essential for starch synthesis in the leaf and seed endosperm of rice (*Oryza sativa* L.). Plant Mol Biol **65**: 531–546

Lemaire SD, Collin V, Keryer E, Quesada A, Miginiac-Maslow M (2003) Characterization of thioredoxin y, a new type of thioredoxin identified in the genome of *Chlamydomonas reinhardtii*. FEBS Lett **543**: 87–92

Leprince O, Bronchart R, Deltour R (1990) Changes in starch and soluble sugars in relation to the acquisition of desiccation tolerance during maturation of *Brassica campestris* seed. Plant, Cell & Environment **13**: 539–546

Leterrier M, Holappa LD, Broglie KE, Beckles DM (2008) Cloning, characterisation and comparative analysis of a starch synthase IV gene in wheat: functional and evolutionary implications. BMC Plant Biol **8**: 98

Li J, Almagro G, Muñoz FJ, Baroja-Fernández E, Bahaji A, Montero M, Hidalgo M, Sánchez-López AM, Ezquer I, Sesma MT, et al (2012) Post-translational redox modification of ADP-glucose pyrophosphorylase in response to light is not a major determinant of fine regulation of transitory starch accumulation in Arabidopsis leaves. Plant Cell Physiol **53**: 433–444

Lin TP, Caspar T, Somerville C, Preiss J (1988a) Isolation and characterization of a starchless mutant of *Arabidopsis thaliana* (L.) Heynh lacking ADPglucose pyrophosphorylase activity. Plant Physiol **86**: 1131–1135

Lin TP, Caspar T, Somerville CR, Preiss J (1988b) A starch deficient mutant of *Arabidopsis thaliana* with low ADPglucose pyrophosphorylase activity lacks one of the two subunits of the enzyme. Plant Physiol **88**: 1175–1181

Lin Y, Ulanov AV, Lozovaya V, Widholm J, Zhang G, Guo J, Goodman HM (2006) Genetic and transgenic perturbations of carbon reserve production in Arabidopsis seeds reveal metabolic interactions of biochemical pathways. Planta **225**: 153–164

Li Y, Beisson F, Pollard M, Ohlrogge J (2006) Oil content of Arabidopsis seeds: the influence of seed anatomy, light and plant-to-plant variation. Phytochemistry **67**: 904–915

Lloyd JR, Kossmann J, Ritte G (2005) Leaf starch degradation comes out of the shadows. Trends Plant Sci **10**: 130–137

Lohmeier-Vogel EM, Kerk D, Nimick M, Wrobel S, Vickerman L, Muench DG, Moorhead GBG (2008) Arabidopsis At5g39790 encodes a chloroplast-localized, carbohydrate-binding, coiled-coil domain-containing putative scaffold protein. BMC Plant Biol **8**: 120

Lomako J, Lomako WM, Whelan WJ, Marchase RB (1993) Glycogen contains phosphodiester groups that can be introduced by UDPglucose: glycogen glucose 1-phosphotransferase. FEBS Lett **329**: 263–267

Lorberth R, Ritte G, Willmitzer L, Kossmann J (1998) Inhibition of a starch-granule-bound protein leads to modified starch and repression of cold sweetening. Nat Biotechnol **16**: 473–477

Lunn JE, Feil R, Hendriks JHM, Gibon Y, Morcuende R, Osuna D, Scheible W-R, Carillo P, Hajirezaei M-R, Stitt M (2006) Sugar-induced increases in trehalose 6-phosphate are correlated with redox activation of ADPglucose pyrophosphorylase and higher rates of starch synthesis in *Arabidopsis thaliana*. Biochem J **397**: 139–148

Lu Y, Steichen JM, Yao J, Sharkey TD (2006) The role of cytosolic α-glucan phosphorylase in maltose metabolism and the comparison of amylomaltase in Arabidopsis and *Escherichia coli*. Plant Physiol **142**: 878–889

Lu Y, Gehan JP, Sharkey TD (2005) Daylength and circadian effects on starch degradation and maltose metabolism. Plant Physiology **138**: 2280–2291

Lu Y, Sharkey TD (2004) The role of amylomaltase in maltose metabolism in the cytosol of photosynthetic cells. Planta **218**: 466–473

MacGregor AW (1991) The effect of barley structure and composition on malt duality. *In* Proceedings of the European Brewery Convention Congress, Lisbon, Portugal, pp. 37–42.

Mansfield SG, Briarty LG (1992) Cotyledon cell development in *Arabidopsis thaliana* during reserve deposition. Can J Bot **70**: 151–164

Ma Y, Baker RF, Magallanes-Lundback M, DellaPenna D, Braun DM (2008) Tie-dyed1 and sucrose export defective1 act independently to promote carbohydrate export from maize leaves. Planta **227**: 527–538

Mazanec K, Dycka F, Bobalova J (2011) Monitoring of barley starch amylolysis by gravitational field flow fractionation and MALDI-TOF MS. J Sci Food Agric **91**: 2756–2761

McDonald AML, Stark JR, Morrison WR, Ellis RP (1991) The composition of starch granules from developing barley genotypes. Journal of Cereal Science **13**: 93–112

McPherson AE, Jane J (1999) Comparison of waxy potato with other root and tuber starches. Carbohydrate Polymers **40**: 57–70

Meyer Y, Vignols F, Reichheld JP (2002) Classification of plant thioredoxins by sequence similarity and intron position. Meth Enzymol **347**: 394–402

Michalska J, Zauber H, Buchanan BB, Cejudo FJ, Geigenberger P (2009) NTRC links built-in thioredoxin to light and sucrose in regulating starch synthesis in chloroplasts and amyloplasts. Proc Natl Acad Sci USA **106**: 9908–9913

Mikami B, Yoon HJ, Yoshigi N (1999) The crystal structure of the sevenfold mutant of barley β-amylase with increased thermostability at 2.5 A resolution. J Mol Biol **285**: 1235–1243

Mikkelsen R, Baunsgaard L, Blennow A (2004) Functional characterization of α-glucan,water dikinase, the starch phosphorylating enzyme. Biochem J **377**: 525–532

Mikkelsen R, Blennow A (2005) Functional domain organization of the potato α-glucan, water dikinase (GWD): evidence for separate site catalysis as revealed by limited proteolysis and deletion mutants. Biochemical Journal **385**: 355–361

Minchin PEH, Thorpe MR (1987) Measurement of unloading and reloading of photo-assimilate within the stem of bean. J Exp Bot **38**: 211–220

Miquel M, Browse J (1995) Lipid biosynthesis in developing seeds. Seed development and germination, Kigel J. and Galli G. Marcel Dekker, New York, pp 169–193

Mizuno K, Kawasaki T, Shimada H, Satoh H, Kobayashi E, Okumura S, Arai Y, Baba T (1993) Alteration of the structural properties of starch components by the lack of an isoform of starch branching enzyme in rice seeds. J Biol Chem **268**: 19084–19091

Morell M, Bloom M, Preiss J (1988) Affinity labeling of the allosteric activator site(s) of spinach leaf ADP-glucose pyrophosphorylase. J Biol Chem **263**: 633–637

Morell MK, Blennow A, Kosar-Hashemi B, Samuel MS (1997) Differential expression and properties of starch branching enzyme isoforms in developing wheat endosperm. Plant Physiol **113**: 201–208

Morell MK, Kosar-Hashemi B, Cmiel M, Samuel MS, Chandler P, Rahman S, Buleon A, Batey IL, Li Z (2003) Barley sex6 mutants lack starch synthase IIa activity and contain a starch with novel properties. Plant J **34**: 173–185

Mouille G, Maddelein ML, Libessart N, Talaga P, Decq A, Delrue B, Ball S (1996) Preamylopectin processing: a mandatory step for starch biosynthesis in plants. Plant Cell **8**: 1353–1366

Musgrave M, Allen J, Blasiak J, Tuominen L, Kuang A (2008) In vitro seed maturation in *Brassica rapa* L.: relationship of silique atmosphere to storage reserve deposition. Environmental and Experimental Botany **62**: 247–253

Myers AM, Morell MK, James MG, Ball SG (2000) Recent progress toward understanding biosynthesis of the amylopectin crystal. Plant Physiol **122**: 989–997

Nakamura Y, Utsumi Y, Sawada T, Aihara S, Utsumi C, Yoshida M, Kitamura S (2010) Characterization of the reactions of starch branching enzymes from rice endosperm. Plant Cell Physiol **51**: 776–794

Narindrasorasak S, Bridger WA (1977) Phosphoenolypyruvate synthetase of *Escherichia coli*: molecular weight, subunit composition, and identification of phosphohistidine in phosphoenzyme intermediate. J Biol Chem **252**: 3121–3127

Nielsen MM, Seo E-S, Bozonnet S, Aghajari N, Robert X, Haser R, Svensson B (2008) Multi-site substrate binding and interplay in barley α-amylase 1. FEBS Letters **582**: 2567–2571

Nielsen TH, Deiting U, Stitt M (1997) A β-amylase in potato tubers is induced by storage at low temperature. Plant Physiol **113**: 503–510

Nielsen TH, Wischmann B, Enevoldsen K, Moller BL (1994) Starch phosphorylation in potato tubers proceeds concurrently with de novo biosynthesis of starch. Plant Physiol **105**: 111–117

Niittylä T, Messerli G, Trevisan M, Chen J, Smith AM, Zeeman SC (2004) A previously unknown maltose transporter essential for starch degradation in leaves. Science **303**: 87–89

Nikuni Z (1978) Studies on starch granules. Starch/Stärke **30**: 105–111

Noiraud N, Maurousset L, Lemoine R (2001) Identification of a mannitol transporter, AgMaT1, in celery phloem. Plant Cell **13**: 695–705

Norton G, Harris JF (1975) Compositional changes in developing rape seed (*Brassica napus* L.). Planta **123**: 163–174

Nugent AP (2005) Health properties of resistant starch. Nutrition Bulletin **30**: 27–54

Oates CG (1997) Towards an understanding of starch granule structure and hydrolysis. Trends in Food Science & Technology **8**: 375–382

O'Neill EC, Field RA (2015) Underpinning starch biology with in vitro studies on carbohydrate-active enzymes and biosynthetic glycomaterials. in vitro 136

O'Neill CM, Gill S, Hobbs D, Morgan C, Bancroft I (2003) Natural variation for seed oil composition in *Arabidopsis thaliana*. Phytochemistry **64**: 1077–1090

Oostergetel GT, van Bruggen EFJ (1989) On the origin of a low angle spacing in starch. Starch/Stärke **41**: 331–335

Orzechowski S (2008) Starch metabolism in leaves. Acta Biochimica Polonica **55**: 435–445

O'Sullivan AC, Perez S (1999) The relationship between internal chain length of amylopectin and crystallinity in starch. Biopolymers **50**: 381–390

Pang PP, Pruitt RE, Meyerowitz EM (1988) Molecular cloning, genomic organization, expression and evolution of 12S seed storage protein genes of *Arabidopsis thaliana*. Plant Mol Biol **11**: 805–820

Pascual MB, Mata-Cabana A, Florencio FJ, Lindahl M, Cejudo FJ (2011) A comparative analysis of the NADPH thioredoxin reductase C-2-Cys peroxiredoxin system from plants and cyanobacteria. Plant Physiol **155**: 1806–1816

Patrick JW (2013) Does Don Fisher's high-pressure manifold model account for phloem transport and resource partitioning? Front Plant Sci **4**: 184

Patrick JW (1997) Phloem unloading: sieve element unloading and post-sieve element transport. Annual Review of Plant Physiology and Plant Molecular Biology **48**: 191–222

Patron NJ, Keeling PJ (2005) Common evolutionary origin of starch biosynthetic enzymes in green and red Algae. Journal of Phycology **41**: 1131–1141

Pérez S, Bertoft E (2010) The molecular structures of starch components and their contribution to the architecture of starch granules: a comprehensive review. Starch/Stärke **62**: 389–420

Periappuram C, Steinhauer L, Barton DL, Taylor DC, Chatson B, Zou J (2000) The plastidic phosphoglucomutase from Arabidopsis. A reversible enzyme reaction with an important role in metabolic control. Plant Physiol **122**: 1193–1199

Pettersson G, Ryde-Pettersson U (1990) Model studies of the regulation of the Calvin photosynthesis cycle by cytosolic metabolites. Biomed Biochim Acta **49**: 723–732

Posewitz MC, Smolinski SL, Kanakagiri S, Melis A, Seibert M, Ghirardi ML (2004) Hydrogen photoproduction is attenuated by disruption of an isoamylase gene in *Chlamydomonas reinhardtii*. Plant Cell **16**: 2151–2163

Posternak T (1935) Sur le phosphore des amidons. Carbohydrate Research **298**: 319–326

Prasch CM, Ott KV, Bauer H, Ache P, Hedrich R, Sonnewald U (2015) β-amylase1 mutant Arabidopsis plants show improved drought tolerance due to reduced starch breakdown in guard cells. J Exp Bot **66**: 6059–6067

Pyl E-T, Piques M, Ivakov A, Schulze W, Ishihara H, Stitt M, Sulpice R (2012) Metabolism and growth in Arabidopsis depend on the daytime temperature but are temperature-compensated against cool nights. Plant Cell **24**: 2443–2469

Ral J-P, Derelle E, Ferraz C, Wattebled F, Farinas B, Corellou F, Buléon A, Slomianny M-C, Delvalle D, d'Hulst C, et al (2004) Starch division and partitioning. A mechanism for granule propagation and maintenance in the picophytoplanktonic green alga *Ostreococcus tauri*. Plant Physiol **136**: 3333–3340

Rasse DP, Tocquin P (2006) Leaf carbohydrate controls over Arabidopsis growth and response to elevated CO_2: an experimentally based model. New Phytologist **172**: 500–513

Razem FA, Davis AR (1999) Anatomical and ultrastructural changes of the floral nectary of *Pisum sativum* L. during flower development. Protoplasma **206**: 57–72

Recondo E, Leloir LF (1961) Adenosine diphosphate glucose and starch synthesis. Biochem Biophys Res Commun **6**: 85–88

Reinders A, Sivitz AB, Hsi A, Grof CPL, Perroux JM, Ward JM (2006) Sugarcane ShSUT1: analysis of sucrose transport activity and inhibition by sucralose. Plant Cell Environ **29**: 1871–1880

Reinders A, Sivitz AB, Starker CG, Gantt JS, Ward JM (2008) Functional analysis of LjSUT4, a vacuolar sucrose transporter from *Lotus japonicus*. Plant Mol Biol **68**: 289–299

Reinders A, Sivitz AB, Ward JM (2012) Evolution of plant sucrose uptake transporters. Front Plant Sci **3**: 22

Rennie EA, Turgeon R (2009) A comprehensive picture of phloem loading strategies. PNAS **106**: 14162–14167

Riesmeier JW, Willmitzer L, Frommer WB (1994) Evidence for an essential role of the sucrose transporter in phloem loading and assimilate partitioning. EMBO J **13**: 1–7

Ritchie S, Swanson SJ, Gilroy S (2000) Physiology of the aleurone layer and starchy endosperm during grain development and early seedling growth: New insights from cell and molecular biology. Seed Science Research **10**: 193–212

Ritte G, Eckermann N, Haebel S, Lorberth R, Steup M (2000) Compartmentation of the starch-related R1 protein in higher plants. Starch/Stärke **52**: 145–149

Ritte G, Heydenreich M, Mahlow S, Haebel S, Kötting O, Steup M (2006) Phosphorylation of C6- and C3-positions of glucosyl residues in starch is catalysed by distinct dikinases. FEBS Letters **580**: 4872–4876

Ritte G, Lloyd JR, Eckermann N, Rottmann A, Kossmann J, Steup M (2002) The starch-related R1 protein is an α-glucan, water dikinase. Proc Natl Acad Sci U S A **99**: 7166–7171

Ritte G, Scharf A, Eckermann N, Haebel S, Steup M (2004) Phosphorylation of transitory starch is increased during degradation. Plant Physiol **135**: 2068–2077

Ritte G, Steup M, Kossmann J, Lloyd JR (2003) Determination of the starch-phosphorylating enzyme activity in plant extracts. Planta **216**: 798–801

Robin JP, Mercier C, Charbonniere R, Guilbot A (1974) Lintnerized starches. gel filtration and enzymatic studies of insoluble residues from prolonged acid treatment of potato starch. Cereal chemistry

Ruan Y-L (2012) Signaling role of sucrose metabolism in development. Mol Plant **5**: 763–765

Ruan Y-L, Jin Y, Huang J (2009) Capping invertase activity by its inhibitor. Plant Signaling & Behavior **4**: 983–985

Ruan Y-L, Llewellyn DJ, Furbank RT (2001) The control of single-celled cotton fiber elongation by developmentally reversible gating of plasmodesmata and coordinated expression of sucrose and K+ transporters and expansin. Plant Cell **13**: 47–60

Ruan Y-L, Llewellyn DJ, Furbank RT, Chourey PS (2005) The delayed initiation and slow elongation of fuzz-like short fibre cells in relation to altered patterns of sucrose synthase expression and plasmodesmata gating in a lintless mutant of cotton. J Exp Bot **56**: 977–984

Ruan Y-L, Xu S-M, White R, Furbank RT (2004) Genotypic and developmental evidence for the role of plasmodesmatal regulation in cotton fiber elongation mediated by callose turnover. Plant Physiol **136**: 4104–4113

Russin WA, Evert RF, Vanderveer PJ, Sharkey TD, Briggs SP (1996) Modification of a specific class of plasmodesmata and loss of sucrose export ability in the sucrose export defective 1 maize mutant. Plant Cell **8**: 645–658

Rydberg U, Andersson L, Andersson R, Aman P, Larsson H (2001) Comparison of starch branching enzyme I and II from potato. Eur J Biochem **268**: 6140–6145

Safford R, Jobling SA, Sidebottom CM, Westcott RJ, Cooke D, Tober KJ, Strongitharm BH, Russell AL, Gidley MJ (1998) Consequences of antisense RNA inhibition of starch branching enzyme activity on properties of potato starch. Carbohydrate Polymers **35**: 155–168

Sage RF (1994) Acclimation of photosynthesis to increasing atmospheric CO_2: The gas exchange perspective. Photosyn Res **39**: 351–368

Sage RF (1990) A model describing the regulation of ribulose-1,5-bisphosphate carboxylase, electron transport, and triose phosphate use in response to light intensity and CO_2 in C3 Plants. Plant Physiol **94**: 1728–1734

Samec M (1914) Studien über Pflanzenkolloide, IV. Die Verschiebungen des Phosphorgehaltes bei der Zustandsänderungen und dem diastatischen Abbau der Stärke. Kolloidchem Beih **4**: 2–54

Santelia D, Kötting O, Seung D, Schubert M, Thalmann M, Bischof S, Meekins DA, Lutz A, Patron N, Gentry MS, et al (2011) The phosphoglucan phosphatase like sex Four2 dephosphorylates starch at the C3-position in Arabidopsis. Plant Cell **23**: 4096–4111

Santelia D, Zeeman SC (2011) Progress in Arabidopsis starch research and potential biotechnological applications. Curr Opin Biotechnol **22**: 271–280

Satoh H, Nishi A, Yamashita K, Takemoto Y, Tanaka Y, Hosaka Y, Sakurai A, Fujita N, Nakamura Y (2003) Starch-branching enzyme I-deficient mutation specifically affects the structure and properties of starch in rice endosperm. Plant Physiol **133**: 1111–1121

Sauer N (2007) Molecular physiology of higher plant sucrose transporters. FEBS Lett **581**: 2309–2317

Schaffer AA, Petreikov M (1997) Sucrose-to-starch metabolism in tomato fruit undergoing transient starch accumulation. Plant Physiol **113**: 739–746

Scheidig A, Fröhlich A, Schulze S, Lloyd JR, Kossmann J (2002) Downregulation of a chloroplast-targeted β-amylase leads to a starch-excess phenotype in leaves. Plant J **30**: 581–591

Schürmann P (2003) Redox signaling in the chloroplast: the ferredoxin/thioredoxin system. Antioxid Redox Signal **5**: 69–78

Schürmann P, Buchanan BB (2008) The ferredoxin/thioredoxin system of oxygenic photosynthesis. Antioxid Redox Signal **10**: 1235–1274

Schurmann P, Jacquot J-P (2000) Plant thioredoxin systems revisited. Annu Rev Plant Physiol Plant Mol Biol **51**: 371–400

Schwall GP, Safford R, Westcott RJ, Jeffcoat R, Tayal A, Shi YC, Gidley MJ, Jobling SA (2000) Production of very-high-amylose potato starch by inhibition of SBE A and B. Nat Biotechnol **18**: 551–554

Schwender J, Ohlrogge JB, Shachar-Hill Y (2003) A flux model of glycolysis and the oxidative pentose phosphate pathway in developing *Brassica napus* embryos. J Biol Chem **278**: 29442–29453

Scialdone A, Mugford D, Feike D, Skeffington AW, Borrill P, Graf A, Smith AM, Howard M (2013) Arabidopsis plants perform arithmetic division to prevent starvation at night. eLife. doi: p. e00669

Sehnke PC, Chung HJ, Wu K, Ferl RJ (2001) Regulation of starch accumulation by granule-associated plant 14-3-3 proteins. Proc Natl Acad Sci USA **98**: 765–770

Serrato AJ, Fernández-Trijueque J, Barajas-López J-D, Chueca A, Sahrawy M (2013) Plastid thioredoxins: a "one-for-all" redox-signaling system in plants. Front Plant Sci. doi: 10.3389/fpls.2013.00463

Serrato AJ, Pérez-Ruiz JM, Spínola MC, Cejudo FJ (2004) A novel NADPH thioredoxin reductase, localized in the chloroplast, which deficiency causes hypersensitivity to abiotic stress in *Arabidopsis thaliana*. J Biol Chem **279**: 43821–43827

Seung D, Thalmann M, Sparla F, Hachem MA, Lee SK, Issakidis-Bourguet E, Svensson B, Zeeman SC, Santelia D (2013) *Arabidopsis thaliana* AMY3 is a unique redox-regulated chloroplastic α-amylase. Journal of Biological Chemistry **288**: 33620–33633

Shibanuma K, Takeda Y, Hizukuri S, Shibata S (1994) Molecular structures of some wheat starches. Carbohydrate Polymers **25**: 111–116

Silva PMFR da, Eastmond PJ, Hill LM, Smith AM, Rawsthorne S (1997) Starch metabolism in developing embryos of oilseed rape. Planta **203**: 480–487

Silver DM, Silva LP, Issakidis-Bourguet E, Glaring MA, Schriemer DC, Moorhead GBG (2013) Insight into the redox regulation of the phosphoglucan phosphatase SEX4 involved in starch degradation. FEBS Journal **280**: 538–548

Skeffington AW, Graf A, Duxbury Z, Gruissem W, Smith AM (2014) Glucan, water dikinase exerts little control over starch degradation in Arabidopsis leaves at night. Plant Physiol **165**: 866–879

Slewinski TL, Baker RF, Stubert A, Braun DM (2012) Tie-dyed 2 encodes a callose synthase that functions in vein development and affects symplastic trafficking within the phloem of maize leaves. Plant Physiol **160**: 1540–1550

Slewinski TL, Braun DM (2010) Current perspectives on the regulation of whole-plant carbohydrate partitioning. Plant Science **178**: 341–349

Slewinski TL, Meeley R, Braun DM (2009) Sucrose transporter 1 functions in phloem loading in maize leaves. J Exp Bot **60**: 881–892

Smith AM (2008) Prospects for increasing starch and sucrose yields for bioethanol production. Plant J **54**: 546–558

Smith AM, Coupland G, Dolan L, Harberd N, Jones J, Martin C, Sablowski R, Amey A (2009) Plant Biology. Garland Science

Smith AM, Stitt M (2007) Coordination of carbon supply and plant growth. Plant Cell Environ **30**: 1126–1149

Smith AM, Zeeman SC, Smith SM (2005) Starch degradation. Annual Review of Plant Biology **56**: 73–98

Sokolov LM, Dominguez-Solis JR, Allary A-L, Buchanan BB, Luan S (2006) A redox-regulated chloroplast protein phosphatase binds to starch diurnally and functions in its accumulation. Proceedings of the National Academy of Sciences of the United States of America **103**: 9732–9737

Sopanen T, Laurière C (1989) Release and activity of bound β-Amylase in a germinating barley grain. Plant Physiol **89**: 244–249

Sparla F, Costa A, Lo S, Pupillo P, Trost P (2006) Redox regulation of a novel plastid-targeted β-amylase of Arabidopsis. Plant Physiology **141**: 840–850

Srivastava AC, Ganesan S, Ismail IO, Ayre BG (2008) Functional characterization of the Arabidopsis AtSUC2 sucrose/H+ symporter by tissue-specific complementation reveals an essential role in phloem loading but not in long-distance transport. Plant Physiol **148**: 200–211

Stadler R, Wright KM, Lauterbach C, Amon G, Gahrtz M, Feuerstein A, Oparka KJ, Sauer N (2005) Expression of GFP-fusions in Arabidopsis companion cells reveals non-specific protein trafficking into sieve elements and identifies a novel post-phloem domain in roots. Plant J **41**: 319–331

Stanley D, Fitzgerald AM, Farnden KJF (2002) Characterisation of putative α-amylases from apple (*Malus domestica*) and *Arabidopsis thaliana*. Biologia **5**: 137–148

Stanley D, Rejzek M, Naested H, Smedley M, Otero S, Fahy B, Thorpe F, Nash RJ, Harwood W, Svensson B, et al (2011) The role of aα-glucosidase in germinating barley grains. Plant Physiol **155**: 932–943

Stinard PS, Robertson DS, Schnable PS (1993) Genetic isolation, cloning, and analysis of a mutator-induced, dominant antimorph of the maize amylose extender 1 locus. Plant Cell **5**: 1555–1566

Stitt M (1996) Metabolic Regulation of Photosynthesis. *In* Baker NR ed. Photosynthesis and the Environment. Springer Netherlands, Dordrecht, pp 151–190

Stitt M, Gerhardt R, Kürzel B, Heldt HW (1983) A role for fructose 2,6-bisphosphate in the regulation of sucrose synthesis in spinach leaves. Plant Physiol **72**: 1139–1141

Stitt M, Gibon Y, Lunn JE, Piques M (2007) Multilevel genomics analysis of carbon signalling during low carbon availability: coordinating the supply and utilisation of carbon in a fluctuating environment. Funct Plant Biol **34**: 526–549

Stitt M, Kürzel B, Heldt HW (1984) Control of photosynthetic sucrose synthesis by fructose 2,6-bisphosphate: II. partitioning between sucrose and starch. Plant Physiol **75**: 554–560

Stitt M, Quick WP (1989) Photosynthetic carbon partitioning: its regulation and possibilities for manipulation. Physiologia Plantarum **77**: 633–641

Stitt M, Zeeman SC (2012) Starch turnover: pathways, regulation and role in growth. Current Opinion in Plant Biology **15**: 282–292

Streb S, Eicke S, Zeeman SC (2012) The simultaneous abolition of three starch hydrolases blocks transient starch breakdown in Arabidopsis. J Biol Chem **287**: 41745–41756

Streb S, Delatte T, Umhang M, Eicke S, Schorderet M, Reinhardt D, Zeeman SC (2008) Starch granule biosynthesis in Arabidopsis is abolished by removal of all debranching enzymes but restored by the subsequent removal of an endoamylase. Plant Cell **20**: 3448–3466

Streb S, Zeeman SC (2012) Starch Metabolism in Arabidopsis. Arabidopsis Book. doi: 10.1199/tab.0160

Sun Z, Henson CA (1990) Degradation of native starch granules by barley α-glucosidases. Plant Physiol **94**: 320–327

Sun ZT, Henson CA (1991) A quantitative assessment of the importance of barley seed α-amylase, β-amylase, debranching enzyme, and α-glucosidase in starch degradation. Arch Biochem Biophys **284**: 298–305

Szydlowski N, Ragel P, Hennen-Bierwagen TA, Planchot V, Myers AM, Mérida A, d'Hulst C, Wattebled F (2011) Integrated functions among multiple starch synthases determine both amylopectin chain length and branch linkage location in Arabidopsis leaf starch. J Exp Bot **62**: 4547–4559

Szydlowski N, Ragel P, Raynaud S, Lucas MM, Roldán I, Montero M, Muñoz FJ, Ovecka M, Bahaji A, Planchot V, et al (2009) Starch granule initiation in Arabidopsis requires the presence of either class IV or class III starch synthases. Plant Cell **21**: 2443–2457

Tabata S, Hizukuri S (1971) Studies on starch phosphate. Part 2. Isolation of glucose-3-phosphate and maltose phosphate by acid hydrolysis of potato starch. Starch/Staerke **23**: 267–272

Tabata S, Nagata K, Hizukuri S (1975) Studies on Starch Phosphates. Part 3. On the Esterified Phosphates in Some Cereal Starches. Starch/Stärke **27**: 333–335

Taiz L, Zeiger E (2010) Plant Physiology, 5th edition. Sinauer Associates

Takaha T, Yanase M, Okada S, Smith SM (1993) Disproportionating enzyme (4-α-glucanotransferase; EC 2.4.1.25) of potato. Purification, molecular cloning, and potential role in starch metabolism. J Biol Chem **268**: 1391–1396

Takeda Y, Hizukuri S (1981) Re-examination of the action of sweet-potato β-amylase on phosphorylated (1→4)-χ-d-glucan. Carbohydrate Research **89**: 174–178

Takeda Y, Hizukuri S (1982) Location of phosphate groups in potato amylopectin. Carbohydr Res 321–327

Takeda Y, Shitaozono T, Hizukuri S (1988) Molecular structure of corn starch. Starch/Stärke **40**: 51–54

Takeda Y, Takeda C, Mizukami H, Hanashiro I (1999) Structures of large, medium and small starch granules of barley grain. Carbohydrate Polymers **38**: 109–114

Tester RF, Karkalas J, Qi X (2004) Starch-composition, fine structure and architecture. Journal of Cereal Science **39**: 151–165

Tetlow IJ, Beisel KG, Cameron S, Makhmoudova A, Liu F, Bresolin NS, Wait R, Morell MK, Emes MJ (2008) Analysis of protein complexes in wheat amyloplasts reveals functional interactions among starch biosynthetic enzymes. Plant Physiol **146**: 1878–1891

Tetlow IJ, Wait R, Lu Z, Akkasaeng R, Bowsher CG, Esposito S, Kosar-Hashemi B, Morell MK, Emes MJ (2004) Protein phosphorylation in amyloplasts regulates starch branching enzyme activity and protein–protein interactions. Plant Cell **16**: 694–708

Tiessen A, Hendriks JHM, Stitt M, Branscheid A, Gibon Y, Farré EM, Geigenberger P (2002) Starch synthesis in potato tubers is regulated by post-translational redox modification of ADP-glucose pyrophosphorylase: a novel regulatory mechanism linking starch synthesis to the sucrose supply. Plant Cell **14**: 2191–2213

Tiessen A, Prescha K, Branscheid A, Palacios N, McKibbin R, Halford NG, Geigenberger P (2003) Evidence that SNF1-related kinase and hexokinase are involved in separate sugar-signalling pathways modulating post-translational redox activation of ADP-glucose pyrophosphorylase in potato tubers. Plant J **35**: 490–500

Topping D (2007) Cereal complex carbohydrates and their contribution to human health. Journal of Cereal Science **46**: 220–229

Trethewey RN, ap Rees T (1994) A mutant of *Arabidopsis thaliana* lacking the ability to transport glucose across the chloroplast envelope. Biochem J **301 (Pt 2)**: 449–454

Tsai CY (1974) The function of the waxy locus in starch synthesis in maize endosperm. Biochem Genet **11**: 83–96

Tuncel A, Cakir B, Hwang S-K, Okita TW (2014) The role of the large subunit in redox regulation of the rice endosperm ADP-glucose pyrophosphorylase. FEBS J **281**: 4951–4963

Upmeyer DJ, Koller HR (1973) Diurnal trends in net photosynthetic rate and carbohydrate levels of soybean leaves. Plant Physiol **51**: 871–874

Utsumi Y, Nakamura Y (2006) Structural and enzymatic characterization of the isoamylase1 homo-oligomer and the isoamylase1-isoamylase2 hetero-oligomer from rice endosperm. Planta **225**: 75–87

Utsumi Y, Utsumi C, Sawada T, Fujita N, Nakamura Y (2011) Functional diversity of isoamylase oligomers: the ISA1 homo-oligomer is essential for amylopectin biosynthesis in rice endosperm. Plant Physiol **156**: 61–77

Valerio C, Costa A, Marri L, Issakidis-Bourguet E, Pupillo P, Trost P, Sparla F (2011) Thioredoxin-regulated β-amylase (BAM1) triggers diurnal starch degradation in guard cells, and in mesophyll cells under osmotic stress. J Exp Bot **62**: 545–555

van Bel AJE (2003) Transport phloem: low profile, high impact. Plant Physiol **131**: 1509–1510

van Bel AJE (1996) Interaction between sieve element and companion cell and the consequences for photoassimilate distribution. Two structural hardware frames with associated physiological software packages in dicotyledons? J Exp Bot **47**: 1129

van Bel AJE (1993) Strategies of phloem loading. Annual Review of Plant Physiology and Plant Molecular Biology **44**: 253–281

Ventriglia T, Kuhn ML, Ruiz MT, Ribeiro-Pedro M, Valverde F, Ballicora MA, Preiss J, Romero JM (2008) Two Arabidopsis ADP-glucose pyrophosphorylase large subunits (APL1 and APL2) are catalytic. Plant Physiol **148**: 65–76

Vigeolas H, van Dongen JT, Waldeck P, Huhn D, Geigenberger P (2003) Lipid storage metabolism is limited by the prevailing low oxygen concentrations within developing seeds of oilseed rape. Plant Physiol **133**: 2048–2060

Vijn I, Smeekens S (1999) Fructan: more than a reserve carbohydrate? Plant Physiol **120**: 351–360

Viksø-Nielsen A, Blennow A, Jørgensen K, Kristensen KH, Jensen A, Møller BL (2001) Structural, physicochemical, and pasting properties of starches from potato plants with repressed r1-gene. Biomacromolecules **2**: 836–843

Wang Q, Monroe J, Sjolund RD (1995) Identification and characterization of a phloem-specific β-amylase. Plant Physiol **109**: 743–750

Wang X, Xue L, Sun J, Zuo J (2010) The Arabidopsis BE1 gene, encoding a putative glycoside hydrolase localized in plastids, plays crucial roles during embryogenesis and carbohydrate metabolism. J Integr Plant Biol **52**: 273–288

Wattebled F, Dong Y, Dumez S, Delvallé D, Planchot V, Berbezy P, Vyas D, Colonna P, Chatterjee M, Ball S, et al (2005) Mutants of Arabidopsis lacking a chloroplastic isoamylase accumulate phytoglycogen and an abnormal form of amylopectin. Plant Physiol **138**: 184–195

Wattebled F, Planchot V, Dong Y, Szydlowski N, Pontoire B, Devin A, Ball S, D'Hulst C (2008) Further evidence for the mandatory nature of polysaccharide debranching for the aggregation of semicrystalline starch and for overlapping functions of debranching enzymes in Arabidopsis leaves. Plant Physiol **148**: 1309–1323

Weber A, Servaites JC, Geiger DR, Kofler H, Hille D, Gröner F, Hebbeker U, Flügge UI (2000) Identification, purification, and molecular cloning of a putative plastidic glucose translocator. Plant Cell **12**: 787–802

Weber H, Borisjuk L, Wobus U (2005) Molecular physiology of legume seed development. Annual Review of Plant Biology **56**: 253–279

Weiner H, Stitt M, Heldt HW (1987) Subcellular compartmentation of pyrophosphate and alkaline pyrophosphatase in leaves. Biochimica et Biophysica Acta (BBA) - Bioenergetics **893**: 13–21

Werner D, Gerlitz N, Stadler R (2011) A dual switch in phloem unloading during ovule development in Arabidopsis. Protoplasma **248**: 225–235

Wiesenborn DP, Orr PH, Casper HH, Tacke BK (1994) Potato starch paste behavior as related to some physical/chemical properties. Journal of Food Science **59**: 644–648

Xuan YH, Hu YB, Chen L-Q, Sosso D, Ducat DC, Hou B-H, Frommer WB (2013) Functional role of oligomerization for bacterial and plant SWEET sugar transporter family. PNAS **110**: E3685–E3694

Yu TS, Kofler H, Häusler RE, Hille D, Flügge UI, Zeeman SC, Smith AM, Kossmann J, Lloyd J, Ritte G, et al (2001) The Arabidopsis *sex1* mutant is defective in the R1 protein, a general regulator of starch degradation in plants, and not in the chloroplast hexose transporter. Plant Cell **13**: 1907–1918

Yu TS, Lue WL, Wang SM, Chen J (2000) Mutation of Arabidopsis plastid phosphoglucose isomerase affects leaf starch synthesis and floral initiation. Plant Physiol **123**: 319–326

Yu T-S, Zeeman SC, Thorneycroft D, Fulton DC, Dunstan H, Lue W-L, Hegemann B, Tung S-Y, Umemoto T, Chapple A, et al (2005) α-amylase is not required for breakdown of transitory starch in Arabidopsis leaves. J Biol Chem **280**: 9773–9779

Zanella M, Borghi GL, Pirone C, Thalmann M, Pazmino D, Costa A, Santelia D, Trost P, Sparla F (2016) β-amylase 1 (BAM1) degrades transitory starch to sustain proline biosynthesis during drought stress. J Exp Bot erv572

Zeeman SC, Delatte T, Messerli G, Umhang M, Stettler M, Mettler T, Streb S, Reinhold H, Kötting O (2007a) Starch breakdown: recent discoveries suggest distinct pathways and novel mechanisms. doi: 10.1071/FP06313

Zeeman SC, Kossmann J, Smith AM (2010) Starch: its metabolism, evolution, and biotechnological modification in plants. Annual Review of Plant Biology **61**: 209–234

Zeeman SC, Northrop F, Smith AM, ap Rees T (1998) A starch-accumulating mutant of *Arabidopsis thaliana* deficient in a chloroplastic starch-hydrolysing enzyme. The Plant Journal **15**: 357–365

Zeeman SC, ap Rees T (1999) Changes in carbohydrate metabolism and assimilate export in starch-excess mutants of Arabidopsis. Plant, Cell & Environment **22**: 1445–1453

Zeeman SC, Smith SM, Smith AM (2007b) The diurnal metabolism of leaf starch. Biochem J **401**: 13–28

Zeeman SC, Thorneycroft D, Schupp N, Chapple A, Weck M, Dunstan H, Haldimann P, Bechtold N, Smith AM, Smith SM (2004) Plastidial α-glucan phosphorylase is not required for starch degradation in Arabidopsis leaves but has a role in the tolerance of abiotic stress. Plant Physiol **135**: 849–858

Zhang X, Myers AM, James MG (2005) Mutations affecting starch synthase III in Arabidopsis alter leaf starch structure and increase the rate of starch synthesis. Plant Physiol **138**: 663–674

Zhou J, Theodoulou F, Sauer N, Sanders D, Miller AJ (1997) A kinetic model with ordered cytoplasmic dissociation for SUC1, an Arabidopsis H+/sucrose cotransporter expressed in Xenopus oocytes. J Membr Biol **159**: 113–125

RINGRAZIAMENTI

I miei più sinceri ringraziamenti vanno alla Prof.ssa Francesca Sparla, per essere stata un'ottima guida durante il dottorato ed avermi dato la preziosa opportunità di svolgere questo percorso nel Laboratorio di Biologia Redox dei Sistemi Vegetali. Ringrazio per questo, per le sue vivaci domande e per i numerosi spunti anche il Prof. Paolo Trost. Grazie anche al Dr. Mirko Zaffagnini per i preziosi consigli e la simpatia. Sono grata inoltre a tutti i ragazzi e ragazze dell'Orto Botanico di Bologna, dottorandi/e e studenti/esse, per il tempo trascorso insieme.

Inoltre, ringrazio moltissimo la Dr.ssa Diana Santelia dell'Università di Zurigo per avermi accolta con disponibilità e fiducia nel suo laboratorio e per avermi dato l'opportunità di svolgere alcuni preziosi esperimenti. Oltre a Lei, vorrei ringraziare anche il Dr. David Seung per i suggerimenti e per avermi gentilmente messo a disposizione i cloni di AtBAM1 e AtAMY3. Ringrazio Diana P., Daniel, Arianna, Matthias e tutto il gruppo del Prof. Martinoia, che mi hanno aiutata ad ambientarmi in laboratorio, e Martina Zanella, per l'ospitalità e le vivaci conversazioni. Ringrazio anche il Dr. Peter Hunziker e i suoi collaboratori del "Functional Genomics Center Zürich" per l'aiuto nel condurre e analizzare gli esperimenti di spettrometria di massa.

Un ringraziamento va anche alla Dott.ssa Simona Fermani del Dipartimento di Chimica "Giacomo Ciamician" di Bologna ed al Prof. Alex Costa dell'Università degli Studi di Milano.